Universität für Bodenkultur Wien

Department of Forest and Soil Sciences

Institute of Silviculture
Inst. Head/Supervisor: Univ.Prof. Dipl.-Ing. Dr. Huber Hasenauer

INTEGRATION OF IN-SITU AND REMOTELY SENSED DATA TO ASSESS THE STATE OF FOREST RESOURCES ACROSS EUROPE.

Dissertation to obtain the doctoral degree (Dr. Nat. Techn.) at
The University of Natural Resources and Life Sciences (BOKU), Vienna

Submitted by
Adam Moreno

Vienna, Austria, July 2016

Preface

This work is a cumulative dissertation consisting of 4 individual peer-reviewed papers, 2 first author and 2 second author, and 1 first author paper under revision for submission. The papers can be found in the Appendix. The formatting of the papers varies due to the style of the various journals.

This document provides the framework demonstrating the links between all of the papers and how they are used to accomplish a larger research goal. The specific methodologies, results and discussions that underlie each paper can be found in the Appendix.

Citations to this work should refer to: Moreno, A., 2016. Integration of in-situ and remotely sensed data to assess the state of forest resources across Europe. PhD. Dissertation. University of Natural Resources and Life Sciences, Vienna or by reference to the individual papers.

Acknowledgments

This work was funded by the European Union Seventh Framework Programme under 584 grant agreement n°311970 (FORMIT) and involved the collaboration of scientists from 11 different countries who contributed to obtaining and processing the national forest inventory data that I use. Also, I could not have done this study without the hard work of those researchers that produce gridded data products and make them publically available.

I would like to thank my colleagues here at BOKU that helped me throughout my time in Vienna; Dipl.-Ing. Dr. Christopher Thurnher, Dipl.-Ing. Dr.Elisabeth Poetzelsberger, my advisor Univ. Prof. DI Dr. Hubert Hasenauer and my office mate and partner in science Dipl.-Ing. Mathias Neumann. I would also like to thank several other people who helped me professionally including; Dipl.-Ing. Dr.nat.techn. Silvia Winter, Dr. Maosheng Zhao, and Dr. Steve Running. I would like to thank my family who has helped me get to this point, and all throughout my academic career, supporting me both emotionally and logistically while living overseas. Most of all, I would like to thank my wife, Loretta Moreno, for her continued support and encouragement.

List of Papers

1. **Moreno, A.,** Hasenauer, H., 2015. Spatial downscaling of European climate data. Int. J. Climatol.
2. Neumann, M., **Moreno, A.,** Mues, V., Härkönen, S., Mura, M., Bouriaud, O., Lang, M., Achten, W.M.J., Thivolle-Cazat, A., Bronisz, K., Merganič, J., Decuyper, M., Alberdi, I., Astrup, R., Mohren, F., Hasenauer, H., 2016. Comparison of carbon estimation methods for European forests. For. Ecol. Manage. 361, 397–420.
3. Neumann, M., **Moreno, A.,** Thurnher, C., Mues, V., Härkönen, S., Mura, M., Bouriaud, O., Lang, M., Cardellini, G., Thivolle-Cazat, A., Bronisz, K., Merganič, J., Alberdi, I., Astrup, R., Mohren, F., Zhao, M., Hasenauer, H., 2016b. Creating a Regional MODIS Satellite-Driven Net Primary Production Dataset for European Forests. Remote Sens. 8, 1–18.
4. **Moreno, A.,** Neumann, M., Hasenauer, H., 2016. Optimal resolution for linking remotely sensed and forest inventory data in Europe. Remote Sens. Environ. 183.
5. **Moreno, A.**, Neumann, M, Hasenauer, H. In revision for submission. “The state of forest resources across Europe“

Abstract

Climate change will affect forests globally, having varying effects across landscapes. Repercussions of a shifting climate on forest processes require ecosystems to be studied on large scales. To quantify future shifts, anomalies and trends in biophysical drivers and their effects on forest resources, the current state of forest structure must first be known. In European forests, management is also a major driver of forest productivity and structure. To assess the effectiveness of large scale forest management, a spatially explicit landscape level outlook must be taken. In Europe, data on climate and forests in a form that would allow spatial analysis, with local level resolution on a continental scale, is difficult to access or limited in availability. In this study, a pan-European spatially explicit data set of forest characteristics on a 0.133° resolution is derived which represent the decade 2000-2010. A daily pan-European climate data set on a $1km^2$ resolution is also created, which is more accurate than previously available gridded data products. This data is then used to calculate improved, remotely sensed forest productivity estimates. The study also outlines the collation of the largest European plot-level national forest inventory (NFI) data set from 14 countries and quantifies an optimal resolution to link NFI and remotely sensed data of between 0.0664° and 0.266°. An algorithm is developed that links NFI and remotely sensed data to create a gridded pan-European forest structure data set. Bias in the data is less than 1% of NFI values and the mean absolute error is less than the standard deviation. Comparing against other data sources measuring similar values indicates that the new data has realistic values in areas where no NFI data was originally present. Preliminary analysis suggests that climate places limits on forest structure, which can alter future forest management options under a changing climate.

Kurzfassung

Die Wälder der Erde werden durch den weltweiten Klimawandel auf verschiedene Weise beeinflusst. Um die Auswirkungen von Veränderungen in den Prozessen und Kreisläufen von Wälder zu untersuchen, sind großskalige und weitreichende Studien erforderlich. Hier sind besonders Informationen zu Anomalien und Trends in den Wachstumsprozessen von besonderer Wichtigkeit. In den Wäldern Europas ist zusätzlich die Waldbewirtschaftung ein wichtiger Faktor. Um die Effektivität von Bewirtschaftungsformen zu beurteilen, sind ebenso groß-skalige Studien essentiell. Da in Europe die hierfür erforderlichen Daten nicht ausreichend verfügbar sind, ist das Hauptziel dieser Arbeit eine räumlich explizite Datengrundlage für Europa zu entwickeln, die es erlaubt verschiedene Information über die Wälder Europas anzubieten. Dieser Datensatz repräsentiert den Zeitraum 2000 bis 2010 mit einer räumlichen Auflösung von 0.133°. Zu diesem Zwecke wurde ein Klimadatensatz mit einer Auflösung von 1 km aus verfügbaren Daten durch „downscaling“ entwickelt. Damit wurde ein verbesserter Datensatz zu Netto Primärproduktion von Wald gerechnet, der zusätzlich räumlich explizite Satellitendaten nutzt. Diese Arbeit beschreibt in weiterer Folge die Sammlung und Harmonisierung terrestrischer Referenzdaten in Form von Waldinventurdaten aus 14 Europäischen Ländern und ermittelt jene räumliche Auflösung, die für die Verknüpfung mit Fernerkundungsdaten optimal ist. Ein Algorithmus wurde entwickelt um aus Terrestrische Inventurdaten und Fernerkundungsdaten die eingangs erwähnten räumlich expliziten Datengrundlage zu erstellen. Der Bias ist weniger als 1 % im Vergleich zu den Referenzdaten und der mittlere Absolutfehler ist kleiner als die Standardabweichung. Ein Vergleich mit publizierten Daten anderer Studien zeigt, dass dieser neue Datensatz realistische Werte liefert auch für Länder, wo keine Referenzdaten verfügbar waren. vorläufige Ergebnisse legen nahe, dass das Klima ein limitierende Faktor in dem Aufbau und den Strukturen Europas Wälder sein kann. Dies kann zu einer Optimierung zukünftiger Waldbewirtschaftung beitragen mit dem Ziel der Abschwächung des weltweiten Klimawandels.

Table of Contents

1. Introduction

Climate change is projected to alter vegetation states and dynamics globally (Cramer et al. 2001). The states and processes that regulate forest ecosystems determine the ecosystem services that forests provide to society and the earth system as a whole (Kremen 2005). Europeans are heavily dependent on the health of forests and their continued provision of ecosystems services into perpetuity (Daily et al. 1999). Further, European forests are estimated to include over 1/3 of the world's temperate forest carbon sink, giving them global importance for commerce and to combat climate change (Pan et al. 2011). To assess the impact future climate change will have on European forests, and the resources they provide, it is imperative to first understand the current state of these forests and the spatial distribution of various forest characteristics (Cramer et al. 2001).

Europe is made up of 23 countries with its forests spanning across political borders. The forest area of individual countries rarely covers more than 10% of the total forest in Europe (United Nation's Food and Agriculture Organization 2015). Therefore, to fully understand forests throughout Europe, research must be done on the European scale. Lack of available and accessible forest and climate data in Europe make large scale, locally relevant studies difficult or impossible (Moreno and Hasenauer 2015; Moreno, Neumann, and Hasenauer 2016b).

Climate data, necessary for any climate change related work in Europe, is restricted to interpolated data on a 0.25° resolution – not a fine enough resolution to see local level effects such as topography (Moreno and Hasenauer 2015). Individual weather stations in Europe are not linked via an overarching database or methodology, as can be found in the United States. Weather station data must be collected from individual countries and requests may be subject to the approval of each nation. Often national data portals are difficult to navigate and, as is the case for Finland, even require knowledge of programming to access. Access to an entire country's data set is often limited or restricted. These regulatory hurdles make the creation of finer resolution interpolations, or interpolations using alternate methods difficult or statistically implausible in certain areas of Europe. The size of the resolution dictates which forest-climate interactions can be studied. For example, with a resolution of 0.25°, one cannot study orographic climate effects on forests or differing effects on various species groups.

Data accessibility and availability describing the state of European forests are not much different than the aforementioned challenges of obtaining climate data. National Forest Inventory (NFI) data is also not integrated into a common database for public accessibility (Neumann, Moreno, Thurnher, et al. 2016). Currently, there are only 3 countries that provide plot-level data online for public access: France, Spain and Italy. Apart from these three countries, accessing NFI data online is typically limited to country-level statistics and does not provide plot-level data for recalculation or spatial analysis, thereby not allowing spatial assessments of forests that transcend political boundaries. For example, the current state of NFI data prevents assessing how climatic gradients limit forest structure and how forest policies spatially affect timber supply.

Unlike other large forested regions, e.g., The United States, Canada, Russia, and Brazil, Europe is made of a myriad of countries, cultures, languages, policies and hurtles to data access. This makes creating data sets that cover all of Europe, not only a technical and scientific challenge, but an inter-personal, political and logistical one as well. There have been several attempts to make data sets that describe the state of European forest structure (Brus et al. 2011; Gallaun et al. 2010; Naudts et al. 2016; Vilén et al. 2012). These data sets however, are not provided in a publically available repository or are completely inaccessible. Further, these datasets only focus on one particular aspect of forest structure and rely on varying methods and input data sets for their creation, making them spurious to compare or combine. There have also been efforts at other scales to map forest structure and dynamics, both globally (Crowther et al. 2015; Running et al. 2004; Simard et al. 2006), and regionally (Dong et al. 2003; Hasenauer et al. 2012; Maselli et al. 2014). However, scale dictates the accuracy of the data. Data produced for global analyses can result in lower accuracy on continental or regional scales. Data made on the regional scale is, of course, limited to that particular region and uses a particular method, which can vary from region to region, making comparison or collation of these data sets difficult.

Pan-European, integrated, spatially explicit datasets on various aspects of forest structure and climate would allow for the types of assessments that are necessary to quantify European forests' vulnerability to climate change and the effectiveness of different forest management practices across the landscape. These types of data sets could also act as a quality check against other global data sets that are used for policy decisions, such as the United Nations Food and Agriculture Organization's Forest Resource Assessment (FAO FRA), which heavily influence policy decisions.

In this study: a daily pan-European climate data set on a 1x1km resolution is created; a European focused MODerate resolution Imaging Spectroradiometer (MODIS) based forest productivity estimate is derived; the largest plot-level forest inventory data set that currently exists in Europe is collated; the optimal resolution on which to combine NFI and remotely sensed data is quantified; and a spatially explicit pan-European gridded data set of forest characteristics is produced. Various aspects of the interplay between forest structure, management and climate are then analyzed utilizing this data.

2. Objectives and outline

The goal of this study was to develop the data necessary to spatially analyze the state of forest resources across Europe and then to begin to analyze the interplay between forest management, forest productivity, forest structure, and climate. There were several steps necessary to accomplishing this task, each of which has contributed to the body of knowledge on climate, forests and data integration (Figure 1).

The first steps were to downscale climate data and to collate national forest inventory (NFI) data throughout Europe (Figure 1). The climate data and the NFI data were then used to derive and validate European forest focused remotely sensed net primary production (NPP) estimates. NFI data and remotely sensed data were then combined to create a pan-European forest

characteristics data set. To combine these data for analysis, the optimal resolution on which to link the data to maximize the confidence in the output data, was quantified. The optimal resolution and the NPP estimates were then used, along with several other datasets, within an algorithm developed in this study, to gap fill NFI data into areas where NFI data was not present. The result was a pan-European data set of forest characteristics representing the mean values for the decade 2000-2010. Using all of the data created in this study, the state of forest resources throughout Europe was analyzed in ways that had hitherto been infeasible. The individual objectives of the study are:

1. Spatially downscale daily European climate data
2. Collate NFI data throughout Europe
3. Derive new forest productivity estimates for Europe
4. Determine the most accurate resolution on which to combine NFI and remotely sensed data
5. Combine NFI and remotely sensed data to produce pan-European spatially explicit data sets of forest characteristics
6. Utilize new data products to analyze the state of forest resources.

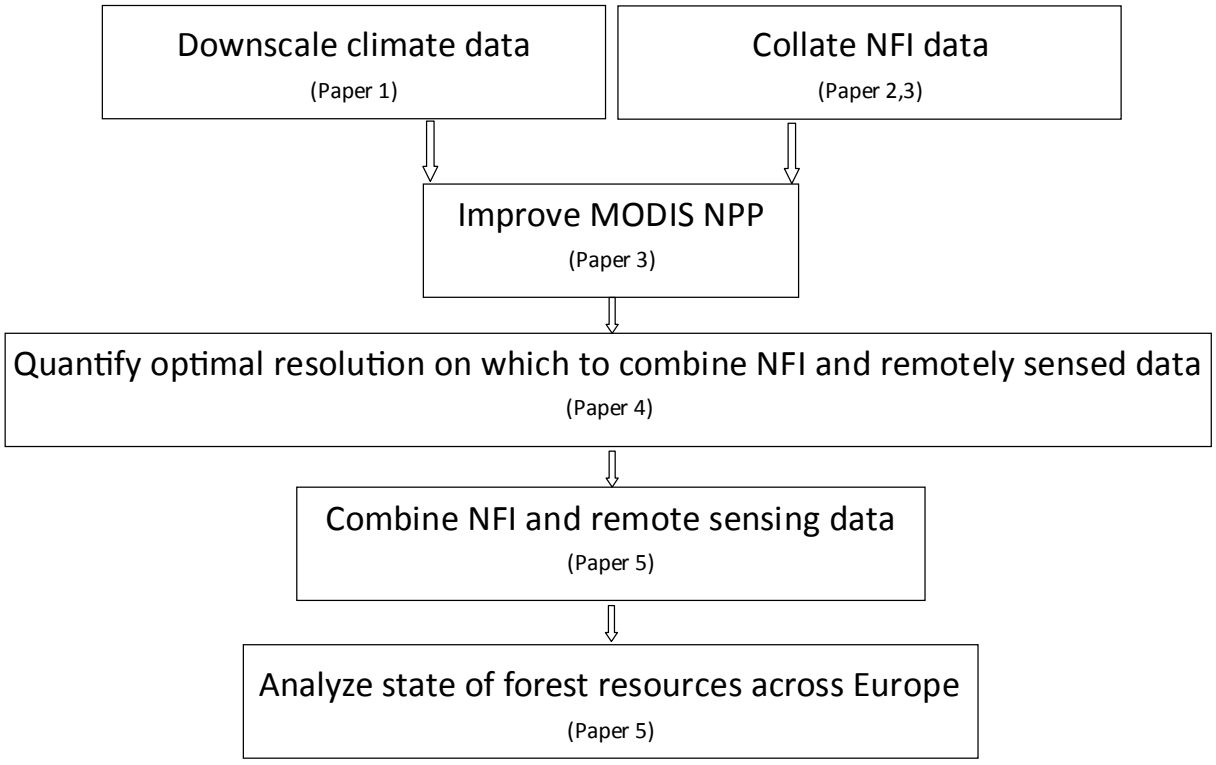

Figure 1: Flowchart of research. (Paper # where this research is explained in greater detail)

3. Data

Diverse spatially and temporally explicit data sets that cover content from climate to forest structure in Europe were used in this study (Table 1). These data sets were derived using a myriad of methods from different sources for varying purposes, and range in scale from jurisdictions to global coverage. These data include in-situ point data which were collected on the ground and remotely sensed, gridded, data which cover a large area. Various statistics on the national and sub-national level were also utilized. Some of these datasets had a temporal component which had to be reconciled with those data that did not. The aspects of the environment that were covered by these data sets include: climate, land cover-type, forest characteristics, biogeographical regions, vegetative productivity, and topography.

Table 1: Data products used in this study. Type can be gridded, plot level (points), or stats which indicates aggregated statistics. Temporal indicates if time was taken into account when dealing with this data set. Subject describes the area of interest of the data product. Paper indicates in which publication throughout this study the data set was used.

Data Set	Scale	Type	Temporal	Subject	Paper
E-OBS	Europe	Gridded	Yes	Climate	1
WorldClim	Globe	Gridded	No	Climate	1
Weather Stations	Country	Point	Yes	Climate	1
Forest Inventory	Country	Point	Yes	Forest	2,3,4,5
MODIS Land Cover	Globe	Gridded	No	Cover Type	3,4,5
Global Land Cover 2000	Globe	Gridded	No	Cover Type	4
CORINE Land Cover	Europe	Gridded	No	Cover Type	4
EFI Tree Species	Europe	Gridded	No	Cover Type	4,5
Biogeo. Regions	Europe	Gridded	No	Biogeography	5
MODIS % Forest	Global	Gridded	No	Forest	5
MODIS LAI/FPAR	Globe	Gridded	Yes	Productivity	3,5
MODIS NPP + Trend	Globe	Gridded	Yes	Productivity	3,5
Tree Canopy height	Globe	Gridded	No	Forest	5
GTOPO30 DEM	Globe	Gridded	No	Topography	3,5
Forest Area	Europe	Gridded	No	Forest	5
FAO FRA	Globe	Stats	No	Forest	5
EFIScen	Jurisdiction	Stats	No	Forest	5

4. Methods

4.1. Workflow

Each paper developed in this study was a step towards the goal of spatially analyzing European forest resources (Figure 1). Paper 1 describes the effort to create a daily 1km² resolution climate data set of precipitation and minimum and maximum temperature across Europe from 1950 to 2012. Paper 2 begins to examine the uncertainties in carbon and biomass estimates when combining NFI data from various countries which use different calculation methods. Paper 3 outlines the collation of NFI data sets throughout Europe, describing the newly derived MODIS forest NPP estimates - driven by the downscaled climate data - and compares these estimates with those derived from NFI data. Paper 4 quantifies the optimal resolution on which to combine NFI and remotely sensed data, outlining the benefits and drawbacks of different resolutions on the European scale. Paper 5 describes the algorithm used to combine the collated NFI and remotely sensed data to create a pan-European data set on forest characteristics, compares this data set with previously produced ones from other organizations, and begins to assess the state of European forest resources. To exemplify the benefits of this work, also included in this study are current research concepts that are building upon this work and example preliminary results of work that is yet to be published.

4.2. Downscale Climate data

The previous state of climate data in Europe was restricted to a 0.25˚ (30km^2) resolution and came from the European Observation (E-OBS) dataset. E-OBS was downscaled to 0.0083˚(1km^2) using WorldClim data and a delta method algorithm designed in the study (Moreno and Hasenauer 2015). A monotone cubic interpolation was used, which preserves the large resolution mean values from E-OBS, but with the finer resolution, relative scaling of WorldClim. The downscaled datasets include daily precipitation and minimum and maximum temperature all on a 0.0083˚ resolution from 1950-2012.

4.3. Collate and NFI data

National Forest Inventory (NFI) data in Europe is collected by individual countries and is not housed in one common repository for public or scientific use. Therefore, to study NFI data on the European scale, data must be collected from individual countries. As spatially explicit data was needed for analysis, the publicly available data from various countries' forest agency's websites was not sufficient because this data is typically only given on country level aggregates. Plot level data was collated from 14 different countries including: Austria, Germany, Spain, Italy, Romania, Netherlands, Belgium, France, Poland, Estonia, Czech Republic, Finland, Norway and Sweden (Neumann, Moreno, Thurnher, et al. 2016). Data from all countries were then harmonized to the

most limiting country values. For example, age classes for every country were converted to 20-year time steps, up to 140 years, which was the coarsest time step of any country. As part of this harmonization process, the effect different biomass functions in the different countries has on the total biomass estimates, was quantified (Neumann, Moreno, Mues, et al. 2016). This plot level NFI data set is the largest in Europe, including 238,834 plots and spanning the entire European latitudinal gradient.

4.4. Improve MODIS NPP

To make MODIS NPP data more accurate on the European scale, the downscaled climate data was used to drive the MOD17 algorithm. MOD17 takes vapor pressure deficit (VPD) and shortwave solar radiation (SRad) as two inputs that previously did not exist spatially for Europe (Neumann, Moreno, Thurnher, et al. 2016). The MtClim algorithm was used in conjunction with the GTOPO30 digital elevation model and the downscaled climate data to produce VPD and SRad. The MOD17 algorithm was then run using this new data and compared with the newly derived NPP data with estimates derived from NFI data.

4.5. Determine Optimal Resolution

To determine the optimal resolution on which to combine the NFI and remotely sensed data three factors that are affected by resolution aggregation were analyzed: loss of spatial information, agreement between remotely sensed and NFI data, and the standard error of the underlying NFI data (Moreno, Neumann, and Hasenauer 2016a). These three factors were assessed as data was aggregated from the native resolution of 0.0083˚ (NR) to: 2xNR, 4xNR, 8xNR, 16xNR, 32xNR, 64xNR, and 128xNR. Loss of spatial information was assessed by calculating Shannon's Equitability Index (SEI) for all of the NR cells that make up an aggregated cell. The lower the SEI, the higher the heterogeneity within a cell, and thus the more loss of information that will occur when the cells are aggregated to 1 value. Agreement between remotely sensed and NFI data was assessed by using a confusion matrix between the NFI data and 4 remotely sensed land cover datasets. Aggregation of both the remotely sensed land cover data and the NFI data was done using the rules for classification of the remotely sensed land cover data set in question. The standard error of the NFI data was calculated based on the basal area, height and age at each aggregation step.

To quantify the optimal resolution, a normalized curve was produced representing the three factors assessed and they were summed. The optimal resolution is then the resolution at the point where the slope of the resultant curve flattens off. At this inflection point there is a diminishing benefit to aggregation.

4.6. Combine NFI and Remote Sensing data

To analyze forests throughout all of Europe, forest characteristic data is required in both areas where NFI data is present and where it isn't. Combing NFI with remotely sensed data is often used to produce such data on country scales. An algorithm involving clustering and nearest neighbors was developed to combine NFI with the remotely sensed data to create a pan-European data set (Moreno, Neumann, and Hasenauer 2016b) (Figure 2). To gap-fill areas without NFI data, the algorithm first uses a combination of remotely sensed co-variates that can delineate forest types and structures from one another. The co-variates used were: MODIS NPP, MODIS NPP trend, canopy height and climate site quality (based on average decadal shortwave radiation, vapor pressure deficit, and growing season based on MODIS LAI). Clustering was first done by bioregion and cover type. Then a further clustering using a k-means process was done to further delineate forest types. It was upon these clusters that the nearest neighbor algorithm was performed. The way in which clustering was done and how many nearest neighbors were used and how they were combined was decided through a parameterization process which minimized the difference in bias and the three moments (variance, skewness and kurtosis) of the overall European level distribution.

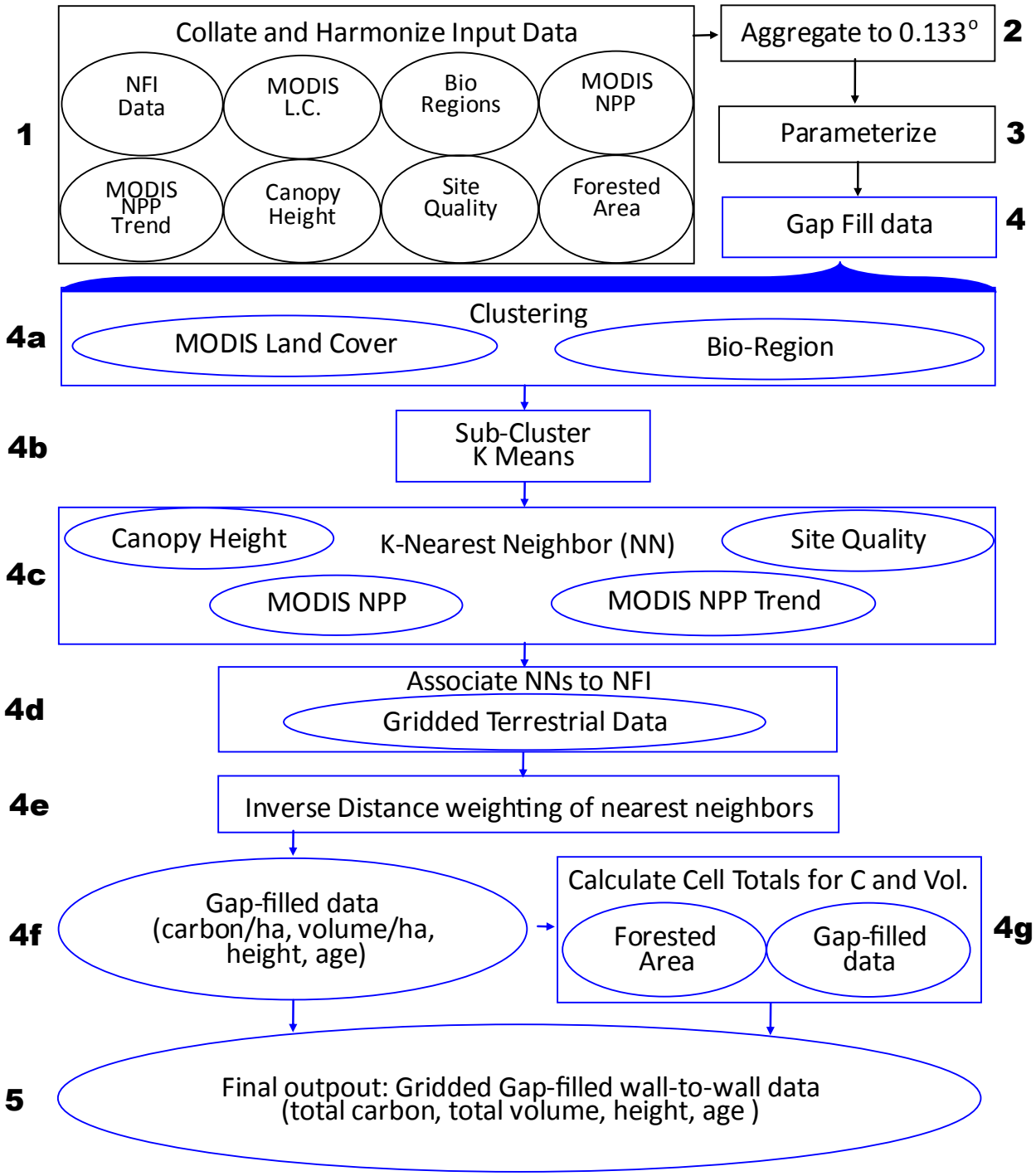

Figure 2: Algorithm Flow-Chart. There are 6 steps in the methodology: 1) Collate Input Data, 2) Data aggregation, 3) Parameterization, 4) Gap-filling, 5) Final outputs. Gap filling is shown in more detail with steps 4a to 4g. Ovals represent data sets and rectangles represent processes. Ovals inside rectangles indicate that this data set was used within this process.

4.7. Analyze the state of forest resources across Europe

Estimates on forest characteristics from this study were compared with several previously produced datasets and statistics. Combining carbon/hectare and volume/hectare estimates with forest area, country level carbon, and volume totals was carried out, which was then compared to FAO data. Age and height were also compared with jurisdictional-level statistics and a global data set, respectively.

Utilizing all of the data produced from this work, the effects forest management, climate and land-use change has on forest characteristics and structure, is being analyzed. The analysis of the impact forest management has had on forest productivity is being done by comparing NPP from areas inside and outside conservation zones. Beyond quantifying the absolute difference in NPP, the robustness of forests to climate anomalies was also analyzed. The effect land-use change has on NPP will be quantified by using NPP trended by climate and then assessing the relative difference from before and after land-use change. The climate limits set on forest structure will be quantified by assessing the maximum values of forest structures by various climate gradients, as quantified through cross-validation.

5. Analysis and Results

Assessing the current state of forest resources throughout Europe allows one to quantify the limits that climate has placed on forest structure, the impact forest management has throughout the continent and the affect land-use change has on productivity. To conduct such analyses one needs spatially explicit data on forest characteristics at a resolution finer than country borders. The previously available data in Europe on forest structure and climate either did not cover the entire continent, was not on an appropriate resolution for local level analysis, unavailable, or on a scale that did not maximize accuracy on the European scale. Therefore, before forest resources throughout Europe could be analyzed, forest structure and climate data necessary to achieve this goal, needed to be produced. Through achieving this goal a diverse assemblage of point and gridded data sets describing various aspects of forest ecosystems, e.g., climate, productivity, forest characteristics, etc. were collated and integrated. Methods and analyses which contribute to the scientific body of knowledge on climate, data integration and forest structure in Europe were also developed.

Climate gradients, such as orographic effects, were sought for analysis but were prohibited by the resolution of the previously available data sets. The downscaled climate data provides the ability to analyze such gradients and has increased accuracy compared to the existing European climate data in the three variables assessed: precipitation, minimum temperature and maximum temperature. After downscaling, the continental-scale distribution of precipitation and temperature values, and the accuracy at weather stations that were used in the derivation of the original E-OBS climate data, did not change. The increased accuracy in the downscaled data set is found primarily in the temperature variables (Figure 3) at weather stations that were not used in the derivation of the original E-OBS data set. Bias, mean absolute error (MAE) and root mean

squared error (RMSE) decrease for all variables when compared to the original E-OBS and analyzing against weather stations that were not used in the derivation of E-OBS. The most improvement is seen in temperature because the major benefit of the downscaling is incorporating elevation into the data set which has a larger impact on temperature than on precipitation.

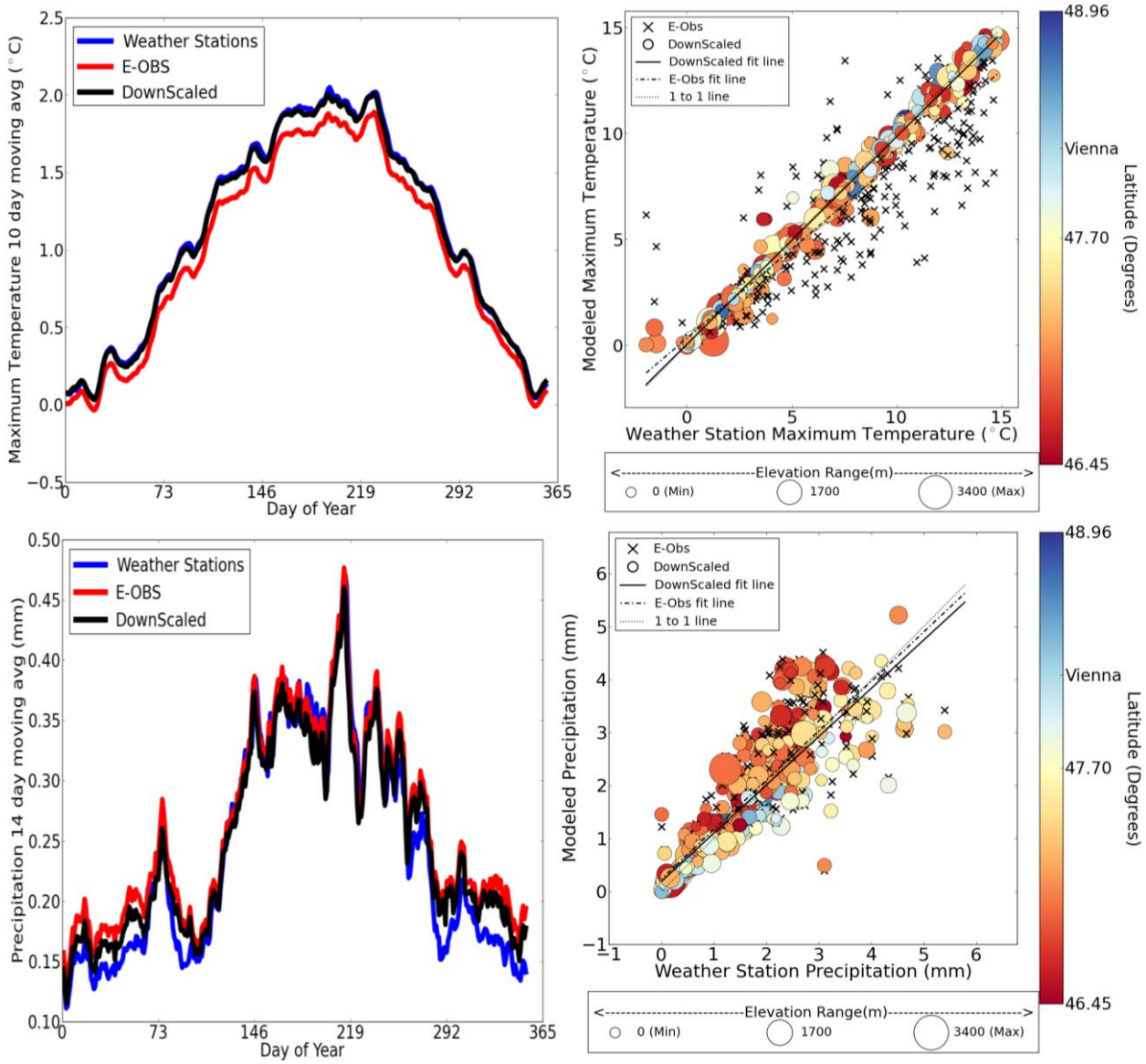

Figure 3: Validation of E-OBS and Downscaled data against weather station data from Austria. None of these stations were used to create E-OBS. Minimum Temperature, Maximum Temperature and Precipitation are shown. Left column gives daily averages for years 2000-2012 of all stations. Right column shows weather station data (x-axis) versus E-OBS and Downscaled data (y-axis). Size of downscaled points (circles) indicates the elevation of the station at that point. The color of the downscaled points indicates latitude of the corresponding weather station.

National forest inventories (NFI) provide information on forest characteristics that cannot currently be measured from space, e.g., age, basal area, branch biomass, etc. To spatially analyze forest characteristics across all of Europe such data is needed. Each country in Europe collects, archives, and distributes their own NFI data. To date, there has never been a data set that contains plot-level information for every European country. NFI data from 14 different countries throughout Europe was collated. The collated NFI data set spans all latitudes in Europe and all designated bioregions and is currently the largest plot-level NFI data set in Europe; though it does not cover the entire continent. To create a pan-European data set of forest characteristics, an algorithm was developed to gap fill areas where NFI data was not present.

A combination of clustering and nearest neighbor analysis was used to develop the gap filling algorithm. The algorithm incorporates data that covers all of Europe to delineate similar forests from areas where NFI data exists in the data set with areas where NFI data does not exist. Using these groups of similar forests, the algorithm could then gap fill NFI data all over Europe. To delineate groups of similar forests, the algorithm used six pan-European gridded data sets: Bioregion, covertype, canopy height, site quality, MODIS net primary production (NPP) and NPP trend.

Global NPP data is driven by a global climate data set that is on a 1.875° resolution (220x220km), which does not encapsulate local-level climate effects. To incorporate local-level effects into the NPP estimates, the downscaled climate data was used along with the MOD17 algorithm to derive new NPP estimates of European forests. A regionally-focused productivity estimate allows for more accurate delineations of forests for the purposes of gap filling NFI data into areas where NFI data was not present. The global MODIS NPP data set over-estimates compared to the NFI derived NPP data set by 26% of the NFI NPP mean (Figure 4). After using the newly downscaled climate data within the MOD17 algorithm, the difference between MODIS NPP and NFI NPP decreased to 7%. Only in Germany and Poland did the difference increase after using the new climate data.

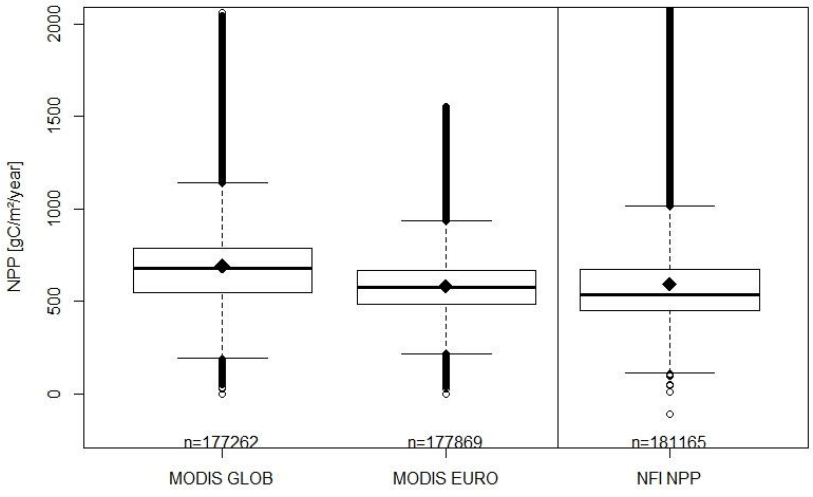

Figure 4: Decadal average (2000-2010) of European net primary production of the Global MODIS MOD17 data set (MODIS GLOB); the newly derived European focused MODIS MOD17 product (MODIS EURO); and the NFI derived NPP estimates (NFI NPP) on a 1km resolution.

After creating new NPP estimates of European forests and collating NFI data, it was then possible to integrate the array of remotely sensed gridded data with the ground based point NFI data. However, before proceeding with data integration, one common spatial resolution needed to be decided upon. Using the highest resolution of the remotely sensed data (1km^2) for data integration does not result in the maximum level of statistical confidence (Moreno, Neumann, and Hasenauer 2016a). The effect aggregation has on the integration of remotely sensed and point data was quantified to determine the appropriate resolution. Three factors were analyzed that determine the quality of combined NFI and gridded data at various aggregation steps: i) loss of spatial information; ii) agreement between remotely sensed and NFI data; and iii) the standard error of the underlying NFI data (Figure 5). The loss of spatial information steadily increases with aggregation, but asymptotes towards the large aggregation steps. The agreement between remotely sensed and NFI data hits a maximum at 0.0664° resolution. The standard error of the underlying NFI data decreases with aggregation. When these three factors are normalized and summed together, it is evident that the loss of spatial information is outpaced by the decrease in standard error and that the maxima in agreement creates an inflection point where there are diminishing benefits to aggregation. This gives statistical empirical justification that resolutions between 0.0664° and 0.266° produce the most accurate estimates on which to combine the NFI and remotely sensed data in Europe. For this reason, a resolution of 0.133° was chosen to integrate the remotely sensed and NFI data.

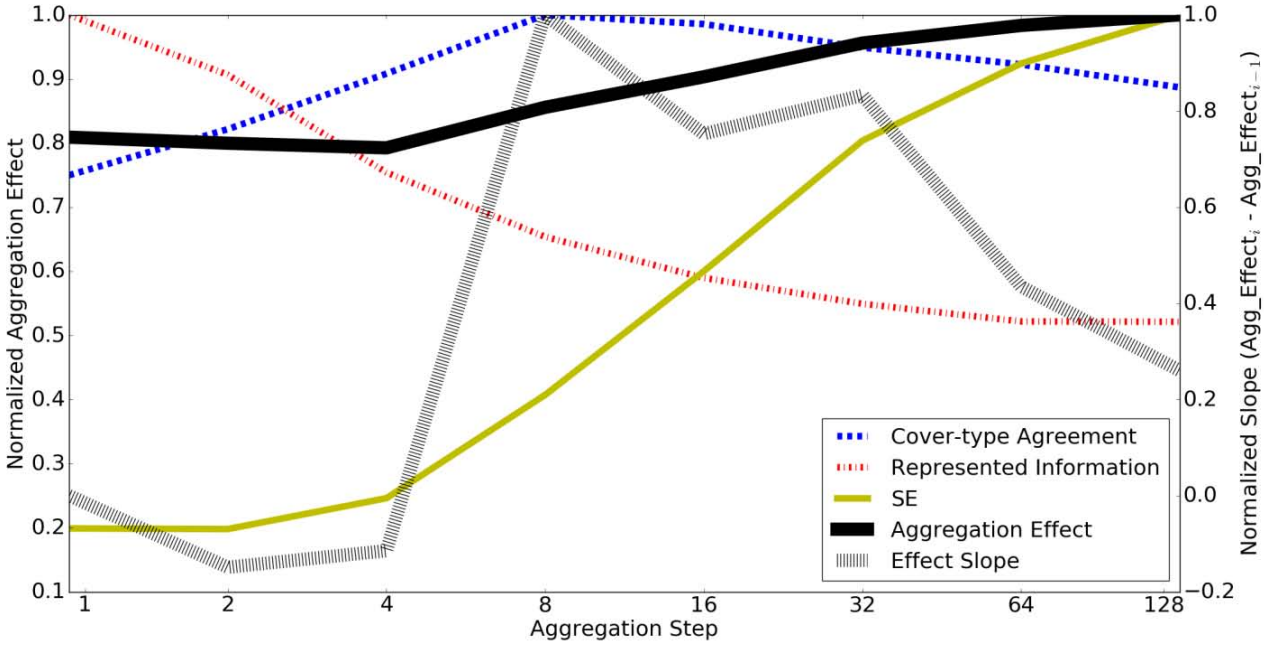

Figure 5: Three normalized effects of aggregation: Represented Information, Cover-type agreement, and the Standard Error (SE) of the underlying NFI data. Aggregation Effect is the normalized sum of the 3 curves. Effect Slope is the Aggregation Effect value minus the preceding Aggregation Effect value.

Using the optimized resolution with the newly produced MODIS NPP data, and other remotely sensed data products (MODIS LAI based growing season, SRad, VPD, and canopy height), NFI data was gap-filled into areas where NFI data was not present. The resulting data sets on which this study focuses are of 4 different forest characteristics: carbon/ha, volume/ha, age, and height (Figure 6). The error varies by forest characteristic and through space. Every data set has a bias of less than 1% from the mean NFI data value. The mean absolute errors of all 4 data sets, assessed through cross-validation, are smaller than the standard deviations of the NFI data, which means that the error associated with each cell is within the variation of the data. The high number of plots in lower elevations led to more accurate estimates, rather than at higher elevations. The pan-European data tends to underestimate at middle latitudes (48° to 58°) and overestimate in the south and north. The country with the highest underestimation in carbon and volume is the Czech Republic. Italy has the largest overestimation in height and Estonia has the highest overestimation in age. The newly produced data was then compared against previously produced datasets.

Carbon/ha values were combined with forest area data to compare total carbon estimates against those from FAO data (Figure 7). This comparison shows that using a combination of forest area data sets and the new data on carbon/ha creates a total European carbon stock of 11,003 million tons which is less than 10% over the FAO estimate of 10,093 million tons carbon. For countries where NFI data was present the difference is 5%.

Forest characteristics were then quantified across various gradients, e.g., latitude and elevation, which was hitherto not possible (Figure 8). Different forest characteristics were also combined to assess the state of forest resources using gradients that could not be done with the previous state of data availability. For example, using this analysis, it can be shown that elevation has a sinusoidal effect on carbon/ha, and the highest carbon/ha values found in the age class 60-80 years old, broadleaf and mixed forests, and in mid latitudes (Figure 8).

Forest resources can be quantified using data on forest characteristics, for example, carbon stocks, volume, age and height, and by fluxes (such as NPP). Using the data sets developed during this study that describe the state of forest resources across Europe, work has begun on analyzing the effect that forest management has had on carbon storage and NPP. This data is now being used to analyze the effect that land use change and drought has on NPP in Europe. The limitations climate gradients put on forest management and forest structure are also being examined (Figure 9). Preliminary results on the climate limitations on forest structure show that maximum stand densities vary greatly with temperature and precipitation. Maximum stand densities are less affected by cold climates than they are by hot climates. Maximum stand densities follow an overshoot curve when graphed against precipitation, with very low stand densities in dry regions and a maximum of approximately 4mm of average daily precipitation. Volume/ha has clear climactic zones associated with high and low values within the distinct climactic triangle area in Europe.

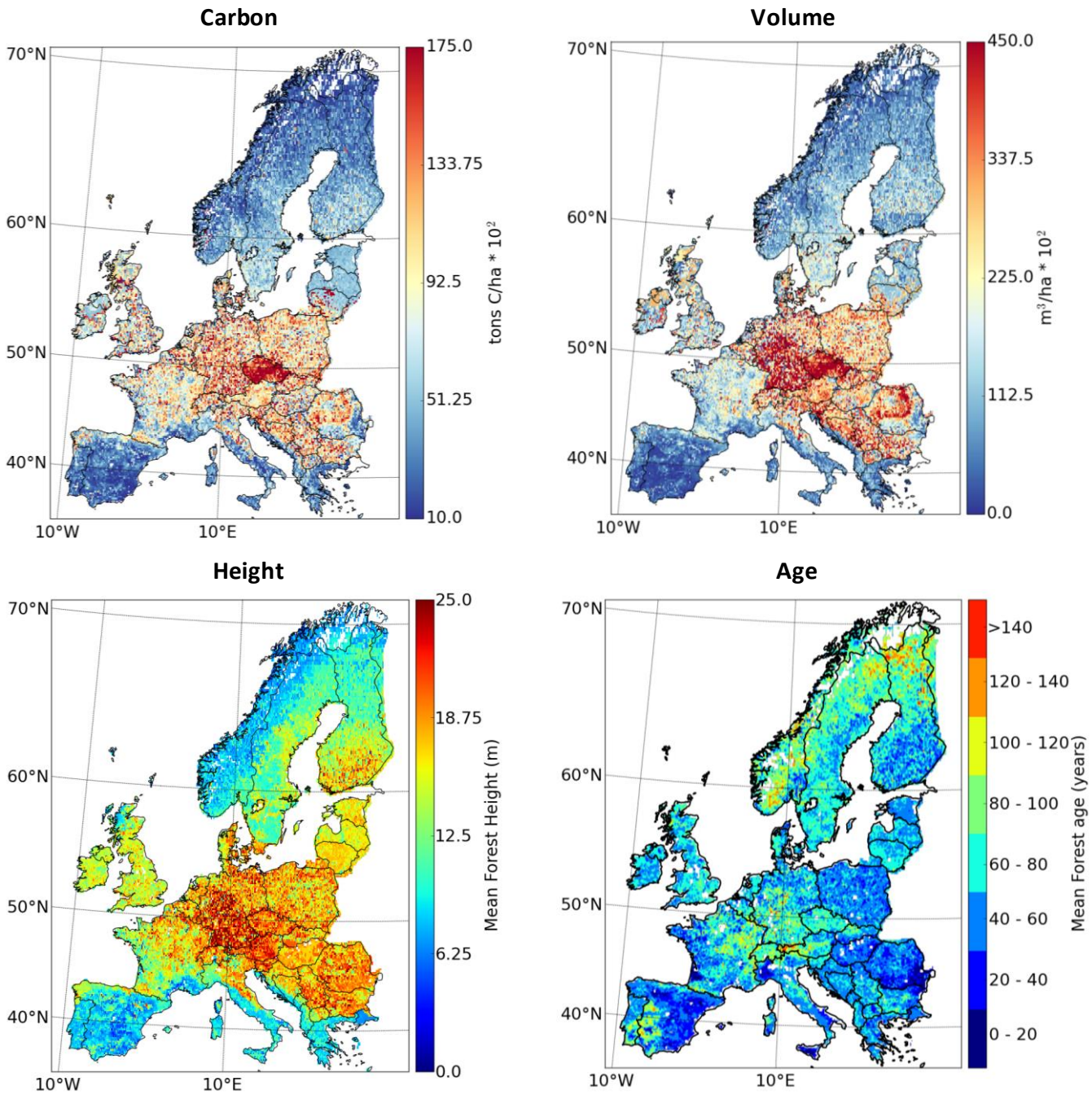

Figure 6: Total Live Tree Carbon / ha (tons C/ha*102), Volume/ha (m3/ha*102), Height (m), Mean tree age (age classes in years). 0.133° resolution. The total live tree carbon and total volume result from multiplying the c/ha and the m3/ha by the total number of hectares of forest within each cell respectively. Height and mean tree age are unaffected by forest area.

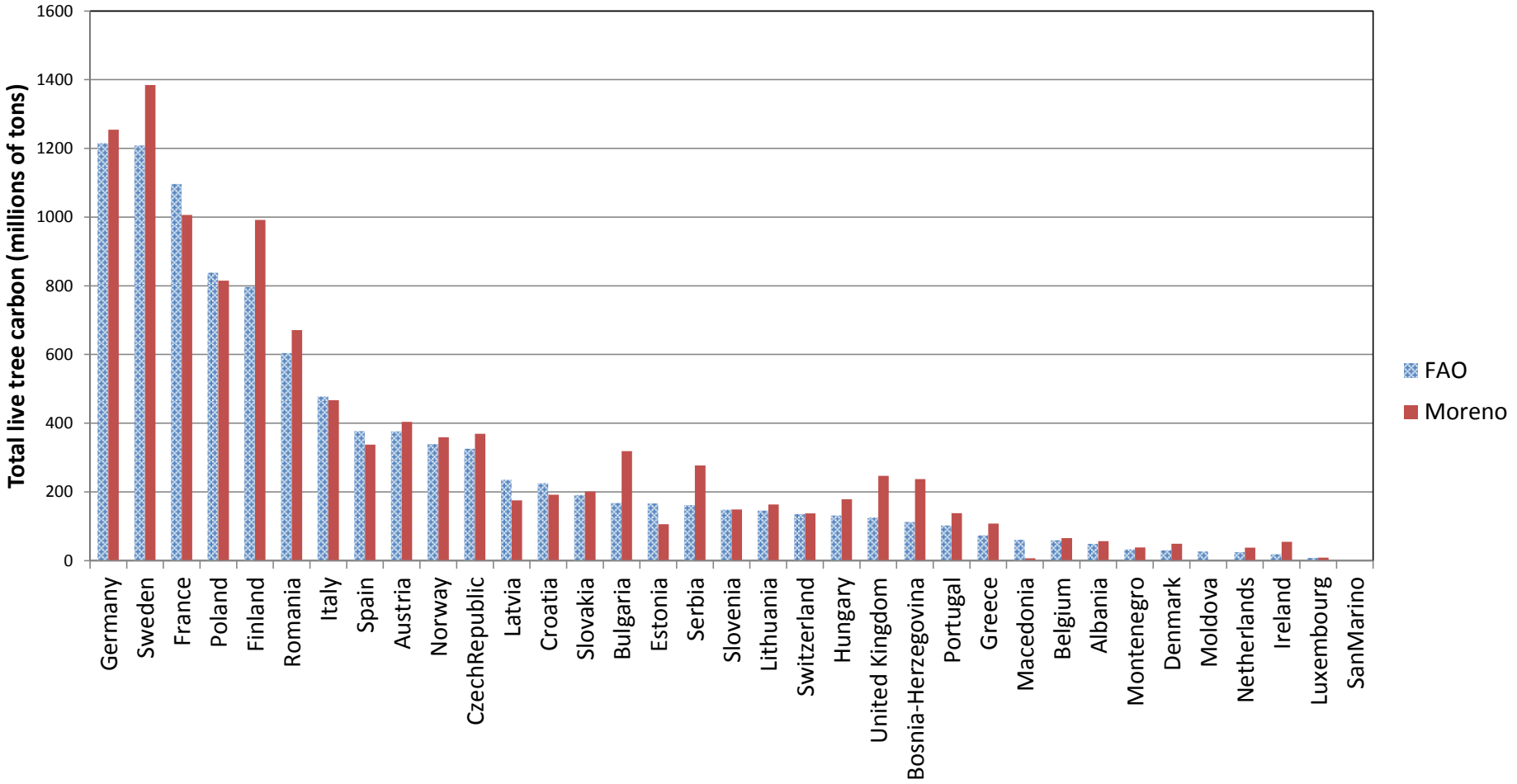

Figure 7: Total live tree carbon by country from the FAO and this study (Moreno)

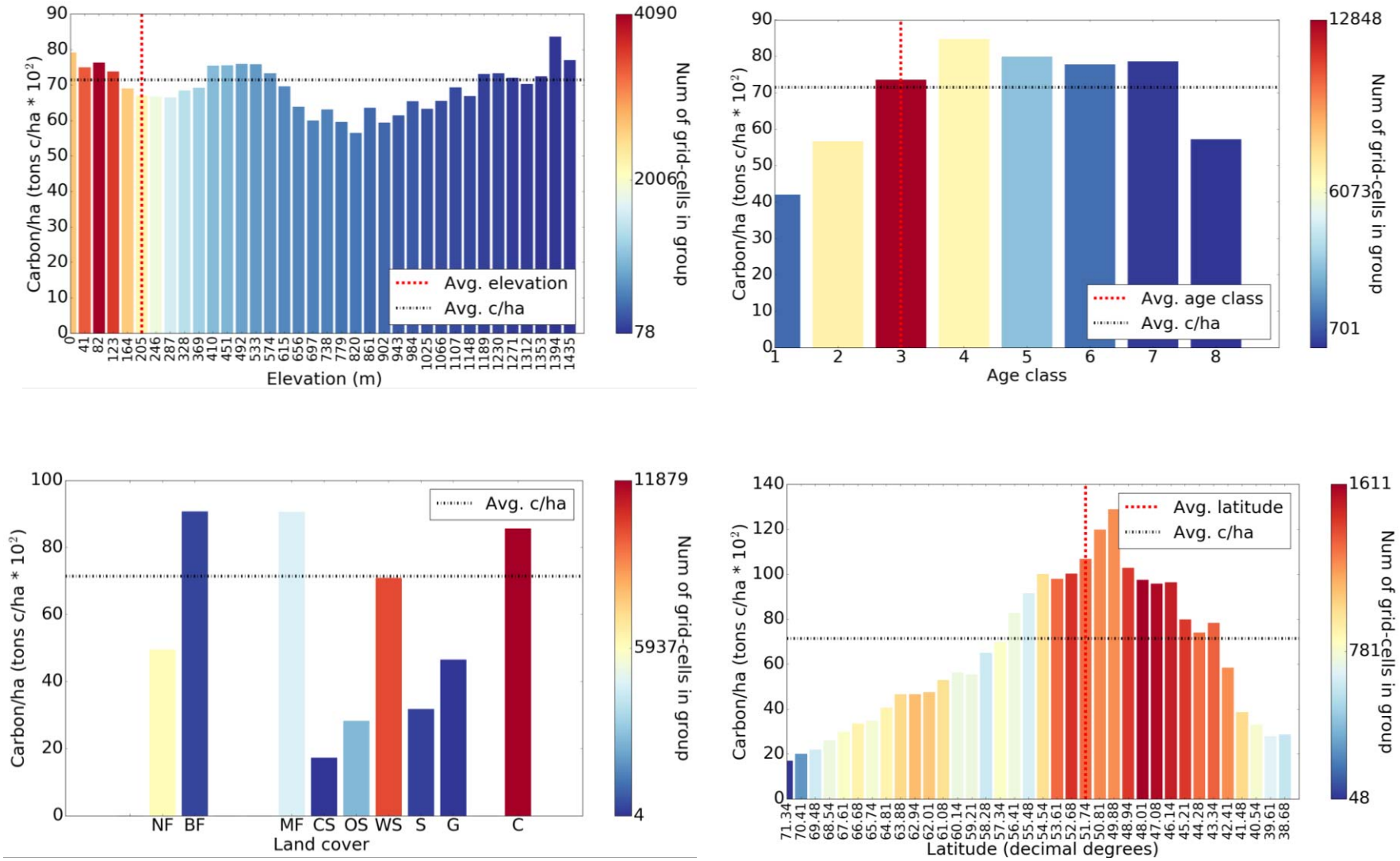

Figure 8: Live tree carbon/ha by elevation, age class, land cover type, and latitude. Color indicates the number of grid cells found in the group. Covertypes: NF – Needle leaf Forest, BF – Broad Leaf Forest, MF – Mixed Forest, CS – Closed shrublands, OS – Open shrublands, WS – Woody savannah, S – Savannah, G – Grassland, C – Crop lands. Age Classes: 1 – 1 to 20, 2 – 21 to 40, 3 – 41 to 60, 4 – 61 to 80, 5 – 81 to 100, 6 – 101 to 120, 7 – 121 to 140, 8 - >140.

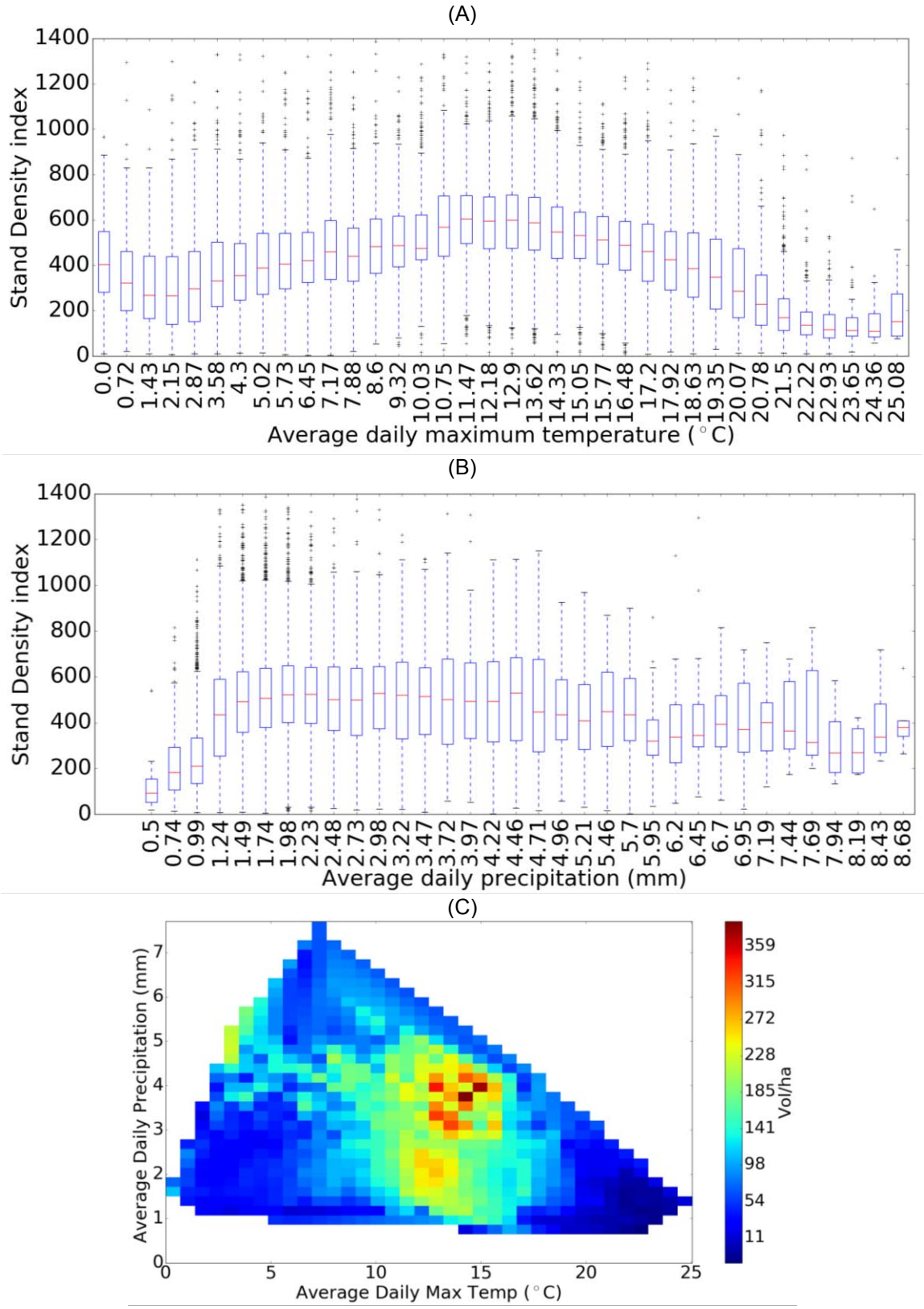

Figure 9: Climate limitations to forest management across Europe. A) Temperature vs. Stand Density Index. B) Precipitation vs. Stand Density Index. C) Precipitation and Temperature vs. Vol/ha.

6. Discussion

Spatial information allows for rapid assessment of forest characteristic values across political boundaries. For example, upon visual inspection, it is quickly evident that the Czech Republic has by far the highest reported carbon/ha values of any other country in Europe (Figure 6). Further, there is a distinct difference in volume/ha values when crossing the border between France and Germany. These differences could be real or an artifact of the NFI collection and reporting process; but this difference is easy to see and recognize when data is spatially displayed. These maps also make it easy to see that the average height of trees are highest throughout central Europe, and that the area with the oldest average tree ages are in western Austria and in the northern-most latitudes.

Comparing forest characteristics data from this study against other data sets give us the opportunity to identify discrepancies and possible errors. Using a combination of forest area maps, the carbon/ha values can come within 10% of FAO estimates (Figure 7). However, using just one forest area map will produce estimates of 20 - 25% greater than FAO estimates, with large differences from country to country. This indicates that the forest area data used has a large influence on derived carbon stock totals. In the FAO data, each country uses different information on forest area to calculate their individual totals. This makes it difficult to exactly replicate FAO data. However, comparing the new pan-European gridded data with FAO indicate that the NFI derived carbon/ha values from this study, in conjunction with the gap filling algorithm, can produce realistic results.

It is now possible to compare forest characteristics across different gradients (Figure 8). This kind of analysis shows how forests behave over the entire continent and how forest management has had an impact. For example, the age distribution throughout all of Europe matches the common rotation lengths implemented by forest managers with the majority of forests being 41-60 years old. After this age class, trees are typically harvested which results in less forests being 61-80 years old. If rotation lengths were extended, on average, by another 10-20 years, then Europe could store up to 12% more carbon/ha in their forests. The prevalence of Norway Spruce throughout Europe may be lowering the potential carbon storage of European forests, as needle leaf forests tend to contain less carbon/ha than broadleaf species. The high carbon/ha values in croplands indicate remnant forests that are preserved amongst agricultural systems, and reflect more of a conservation approach to forest management that can store high amounts of carbon/ha. The elevation effect on carbon/ha shows that there is a sinusoidal curve with several peaks and troughs. The cause behind this effect will require further investigation as it could be caused by ecology or management. Latitude appears to have a clear impact on carbon/ha, showing a strong ecological influence that climate and solar radiation place upon forest management.

Spatial information on forest resources and climate can be used to assess the various effects climate and forest management has on forests. Three different aspects of forests are being analyzed throughout Europe: forest management's impact on carbon stocks and fluxes, land-use change effect of productivity and climate's effect on forest structure and forest management options.

Studying forest management's impact on carbon stocks and fluxes will take advantage of all of the data that was created throughout this study. The gridded data on forest carbon will be used to estimate carbon stocks, and the new MODIS NPP values to estimate fluxes. These stocks and fluxes will then be detrended by the newly downscaled climate data, latitude and elevation to remove factors that influence carbon, but that forest management can not affect. This step isolates the forest management influence on carbon and carbon fluxes. Then the newly created pan-European data on other forest characteristics, e.g., age, diameter, and basal area, and locations of conserved forest areas, will be used to quantify the affect forest management has had on the carbon stocks and fluxes.

Land-use change is identified as one of the globe's primary anthropogenic carbon emission sources (West et al. 2004). The quantity of exactly how much carbon uptake is gained or lost in Europe through land-use change will be assessed. To accomplish this, the new European MODIS NPP will be detrended by the climate data and used along with CORINE land cover to assess how changes in land-use are affecting the vegetative landscapes' ability to sequester carbon.

Assessing climate's effect on forest structure and management options will utilize the climate data along with the gridded data on forest characteristics (Figure 9). Forests in Europe are under all levels of forest management intensity. By quantifying the variability and maximums of various forest characteristics that management can affect in climate space, the limits to forest management as dictated by climate can be quantified. This can then show how a changing climate could affect forest management options in the future and the limit forest management has to change forest structure under different climate regimes. Preliminary results indicate that climate clearly limits the maximum stand density that can exist on the landscape (Figure 9). Assuming that the data on stand density reflects all levels of forest management, including a close-to-natural management system, by focusing on the upper whiskers of the box plots the effect a particular climate variable can have on forest structure becomes evident. Temperature has a strong effect on stand density, especially towards the higher average maximum temperatures. Precipitation has an even stronger effect at both high and low daily precipitations. Clear climactic zones exist for high vol/ha values. These zones are on the border of European climate space. With the shape of European climate space uncertain under future climate change, especially in regards to precipitation, it is possible that the high vol/ha zone could lie outside Europe's future climate space. As temperature is expected to rise, Europe's climate space will move towards the bottom right of the triangle (Figure 9). This area starts to show the lowest vol/ha values in Europe. This means that the prospect of climate change currently leaves the future of forest management and timber supply in Europe unknown (Figure 9).

7. Conclusion

The new data sets derived through this study allow for analyses of forest resources across gradients that have in the past been limited to country-level assessments. Climate data is now on a resolution that allows the assessment of differences in topography, covertypes and land-uses. The climate data is also on the resolution required to improve remotely sensed estimates

of forest productivity, which was done by implementing the MOD17 algorithm with the downscaled climate data. To quantify the improvement of the NPP estimates, NFI data for 14 different European countries was collated and used to calculate NFI based NPP estimates. To derive forest characteristics across all of Europe, including those areas where NFI data was not present, the collated NFI data and remotely sensed data were combined within a clustering/nearest neighbor algorithm. However, a direct link cannot be used between NFI and remotely sensed data, because NFIs are point data and are provided with falsified locations and a remotely sensed cell covers an area at least 2 orders of magnitude larger than that of an NFI plot. Thus, the optimal resolution was quantified on which a statistically justifiable connection can be made between NFI and remote sensing data. Using all of the data produced, along with some additional remotely sensed data, and the optimal resolution for linking this data, an algorithm was developed which created new data on forest characteristics across Europe. These datasets allow for the large scale studies of forests, forest productivity and how they relate to climate all throughout Europe, which was not possible with the previous state of data accessibility in Europe.

The data on this resolution should be used to study landscape-scale ecosystems. That is to say, that with a resolution of 16x16km, the values per cell should not be interpreted in the same way as plot-level NFI data. Each cell represents average values for forests and should be interpreted with the forest area within a cell taken into account. For example, carbon/ha values may be high but the amount of forest per cell may result is low total carbon estimates. Also, age in this study indicates the average age of all trees, which leads to older age class values being found in savannahs and open shrub lands. Even though these cover types contain very few trees, on average, these trees are older than the average age of trees found in other cover types.

Empirical data can now be used to assess forests throughout Europe. The analyses that implement the data derived in this study can give a more accurate spatial depiction of the effect forest management has on the carbon cycle, the impact land-use has on the carbon sequestering ability of landscapes, and how climate influences forest structure throughout Europe.

Further, these data sets allow for quick and easy quality assessments of the data reported by different countries to larger overarching projects, such as FAO studies. The visual representation of the gridded data allows people to quickly see if there is reasonable justification for outlier values or if there is a possible error.

This work removes political borders and policy obstacles to furthering forest research throughout Europe. Understanding the spatial distribution of forest structure characteristics is vital for inferring the future of forest ecosystems that Europeans rely upon for their recreation, economy, food, and cultural heritage. Ecological principles do not obey political borders and country-level statistics are not sufficient for discovering unknown dynamics that are occurring throughout Europe, such as climate change, bark beetle outbreaks, persistent nitrogen deficiencies caused by CO_2 fertilization, reaction to landscape-level management policies, or the effect of large-scale nitrogen deposition. This work helps to make the hard work of these individual institutions relevant to topics that are larger than any one country and that affect all life in Europe and around the globe.

8. References

Brus, D. J., G. M. Hengeveld, D. J. J. Walvoort, P. W. Goedhart, a. H. Heidema, G. J. Nabuurs, and K. Gunia. 2011. “Statistical Mapping of Tree Species over Europe.” *European Journal of Forest Research* 131(1): 145–57. http://link.springer.com/10.1007/s10342-011-0513-5 (October 14, 2014).

Cramer, Wolfgang, Alberte Bondeau, F. Ian Woodward, I. Colin Prentice, Richard A. Betts, Victor Brovkin, Peter M. Cox, Veronica Fisher, Jonathan A. Foley, Andrew D. Friend, Chris Kucharik, Mark R. Lomas, Navin Ramankutty, Stephen Sitch, Benjamin Smith, Andrew White, and Christine Young-Molling. 2001. “Global Response of Terrestrial Ecosystem Structure and Function to CO2 and Climate Change: Results from Six Dynamic Global Vegetation Models.” *Global Change Biology* 7(4): 357–73.

Crowther, T. W., H. B. Glick, K. R. Covey, C. Bettigole, D. S. Maynard, S. M. Thomas, J. R. Smith, G. Hintler, M. C. Duguid, G. Amatulli, M.-N. Tuanmu, W. Jetz, C. Salas, C. Stam, D. Piotto, R. Tavani, S. Green, G. Bruce, S. J. Williams, S. K. Wiser, M. O. Huber, G. M. Hengeveld, G.-J. Nabuurs, E. Tikhonova, P. Borchardt, C.-F. Li, L. W. Powrie, M. Fischer, a. Hemp, J. Homeier, P. Cho, a. C. Vibrans, P. M. Umunay, S. L. Piao, C. W. Rowe, M. S. Ashton, P. R. Crane, and M. a. Bradford. 2015. “Mapping Tree Density at a Global Scale.” *Nature*. http://www.nature.com/doifinder/10.1038/nature14967.

Daily, Gretchen. C., Susan Alexander, Paul. R. Ehrlich, Larry Goulder, Jane Lubchenco, Pamela A. Matson, Harold A. Mooney, Sandra Postel, Stephen H. Schneider, David Tilman, and George. M. Woodwell. 1999. “Ecosystem Services: Benefits Supplied to Human Societies by Natural Ecosystems.” *Issues in Ecology* 4(4): 1–12.

Dong, J, R K Kaufmann, R B Myneni, C J Tucker, P E Kauppi, J Liski, W Buermann, V Alexeyev, and M K Hughes. 2003. “Remote Sensing Estimates of Boreal and Temperate Forest Woody Biomass: Carbon Pools, Sources, and Sinks.” *Remote Sensing of Environment* 84(3): 393–410.

Gallaun, Heinz, Giuliana Zanchi, Gert Jan Nabuurs, Geerten Hengeveld, Mathias Schardt, and Pieter J. Verkerk. 2010. “EU-Wide Maps of Growing Stock and above-Ground Biomass in Forests Based on Remote Sensing and Field Measurements.” *Forest Ecology and Management* 260(3): 252–61. http://dx.doi.org/10.1016/j.foreco.2009.10.011.

Hasenauer, Hubert, Richard Petritsch, Maosheng Zhao, Celine Boisvenue, and Steven W. Running. 2012. “Reconciling Satellite with Ground Data to Estimate Forest Productivity at National Scales.” *Forest Ecology and Management* 276: 196–208. http://dx.doi.org/10.1016/j.foreco.2012.03.022.

Kremen, Claire. 2005. “Managing Ecosystem Services: What Do We Need to Know about Their Ecology?” *Ecology Letters* 8(5): 468–79.

Maselli, F., M. Chiesi, M. Mura, M. Marchetti, P. Corona, and G. Chirici. 2014. “Combination of Optical and LiDAR Satellite Imagery with Forest Inventory Data to Improve Wall-to-Wall Assessment of Growing Stock in Italy.” *International Journal of Applied Earth Observation and Geoinformation* 26(1): 377–86.

Moreno, Adam, and Hubert Hasenauer. 2015. “Spatial Downscaling of European Climate Data.” *International Journal of Climatology*.

Moreno, Adam, Mathias Neumann, and Hubert Hasenauer. 2016a. “Optimal Resolution for Linking Remotely Sensed and Forest Inventory Data in Europe.” *Remote Sensing of Environment* 183: 109–19. http://dx.doi.org/10.1016/j.rse.2016.05.021.

Moreno, Adam, Mathias Neumann, and Hubert Hasenauer. 2016b. “The State of Forest Resources across Europe.” *Remote Sensing* In progres.

Naudts, Kim, Yiying Chen, Matthew J. McGrath, James Ryder, Aude Valade, Juliane Otto, and Sebastiaan Luyssaert. 2016. “Europe’s Forest Management Did Not Mitigate Climate Warming.” *Science* 351(6273): 597–601.

Neumann, Mathias, Adam Moreno, Volker Mues, Sanna Härkönen, Matteo Mura, Olivier Bouriaud, Mait Lang, Wouter M.J. Achten, Alain Thivolle-Cazat, Karol Bronisz, Ján Merganič, Mathieu Decuyper, Iciar Alberdi, Rasmus Astrup, Frits Mohren, and Hubert Hasenauer. 2016. “Comparison of Carbon Estimation Methods for European Forests.” *Forest Ecology and Management* 361: 397–420. http://linkinghub.elsevier.com/retrieve/pii/S0378112715006398.

Neumann, Mathias, Adam Moreno, Christopher Thurnher, Volker Mues, Sanna Härkönen, Matteo Mura, Olivier Bouriaud, Mait Lang, and Giuseppe Cardellini. 2016. “Creating a Regional MODIS Satellite-Driven Net Primary Production Dataset for European Forests.” *Remote Sensing*: 1–18.

Pan, Yude, Richard a Birdsey, Jingyun Fang, Richard Houghton, Pekka E Kauppi, Werner a Kurz, Oliver L Phillips, Anatoly Shvidenko, Simon L Lewis, Josep G Canadell, Philippe Ciais, Robert B Jackson, Stephen W Pacala, a David McGuire, Shilong Piao, Aapo Rautiainen, Stephen Sitch, and Daniel Hayes. 2011. “A Large and Persistent Carbon Sink in the World’s Forests.” *Science (New York, N.Y.)* 333(6045): 988–93.

Running, Steven W., Ramakrishna R. Nemani, Faith Ann Heinsch, Maosheng Zhao, Matt Reeves, and Hirofumi Hashimoto. 2004. “A Continuous Satellite-Derived Measure of Global Terrestrial Primary Production.” *BioScience* 54(6): 547.

Simard, Marc, Keqi Zhang, Victor H Rivera-monroy, Michael S Ross, Pablo L Ruiz, Edward Castañeda-moya, Robert R Twilley, and Ernesto Rodriguez. 2006. “Mapping Height and Biomass of Mangrove Forests in Everglades National Park with SRTM Elevation Data.” *Photogrammetric Engineering Remote Sensing* 72(3): 299–311. http://www.scopus.com/inward/record.url?eid=2-s2.0-33644677069&partnerID=40&md5=7b0d066e192f884cbe0c04a6129014e0.

United Nation’s Food and Agriculture Organization. 2015. NATIONS, FOOD AND AGRICULTURE ORGANIZATION OF THE UNITED Rome, 2015 *Global Forest Resources Assessment 2015: How Are the World’s Forests Changing?* http://www.fao.org/forestry/fra2005/en/.

Vilén, T., K. Gunia, P. J. Verkerk, R. Seidl, M. J. Schelhaas, M. Lindner, and V. Bellassen. 2012. “Reconstructed Forest Age Structure in Europe 1950-2010.” *Forest Ecology and Management* 286: 203–18.

West, Tristram O, Gregg Marland, Anthony W King, Wilfred M Post, Atul K Jain, and Kenneth Andrasko. 2004. “Carbon Management Response Curves: Estimates of Temporal Soil Carbon Dynamics.” *Environmental management* 33(4): 507–18.

9. Appendix

9.1. Paper 1

Moreno, A., Hasenauer, H., 2015. Spatial downscaling of European climate data. Int. J. Climatol.

INTERNATIONAL JOURNAL OF CLIMATOLOGY
Int. J. Climatol. (2015)
Published online in Wiley Online Library
(wileyonlinelibrary.com) DOI: 10.1002/joc.4436

RMetS
Royal Meteorological Society

Spatial downscaling of European climate data

Adam Moreno* and Hubert Hasenauer

Institute of Silviculture, University of Natural Resources and Life Sciences, Vienna, Austria

ABSTRACT: E-OBS(European Observations) is a gridded climate data set which contains maximum temperature, minimum temperature, and precipitation on a daily time step. The data can be as fine as 0.25° in resolution and extends over the entire European continent and parts of Africa and Asia. However, for studying regional or local climatic effects, a finer resolution would be more appropriate. A continental data set with resolution would allow research that is large in scale and still locally relevant. Until now, a climate data set with high spatial and temporal resolution has not existed for Europe. To fulfil this need, we produced a downscaled version of E-OBS, applying the delta method, which uses WorldClim climate surfaces to obtain a $0.008\overline{3}°$ (about 1×1 km) resolution climate data set on a daily time step covering the European Union. The new downscaled data set includes minimum and maximum temperature and precipitation for the years 1951–2012. It is analysed against weather station data from six countries: Norway, Germany, France, Italy, Austria, and Spain. Our analysis of the downscaled data set shows a reduction in the mean bias error of 3 °C for mean daily minimum temperature and of 4 °C for mean daily maximum temperature. Daily precipitation improved by 0.15 mm on average for all weather stations in the validation. The entire data set is freely and publically available at ftp://palantir.boku.ac.at/Public/ClimateData.

KEY WORDS temperature; precipitation; climate; Europe; downscaling; E-OBS; elevation; WorldClim

Received 17 March 2015; Revised 5 June 2015; Accepted 8 June 2015

1. Introduction

Climate data are essential for understanding and modelling many ecological processes (VEMAP Members, 1995; Haylock *et al.*, 2008; Waring and Running, 2010). Gridded climate data provide information for every point across a landscape. These gridded data sets are essential for performing climate analyses, understanding biogeochemical processes, and for use in conjunction with satellite data and models.

Nearly 20 years ago, the first daily large-scale, fine-resolution climate data sets of the entire United States became available with the development of PRISM and Daymet with 1×10 km and 500×500 m resolutions respectively; both were limited by the digital elevation model resolution (Daly *et al.*, 1994; Thornton *et al.*, 1997). The availability of high-resolution, large-scale climate data sets has enabled more detailed studies of the climate's impact on epidemiology, ecology, agriculture, and genetics across United States (Guo *et al.*, 2006; Wimberly *et al.*, 2008; Luedeling *et al.*, 2009; Jay *et al.*, 2012). Large-scale, fine-resolution climate data sets in the United States are possible because of the easy accessibility policies to weather station data. Researchers studying Europe have been limited by the current state of climate data policy.

The absence of a comprehensive European weather network, a result of the continents administrative and cultural heterogeneity, makes obtaining weather station data very difficult and costly. European weather stations lack the density needed for daily interpolations to be made at high resolution and at regional-scales (Wijngaard *et al.*, 2003; Daly, 2006). Compounding the problem of data accessibility for climate interpolation throughout Europe, the quantity, quality, accessibility, and format of weather data varies from country to country (Wijngaard *et al.*, 2003). Many countries or geographic regions in Europe have their own locally produced interpolated gridded climate data sets that were possible because of access to the local weather station data network (Hofstra *et al.*, 2009; Isotta *et al.*, 2014; Masson and Frei, 2015). These data sets however use different methods and assumptions making harmonization difficult to obtain a single continental data set.

The ENSEMBLES group runs the European Climate Assessment & Data set (ECA&D) project which has gathered 7852 weather stations. Using this weather station network, they developed an interpolated gridded climate data set. This data set, referred to as European Observations (E-OBS), covers Europe on a daily time step (Haylock *et al.*, 2008). The resolution of the E-OBS data set is on a 0.25° regular grid (approximately 30×30 km). The coarseness of the gridded data is a result of station density limitations but is sufficient for studies performed at continental scale.

For studying orographic effects on climate, performing regional climate change analysis, and providing knowledge of spatial and temporal climate dynamics to users, it is essential to have high-resolution information (Frei and Schaer, 1998). Climate data at continental scales in high

* Correspondence to: A. Moreno, Institute of Silviculture, University of Natural Resources and Life Sciences, Vienna, Peter Jordan Straße 82, A-1190 Vienna, Austria. E-mail: adam.moreno@boku.ac.at

resolution allow large-scale research efforts to provide insights which are locally relevant. A 1×1 km resolution data set permits more accurate simulations of carbon and water fluxes than the currently available 50×50 km or 10×10 km resolutions climate data sets (Turner *et al.*, 1996). Researchers with the ability to address fine scale issues while maintaining a large spatial outlook may better assist managers in decision making by providing information about processes on both local and landscape scales (Turner *et al.*, 1996; Seidl *et al.*, 2013). Furthermore, climate data at a resolution of 1×1 km ($0.008\overline{3}°$ or 30 arc seconds) can be used in conjunction with remote sensing products such as Moderate Resolution Imaging Spectroradiometer (MODIS) gross primary production and net primary production products that require such data for their processing algorithms (Zhao *et al.*, 2005). Therefore having a climate data set at a 1×1 km resolution combined with other data sets or algorithms provides a better understanding of the spatio–temporal complexities of European landscapes at various scales.

In Europe, scientists are forced to focus either on individual countries or regions using national data sets (Hasenauer *et al.*, 2003; Venäläinen *et al.*, 2005; Maselli *et al.*, 2012). Another common way to study climate on larger scales in Europe is to use point data, from weather stations or flux towers, as representive of larger areas (Janssens *et al.*, 2001; Ciais *et al.*, 2005). In addition, research performed at larger scales with low-resolution data lack the ability to analyse local level climate effects (Lorenz *et al.*, 2012; Hawkins *et al.*, 2013). However, to compare climate data from multiple regions of Europe, some sort of harmonization is required. The aforementioned data can prevent discrepancies between country boundries that result from different methodologies and weather station networks. A unified data set, covering the entirety of Europe, while maintaining fine-resolution information would reduce errors, uncertainty, and inconsistencies.

The aim of this study is to advance the current scientific understanding of both local level processeses and landscape level dynamics by developing a Pan-European high-resolution climate data set. A lack of accessibility to primary data collected from weather stations prevents direct interpolation of a gridded data set with a resolution of 1×1 km on a European scale. This limitation makes downscaling previously interpolated climate data the only option to create high-resolution data for all of Europe. The objective of this study is to downscale the E-OBS data set using WorldClim data (Hijmans *et al.*, 2005). We produced a new downscaled climate data set which covers the European continent. It includes daily minimum and maximum temperature and precipitation at a $0.008\overline{3}°$ (approximately 1×1 km) resolution for the years 1950–2012. To reach our objective we

1. Create an algorithm to downscale E-OBS data using WorldClim data.
2. Evaluate random variation and/or error resulting from the downscaling algorithm.
3. Validate the downscaled results against weather station data not used in the original E-OBS interpolation.

2. Data

Two data sets were used in the downscaling process: E-OBS version 8.0 at 0.25° resolution (approximately 30 km) obtained on 25 April 2013 and WorldClim version 1.4 release 3 at a $0.008\overline{3}°$ resolution (approximately 1 km) obtained on 22 February 2013.

2.1. European Observations

E-OBS is an interpolated gridded daily climate data set that covers all of Europe, including portions of Russia, Asia, and Africa from 1950 to the present (Haylock *et al.*, 2008). Several parameters are included in this data set: daily mean temperature, maximum temperature, minimum temperature, precipitation, and sea level pressure. These data are available on various resolutions including on a regular grid with 0.25° and 0.5° resolutions

The E-OBS data set was created using a hybrid approach of Kriging and a thin-plate spline (Journal and Huijbregts, 1978; Haylock *et al.*, 2008). The authors of E-OBS first generated monthly means using the spline technique. Kriging was used to interpolate daily differences from the monthly mean. This difference was then applied to the monthly mean to obtain a daily value. E-OBS used 7852 weather stations throughout Europe for the release used in this study. Only 61% of which were publicly available to others outside the ENSEMBLE group. E-OBS has an uneven underlying weather station density across Europe which creates areas of high and low uncertainty (Haylock *et al.*, 2008).

2.2. WorldClim

WorldClim is a set of climate surfaces designed to provide long-term monthly averages of several climate variables (Hijmans *et al.,* 2005). Every cell has 12 values for each parameter, one value for each month. These values are the monthly means over the entire time period that was available for interpolation. WorldClim monthly mean variables include minimum and maximum temperature, precipitation, and 19 derived bioclimatic variables, which were not used in our study. WorldClim data are available at a $0.008\overline{3}°$ resolution globally.

WorldClim is developed using ANUSPLIN (Hutchinson, 2004), a thin-plate smoothing spline procedure as described in Hutchinson (Hutchinson, 1995). Hijmans *et al.* (2005), the developers of WorldClim, obtained input data from various sources globally consisting of 47 554 weather stations. In addition to climate data, they use two different digital elevation models (DEM) for interpolation. The two DEMs used were the Shuttle Radar Topography Mission (SRTM) (Farr *et al.*, 2007) and the GTOPO30 from the United States Geological Survey (USGS). Several problems exist associated with the input data sets. First, the authors of WorldClim note that there were problems matching weather station elevation with

DEM elevation; many times they simply did not match. Second – and relevant to our study – the authors explicitly note that obtaining weather station data in Europe was difficult. Finally, precipitation uncertainty is higher in mountainous regions. Many studies use WorldClim data to study ecosystems in areas with a lack of climate data (Nekola and Brown, 2007; Peterson and Nakazawa, 2007; Peterson *et al.*, 2007; Hawkins, 2010). Studies have found the accuracy of WorldClim data varies seasonally (Ezzine *et al.*, 2014).

3. Methods

3.1. Downscaling procedure

The conceptual framework is to use the fine-resolution WorldClim data to adjust the course resolution E-OBS cells to obtain our desired 1×1 km resolution daily. We applied a spatial delta method with a monotone cubic interpolation of anomalies (Mote and Salathe, 2010; Mosier *et al.*, 2014).

Columns 118–298 and rows 16–163 of the original E-OBS gridded data were downscaled due to data storage and computation limitations. The latitude and longitude of the upper left corner are 71.33°N, 10.833°W and the lower right hand corner are 34.583°N, 34.2499°E.

We used the delta method for downscaling, similar to the Piecewise Cubic Hermite Interpolating Polynomials (PCHIP) method described in Mosier *et al.* (Mosier *et al.*, 2014). This method uses climate data sets at different spatio–temporal resolutions to derive a new data set with a desired spatio–temporal resolution. This specific method is essentially a monotone cubic interpolation that varies the calculation of anomalies based on whether we are calculating temperature or precipitation.

To begin downscaling, in step 1, we upscaled the WorldClim data to the E-OBS resolution of 30×30 km (Figure 1). We averaged the WorldClim cells within each 30×30 km area for upscaling.

In step 2, we calculated the difference between the upscaled WorldClim cell and the E-OBS cell (Figure 1). The calculations in our algorithm for temperature are different than those for precipitation (Equations (1) and (2)). The difference in calculations was to prevent negative precipitation values which can occur with a simple subtraction:

$$\mathrm{d}T = \mathrm{WC} - E \tag{1}$$

$$\mathrm{d}P = E/\mathrm{WC} \tag{2}$$

where $\mathrm{d}T$ is the difference for temperature, $\mathrm{d}P$ is the difference for precipitation, WC is the upscaled WorldClim value, and E is the E-OBS value.

In step 3, we step through each cell of the WorldClim gridded data, one at a time, retrieving the value of the cell which was then be used in step 5 (Figure 1). This location was also found on the 30×30 km difference cells. Note that WorldClim data are given on monthly time steps and all calculations used the appropriate month's data.

During step 4, we calculated the weighted difference of the selected 30×30 km cell and that of the three adjacent 30×30 km cells (Figure 1). These four differences were weighted by the distance from the downscaling point to each 30×30 km cell. We then summed the weighted differences for the final difference value. If the downscaling point was in the centre of an E-OBS cell, then it is influenced only by that cell. If the downscaling point was located in a cell corner, then it was influenced almost equally by all four different cells. This avoided artificial delineations when moving from one E-OBS cell to another.

In step 5, we calculated the final downscaled value using the original WorldClim value and the summed inverse distance-weighted difference value from step 4 (Figure 1). The formulas for final downscaled cell values are

$$\mathrm{v}T = \mathrm{wc} - \mathrm{d}F \tag{3}$$

$$\mathrm{v}P = \mathrm{wc} \times \mathrm{d}F \tag{4}$$

where $\mathrm{v}T$ is the final downscaled cell value for daily temperature, $\mathrm{v}P$ is the final cell value for daily precipitation, $\mathrm{d}F$ is the sum of the weighted differences, and wc is the original 1×1 km WorldClim value.

3.2. Evaluation method

Evaluation of the downscaled and E-OBS data was performed to ensure that no added random variation or increased error occurred from the downscaling procedure. The evaluation compared weather station data used to create the original E-OBS with the corresponding grid point in our downscaled data and E-OBS data with (Table 1).

All statistics from Willmott and Matsuura (Willmott and Matsuura, 2006) were calculated for both E-OBS and the downscaled data sets (derived data) *versus* the corresponding weather station data. We calculate the mean ($\bar{x}$), the minimum, and maximum values of all three data sets. For E-OBS and the downscaled data, we calculate the mean biased error (MBE) which equals the mean difference between the derived data sets and the weather stations; this value represents the overall bias in the data set. The mean absolute error (MAE) is the mean absolute residual between the derived and weather station data; this value represents the mean residual – whether above or below – between the derived and the weather station data. The root mean square error (RMSE) is the square root of the mean squared residual between the weather station values and the derived values; this value is similar to the MAE except that it is more sensitive to outliers in the residuals. The squared Pearson's correlation coefficient (R^2) is the measure of the linear relationship between two data sets. In addition to the Willmott and Matsuura (2006) statistics, we calculated the linear error in probability space (LEPS) and the critical success index (CSI) as calculated in Hofstra *et al.* (Hofstra *et al.*, 2008). The LEPS is calculated as such:

$$\mathrm{LEPS} = \frac{\left|P_{\mathrm{v}} - 0.5\right| - \left|P_{\mathrm{f}} - P_{\mathrm{v}}\right|}{0.25} \tag{5}$$

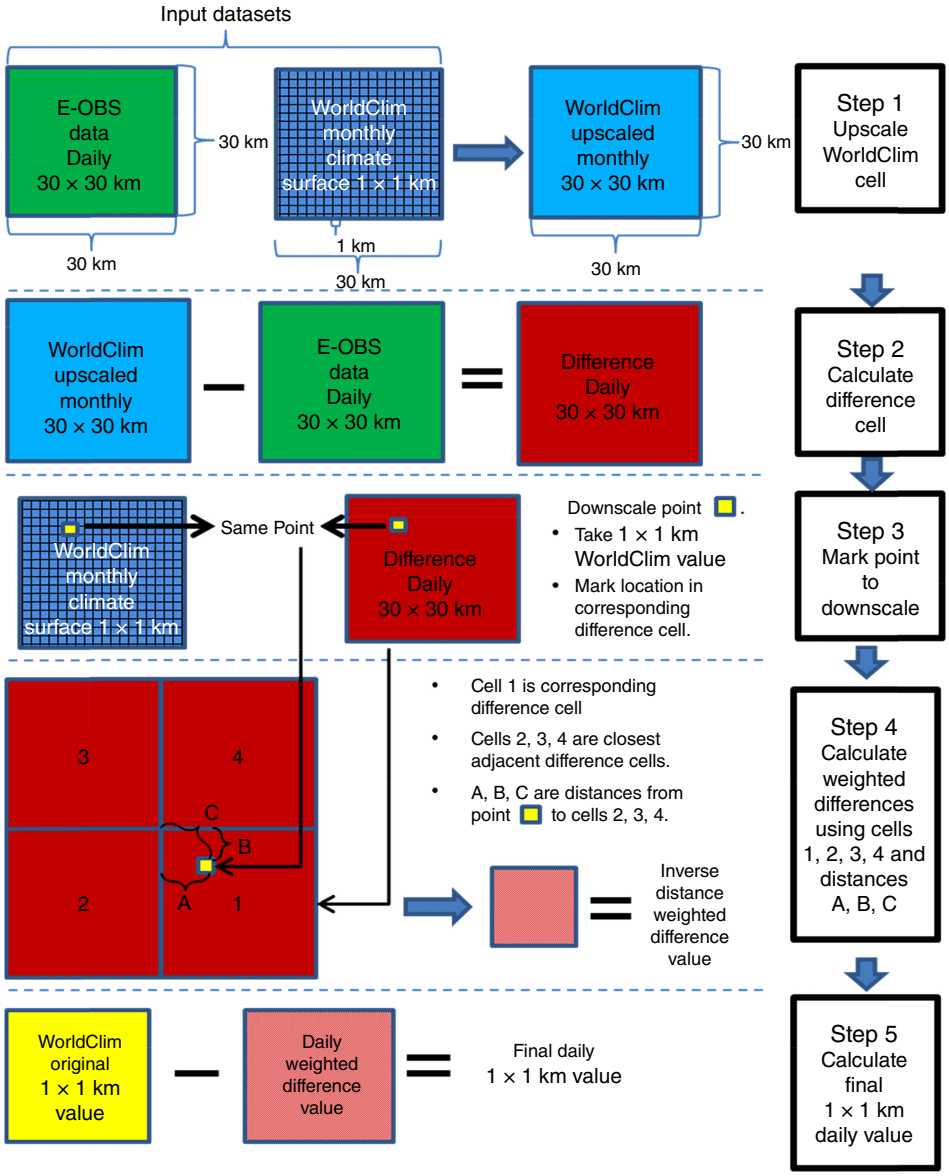

Figure 1. Methodology flow diagram for the delta downscaling algorithm.

where P_v is the probability of occurrence of the weather station value in the weather station data's cumulative distribution function (CDF). P_f is the probability of occurrence of the derived data value in the weather station data's CDF. This particular LEPS equation gives values from −1 (no skill) to 1 (prefect skill). A 0 value is given if the median value (probability = 0.5) of the weather station data is given as a derived value on every data point. The benefit of using LEPS is that calculating error in probability space gives better scores to derived values that come close to extreme observed values and worse scores to derived value that do not accurately predict median values. LEPS requires a normal distribution – because in the precipitation (Prcp) CDF 0 is both an extreme value and close to the median value – which is not present in the precipitation data set, therefore we did not provide an LEPS value for precipitation. For precipitation, we calculated the CSI which measures the success of the derived data sets in capturing rain days. CSI is calculated as such:

$$\mathrm{CSI} = \frac{\text{hits}}{\text{hits} + \text{misses} + \text{false alarms}} \tag{6}$$

where hits represent the number of days when rain was observed in the weather station data and predicted in the derived data. Misses are the number of days when rain was observed but not predicted, and false alarms are the number of days when rain was predicted but not observed. For all variables, we also calculated the CSI for extreme high and extreme low values. Where extreme high values are defined as those values above the 95th percentile of the weather station CDF and extreme low values are those values below the 5th percentile of the weather station data. A value of 1 means perfect skill and 0 means no skill.

We used weather station data from Norway, Italy, Germany, France, and Spain. The weather station data were obtained from the E-OBS website and cover the

Table 1. Evaluation/validation results of original E-OBS and the downscaled data *versus* weather station data.

			Weather station	E-OBS						Downscaled						
			$\bar{x}$(min, max)	$\bar{x}$(min, max)	MBE (MAE)	RMSE	R^2	LEPS	CSI (low, high)	$\bar{x}$(min, max)	MBE (MAE)	RMSE	R^2	LEPS	CSI (low, high)	# Stations
Validation	Austria	T_{min} (°C)	3.8 (−30.8, 26.1)	3.1 (−25.9, 23.2)	−0.6 (2.5)	3.2	0.72	0.65	NA (0.46, 0.31)	3.98 (−25.2, 23.4)	0.2 (2.2)	2.8	0.89	0.7	NA (0.47, 0.41)	434
		T_{max} (°C)	13.1 (−26.1, 39.5)	11.7 (−20.7, 38.4)	−1.4 (3.4)	4.5	0.82	0.61	NA (0.39, 0.29)	12.92 (−20.9, 38.7)	−0.2 (2.4)	3.2	0.99	0.74	NA (0.51, 0.46)	434
		Prcp (mm)	2.9 (0, 1099.8)	3.1 (0.0, 166)	0.3 (3.4)	7.9	0.75	NA	0.54 (0.61, 0.12)	2.95 (0.0, 159.4)	0.1 (3.3)	7.7	0.77	NA	0.51 (0.6, 0.16)	449
Evaluation	Norway	T_{min} (°C)	−1.3 (−84, 31)	−2.2 (−50.9, 19.3)	−1.0(1.7)	2.1	0.95	0.80	NA (0.74, 0.36)	−1.5 (−50, 20.8)	−0.2 (1.5)	2.0	0.90	0.83	NA (0.71, 0.54)	17
		T_{max} (°C)	9.3 (−21, 34.2)	8.4 (−23.7, 32.5)	−0.9 (2.0)	2.2	0.99	0.75	NA (0.59, 0.48)	8.2 (−23.8, 31.7)	−1.1 (1.6)	1.8	0.93	0.81	NA (0.66, 0.58)	4
		Prcp (mm)	3.2 (0, 99.6)	3.3 (0.0, 104.3)	0.1 (1.1)	2.7	0.91	NA	0.80 (0.80, 0.53)	3.3 (0.0, 113.1)	0.1 (1.1)	2.5	0.92	NA	0.80 (0.79, 0.64)	55
	Germany	T_{min} (°C)	4.4 (−32.8, 85.8)	4.6 (−29.7, 23.3)	0.2 (1.1)	1.9	0.70	0.84	NA (0.65, 0.61)	4.6 (−30.2, 22.7)	0.2 (1.1)	2.0	0.84	0.84	NA (0.65, 0.68)	47
		T_{max} (°C)	12.4 (−28.9, 74.8)	13.0 (−21.0, 39.3)	0.6 (1.2)	2.4	0.66	0.86	NA (0.57, 0.73)	12.9 (−22.0, 39.3)	0.5 (1.2)	2.6	0.64	0.85	NA (0.56, 0.79)	47
		Prcp (mm)	2.3 (0, 99.4)	2.1 (0.0, 97.2)	−0.2 (0.9)	2.4	0.81	NA	0.80 (0.82, 0.48)	2.1 (0.0, 95.0)	−0.2 (0.8)	2.3	0.88	NA	0.82 (0.82, 0.56)	46
	France	T_{min} (°C)	7.7 (−39.8, 27.6)	7.2 (−22.0, 25)	−0.5 (1.1)	1.8	0.65	0.80	NA (0.64, 0.62)	7.2 (−21.6, 25.6)	−0.5 (1.1)	1.7	0.74	0.81	NA (0.68, 0.68)	23
		T_{max} (°C)	16.1 (−22.8, 41.9)	16.0 (−14.9, 40.6)	−0.1 (1.1)	1.9	0.71	0.86	NA (0.67, 0.68)	16.0 (−15.7, 40.9)	−0.1 (0.9)	1.9	0.91	0.88	NA (0.72, 0.76)	24
		Prcp (mm)	2.1 (0, 99.0)	1.9 (0.0, 119.5)	−0.2 (1.0)	3.1	0.62	NA	0.74 (0.82, 0.47)	1.9 (0.0, 117.1)	−0.2 (1.0)	3.1	0.80	NA	0.73 (0.81, 0.54)	18
	Spain	T_{min} (°C)	9.5 (−21.0, 30.5)	8.8 (−19.6, 26.7)	−0.7 (2.7)	3.6	0.09	0.51	NA (0.29, 0.26)	8.6 (−22.5, 25.6)	−0.9 (3.1)	4.1	0.03	0.45	NA (0.24, 0.31)	16
		T_{max} (°C)	19.6 (−8.2, 47.2)	18.9 (−13.7, 47.3)	−0.7 (3.1)	4.1	0.87	0.54	NA (0.36, 0.19)	18.8 (−17.2, 47.0)	−0.8 (3.2)	4.4	0.78	0.53	NA (0.33, 0.27)	38
		Prcp (mm)	2.1 (0, 99.8)	1.6 (0.0, 133.6)	−0.4 (2.4)	6.5	0.12	NA	0.40 (0.70, 0.11)	1.7 (0.0, 164.4)	−0.4 (2.4)	6.6	0.06	NA	0.42 (0.70, 0.14)	18
	Italy	T_{min} (°C)	6.3 (−24.3, 45.1)	8.2 (−18.0, 27.8)	1.9 (2.4)	3.5	0.96	0.69	NA (0.20, 0.74)	7.6 (−20.1, 28.1)	1.3 (1.9)	3.0	0.89	0.76	NA (0.34, 0.79)	5
		T_{max} (°C)	13.8 (−20.6, 44.4)	17.1 (−10.6, 41.2)	3.3 (3.7)	5.7	0.93	0.60	NA (0.05, 0.79)	16.2 (−14.0, 40.9)	2.5 (2.8)	5.0	0.74	0.69	NA (0.19, 0.79)	5
		Prcp (mm)	1.7 (0, 99.8)	2.4 (0.0, 178.0)	0.7 (1.8)	6.2	0.01	NA	0.62 (0.82, 0.26)	2.2 (0.0, 143.6)	0.5 (1.7)	5.4	0.00	NA	0.62 (0.81, 0.39)	8
All evaluation stations		T_{min} (°C)	5.0 (−84.0, 85.8)	4.9 (−50.9, 27.8)	−0.2 (1.5)	2.2	0.91	0.77	NA (0.56, 0.50)	4.9 (−50.0, 28.1)	−0.1 (1.5)	2.3	0.90	0.77	NA (0.55, 0.59)	108
		T_{max} (°C)	15.4 (−28.9, 74.8)	15.5 (−23.7, 47.3)	0.1 (1.9)	3.0	0.87	0.76	NA (0.49, 0.53)	15.4 (−23.8, 47.0)	0.0 (1.9)	3.1	0.85	0.76	NA (0.49, 0.61)	118
		Prcp (mm)	2.6 (0.0, 99.8)	2.5 (0.0, 178.0)	−0.1 (1.2)	3.3	0.88	NA	0.75 (0.80, 0.42)	2.5 (0.0, 164.4)	−0.1 (1.2)	3.2	0.90	NA	0.75 (0.79, 0.52)	145

$\bar{x}$(min, max) provide the mean and the minimum and maximum values of the data set. The mean bias error (MBE) is the weather station data minus the modelled data averaged over the number of stations, and the mean absolute error (MAE) is the average absolute value of MBE. The root mean squared error (RMSE) provides the root mean squared error. Number of stations gives us the number of weather stations that were used in this evaluation and validation.

time period 1951–2012, the same period of time the gridded data covers. We downloaded minimum temperature (T_{min}), maximum temperature (T_{max}), and Prcp data for every available station for each country. We chose these countries because they cover a large portion of Europe and span the continental latitudinal gradient. E-OBS current data portal made obtaining weather station data time consuming not allowing us to use the entire ENSEMBLE weather station data set.

Every station was analysed individually using the mean of each variable over the entire time period. This analysis was spatially explicit but temporally averaged. We also analysed every individual day averaged over all of the stations and years. This method is daily explicit but averaged over space and years. Finally, we also evaluated all available stations and days averaged together (Table 1).

3.3. Validation method

We validated our downscaled data and E-OBS data with the corresponding grid cell of weather stations in an independent data set, from Austria, not used to create the original E-OBS, as opposed to the evaluation that used data that were used to create E-OBS. We performed a validation to assess improvement in accuracy and precision as a result of downscaling using the same statistics we described in the evaluation method section. Austrian weather station data were obtained from the Austrian Central Institute for Meteorology and Geodynamics (ZAMG) and contain all of Austria's weather stations (Hasenauer *et al.*, 2003). Twenty-four stations that were used to create E-OBS were removed (ECA&D provide a list with the location of stations included in their interpolation). There were over 430 weather stations used to validate each variable for the time period 2000–2012. Some of these stations are replacements and so have identical locations as their antecedents giving 250 independent locations. The time period is due to data availability (Table 1). Austria is a representative country for a European climate validation. Austria has a heterogeneous landscape caused by the Alps mountain range, an abundance of large water bodies, and a location within Europe where it is influenced by Nordic, Mediterranean, and inner-continental weather patterns. All of these factors give Austria a very dynamic area on which to analyse climate. We also chose Austria because of data availability.

We analysed every weather station individually averaged daily throughout the entire time period. We also analysed the daily average over all stations throughout the entire time period (Figure 6). We used a downscaling algorithm and not an interpolation of weather stations making a cross-validation impossible.

4. Analysis and results

Our analysis performs three steps to meet the objectives of the study. (1) We first visually assess the spatial pattern of the downscaled data compared to the original E-OBS – to ensure overall continuity between the two data sets (downscaled gridded data). (2) We evaluate the downscaled and original E-OBS data *versus* weather station data – which were used in the original E-OBS interpolation – for any change due to downscaling (evaluation). (3) We validate the downscaled and original E-OBS data *versus* weather stations that were not used in the original E-OBS interpolation. The validation analyses accuracy and error by quantifying any change that arose from the downscaling process (validation).

4.1. Downscaled gridded data

We produced gridded data of minimum temperature, maximum temperature, and precipitation of Europe at a 1×1 km resolution on a daily time step from year 1950 until 2012. The downscaling procedure should enhance local level climate features, such as those created by topography, while maintaining the continental scale pattern of E-OBS. We ensure continental scale continuity between our downscaled data and the original E-OBS by visually assessing gridded data examples for differences and plotting the CDF of both gridded data.

As the data set contains over 54 000 daily gridded data, we assessed a yearly average gridded data set to test the visual differences between the original and downscaled gridded data. No visual differences are apparent in spatial pattern between the original and downscaled versions (Figure 2(a) and (b)). Further, the value ranges of both gridded data are similar (−9 min, 29 max). The CDFs of both data sets indicate that the downscaling did not affect the overall values (Figure 2(c)). The overlay of the CDFs demonstrates that at the continental scale both gridded data have the same distribution of values.

Next, we were interested in how our procedure affected local scale climate features; thus we focused on the Iberian Peninsula centred on Madrid, because of its local scale climatic differences caused by elevation variation, to enhance the visible effect of the downscaling (Figure 3). Figure 3 shows that there are much finer scale temperature features, caused by the incorporation of elevation effects, in the downscaled version than in the original. Figures 2 and 3, therefore, indicate that we have increased local level features while maintaining the overall continental scale pattern.

As explained in the methods section, downscaling precipitation uses different equations than downscaling temperature. Thus, we sought to ensure that downscaling precipitation had also maintained the continental scale pattern. Visually, both the E-OBS, the downscaled map and value ranges of precipitation are the same (Figure 4(a) and (b)). When viewed at this continental scale, the local level effects of downscaling are already apparent as Figure 4(b) appears sharper than Figure 4(a). The CDF's of both data sets are almost identical at this scale as they overlay one another (Figure 4(c)).

4.2. Evaluation

The evaluation examines change that occurred during the downscaling procedure at the points used to create E-OBS.

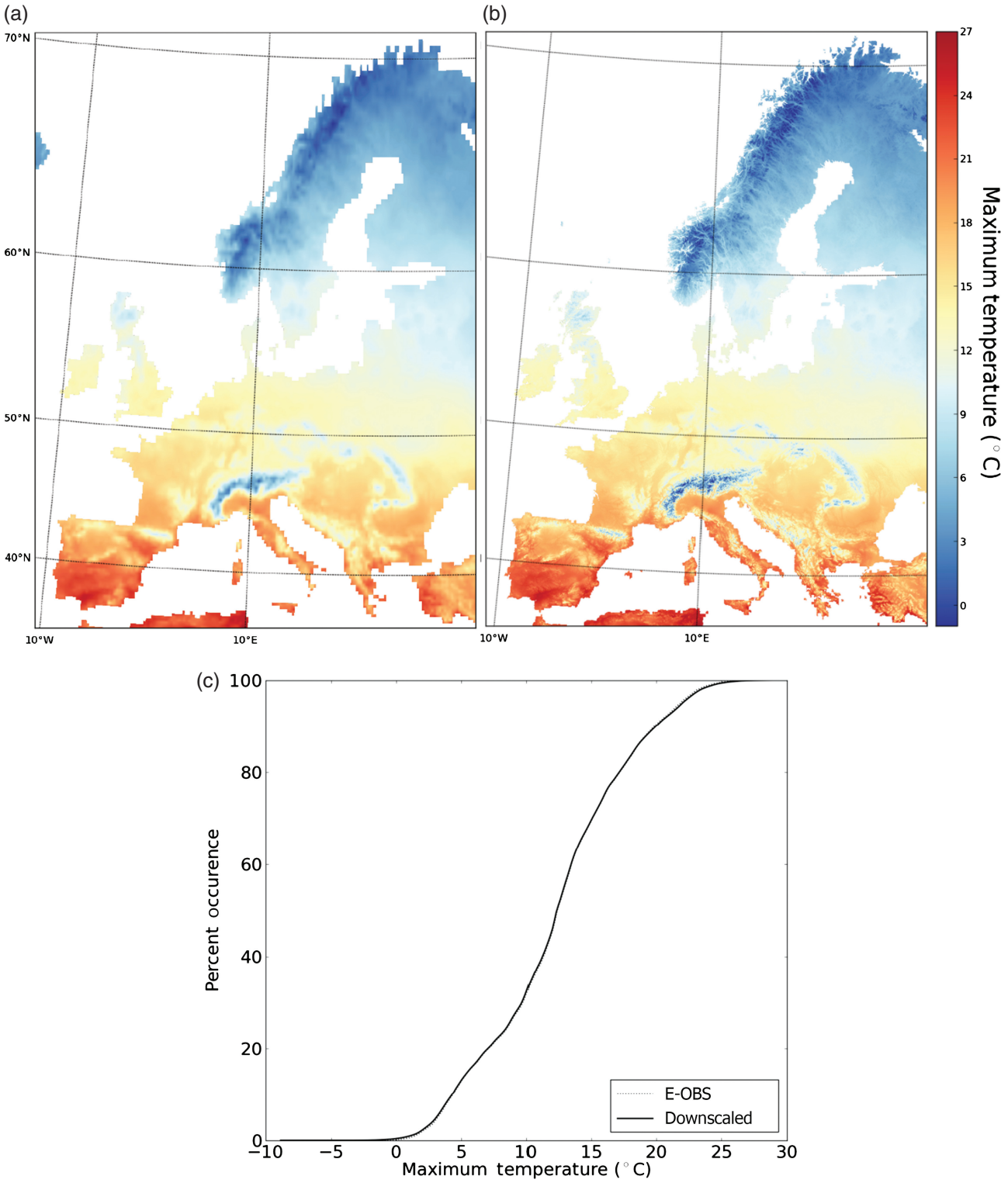

Figure 2. (a) Original E-OBS average daily T_{max} for year 2001. (b) Downscaled average daily T_{max} for year 2001. (c) Cumulative distribution function of average daily T_{max} for year 2001 (downscaled climate data, solid; original E-OBS, dotted). The lines overlay one another.

E-OBS' spline-based spatial interpolation and weather station density indicate that E-OBS should accurately represent the station points. The downscaling algorithm may modify every point on the gridded data not knowing which points were used for the E-OBS interpolation. The sparse density of the weather station network used to interpolate the original E-OBS means that the cells will have values close to that of the weather station data; therefore, we assume high confidence in E-OBS data at locations of weather stations used for the original E-OBS interpolation. There is a chance that we can reduce accuracy through downscaling at those points because our algorithm has no knowledge of the location of weather stations.

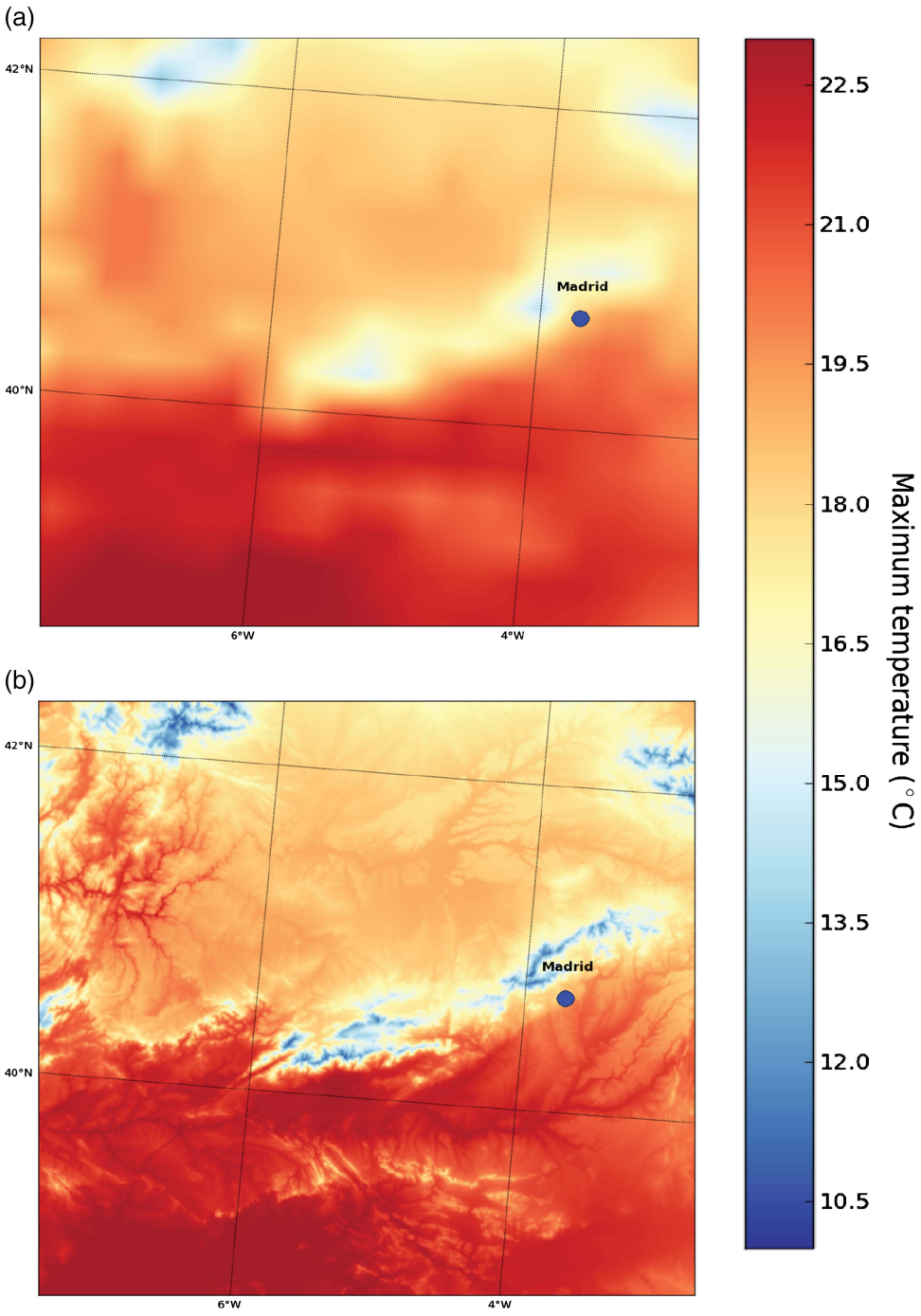

Figure 3. Original E-OBS average daily T_{max} and downscaled average daily T_{max} for year 2001.

The results show that accuracy consistently remained equal between the two data sets. For all countries, the results show similar variation and error between the original and downscaled data (Table 1, Figure 5). The greatest overall difference in MBE is 0.1 °C in both minimum and maximum temperature. Precipitation is underestimated in both the original E-OBS and the downscaled version by 0.1 mm per weather station per year. However, the similarities between the two data sets are different for individual countries. Northern countries have more similarities than southern countries between the original and the downscaled data sets. RMSE and bias (MBE) for Germany and France improve or remain the same for all measures across all variables, with the exception of T_{max} in Germany which has a higher root mean RMSE and lower R^2 value. Downscaled data set for Norway has an increase in bias and a decrease in R^2 values but a decrease in RMSE for temperature. Although the R^2 values drop, they still remain over 0.9. Precipitation for Norway improves with downscaling (Table 1, Figure 5).

The LEPS values for all evaluation stations remain the same after downscaling at 0.77 and 0.76 for T_{min} and T_{max}, respectively. The LEPS values of the individual countries all increase or remain the same after downscaling with the

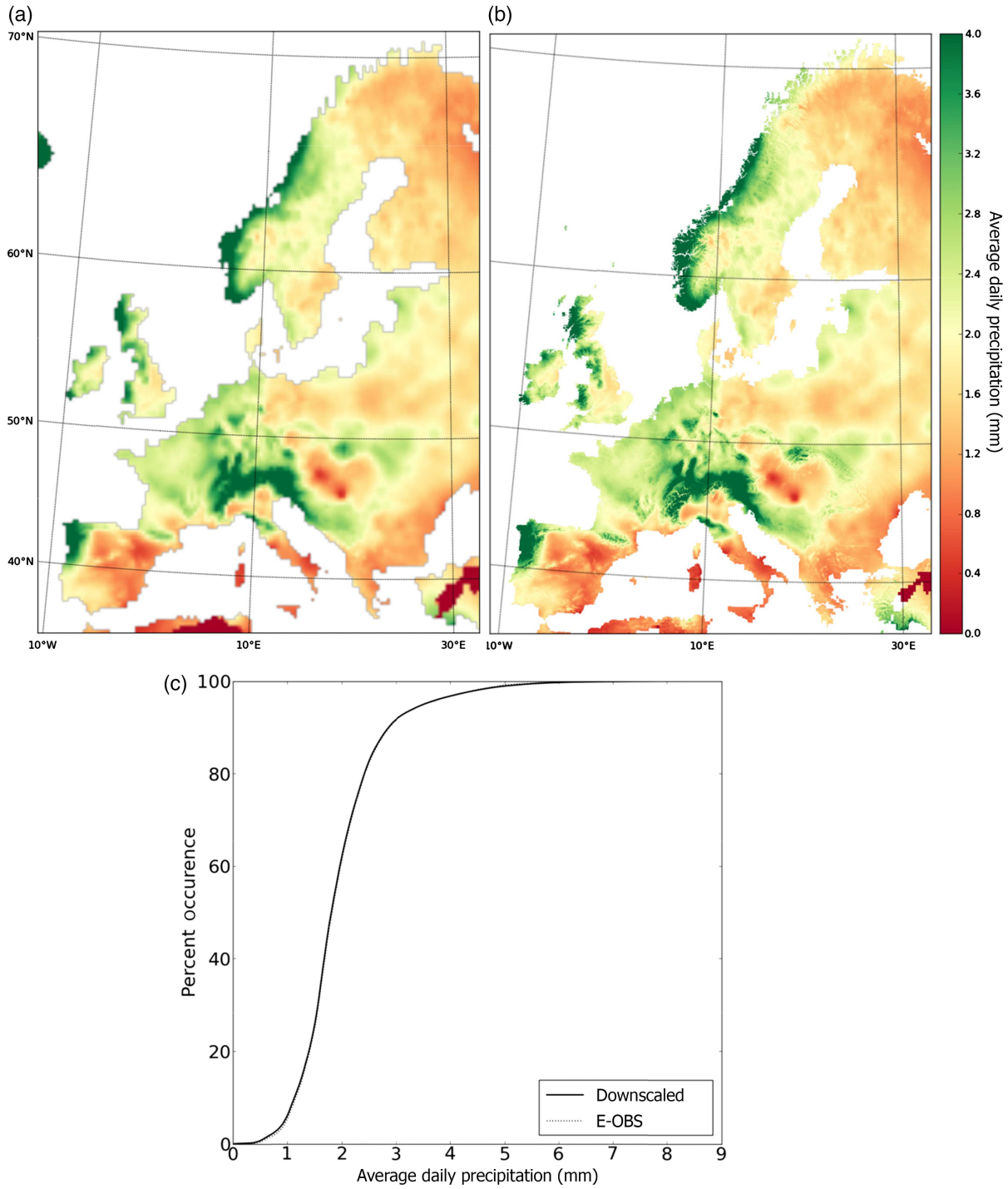

Figure 4. (a) Original E-OBS average daily precipitation for year 2001. (b) Downscaled average daily precipitation for year 2001. (c) Cumulative distribution function of average daily precipitation for year 2001 (downscaled climate data, solid; original E-OBS, dotted). The lines overlay one another.

exception of T_{min} of Spain which decreases from 0.51 to 0.45. The Prcp CSI values for of all evaluation stations remain the same after downscaling at 0.75. The CSI low values of all evaluation stations for all variables remain the same after downscaling. The CSI high values increase for all variables with the largest increase in Prcp from 0.42 in the original E-OBS to 0.52 in the downscaled version.

Spain and Italy have high bias and error and low R^2 values for precipitation in the original and downscaled data sets. Minimum temperature in Spain has high RMSE and low R^2 values in both the original and downscaled data sets. In Spain and Italy, for every variable downscaling created higher bias and RMSE and lower R^2 values than the original data.

Seasonally E-OBS underestimates temperature in the winters and overestimates in the summer. The temperature seasonality difference for both the original and downscaled data sets never exceeds 0.01 °C. The modelled

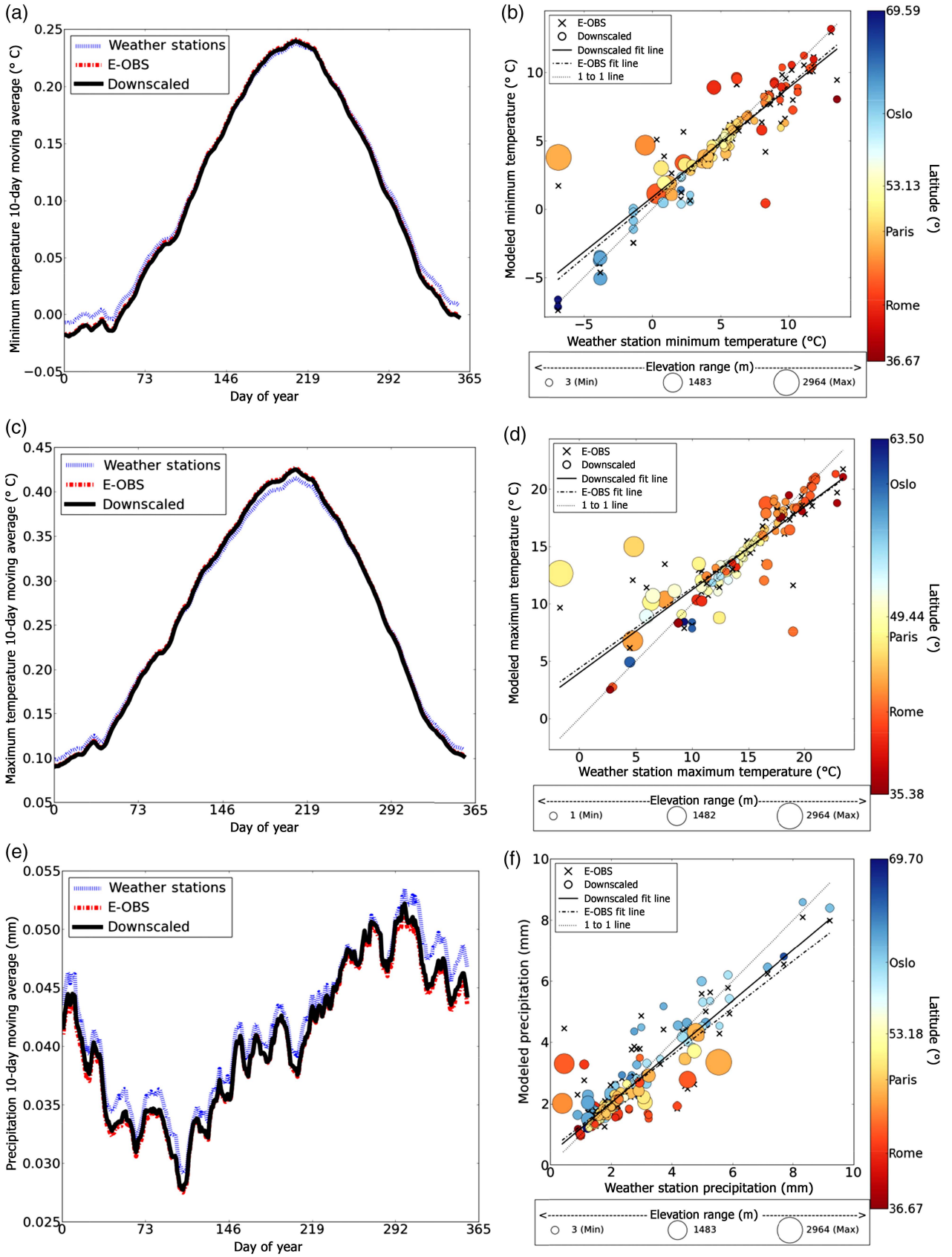

Figure 5. Evaluation of E-OBS and downscaled data against weather station data from Norway, Germany, France, Spain, and Italy. All of these stations were used to create E-OBS. Minimum temperature, maximum temperature, and precipitation are shown. Left column gives daily averages for years 1950–2012 of all stations. Right column shows weather station data (x-axis) *versus* E-OBS and downscaled data (y-axis). Size of downscaled points indicates the elevation of the station at that point. The colour of the downscaled points (circles) indicates latitude of the corresponding weather station.

data sets consistently underestimate precipitation seasonally but never more that by 0.0025 mm per day. Downscaled daily precipitation is consistently more accurate than E-OBS (Figure 5).

The scatter plot in Figure 5 shows that both the original E-OBS and the downscaled version (interpolated data) minimum temperature values best fit weather station data between 1 and 7 °C. Interpolated data minimum temperature becomes more accurate towards lower elevations and towards higher latitudes (Figure 5). Maximum temperature is accurate for all temperatures and latitudes however elevation greatly affects accuracy – with lower accuracies occurring at high elevations. Precipitation data have higher accuracy at lower values of precipitation. Interpolated data precipitation is more accurate at higher latitudes and underestimates at lower latitudes. Precipitation accuracy is higher at lower elevations. For all variables, the fit lines for both data sets are similar and close to the 1 to 1 line (Figure 5).

At grid points with weather stations used to produce E-OBS, the downscaling maintains or improves upon the error already incorporated in the original E-OBS data set (Table 1). This evaluation confirms that our downscaling algorithm does not increase error at grid points with which we have high confidence in the original E-OBS.

4.3. Validation

We validated the new data set against an independent data set of over 400 Austrian weather stations that were not used in the original E-OBS interpolation. Downscaled variables have R^2 values of 0.77 or better, a bias of 5% or lower, and an RMSE of 5% or less (Table 1). We improve the bias for T_{max}, T_{min}, and Prcp by 89, 65, and 60% and the RMSE by 29, 11, and 2%, respectively. R^2 values increase for T_{max}, T_{min}, and Prcp by 24, 20, and 3% respectively. All downscaled variables improve compared to the original E-OBS (Table 1, Figure 6).

The LEPS values of T_{min} and T_{max} both increased with downscaling by 9 and 21%, respectively. The CSI low score for T_{min} did not improve much with downscaling with a score of 0.47. The T_{min} CSI high score did improve from 0.31 to 0.41. Both CSI scores for T_{max} improved from 0.39 to 0.51 for the CSI low and from 0.29 to 0.46 for the CSI high. The CSI score for Prcp decreased from 0.54 to 0.51. The Prcp CSI low score remained constant at 0.6. The Prcp CSI high score improved from 0.12 to 0.16.

The seasonal pattern of precipitation matches the weather station data (Figure 6). The absolute values yield the greatest improvement through downscaling in the winter (Figure 6). The downscaled daily values of both T_{min} and T_{max} improved over the original E-OBS values (line graphs Figure 6). Individual station precipitation has higher accuracy at lower absolute values. Precipitation accuracy appears to be independent of elevation and latitude (scatter plots Figure 6). For individual stations, the downscaled precipitation values only slightly changed from the E-OBS values. Although the fit line of the downscaled data is further from the 1 to 1 line than the E-OBS fit line, all other metrics show a slight improvement in precipitation values due to the increase in temporal accuracy (Table 1, Figure 6).

Both T_{min} and T_{max} have a visible temporal improvement with the downscaled curve overlaying that of the weather stations (Figure 6). This pattern is consistent across seasons with no seasonally dependent error (line graphs Figure 6). When viewing individual stations (scatter plots Figure 6), minimum temperature has increased accuracy through downscaling, primarily, by increasing values that were underestimated by E-OBS. Elevation and latitude do not affect the accuracy of downscaled T_{min} (scatter plot Figure 6). The original E-OBS data set tends to underestimates T_{min} to a greater extent relative to the downscaled data (Table 1, Figure 6). The greatest improvement from downscaling can be seen in T_{max}. The downscaled fit line overlays the 1 to 1 line. The downscaled T_{max} values have almost no error as compared to E-OBS values. The magnitude temperature values, elevation, and latitude do not affect the accuracy of the downscaled values, whereas the E-OBS values have more error towards higher temperatures. The original E-OBS had a consistent bias towards underestimating both T_{min} and T_{max} which is removed through downscaling (Table 1, Figure 6).

5. Discussion

A lack of access empirical data from weather stations makes downscaling the original E-OBS data set only option to create a higher resolution gridded data that spans Europe. It is only possible to download 77% of all the weather stations' data sets used to create E-OBS. We were only able to obtain weather station data not used in E-OBS from one country, Austria, which we used for validation. The method we used for downscaling, the delta method, is designed to integrate various data sets with different temporal/spatial scales (Mote and Salathe, 2010; Mosier *et al.*, 2014; Reeves *et al.*, 2014). Although the delta method has been used in numerous studies, its application must be customized to cater to each study's unique parameters which inevitably have slightly different temporal and spatial resolutions.

We produced a downscaled climate data set that increases local scale accuracy while maintaining the continental scale patterns of the E-OBS data set (Figures 2 and 4). Averaged over five countries that span Europe's latitudinal gradient, the new data set maintains the bias and error at points used to create the original E-OBS (Table 1, Figure 5). In Austria, at grid points that contain weather stations not used in the original E-OBS derivation, the downscaling improves all climate variables as shown in our validation (Table 1, Figure 6).

Our downscaling algorithm utilizes the strengths of both input data sets. E-OBS was derived by a Kriging/spline method accounting for distance relationships and expert knowledge. E-OBS provides daily values that are designed for the continental scale. WorldClim's monthly climate surfaces use an interpolation technique with DEMs (SRTM, GTOPO30) incorporating elevation effects on

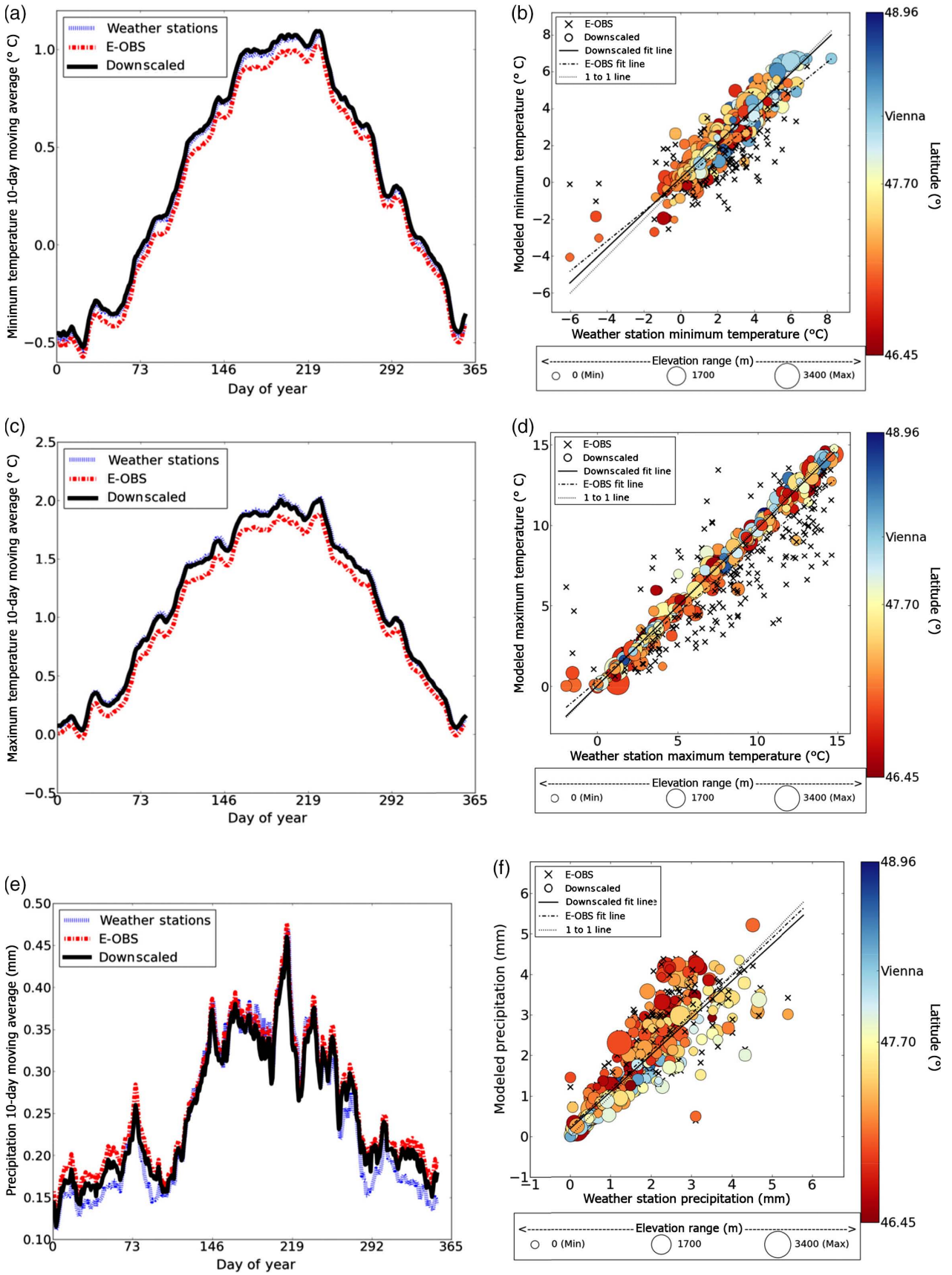

Figure 6. Validation of E-OBS and downscaled data against weather station data from Austria. None of these stations were used to create E-OBS. Minimum temperature, maximum temperature, and precipitation are shown. Left column gives daily averages for years 2000–2012 of all stations. Right column shows weather station data (*x*-axis) *versus* E-OBS and downscaled data (*y*-axis). Size of downscaled points (circles) indicates the elevation of the station at that point. The colour of the downscaled points indicates latitude of the corresponding weather station.

climate. The primary benefit of the downscaling method we used is the incorporation of elevation, through WorldClim, into the E-OBS daily climate data. Temperature is strongly influenced by elevation (through its lapse rate) more so than precipitation. However, one cannot apply a single lapse rate in every location for every day of the year. Lapse rates vary by elevation, latitude, weather type, and season (Stone and Carlson, 1979; Blandford *et al.*, 2008). Lapse rates for precipitation, in particular, are not constant through seasons, regions, or across scales (Daly *et al.*, 1994). Therefore, it is beneficial to incorporate WorldClim into E-OBS because it is based on real world observations (which capture mean local lapse rates), has monthly values, is spatially explicit, and represents the average weather conditions over an extended time period. Because of the nature of the delta method, however, the base ratios between downscaled cells – lapse rates – only change by month and not from year to year.

Table 1 shows that the MBE, for the majority of variables and countries in the evaluation, improved or retained its previous value through downscaling. This result was also found by Mosier *et al.* (Mosier *et al.*, 2014) when comparing downscaled data against stations that were used within the WorldClim interpolation. The R^2 values are all above 0.64 except for $T_{\min}$ and Prcp in Spain and Prcp in Italy. E-OBS had weather stations in these countries that are not publicly available and thus not available for our evaluation. During interpolation, these station values, to which we have access, may have been smoothed by incorporating stations to which we do not have access. It is also important to note that across all statistical measures aggregating all countries together improves both data sets. This again indicates that E-OBS was designed for continental scale studies.

The temperature LEPS values indicate that the downscaled version did not affect the accuracy of E-OBS in probability space meaning that it has the same ability to predict both median values as well as more extreme values as the original E-OBS. The CSI high values increase for all evaluation stations for all variables. This indicates that downscaling has a positive effect on the data set's ability to match extreme high values. CSI values for all variables for all evaluation stations indicate that the downscaled version captures extreme values more than half of the time. Prcp CSI values show that the downscaled version captures rain days 75% of the time. Prcp CSI low values are slightly higher than the Prcp CSI values, indicating that when the downscaled data have a false alarm for a rain-day, it is at least only a low amount of Prcp.

At weather station points not used to create E-OBS, in Austria, the greatest improvement from downscaling is in temperature. This is most likely because of the large effect incorporating elevation into the climate data has on temperature as compared to precipitation. Of all variables, downscaled precipitation has the least improvement. The original WorldClim authors' (Hijmans *et al.*, 2005) explicitly state that they had difficulty in modelling precipitation in mountainous regions. This weakness in WorldClim can explain the lack of improvement in precipitation from our downscaling algorithm when compared against data from a mountainous country such as Austria. Also, we do not perform any new climatological calculations, such as convective precipitation, so we will not capture small precipitation events that were not captured by E-OBS.

The LEPS scores for minimum and maximum temperature of Austria show a positive response to downscaling increasing by 0.05 and 0.13, respectively. This increase in LEPS values along with the decrease in MAE values due to downscaling lead to the conclusion that the downscaled version not only more accurately captures mean temperature values but also extreme values than does the original E-OBS. The CSI score for extreme lows and highs of temperature all improved with downscaling as well. This is to be expected as our method increase/decreases temperature from the E-OBS values which can be interpreted as a mean of the larger area. However, the CSI values for high and low extremes of minimum and maximum temperatures indicate that we still only capture extreme values from 41 to 51% of the time.

The CSI values for precipitation in Austria, on the other hand, have a weaker response to downscaling than temperature. This lack of response is again a demonstration that our method of integrating elevation into the E-OBS data set has more influence on temperature than precipitation.

Considering the daily graphs and the stations scatter plots of Austria together, we show that those errors which occur at individual stations get cancelled out when viewed over time (Figure 6). Thus, the original E-OBS data represent data on the country scale but have much higher error when viewed on a local level. It also shows that at both the local and country scales the downscaled data perform better.

Many studies have used E-OBS to examine various aspects of European ecosystems, making it a widely used and recognized data set (Ziello *et al.*, 2009; Hirschi *et al.*, 2010; Gottfried *et al.*, 2012). Other studies have also examined the validity of E-OBS data itself (Hofstra *et al.*, 2009; Kysely and Plavcova, 2010). These studies compare E-OBS with national gridded climatology or selected weather stations. They found various biases and errors in both temperature and precipitation. Examples of such findings include low levels of precipitation, higher error of precipitation in mountainous regions, and incorrect temperature. Hofstra *et al.* (2009) reports RMSE of temperature of 0.7–0.9 °C and RMSE of 0.85–0.92 mm for Prcp in the United Kingdom and RMSE of 5.77 mm for Prcp in the Alps. Hofstra *et al.* (2009) also reports that over the Alps both absolute error and error as a percent of absolute Prcp are both higher than Prcp error in the United Kingdom. This finding from Hofstra *et al.* (2009) along with the assertion of Hijmans *et al.* (2005) that WordClim does not capture all variation in mountainous precipitation shows that our data will our downscaled precipitation data will also have higher area in mountainous areas. One other source of error in the precipitation data that was not addressed in our study was that of precipitation frequency. We only changed the magnitude of an existing

rain event. We did not create rain events not included in E-OBS.

Maselli *et al.* (2012) created a locally downscaled E-OBS data set for Italy, by applying a regression function for downscaling calibrated for their area of study. They validated their data against ten Italian weather stations for the time period 2000–2009. The authors do not state whether the stations used for analysis were used to create E-OBS or are an independent data set. Our validation against Austrian weather stations and our evaluation of Italian data show reduced bias (MBE) and RMSE for all variables. The Italian downscaled data improve the bias of only the maximum temperature values. As a comparison, the Italian data have an MBE over all stations for minimum temperature of 3.0 while our MBE is 0.2 for Austria and 1.3 for Italy. However, compared to the Italian data, our RMSE values tend to be higher for precipitation and maximum temperature but lower for minimum temperature.

Compounding errors from both of our input data sets, E-OBS and WorldClim, exist and are difficult to quantify. We only downscale grid points that have both WorldClim and E-OBS values. This creates data limitations, mostly from E-OBS, primarily around the coastline making them artificially square. Additionally, a lack of stations in mountainous regions used in our input data sets makes our knowledge of the accuracy in Alpine regions weaker than in other regions. Also, assumptions were made reading ambiguous weather station data in E-OBS, such as inconsistencies in the data collection date and time (Haylock *et al.*, 2008), which could result in fallacious local scale E-OBS outputs and gives less confidence in the weather station data. Also, contradictory elevation data between stations and DEM's used to create WorldClim further weakens confidence in Alpine areas (Hijmans *et al.*, 2005). The extremes of the downscaled data are most likely too conservative as this is also true in E-OBS (Haylock *et al.*, 2008). Incorporating WorldClim will most likely not increase the likelihood of capturing extreme values – which is an increasingly more important aspect of climate data to capture – as WorldClim is itself only a mean value over a long timeframe (Schär *et al.*, 2004). This downscaling method still suffers from the lack of weather station density inherited from both input data sets.

6. Conclusion

We have used the delta method to incorporate E-OBS data ($0.25° \times 0.25°$ resolution, daily) and WorldClim data ($0.008\overline{3}° \times 0.008\overline{3}°$ resolution, monthly climate surface) to produce a new downscaled climate data set, which covers Europe and includes maximum temperature, minimum temperature, and precipitation on a daily time step at a $0.008\overline{3}° \times 0.008\overline{3}°$ resolution (approximately 1×1 km) from 1950 to 2013. This data set will be updated as new E-OBS versions are released. Scientists can use one data set to do research in various areas of Europe at a local level and have results be directly comparable allowing studies of important environmental and economic issues at a local level over a larger landscape than previously possible. We did not increase random variation or error at points used to make the original E-OBS as a result of the downscaling process. The downscaled data also have a higher accuracy and precision than the original E-OBS data at weather stations not used in the original E-OBS interpolation. One major benefit of the method we used for downscaling is that because WorldClim is a global data set, this method can be applied anywhere in the world that already has a low-resolution gridded climate data set.

The most accurate climate data sets with fine resolutions are most likely the national climate data sets; however, those are often difficult, costly, or impossible to obtain and inherently only cover the spatial extent of their particular country. We created these data for those researchers who desire a continental scale data set with a fine resolution and for policy makers or land managers who need locally relevant information on large scales that cross countries and regions in Europe. A better solution would be a European wide interpolation at this resolution such as those that have been done in the United States for over 20 years. However, current infrastructure, policy obstacles, and data sharing culture make such an interpolation with a reasonable level of accuracy unattainable. Until a more coherent, consistent, and open access weather station network is available, downscaling is the only option to create gridded data at this resolution for Europe. This entire data set can be obtained at ftp://palantir.boku.ac.at/Public/ClimateData.

Acknowledgements

We thank Dr Rupert Seidl, Dr Christopher Thurner, Mrs Loretta Moreno, and Dr Phillip Mohebalian for their help in reviewing and revising the article. Data that were downscaled in this article can be obtained at http://www.ecad.eu/download/ensembles/download.php and http://www.worldclim.org/download, and we thank all of the researchers and technicians who make all of these data easily accesible and free. The research leading to these results has received funding from the European Union Seventh Framework Programme under grant agreement n° 311970.

References

Blandford TR, Humes KS, Harshburger BJ, Moore BC, Walden VP, Ye H. 2008. Seasonal and synoptic variations in near-surface air temperature lapse rates in a mountainous basin. *J. Appl. Meteorol. Climatol.* **47**: 249–261, doi: 10.1175/2007JAMC1565.1.

Ciais Ph., Reichstein M, Viovy N, Granier A, Ogée J, Allard V, Aubinet M, Buchmann N, Bernhofer Chr., Carrara A, Chevallier F, De Noblet N, Friend AD, Friedlingstein P, Grünwald T, Heinesch B, Keronen P, Knohl A, Krinner G, Loustau D, Manca G, Matteucci G, Miglietta F, Ourcival JM, Papale D, Pilegaard K, Rambal S, Seufert G, Soussana JF, Sanz MJ, Schulze ED, Vesala T, Valentini R. 2005. Europe-wide reduction in primary productivity caused by the heat and drought in 2003. *Nature* **437**(7058): 529–533. DOI: 10.1038/nature03972.

Daly C. 2006. Guidelines for assessing the suitability of spatial climate data sets. *Int. J. Climatol.* **26**(6): 707–721, doi: 10.1002/joc.1322.

Daly C, Neilson RP, Phillips DL. 1994. A statistical-topographic model for mapping climatological precipitation over mountainous terrain. *J. Appl. Meteorol.* **33**(2): 140–158, doi: 10.1175/1520-0450(1994)033<0140:ASTMFM>2.0.CO;2.

Ezzine H, Bouziane A, Ouazar D. 2014. Seasonal comparisons of meteorological and agricultural drought indices in Morocco using open short time-series data. *Int. J. Appl. Earth Obs. Geoinf.* **26**: 36–48, doi: 10.1016/j.jag.2013.05.005.

Farr TG, Rosen PA, Caro E, Crippen R, Duren R, Hensley S, Kobrick M, Paller M, Rodriguez E, Roth L, Seal D, Shaffer S, Shimada J, Umland J, Werner M, Oskin M, Burbank D, Alsdorf D. 2007. The Shuttle Radar Topography Mission. *Rev. Geophys.* **45**(2): 1944–9208, doi: 10.1029/2005RG000183.

Frei C, Schaer C. 1998. A precipitation climatology of the Alps from high-resolution rain-gauge observations. *Int. J. Climatol.* **18**(8): 873–900.

Gottfried M, Pauli H, Futschik A, Akhalkatsi M, Barančok P, Benito Alonso JL, Coldea G, Dick J, Erschbamer B, Fernández Calzado MR, Kazakis G, Krajči J, Larsson P, Mallaun M, Michelsen O, Moiseev D, Moiseev P, Molau U, Merzouki A, Nagy L, Nakhutsrishvili G, Pedersen B, Pelino G, Puscas M, Rossi G, Stanisci A, Theurillat J-P, Tomaselli M, Villar L, Vittoz P, Vogiatzakis I, Grabherr G. 2012. Continent-wide response of mountain vegetation to climate change. *Nat. Clim. Change* **2**(2): 111–115, doi: 10.1038/nclimate1329.

Guo Y, Gong P, Amundson R, Yu Q. 2006. Analysis of factors controlling soil carbon in the conterminous United States. *Soil Sci. Soc. Am. J.* **70**(2): 601, doi: 10.2136/sssaj2005.0163.

Hasenauer H, Merganicova K, Petritsch R, Pietsch S, Thornton PE. 2003. Validating daily climate interpolations over complex terrain in Austria. *Agric. For. Meteorol.* **119**(1-2): 87–107, doi: 10.1016/S0168-1923(03)00114-X.

Hawkins BA. 2010. Multiregional comparison of the ecological and phylogenetic structure of butterfly species richness gradients. *J. Biogeogr.* **37**(4): 647–656, doi: 10.1111/j.1365-2699.2009.02250.x.

Hawkins E, Fricker TE, Challinor AJ, Ferro CAT, Ho CK, Osborne TM. 2013. Increasing influence of heat stress on French maize yields from the 1960s to the 2030s. *Glob. Change Biol.* **19**(3): 937–47, doi: 10.1111/gcb.12069.

Haylock M, Hofstra N, Tank AK. 2008. A European daily high-resolution gridded data set of surface temperature and precipitation for 1950–2006. *J. Geophys. Res.* **113**: D20119, doi: 10.1029/2008JD010201.

Hijmans RJ, Cameron SE, Parra JL, Jones PG, Jarvis A. 2005. Very high resolution interpolated climate surfaces for global land areas. *Int. J. Climatol.* **25**(15): 1965–1978, doi: 10.1002/joc.1276.

Hirschi M, Seneviratne SI, Alexandrov V, Boberg F, Boroneant C, Christensen OB, Formayer H, Orlowsky B, Stepanek P. 2010. Observational evidence for soil-moisture impact on hot extremes in southeastern Europe. *Nat. Geosci.* **4**(1): 17–21, doi: 10.1038/ngeo1032.

Hofstra N, Haylock M, New M, Jones P, Frei C. 2008. Comparison of six methods for the interpolation of daily, European climate data. *J. Geophys. Res. Atmos.* **113**(21): D21, doi: 10.1029/2008JD010100.

Hofstra N, Haylock M, New M, Jones PD. 2009. Testing E-OBS European high-resolution gridded data set of daily precipitation and surface temperature. *J. Geophys. Res.* **114**(D21): D21101, doi: 10.1029/2009JD011799.

Hutchinson MF. 1995. Interpolating mean rainfall using thin plate smoothing splines. *Int. J. Geogr. Inf. Syst.* **9**(4): 385–403, doi: 10.1080/02693799508902045.

Hutchinson MF. 2004. *Anusplin Version 4.3. Centre for Resource and Environmental Studies*. The Australian National University: Canberra.

Isotta FA, Frei C, Weilguni V, Perčec Tadić M, Lassègues P, Rudolf B, Pavan V, Cacciamani C, Antolini G, Ratto SM, Munari M, Micheletti S, Bonati V, Lussana C, Ronchi C, Panettieri E, Marigo G, Vertačnik G. 2014. The climate of daily precipitation in the Alps: development and analysis of a high-resolution grid dataset from pan-Alpine rain-gauge data. *Int. J. Climatol.* **34**(5): 1657–1675, doi: 10.1002/joc.3794.

Janssens IA, Lankreijer H, Matteucci G, Kowalski AS, Buchmann N, Epron D, Pilegaard K, Kutsch W, Longdoz B, Grunwald T, Montagnani L, Dore S, Rebmann C, Moors EJ, Grelle A, Rannik U, Morgenstern K, Oltchev S, Clement R, Gudmundsson J, Minerbi S, Berbigier P, Ibrom A, Moncrieff J, Aubinet M, Bernhofer C, Jensen NO, Vesala T, Granier A, Schulze E-D, Lindroth A, Dolman AJ, Jarvis PG, Ceulemans R, Valentini R. 2001. Productivity overshadows temperature in determining soil and ecosystem respiration across European forests. *Glob. Change Biol.* **7**(3): 269–278, doi: 10.1046/j.1365-2486.2001.00412.x.

Jay F, Manel S, Alvarez N, Durand EY, Thuiller W, Holderegger R, Taberlet P, François O. 2012. Forecasting changes in population genetic structure of alpine plants in response to global warming. *Mol. Ecol.* **21**(10): 2354–68, doi: 10.1111/j.1365-294X.2012.05541.x.

Journal AG, Huijbregts CJ. 1978. *Mining Geostatistics*. Academic Press: London.

Kysely J, Plavcova E. 2010. A critical remark on the applicability of E-OBS European gridded temperature data set for validating control climate simulations. *J. Geophys. Res.* **115**(D23): D23118.

Lorenz R, Davin EL, Seneviratne SI. 2012. Modeling land-climate coupling in Europe: impact of land surface representation on climate variability and extremes. *J. Geophys. Res. Atmos.* **117**: D20109.

Luedeling E, Zhang M, Girvetz EH. 2009. Climatic changes lead to declining winter chill for fruit and nut trees in California during 1950-2099. *PLoS One* **4**(7): e6166, doi: 10.1371/journal.pone.0006166.

Maselli F, Pasqui M, Chirici G, Chiesi M, Fibbi L, Salvati R, Corona P. 2012. Modeling primary production using a 1 km daily meteorological data set. *Clim. Res.* **54**(3): 271–285, doi: 10.3354/cr01121.

Masson D, Frei C. 2015. Long-term variations and trends of mesoscale precipitation in the Alps: recalculation and update for 1901-2008. *Int. J. Climatol.* , doi: 10.1002/joc.4343.

Mosier TM, Hill DF, Sharp KV. 2014. 30-Arcsecond monthly climate surfaces with global land coverage. *Int. J. Climatol.* **34**: 2175–2188, doi: 10.1002/joc.3829.

Mote PW, Salathe EP Jr. 2010. Future climate in the Pacific Northwest. *Clim. Change* **102**: 29–50, doi: 10.1007/s10584-010-9848-z.

Nekola JC, Brown JH. 2007. The wealth of species: ecological communities, complex systems and the legacy of Frank Preston. *Ecol. Lett.* **10**(3): 188–96, doi: 10.1111/j.1461-0248.2006.01003.x.

Peterson AT, Nakazawa Y. 2007. Environmental data sets matter in ecological niche modelling: an example with Solenopsis invicta and Solenopsis richteri. *Glob. Ecol. Biogeogr.* **17**: 135–144, doi: 10.1111/j.1466-8238.2007.00347.x.

Peterson AT, Papeş M, Eaton M. 2007. Transferability and model evaluation in ecological niche modeling: a comparison of GARP and Maxent. *Ecography* **30**(4): 550–560, doi: 10.1111/j.2007.0906-7590.05102.x.

Reeves MC, Moreno AL, Bagne KE, Running SW. 2014. Estimating climate change effects on net primary production of rangelands in the United States. *Clim. Change* **126**: 429–442, doi: 10.1007/s10584-014-1235-8.

Schär C, Vidale PL, Lüthi D, Frei C, Häberli C, Liniger M, Appenzeller C. 2004. The role of increasing temperature variability in European summer heatwaves. *Nature* **427**(January): 332–336, doi: 10.1038/nature02300.

Seidl R, Eastaugh CS, Kramer K, Maroschek M, Reyer C, Socha J, Vacchiano G, Zlatanov T, Hasenauer H. 2013. Scaling issues in forest ecosystem management and how to address them with models. *Eur. J. For. Res.* **132**(5-6): 653–666, doi: 10.1007/s10342-013-0725-y.

Stone PH, Carlson JH. 1979. Atmospheric lapse rate regimes and their parameterization. *J. Atmos. Sci.* **36**: 415–423.

Thornton PE, Running SW, White MA. 1997. Generating surfaces of daily meteorological variables over large regions of complex terrain. *J. Hydrol.* **190**(3-4): 214–251, doi: 10.1016/S0022-1694(96)03128-9.

Turner DP, Dodson R, Marks D. 1996. Comparison of alternative spatial resolutions in the application of a spatially distributed biogeochemical model over complex terrain. *Ecol. Model.* **90**(68): 53–67.

VEMAP Members. 1995. Vegetation/ecosystem modelling and analysis project: comparing biogeography and biogeochemistry models in a continental-scale study of terrestrial responses to climate change and CO 2 doubling. *Glob. Biogeochem. Cycles* **9**(4): 407–437.

Venäläinen A, Tuomenvirta H, Pirinen P, Drebs A. 2005. A basic finnish climate data set 1961-2000 – description and illustrations. Reports 5, Finnish Meteorological Institute: Helsinki, 1–27.

Waring RH, Running SW. 2010. *Forest Ecosystems: Analysis at Multiple Scales (Google eBook)*. Elsevier.

Wijngaard JB, Klein Tank AMG, Koennen GP. 2003. Homogeneity of 20th century European daily temperature and precipitation series. *Int. J. Climatol.* **23**(6): 679–692, doi: 10.1002/joc.906.

Willmott CJ, Matsuura K. 2006. On the use of dimensioned measures of error to evaluate the performance of spatial interpolators. *Int. J. Geogr. Inf. Sci.* **20**(1): 89–102, doi: 10.1080/13658810500286976.

Wimberly MC, Hildreth MB, Boyte SP, Lindquist E, Kightlinger L. 2008. Ecological niche of the 2003 West Nile virus epidemic in the northern great plains of the United States. *PLoS One* **3**(12): e3744, doi: 10.1371/journal.pone.0003744.

Zhao M, Heinsch FA, Nemani RR, Running SW. 2005. Improvements of the MODIS terrestrial gross and net primary production global data set. *Remote Sens. Environ.* **95**(2): 164–176, doi: 10.1016/j.rse.2004.12.011.

Ziello C, Estrella N, Kostova M, Koch E, Menzel A. 2009. Influence of altitude on phenology of selected plant species in the Alpine region (1971–2000). *Clim. Res.* **39**(1): 227–234, doi: 10.3354/cr00822.

9.2. Paper 2

Neumann, M., **Moreno, A.,** Mues, V., Härkönen, S., Mura, M., Bouriaud, O., Lang, M., Achten, W.M.J., Thivolle-Cazat, A., Bronisz, K., Merganič, J., Decuyper, M., Alberdi, I., Astrup, R., Mohren, F., Hasenauer, H., 2016. Comparison of carbon estimation methods for European forests. For. Ecol. Manage. 361, 397–420.

Forest Ecology and Management 361 (2016) 397–420

Contents lists available at ScienceDirect

Forest Ecology and Management

journal homepage: www.elsevier.com/locate/foreco

Comparison of carbon estimation methods for European forests

Mathias Neumann [a,*], Adam Moreno [a], Volker Mues [b], Sanna Härkönen [c], Matteo Mura [d], Olivier Bouriaud [e], Mait Lang [f], Wouter M.J. Achten [g,o], Alain Thivolle-Cazat [h], Karol Bronisz [i], Ján Merganič [j], Mathieu Decuyper [k,n], Iciar Alberdi [l], Rasmus Astrup [m], Frits Mohren [n], Hubert Hasenauer [a]

[a] Institute of Silviculture, Department of Forest and Soil Sciences, University of Natural Resources and Life Sciences, Vienna, Peter-Jordan-Str. 82, A-1190 Wien, Austria
[b] University Hamburg, Centre for Wood Science, World Forestry Leuschnerstr. 91, D-21031 Hamburg, Germany
[c] Finnish Forest Research Institute, Yliopistokatu 6, BOX 68, FI-80101 Joensuu, Finland
[d] Department of Bioscience and Territory, University of Molise, Contrada Fonte Lappone snc, 86090 Pesche (IS), Italy
[e] Universitatea Stefan del Mare, Suceava, Str. Universitatii, nr. 13, cod postal 720229, Suceava, Romania
[f] Tartu Observatory, 61602 Tõravere, Estonia
[g] KU Leuven – University of Leuven, Division Forest, Nature and Landscape, Celestijnenlaan 200E – 2411, BE-3001 Leuven, Belgium
[h] Technological Institute, Furniture, Environment, Economy, Primary processing and supply (FCBA), 10 rue Galilée, 77420 Champs sur Marne, France
[i] Department of Dendrometry and Forest Productivity, Faculty of Forestry, Warsaw University of Life Sciences, Nowoursynowska 159, 02-787 Warsaw, Poland
[j] Czech University of Life Sciences, Faculty of Forestry and Wood Sciences, Kamycka 1176, 16521 Prague 6, Czech Republic
[k] Wageningen University, Laboratory of Geo-Information Science and Remote Sensing, P.O. Box 47, 6700 AA Wageningen, The Netherlands
[l] INIA-CIFOR, Departamento de Selvicultura y Gestión de los Sistemas Forestales, Ctra. A Coruña, km 7,5, 28040 Madrid, Spain
[m] Norwegian Forest and Landscape Institute, Høgskoleveien 8, Postboks 115, 1431 Ås, Norway
[n] Wageningen University, Forest Ecology and Forest Management Group, P.O. Box 47, 6700 AA Wageningen, The Netherlands
[o] Université Libre de Bruxelles (ULB), Institute for Environmental Management and Land Use Planning (IGEAT), Avenue Franklin D. Roosevelt 50 CP 130/02, B-1050 Brussels, Belgium

ARTICLE INFO

Article history:
Received 4 August 2015
Received in revised form 30 September 2015
Accepted 7 November 2015

Keywords:
Biomass
Carbon
Forest inventory
Allometric biomass functions
Biomass expansion factors
Europe

ABSTRACT

National and international carbon reporting systems require information on carbon stocks of forests. For this purpose, terrestrial assessment systems such as forest inventory data in combination with carbon estimation methods are often used. In this study we analyze and compare terrestrial carbon estimation methods from 12 European countries. The country-specific methods are applied to five European tree species (*Fagus sylvatica* L., *Quercus robur* L., *Betula pendula* Roth, *Picea abies* (L.) Karst. and *Pinus sylvestris* L.), using a standardized theoretically-generated tree dataset. We avoid any bias due to data collection and/or sample design by using this approach. We are then able to demonstrate the conceptual differences in the resulting carbon estimates with regard to the applied country-specific method. In our study we analyze (i) allometric biomass functions, (ii) biomass expansion factors in combination with volume functions and (iii) a combination of both. The results of the analysis show discrepancies in the resulting estimates for total tree carbon and for single tree compartments across the countries analyzed of up to 140 t carbon/ha. After grouping the country-specific approaches by European Forest regions, the deviation within the results in each region is smaller but still remains. This indicates that part of the observed differences can be attributed to varying growing conditions and tree properties throughout Europe. However, the large remaining error is caused by differences in the conceptual approach, different tree allometry, the sample material used for developing the biomass estimation models and the definition of the tree compartments. These issues are currently not addressed and require consideration for reliable and consistent carbon estimates throughout Europe.

1. Introduction

Forests play an integral role in the global carbon cycle. According to the Food and Agriculture Organization (FAO, 2013), forests cover about 31% of the land surface area. Forests store about 2.4 Pg of carbon per year (Pan et al., 2011) and sequester about 30% of the current global CO_2 emissions, thus reducing the atmospheric CO_2 concentration by almost a third (Canadell et al., 2007). In the past the production of timber and fuel wood was the primary objective of forest management (FOREST EUROPE, UNECE, FAO, 2011). Today non timber forest ecosystem services such as clean

* Corresponding author.
E-mail address: mathias.neumann@boku.ac.at (M. Neumann).

http://dx.doi.org/10.1016/j.foreco.2015.11.016
0378-1127/

air and water, protection against natural hazards, and biodiversity are of increasing interest (EUROSTAT, 2012). Following the Kyoto Protocol the forest's ability to store carbon and produce renewable energy in the form of biomass became a focal point in natural resource management. Within Europe (EU-27), 18.3% of the energy is generated from renewable sources, with 67.7% of that consisting of biomass (including renewable waste; EUROSTAT, 2012).

The increasing demand on European forests and their services requires consistency in forest information and monitoring. The primary source of forest information is produced by National Forest Inventories (NFIs), which often vary in terms of their conceptual approaches, sampling designs and data collection systems (Tomppo et al., 2010). Aside from more traditional applications such as monitoring forest resources and the sustainability of forestry, NFI data are of increasing interest for assessing the role of forests in the carbon cycle (e.g., for Kyoto reporting or future climate-related treaties such as the REDD+ Programme; Mohren et al., 2012).

Forest inventories record tree data which are, in turn, used for estimating standing timber volume in m^3/ha. The same tree measures can be used to derive total biomass or carbon content of forest ecosystems in t/ha. Biomass is the dry weight of wood estimated for constant conditions (i.e., oven dried wood samples until a constant weight is reached; Bartelink, 1996; Repola, 2008, 2009 or Cienciala et al., 2006). Carbon accounts for approximately half of this oven dried biomass, which consists mainly of polysaccharides such as cellulose, lignin and hemicellulose (Lamlom and Savidge, 2003; McGroddy et al., 2004).

Two conceptually different approaches are used to assess carbon stocks of forests: (i) the biogeochemical-mechanistic approach, and (ii) the statistical empirical approach. The biogeochemical-mechanistic approach is based on physiological principles of carbon uptake through photosynthesis and carbon loss due to the respiration and decomposition processes. This approach uses energy, water, and nutrient cycles to determine the carbon fluxes of an ecosystem. This method is implemented in large scale carbon cycle models and requires soil data, daily climate information and ecophysiological parameters for the given vegetation or forest ecosystem.

Carbon related outputs include GPP (Gross Primary production), NPP (Net Primary production) as well as stem, root or leaf carbon. Any comparison with terrestrial data such as forest inventory data requires a transfer function (Eastaugh et al., 2013), i.e., converting the model output carbon into tree volume (usually biomass expansion factors). These principles have been implemented in large scale carbon cycle models to circumvent the problem of missing terrestrial data and to provide methodologically consistent carbon cycle information for large regions, continents or even for the whole globe (VEMAP Members, 1995). Examples of models that use such an approach are BIOME BGC (Thornton, 1998; Thornton et al., 2002; Pietsch et al., 2005), CLM (Lawrence et al., 2011) and C-FIX (Veroustraete et al., 2002). A related product, known as the MOD17 product, implements key components of BIOME BGC with additional use of satellite data and provides GPP and NPP estimates on a $0.0083^\circ \times 0.0083^\circ$ resolution (approx. 1×1 km) for the whole globe (Running et al., 2004; Zhao and Running, 2010).

The statistical empirical approach is probably more commonly used in forestry, since it was developed earlier than the biogeochemical approach and requires terrestrial data such as forest inventory data (Tomppo et al., 2010). With this approach, biomass and carbon are estimated by applying (i) allometric biomass functions and/or (ii) biomass expansion factors.

Allometric biomass functions use tree variables such as diameter at breast height and/or tree height for estimating tree biomass. The share of carbon is then estimated using tree carbon fraction factors. In contrast, when using biomass expansion factors, conversion factors are used to transform tree volume into biomass. Volume functions must be used before the application of the expansion factors.

These statistical principles in deriving terrestrial biomass and carbon are also implemented in tree population models such as succession or gap models and typical tree growth models. Predicted volume or tree dimensions such as diameter or height serve as input parameters to apply either biomass functions or biomass expansion factors for calculating the terrestrial biomass in t/ha. Typical examples are succession models like PICUS (Lexer and Hoenninger, 2001; Seidl et al., 2005), LANDCARB (Mitchell et al., 2012), the matrix model EFISCEN (Nabuurs et al., 2000) or tree growth models such as MOSES (Hasenauer, 1994), PROGNAUS (Sterba and Monserud, 1997), SILVA (Pretzsch et al., 2002) or BWINPro (Nagel, 1999).

Allometric biomass and volume functions as well as biomass expansion factors are derived empirically from tree sampling. Destructive sampling, extensive field and lab work are needed to obtain biomass data for the different tree compartments – stem, branches, roots and foliage. Based on these sample data, generalized statistical functions for the different tree compartments or expansion factors are developed and applied to inventory data. Every region or country has different resulting functions and factors (e.g. for Austria Pollanschütz, 1974; for Romania Giurgiu et al., 1972; for Sweden Marklund, 1988; for Finland Repola, 2008, 2009 or for France Vallet et al., 2006). Examples for biomass functions developed for larger regions are Wirth et al. (2004), Muukkonen (2007) or Wutzler et al. (2008). The resulting biomass and carbon estimates strongly depend on the samples, but also on the chosen conceptual approach (i.e., whether biomass functions or biomass expansion factors are used).

Previous studies have shown that throughout many parts of the world, the calculation methods have a large impact on the results for biomass and carbon, both for trees and for tree compartments (Araújo et al., 1999 for Brazil; Westfall, 2012 and MacLean et al., 2014 for Northeastern United States; Guo et al., 2010 for China; Jalkanen et al., 2005 for Sweden, or Thurnher et al., 2013 for Austria). This supports the necessity for a similar study for Europe; however such a study was not done until now.

In Europe, National Forest Inventory data is commonly used for country reporting for international statistics and programs such as the Forest Resource Assessment Program for the Food and Agriculture Organization (FAO), or the Land Use, Land-Use Change and Forestry (LULUCF) report for the United Nations Framework Convention on Climate Change (UNFCCC; Tomppo et al., 2010). However, consistent calculation methods are required to be able to integrate and assess data from various countries for the purpose of assessing climate change mitigation or carbon sequestration potential in European forests (McRoberts et al., 2009; Ståhl et al., 2012).

The purpose of this study is to analyze the different carbon estimation methods covering 12 different countries across Europe and assess the impact of the methodological differences in deriving biomass estimates. Five important tree species in Europe are selected for comparison (*Fagus sylvatica, Quercus robur, Betula pendula, Picea abies* and *Pinus sylvestris*). We are specifically interested in

(i) compiling and assessing country-specific calculation methods for deriving biomass and carbon from NFI data; and
(ii) quantifying the effect of the various calculation methods on resulting biomass and carbon estimates using a standardized theoretical data set.

2. Methods

Europe's forests consist of a variety of ecological and climatic conditions covering different tree species. For our study we select

5 species considered to be important European tree species because they have a large distributional range and a high ecological and economic value. The selected deciduous tree species are (i) *F. sylvatica* L. (European beech), (ii) *Q. robur* L. (Pedunculate oak) and (iii) *B. pendula* Roth (Silver birch) and the two coniferous species, (iv) *P. abies* (L.) Karst. (Norway spruce) and (v) *P. sylvestris* L. (Scots pine).

Q. robur also includes *Quercus petraea* L. and *B. pendula* includes *Betula pubescens* Ehrh., since these species are similar in terms of genetics, shape and properties and thus are usually not distinguished from one another by NFI systems or biomass studies (e.g., Muukkonen, 2007; Repola, 2009; Giurgiu et al., 1972; Ledermann and Neumann, 2006).

Within Europe, each country has its own statistical empirical approach for deriving carbon estimates from National Forest Inventory data (Tomppo et al., 2010). We obtain each of these procedures for our comparative analysis. Below, we describe the methods employed for the 12 countries. For a detailed presentation, by country, we refer to Appendices A–M.

2.1. General carbon calculation approach

Biomass is commonly estimated by separate tree compartments (e.g. Wirth et al., 2004; Seidl et al., 2005; Pietsch et al., 2005; Thurnher et al., 2013). We consider four tree compartments for estimating biomass: (i) stem, (ii) branches, (iii) foliage, and (iv) root (including stump). The general equation for calculating total tree carbon can be expressed as:

$$C_{tree} = CC * (dsm + dbm + dfm + drm) \quad (1)$$

where C_{tree} is the total carbon content of a tree [kg], CC is the carbon fraction [kg/kg] given for each country in Appendix A, dsm is the dry stem biomass [kg], dbm is the dry branch biomass [kg], dfm is the dry foliage biomass [kg] and drm is the dry root biomass [kg]. For each country the species specific carbon calculation methods are compiled (see Appendices A–M).

2.2. Carbon calculations by country

European forests cover a wide range of environmental conditions, as well as large elevation and latitudinal gradients. According to FOREST EUROPE, UNECE, FAO (2011) suggestions to limit the range of these environmental, elevation and latitudinal gradients, we cluster the 12 countries which provide biomass estimation methods for our study into four geographic regions: North Europe, Central-West Europe, Central-East Europe, and South Europe. The underlying assumption is that countries within each region should have similar climatic and biophysical conditions for tree growth and we expect that this will reduce the variation in tree allometry. Table 1 summarizes the 12 country-specific carbon estimation methods and the required tree variables.

All carbon calculation methods use diameter at breast height (DBH) and tree height (H) as input variables. In five countries (Finland, Austria, Germany, the Netherlands, and Romania) additional variables are used: crown ratio (CR), aboveground volume (V), and tree age (A). Six methods use allometric biomass functions, three use biomass expansion factors and four use a combination of both (see Table 1). The carbon calculation method, by country, including the coefficients and the definitions of the tree compartments are given in Appendices A–M. Below, we give a brief summary by region.

2.2.1. Northern Europe

Two countries, Finland and Norway, belong to Northern Europe. In Finland (also representing Estonia) the allometric biomass functions use DBH, tree height, and crown ratio. The models developed for Finland obtain carbon from biomass with a constant carbon fraction of 0.5 (see Appendix B). The carbon estimation approach of Finland is also applied in Estonia since forest biomass functions for Estonia are currently under development (Uri et al., 2010).

The Norwegian methodology uses allometric biomass functions. The method for Norway was developed in Sweden (Marklund, 1988; Petersson and Ståhl, 2006). The models use DBH and tree height as variables (see Appendix C).

F. sylvatica is not native in Finland or Norway, thus it is excluded from the analysis for Northern Europe.

Table 1
Summary on calculation Methods (AF = allometric biomass functions, BEF = biomass expansion factors and volume functions, combi = combination of AF and BEF) and used Variables in the calculations (DBH = diameter at breast height, H = tree height, CR = crown ratio, A = tree age, V = aboveground tree volume), variables in brackets indicate that this variable is only used in some functions.

Region	Country	Method	Variables
North Europe	Finland	AF	DBH, *H*, (CR)
	Norway	AF	DBH, (*H*)
Central-West Europe	Austria	combi	DBH, (*H*, CR, *A*)
	Belgium	combi	DBH, (*H*)
	France	BEF	DBH, (*H*)
	Germany	combi	DBH, *H*, (*V*, *A*)
	Netherlands	BEF	DBH, *A*, (*H*)
Central-East Europe	Czech Republic	combi	DBH, (*H*)
	Poland	AF	DBH, (*H*)
	Romania	BEF	DBH, *H*, *A*
South Europe	Italy	AF	DBH, *H*
	Spain	AF	DBH, (*H*)

2.2.2. Central-Western Europe

Five countries, Austria, Belgium, France, Germany and the Netherlands, belong to Central-Western Europe. The biomass calculation in Austria uses a combination of species-specific form factor functions, biomass expansion factors, and allometric biomass functions. The allometric biomass functions for branch biomass use crown ratio as an additional input variable (Ledermann and Neumann, 2006), while the functions for root biomass use tree age (Wirth et al., 2004). The volume and branch biomass functions use data from Austria, while the foliage and root biomass function obtain their data from other Central European countries (see Appendix D).

The Belgian biomass calculation method is a combination of volume estimation, expansion factors, and allometric biomass functions. The volume prediction (Dagnelie et al., 1985) and the biomass functions of *P. abies* depend on DBH and tree height. All other biomass functions use only DBH as input variable. The volume calculation method and most of the biomass functions mainly use data from Belgium. Some biomass functions are obtained from other countries such as Austria, the Czech Republic, Germany, France, and the Netherlands (see Appendix E).

In France, the biomass calculation method combines volume functions with biomass expansion factors derived from samples in France (INRA, 2004). Foliage biomass is assumed to be a constant proportion of total biomass (see Appendix F). For all species in France a carbon fraction of 0.475 is used (see Appendix A), which differs from most other countries.

In Germany, a combination of volume functions, biomass expansion factors and allometric biomass functions is applied. The volume calculation is implemented in the program BDAT 2.0 (Kublin, 2002). The expansion factors for tree volume vary by tree age and the expansion factors for root biomass vary by aboveground biomass (see Appendix A). The models (except foliage

biomass) are developed with sample material from Germany (see Appendix G).

The method for the Netherlands uses allometric biomass functions to calculate aboveground tree biomass. Aboveground biomass is then separated into tree compartments with proportional biomass fractions. The biomass fractions are derived from tree age and are calculated based on the allometric biomass functions of the EFISCEN project (Schelhaas et al., 1999; Vilén et al., 2005). The biomass calculations for aboveground biomass and the fraction coefficients come from sample material across Europe and the European part of Russia (see Appendix H).

2.2.3. Central-Eastern Europe

Three countries, Czech Republic, Poland, and Romania, belong to Central-Eastern Europe. The Czech Republic biomass calculation method is similar to Austria and Belgium, using a combination of volume functions, expansion factors, and allometric biomass functions. The functions were developed based on sample material from the Czech Republic or former Czechoslovakia (see Appendix I).

In Poland, allometric biomass functions are used for aboveground biomass and expansion factors for belowground biomass. The functions are developed with sample data from Poland, Finland and Central Europe (see Appendix J).

The calculation in Romania uses a combination of volume functions, biomass expansion factors and biomass fractions similar to the Netherlands. The volume functions based on data from Romania (Giurgiu et al., 1972) provide tree volume. After applying biomass expansion factors, the biomass of tree compartments is estimated using biomass fractions from the EFISCEN project (Schelhaas et al., 1999; Vilén et al., 2005) (see Appendix K).

2.2.4. Southern Europe

Two countries, Italy and Spain, belong to Southern Europe. Italy uses allometric biomass functions developed with sample material from Italy for aboveground biomass and expansion factors for root biomass (see Appendix L).

In Spain allometric biomass functions developed with Spanish sample data are used. Similar to France, the carbon fractions in Spain differ from the other countries. Species-specific carbon fractions given by Montero et al. (2005) are used (see Appendix A, and for further details Appendix M).

3. Data

Forests across Europe vary by site conditions, age, and genetics and usually have experienced different forest management. Furthermore, available forest inventory data sets differ according to (i) the sampling design (i.e., fixed area plots vs. angle count sampling), (ii) the measurement methods (i.e., minimum diameter threshold for recording trees) or (iii) the data collection and processing method (i.e., measurement of tree height for every tree vs. applying diameter–height relationships, etc.). These differences in forest data from country to country make a theoretical comparison of the different regional biomass calculation methods difficult (Tomppo et al., 2010).

In order to circumvent this problem we produce a standardized input dataset, which provides all necessary input data for the country-specific models (see Appendices A–M). This ensures that any differences in the results are a consequence of the carbon calculation methods.

3.1. Stand data generation

For creating a standardized data set we use STANDGEN (Kittenberger, 2003), a tool implemented in the framework of the single tree simulation model MOSES (Hasenauer, 1994; Klopf et al., 2011). The STANDGEN tool generates stand data including diameter and location of single trees based on information on diameter distribution (mean and standard deviation), spatial distribution, and aggregation of trees. For each of the five selected tree species, three stands are generated, each with a size of 0.25 hectare (2500 m^2). The three stands differ in mean and standard deviation of tree diameter and represent forest stands at different ages. This takes into account that stand age affects eco-physiological processes such as biomass allocation, stem number, or stocking density. For each species, we generate a young stand (quadratic mean DBH 10 cm with standard deviation 1 cm), a middle-aged stand (30 cm ± 5 cm), and an old stand (50 cm ± 10 cm). Note that we use the quadratic mean DBH to refer to the "average or central tree" representing the tree with the mean basal area. For convenience we consider that a tree with quadratic mean DBH represents a tree with "mean tree biomass". We follow here Eastaugh (2014) showing that the error in this assumption is small. Tree height and age are estimated using species-dependent relationships, crown length is estimated using the DBH-, and height-dependent functions implemented in the MOSES framework (Sterba, 1976; Marschall, 1992; Klopf et al., 2011).

3.2. Stand variables

The generated stands are characterized by the stand variables: mean tree height, height–diameter ratio, crown ratio, stand age, stem number per hectare (N), and basal area per hectare (BA). The two latter variables are calculated as follows.

$$BA = 1/S * \Sigma(DBH^2 * \pi/400) \quad (2)$$

$$N = 1/S * ni \quad (3)$$

where BA is the basal area per hectare [m^2/ha], S is equal to 0.25 ha (the size of the generated stand), DBH is the diameter at breast height (at 1.3 m) [cm], N is the stem number per hectare [trees/ha], and ni is the number of trees per stand. Summary statistics of the generated stand properties available for our study are given in Table 2. Tree height, stand age and basal area increase with increasing DBH, while the height–diameter ratio, crown ratio and stem number decrease, meaning that these stand properties change with age (Table 2).

4. Analysis and results

4.1. Tree carbon estimation

We start our analysis by applying the 12 country specific carbon calculation methods as outlined in Appendices B–M to our standardized tree data set. The data set covers five tree species: (i) *F. sylvatica* L., (ii) *Q. robur* L., (iii) *B. pendula* Roth, (iv) *P. abies* (L.) Karst. and (v) *P. sylvestris* L. (Table 2). We calculate biomass for the tree compartments stem, branch, foliage and roots. The biomass results by compartment are added and multiplied with the carbon fraction (Appendix A) to derive total tree carbon. Since the input data set is identical by species, we ensure that any differences in the results represent (i) differences in the calculation approach, (ii) the statistical coefficients and/or (iii) any additional regional biophysical differences by species. Fig. 1 provides the total carbon in kg per tree versus diameter at breast height (DBH) by

Table 2
Properties of the generated standardized tree dataset separated by stands and species, first column properties of stand with quadratic mean diameter (DBH) of 10 cm, second for DBH of 30 cm, third for DBH 50 cm, Stand age [year] derived from yield tables (see Method section), Stem number is number of trees per hectare [ha^{-1}], Basal area is the area of trees at breast height (1.3 m) per hectare [m^2/ha], Mean height is Lorey's mean height (Lorey, 1878) of all trees in stand [m], Mean H/DBH is the mean height-to-diameter ratio [m/m], Mean CR is mean crown ratio (crown height divided by tree height) [m/m].

	Stand age [year]			Stem number [ha^{-1}]			Basal area [m^2/ha]		
	10 cm	30 cm	50 cm	10 cm	30 cm	50 cm	10 cm	30 cm	50 cm
Picea abies	25	70	150	3404	740	304	27	52	65
Pinus sylvestris	35	115	>130	2776	576	240	22	41	50
Fagus sylvatica	40	85	>140	3064	496	188	24	35	37
Quercus robur	35	90	>130	2248	440	212	18	31	39
Betula pendula	17	75	>120	2148	412	160	17	29	31
	Mean height [m]			Mean H/DBH [m/m]			Mean CR [m/m]		
Picea abies	8.5	22.6	30.9	83	75	59	0.73	0.58	0.46
Pinus sylvestris	6.6	18.8	26.6	65	62	52	0.79	0.61	0.48
Fagus sylvatica	8.7	20.8	26.7	87	69	54	0.71	0.59	0.48
Quercus robur	8.4	25.2	31.5	82	84	66	0.73	0.55	0.47
Betula pendula	8.4	25.3	31.9	81	84	65	0.73	0.55	0.46

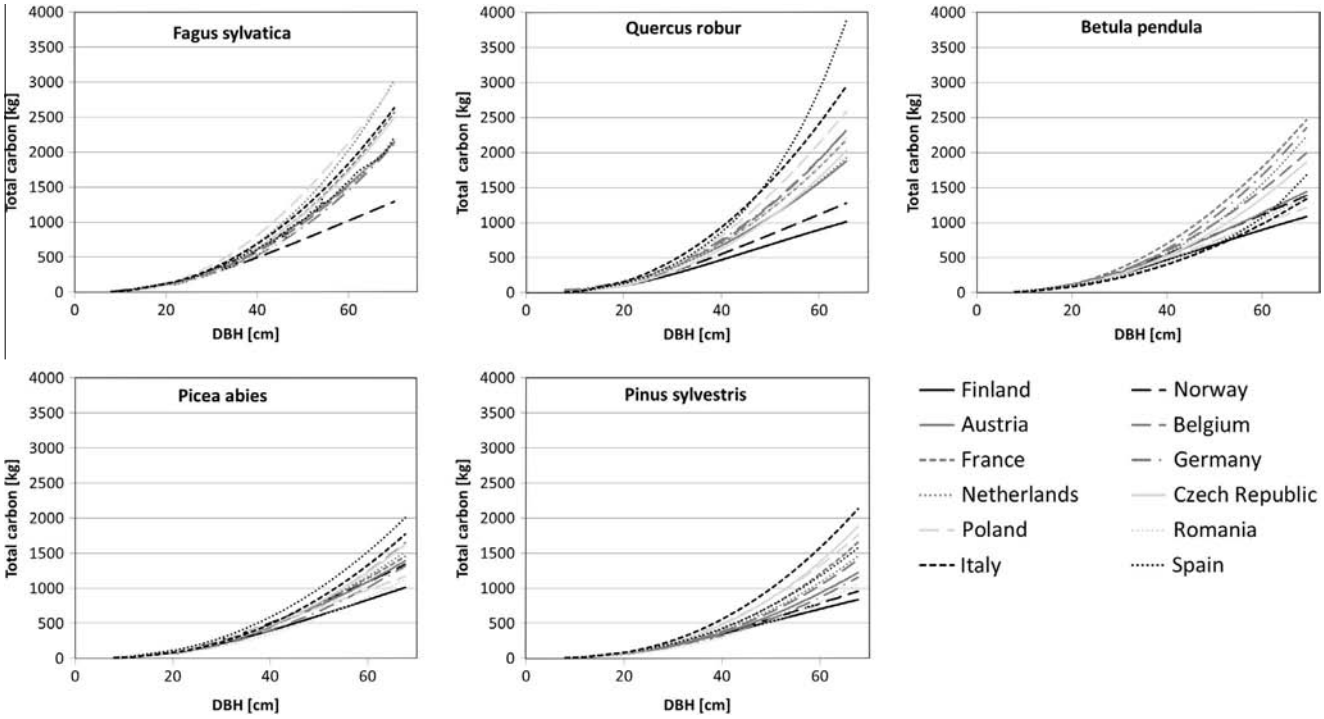

Fig. 1. Tree carbon on tree level [kg/tree] for all countries in this study and for all analyzed tree species, results are grouped by ecoregions (black – North Europe and South Europe, dark gray – Central-West Europe, light gray – Central-East Europe).

species and country. In Fig. 1, and in the following Figs. 2–7, we present curves that originate from the smoothed single tree results.

Strong discrepancies with increasing DBH are evident (Fig. 1) by country. Thus we subsequently group the country-specific results by European forest regions following the definition of the State of Europe's Forests 2011 (FOREST EUROPE, UNECE, FAO, 2011) to address regional biophysical growing conditions resulting from the geographic location, soil and climate conditions, and genetic differences by species across Europe. Country specific biomass estimation methods (Appendices B–M) were developed and calibrated with regional data. Thus the resulting carbon and biomass estimates are expected to capture the different regional biophysical growing conditions. We assign each tree species and country-specific estimation method to each of the four European forest regions. The results for tree carbon in kg per tree versus DBH are ordered by country and grouped by European forest region as shown in Figs. 2–5.

4.2. Tree biomass estimation by compartment

Total tree carbon (Figs. 1–5) is calculated as the sum of the estimated biomass of each compartment (stem, branches, foliage and roots) multiplied by the carbon fraction factor (Eq. (1) and Appendices A–M). Next we evaluate the proportions of the compartment results and their respective discrepancies by species and country across Europe. Since *P. abies* and *F. sylvatica* are the most important coniferous and broadleaf species and cover the vast majority of forest area in Central-East and Central-West Europe, we focus and display here only these two species within these two regions. Fig. 6 presents the trend in the four compartments versus DBH for *P. abies* in Central-West Europe, and Fig. 7 for *F. sylvatica* for Central-East Europe, respectively. We use the identical scaling to show (i) the effect of the different functions by compartment applied and (ii) their contribution to the total tree carbon.

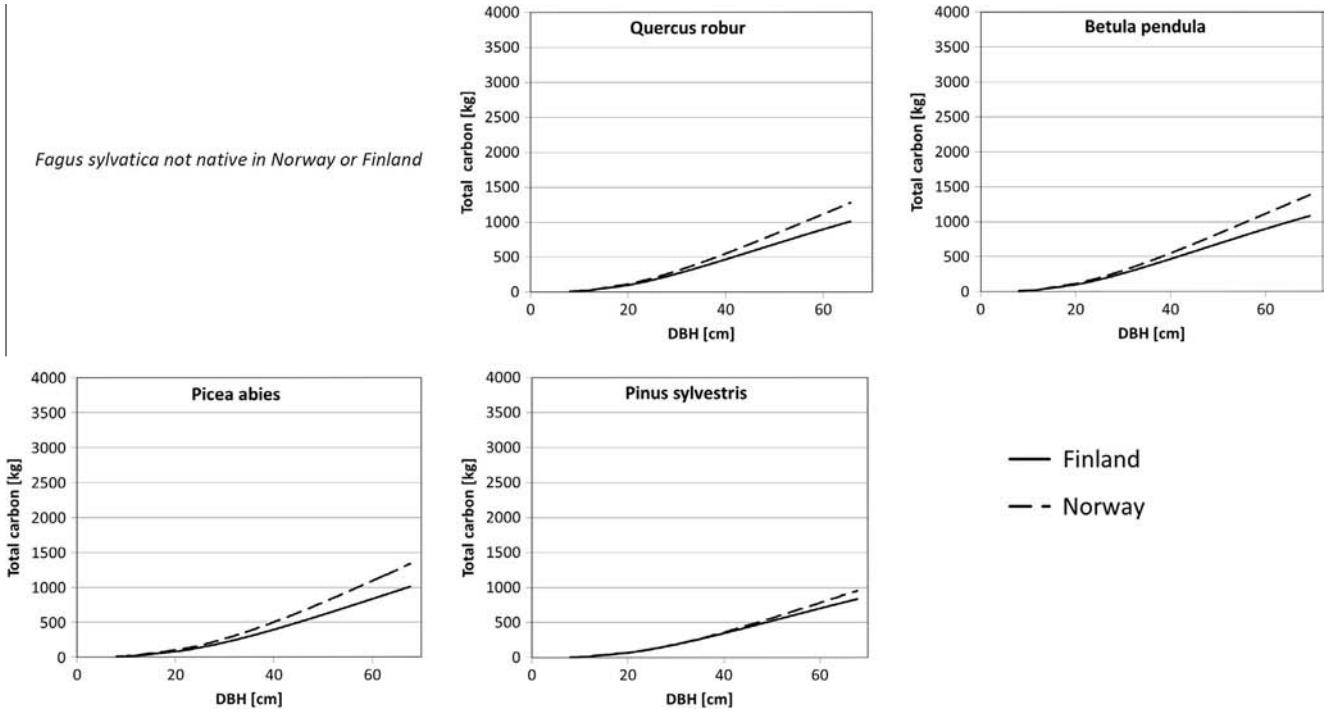

Fig. 2. Tree carbon on tree level [kg/tree] for North Europe and for all analyzed tree species.

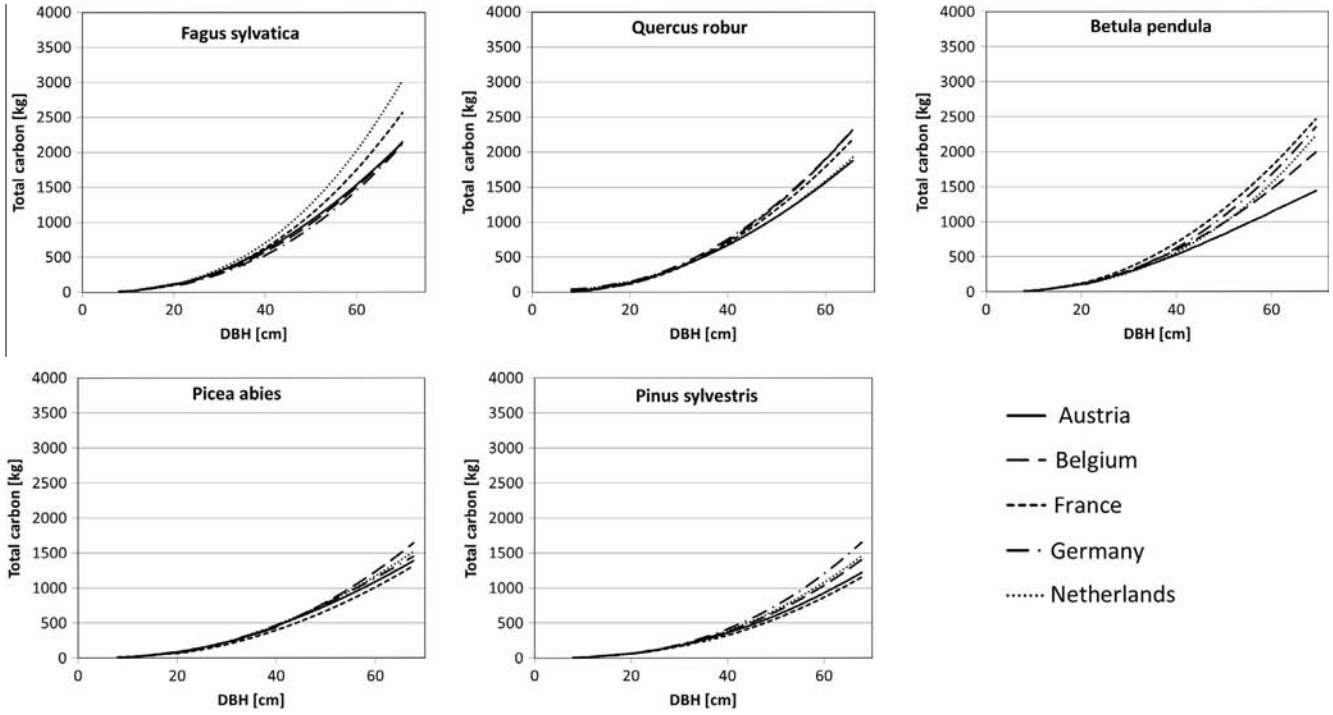

Fig. 3. Tree carbon on tree level [kg/tree] for Central-West Europe and for all analyzed tree species.

4.3. Carbon and biomass of forest stands

The deviations found in the country-specific tree carbon estimates by DBH (see Figs. 1–7) may differ from carbon estimates at the forest stand-level since the number of trees by DBH class varies. In addition, most carbon studies focus on stand level estimates (e.g. t/ha). Therefore, we assess the methodological implications at the forest stand level by country and the species-specific carbon calculation method by deriving forest stand carbon estimates for our generated forest stands. Again, we choose to focus on *P. abies* and *F. sylvatica* and the corresponding three reference stands with a quadratic mean DBH of 10 cm (standard deviation (SD) of DBH distribution 1 cm), 30 cm (SD 5 cm) and 50 cm (SD 10 cm) generated with the tool STANDGEN (see Table 2).

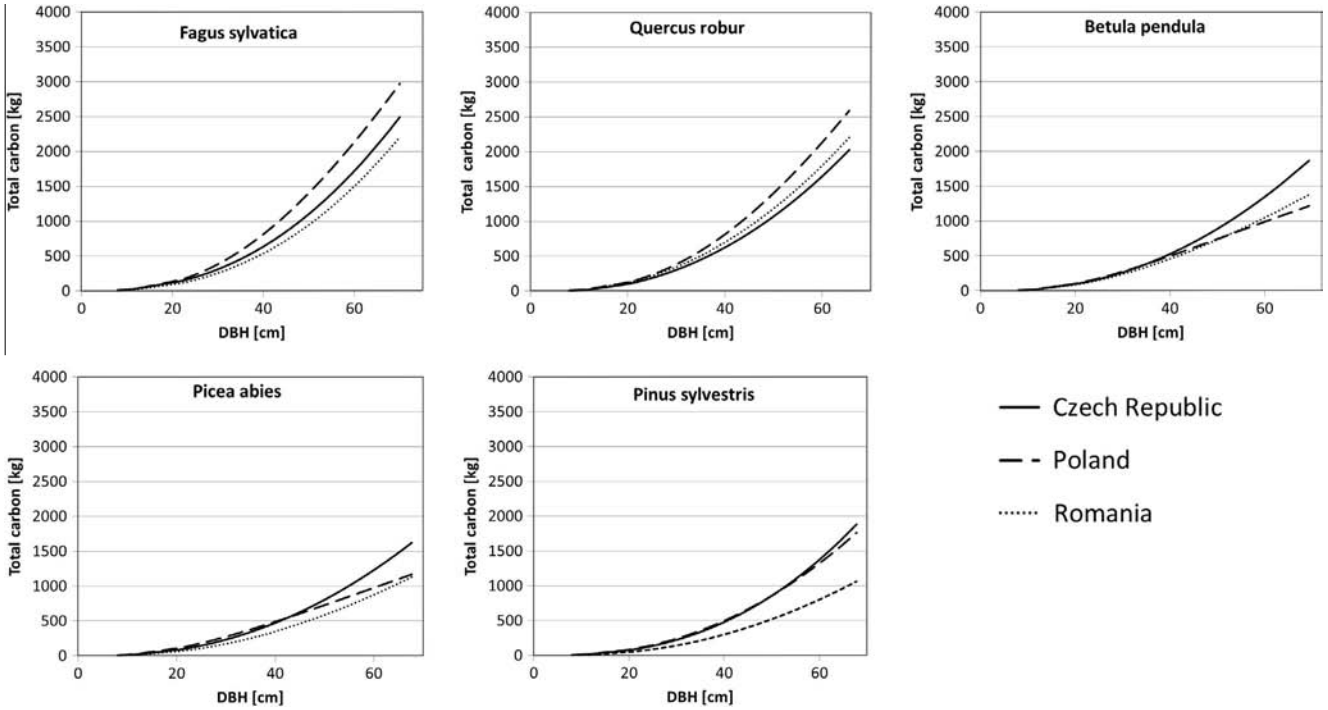

Fig. 4. Tree carbon on tree level [kg/tree] for Central-East Europe and for all analyzed tree species.

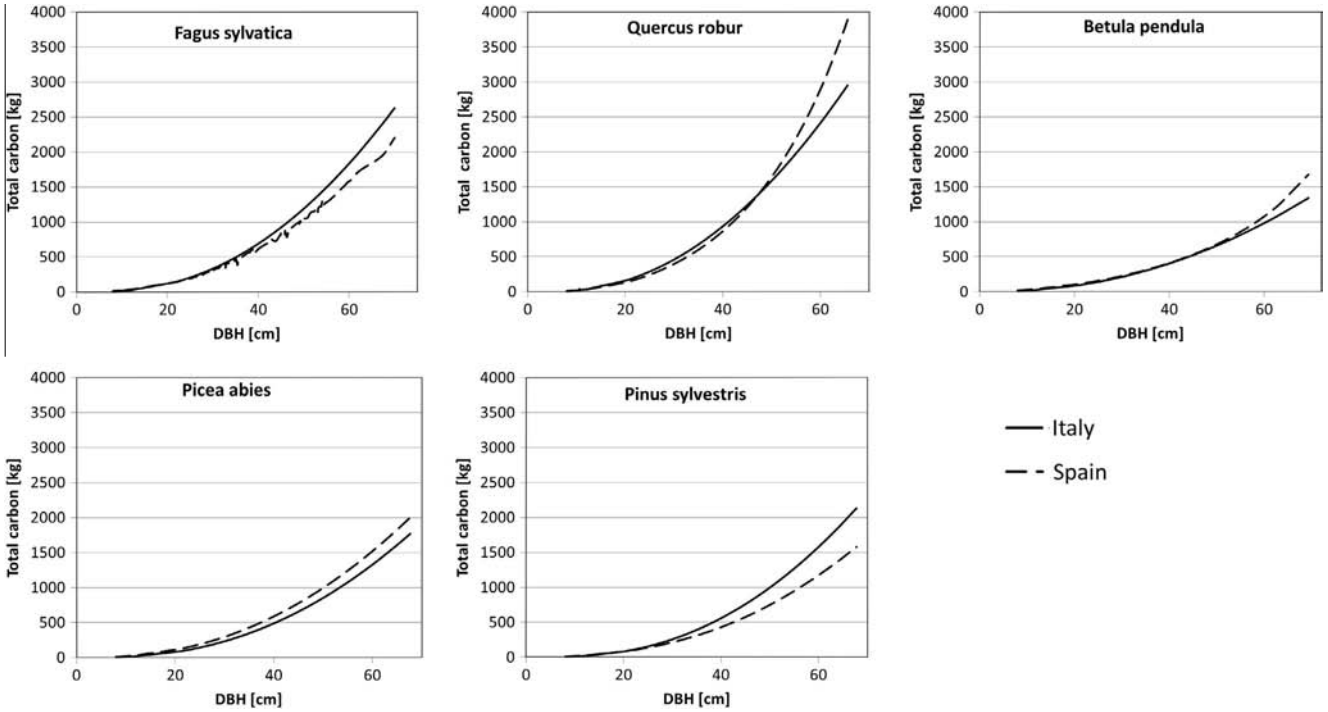

Fig. 5. Tree carbon on tree level [kg/tree] for South Europe and for all analyzed tree species.

For each tree, the biomass and carbon estimation methods are applied. The results for *P. abies* and *F. sylvatica* covering the stem, branch, foliage, root, and total tree biomass plus the tree carbon estimates for each reference stand are given in Tables 3 and 4. Again, we use the quadratic mean DBH representing the tree with mean basal area and mean tree biomass (Eastaugh, 2014). Tables 3 and 4 also provide summary statistics for *P. abies* and *F. sylvatica*. Similar tables for the other species, we provide in Supplementary material (Tables S.1–S.3).

5. Discussion

Carbon estimates by tree species differ substantially by country (see Fig. 1). After grouping the countries by main forest region in Europe (FOREST EUROPE, UNECE, FAO, 2011) to address regional differences, the deviations by species and country within the forest region are found to be smaller, but still evident (Figs. 2–5). The smallest deviations are detected for the North Europe and South

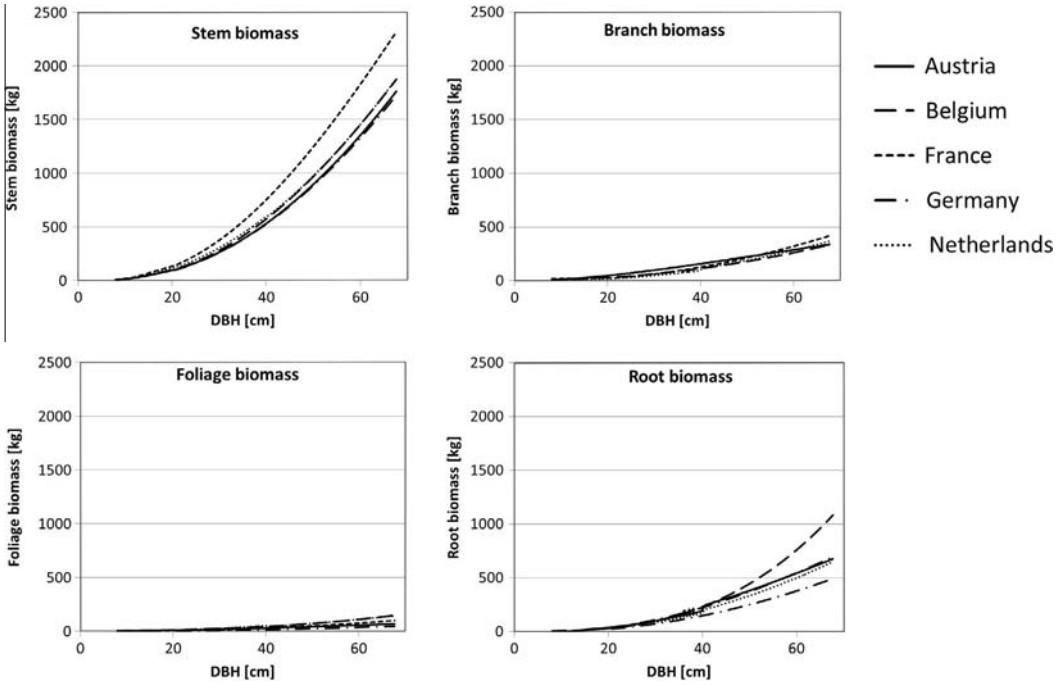

Fig. 6. Biomass in tree compartments on tree level [kg/tree] for *Picea abies* and Central-West Europe.

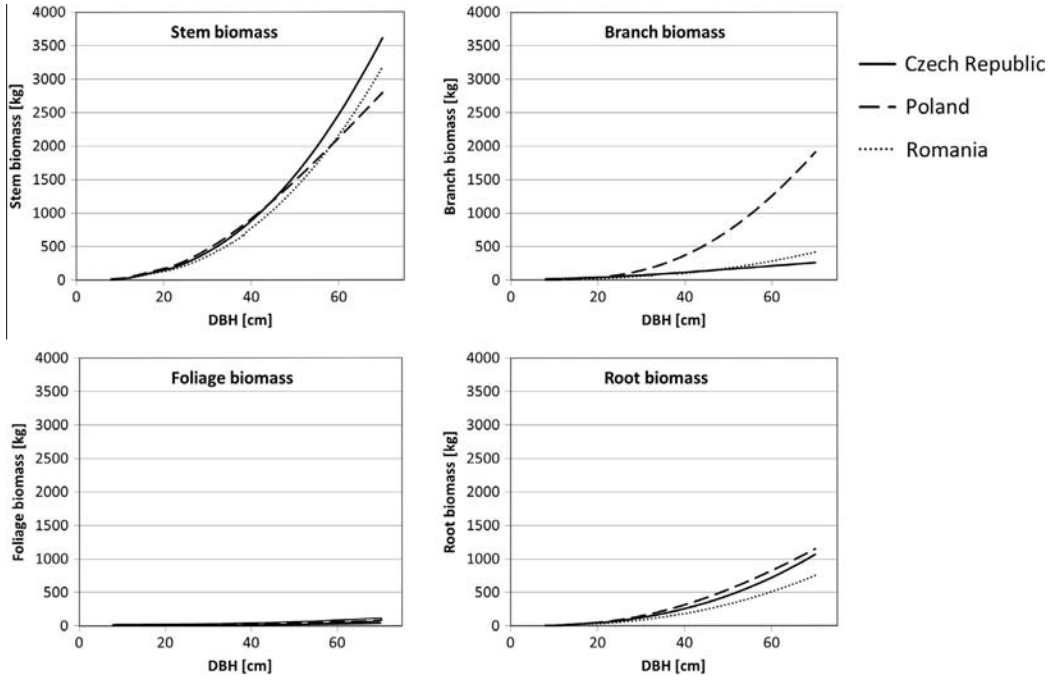

Fig. 7. Biomass in tree compartments on tree level [kg/tree] for *Fagus sylvatica* and Central-East Europe.

Europe regions (Figs. 2 and 5), as compared to Central-West Europe (Fig. 3) and Central-East Europe (Fig. 4). This supports the hypothesis that part of the observed differences can be attributed to environmental growing conditions. The remaining error is caused by the conceptual approach. Stem biomass contributes the largest proportion of total biomass followed by root, branch, and foliage biomass (Figs. 6 and 7). Some unrealistic results are detected, for example in the case of branch biomass for *F. sylvatica* in Poland (Fig. 7).

The results at the stand level (Tables 3 and 4 and Tables S.1–S.3 in Supplementary material) confirm that the differences in tree carbon and biomass in tree compartments at the tree level (Figs. 1–7) can be observed also on the stand level. Tables 3 and 4 further allows quantifying the discrepancies in carbon and biomass observed merely visually in Figs. 1–7. For both *P. abies* and *F. sylvatica,* stem biomass add the largest part to the existing discrepancies in total biomass and carbon followed by branch and root biomass. The average range of stem biomass estimates for all countries and

Table 3
Results for biomass in tree compartments, tree biomass (sum of all compartments) and tree carbon on stand level [t/ha] for *Picea abies*, results arranged according to the 4 Forest regions, first column give the results for the stand with quadratic mean diameter (DBH) of 10 cm, second column for DBH of 30 cm and third column for DBH of 50 cm. At the end of table selected statistics are given for each stand and each biomass and carbon estimate: Mean and Range (Maximum–Minimum) of the country estimates and variation expressed as Range divided by Mean.

Picea abies	Stem biomass [t/ha]			Branch biomass [t/ha]			Foliage biomass [t/ha]			Root biomass [t/ha]			Tree biomass [t/ha]			Tree carbon [t/ha]		
	10 cm	30 cm	50 cm	10 cm	30 cm	50 cm	10 cm	30 cm	50 cm	10 cm	30 cm	50 cm	10 cm	30 cm	50 cm	10 cm	30 cm	50 cm
North Europe																		
Finland	49.6	186.3	232.0	17.1	41.7	42.5	12.6	18.0	12.0	29.8	85.7	118.9	109.0	331.6	405.4	48.2	155.9	197.7
Norway	48.2	217.7	316.6	40.1	80.4	80.1	16.3	27.1	25.0	27.4	91.9	113.0	132.1	417.1	534.6	57.9	193.8	256.1
Central-West Europe																		
Austria	45.8	194.3	300.9	45.4	71.4	70.9	11.9	14.1	13.8	13.9	75.3	125.4	117.0	355.0	510.9	52.6	169.7	249.3
Belgium	43.4	206.9	323.5	29.7	47.5	59.8	18.7	18.6	24.6	14.2	76.1	159.1	105.9	349.1	567.1	43.6	164.0	272.6
France	60.2	276.7	412.2	–	–	–	1.2	5.5	8.2	18.1	83.0	123.7	79.5	365.3	544.1	37.8	172.2	259.7
Germany	37.1	192.1	296.2	68.7	46.5	71.7	4.2	11.5	17.0	33.9	54.9	84.6	143.9	304.9	469.5	69.8	145.6	227.4
Netherlands	41.8	224.6	325.7	22.6	36.1	63.7	12.1	20.2	24.6	11.6	64.8	112.3	88.1	345.7	526.3	44.0	171.9	264.1
Central-East Europe																		
Czech Republic	41.1	215.2	346.9	17.5	21.6	26.4	3.5	5.1	6.6	26.7	83.7	133.8	88.8	325.6	513.7	44.4	161.6	258.1
Poland	73.9	278.5	311.2	14.9	32.2	53.0	10.3	15.5	15.5	22.8	75.0	87.3	121.9	401.2	466.9	60.9	199.5	234.6
Romania	29.9	167.0	246.3	16.2	26.8	45.2	8.7	15.0	18.8	8.3	48.2	81.9	63.1	257.0	392.2	31.6	127.6	197.0
South Europe																		
Italy	45.0	210.4	348.5	24.9	60.7	102.6	–	–	–	20.3	78.6	130.8	90.2	349.7	581.9	45.1	173.4	292.4
Spain	55.1	282.8	483.7	60.3	78.9	87.9	4.2	12.3	19.0	34.7	66.9	83.6	154.3	440.9	674.2	77.1	218.8	338.7
Mean [t/ha]	47.6	221.0	328.6	32.5	49.4	64.0	9.4	14.8	16.8	21.8	73.7	112.9	107.8	353.6	515.6	51.1	171.2	254.0
Range [t/ha]	44.0	115.9	251.7	53.8	58.9	76.2	17.5	22.0	18.4	26.4	43.7	77.3	91.2	183.9	282.0	45.6	91.2	141.8
Range/Mean [%]	92	52	77	166	119	119	185	149	109	121	59	68	85	52	55	89	53	56

Table 4
Results for biomass in tree compartments, tree biomass (sum of all compartments) and tree carbon on stand level [t/ha] for *Fagus sylvatica*, for details on the table and the content please see explanations provided for Table 3.

Fagus sylvatica	Stem biomass [t/ha]			Branch biomass [t/ha]			Foliage biomass [t/ha]			Root biomass [t/ha]			Tree biomass [t/ha]			Tree carbon [t/ha]		
	10 cm	30 cm	50 cm	10 cm	30 cm	50 cm	10 cm	30 cm	50 cm	10 cm	30 cm	50 cm	10 cm	30 cm	50 cm	10 cm	30 cm	50 cm
North Europe																		
Finland	–	–	–	–	–	–	–	–	–	–	–	–	–	–	–	–	–	–
Norway	–	–	–	–	–	–	–	–	–	–	–	–	–	–	–	–	–	–
Central-West Europe																		
Austria	55.9	185.4	241.1	36.0	87.9	110.5	3.3	3.5	3.1	12.7	26.3	32.9	107.8	303.1	387.6	53.9	149.9	195.4
Belgium	48.0	189.8	248.0	19.1	46.9	63.4	3.6	6.5	8.8	21.2	47.7	61.8	91.9	290.8	382.0	45.0	141.0	188.7
France	80.8	247.6	345.6	–	–	–	1.6	5.0	6.9	22.6	69.3	96.8	105.1	321.9	449.2	49.9	151.1	215.2
Germany	43.5	168.9	241.8	29.7	38.7	37.2	3.6	6.5	8.8	31.5	49.8	67.0	108.3	263.9	354.7	54.1	130.2	179.1
Netherlands	79.2	233.1	349.7	13.2	39.7	46.1	5.8	5.4	6.3	34.4	58.6	82.8	132.7	336.8	485.0	66.1	166.4	244.6
Central-East Europe																		
Czech Republic	56.1	209.7	299.5	62.0	36.5	30.6	3.0	3.6	4.0	23.4	62.2	87.2	144.6	312.1	421.2	72.3	154.3	212.3
Poland	80.2	229.7	277.2	14.6	74.7	143.1	3.4	6.4	7.7	23.6	74.6	102.7	121.8	385.3	530.7	60.9	190.4	267.7
Romania	54.1	178.9	262.0	9.0	30.5	34.6	4.0	4.1	4.7	23.5	45.0	62.0	90.6	258.5	363.3	45.3	127.7	183.2
South Europe																		
Italy	63.9	230.2	312.6	21.4	48.8	65.0	–	–	–	17.1	55.8	75.5	102.3	334.8	453.1	51.2	165.5	228.5
Spain	69.3	198.9	260.8	46.5	65.1	76.8	5.0	4.9	4.3	32.4	47.2	50.0	153.2	316.2	391.9	76.6	155.6	198.4
Mean [t/ha]	63.1	207.2	283.8	27.9	52.1	67.5	3.7	5.1	6.1	24.2	53.7	71.9	115.8	312.3	421.9	57.5	153.2	211.3
Range [t/ha]	37.3	78.7	108.6	53.0	57.4	112.5	4.2	3.0	5.6	21.8	48.2	69.8	62.5	126.8	176.1	31.6	62.7	88.6
Range/Mean [%]	59	38	38	190	110	167	114	59	92	90	90	97	54	41	42	55	41	42

stands is 137.2 t/ha for *P. abies* (branch 63.0, root 49.1, and foliage 19.3 t/ha) and 74.8 t/ha for *F. sylvatica* (branch 74.3, root 46.6, and foliage 4.3 t/ha). Although the differences of the root, branch and foliage biomass are smaller in absolute terms, the relative differences are even higher as compared to the stem biomass estimates (Average Range/Mean for stem biomass and all stands for *P. abies* 74% (branch 135%, root 83%, and foliage 148%) and for *F. sylvatica* 45% (branch 156%, root 92%, and foliage 88%) (Tables 3 and 4). Therefor the choice of stem biomass function contributes most to total carbon in absolute terms, but the other compartments have an impact as well, especially in proportion to their results.

Tables 3 and 4 further indicate that these discrepancies differ between the different stands. In the younger forest stands (DBH 10 cm) the ratio of Range and Mean of the tree carbon estimates for *P. abies* is 85% and for *F. sylvatica* of 54% and thus highest as opposed to the two older stands. The same patterns are also visible in the biomass compartments (Tables 3 and 4 and Tables S.1–S.3). This is not detectable from the single tree results (Figs. 1–7) since the scaling hides the results at small DBH. The results for the young trees are very small in absolute values compared to the results of bigger trees (Figs. 1–7). Still the total carbon results of the young stands with DBH 10 cm amount for about a fourth of the results of the old stands with DBH 50 cm (21% for *P. abies* and 28% for *F. sylvatica*; Tables 3 and 4). The large amount of carbon in young stands is caused by the large number of trees per unit area (Table 2), which have an amplifying effect on the single tree results and the differences on forest stand level. Comparing only the carbon of single trees would be misleading because the stem number decreases with age due to competition. Such effects need to be considered if the task is to optimize carbon storage for the purposes of climate change mitigation, such as REDD+ (Canadell et al., 2007; Mohren et al., 2012).

Stand-level results for branch and foliage biomass do not show the same increase based upon DBH as do stem and root biomass. The results show that foliage and branch biomass are constant with a modest increase with stand age. This is consistent with the Pipe Model Theory (Shinozaki et al., 1964a,b) and other research indicating that after canopy closure Leaf Area Index (LAI) is a constant (Waring et al., 1982; He et al., 2012).

Our analysis confirms that the general carbon calculation approach (biomass functions vs. conversion factors) in combination with the specific parameter estimates for deriving biomass functions or conversion factors (Appendices A–M) influences the country-specific results. Differences in carbon estimates across countries are affected by regional conditions. However determining the proportion of the detected deviation that is due to the sampling procedure and methods versus the deviation from environmental conditions (e.g. climate, soil or genetics) or differences in tree allometry remains a key question. Since it is very difficult to know the true biomass amount by compartment and tree species, plausibility checks, such as a careful assessment of the (i) original sample material for calibrating and developing regional biomass estimation methods and the (ii) statistical approach are essential. The empirical sample material for the country-specific estimation methods has large discrepancies (see Tables 5 and 6 for *P. abies* and *F. sylvatica* and Tables S.4–S.6 in the Supplementary material for the remaining species).

Most biomass estimation methods applied in this study use sample data mostly within a DBH range between 10 and 40 cm and lack data from very small or very big trees. Tree heights and ages have similar deficiencies in sample data range (Tables 5 and 6, Tables S.4–S.6 in Supplementary material). This range limitation results in regression functions derived from sample data that may lead to unrealistic estimates if they are extrapolated, particularly for larger, but also smaller tree diameters. Analogously, differences in tree allometry due to forest management or tree genetics can be possible sources of deviation in the carbon and biomass results. Within Europe both management practices (FOREST EUROPE, UNECE, FAO, 2011) and tree genetics vary strongly by tree species (Skrøppa, 2003; Mátyás et al., 2004). This may affect biomass allocation and growth rates (Schmidt-Vogt, 1977; Gruber, 1987; Müller-Starck et al., 1992). Since hardly any references provide information on allometric properties such as crown length, crown width or stem taper or even tree genetics, we cannot examine this in more detail.

The type of estimation method has a large effect on any results and we want to illustrate this for biomass expansion factors versus allometric biomass functions. Biomass expansion factors convert tree volume into biomass by applying a species-specific average conversion factor, independent of age, tree height, etc. Forest management strongly affects the growth rates of stands and thus the tree ring width (Assmann, 1970). Wood density is strongly correlated to tree ring width (MacPeak et al., 1990; Repola, 2006; Ledermann and Neumann, 2006) but also to tree age. It is well known that constant biomass expansion factors tend to overestimate biomass for young trees and underestimate biomass for older trees (Pietsch and Hasenauer, 2002). Allometric biomass functions which derive tree biomass from DBH and/or height were developed to circumvent this problem and include the effect of age in the biomass predictions.

Biomass in tree compartments show higher differences among countries than total biomass estimates (Figs. 6 and 7). Again part of these discrepancies in biomass estimates may be caused by environmental drivers while the rest is an effect of sample material and the estimation methodology. Here it is also important to know the definition of the various tree compartments by country as this also affects the results (Jenkins et al., 2003). For example, the definition of branch or stem biomass for *F. sylvatica* in Poland could be different than in other countries, since the results for total biomass in Poland did not show clear differences in Fig. 4. Unfortunately, in the case of Poland (Muukkonen, 2007) we could not test this hypothesis, since the definition of stem and branch biomass is not given. But there is some evidence in the results of other countries. In France stem biomass includes all branches (Vallet et al., 2006). In most other countries the definition of stem excludes branches as well as the stump (e.g. for Austria Pollanschütz, 1974; for Norway Marklund, 1988). This explains why France has the highest results for stem biomass for *P. abies* (Fig. 6) but only average results for total tree biomass (see Fig. 3 and Table 3).

Similarly, the assigned minimum diameter for root biomass (see Appendices B–M) influences the deviations in root biomass results (Figs. 6 and 7, Tables 3 and 4). For Austria as well as for Norway it is assigned 2 mm (Wirth et al., 2004; Petersson and Ståhl, 2006), while for the Czech Republic or Belgium it is assigned 5 mm (Drexhage and Gruber, 1999; Drexhage and Colin, 2001; Xiao et al., 2003).

All functions in this study use tree diameter to predict the biomass or volume, with many also using tree height (Table 1 and Appendices B–M). Any additional predictor variable decreases the remaining variation and improves the performance of the model (e.g. Ketterings et al., 2001; Ledermann and Neumann, 2006 or Lang et al., 2007). Some models use additional variables such as tree age (Wirth et al., 2004) or tree crown parameters (i.e., crown ratio or crown length; Repola, 2008, 2009; Ledermann and Neumann, 2006). Without tree height or crown height as additional variables the models will assume a constant DBH/height ratio or DBH/crown height ratio. This is an unrealistic assumption since height increment culminates earlier than diameter increment and trees in general modify their crown according to stand density and the light availability (Assmann, 1970). A good example to illustrate the effect of additional variables are root biomass estimates of *P. abies* from Austria and Belgium. Both countries use

Table 5
Properties of the sample material used for volume and biomass functions for *Picea abies* by country and region: if multiple references are used for the compartments in one country, each reference is covered by one row. Given for each reference is DBH (diameter at breast height) and tree height of the sample material, the Origin of the samples (the country where the sample material was collected), the Number of samples, the Age of the sample trees in years as well as the Reference. Boxes with a endash (–) indicate that this information is not given by the reference. For the volume functions used in Czech Republic only the maximum diameter and height of the samples is given (Petráš and Pajtík, 1991).

Forest region	Country	Compartments	DBH [cm]	Height [m]	Origin	No. samples	Age [a]	References
North Europe	Finland	All	1.7–41.7	2.1–35.0	Finland	613	15–164	Repola (2009)
	Norway	Aboveground	0.3–63.4	1.3–35.6	Sweden	551	1–223	Marklund (1988)
		Roots	0.3–63.4	1.3–35.6	Sweden	342	1–223	Petersson and Stahl (2006)
Central-West Europe	Austria	Stem volume	5.0–78.0	10.0–44.0	Austria	9972	–	Pollanschütz (1974)
		Branches	2.4–65.9	2.8–42.6	Austria	3753	35–126	Ledermann and Neumann (2006)
		Foliage	1.8–98.2	2.1–44.8	Switzerland	189	15–270	Burger (1947, 1953)
		Roots	7.6–41.2	6.8–31.7	Temperate Europe	85	16–142	Wirth et al. (2004)
	Belgium	Stem volume	–	–	Belgium	991	–	Dagnelie et al. (1985)
		Branches	2.4–65.9	2.8–42.6	Austria	3753	35–126	Ledermann and Neumann (2006)
		Foliage	4.0–38.0	6.7–25.9	Netherlands	23	9–39	Bartelink (1996)
		Roots	7.6–41.2	6.8–31.7	Temperate Europe	85	16–142	Wirth et al. (2004)
	France	Aboveground	14.3–71.6	–	France	309	–	Vallet et al. (2006)
	Germany	Wood volume	–	–	Germany	–	–	Kublin (2002)
		Foliage	25.0–55.6	22.0–29.8	Germany	7	–	Schwarzmeier (2000)
	Netherlands	Aboveground	0.5–52.0	–	European Russia	222	20–155	Hamburg et al. (1997)
Central-East Europe	Czech Republic	Wood volume	–74.0	–46.0	Czechoslovakia	2111	–	Petráš and Pajtík (1991)
		Foliage, twigs	4.0–92.0	4.0–48.0	Czechoslovakia	265	–	Petráš et al. (1985)
		Roots	5.0–25.0	15 (mean)	N Germany	15	10–40	Drexhage and Gruber (1999)
	Poland	All	0.0–67.5	2.0–42.7	Europe	~1800	–	Muukkonen (2007)
	Romania	Aboveground	–	–	Romania	5403	–	Giurgiu et al. (1972)
South Europe	Italy	All	8.1–81.7	6.0–40.1	NE Italy	93	–	Tabacchi et al. (2011)
	Spain	All (excl. foliage)	9.0–57.5	8.0–29.0	Spain	29 (roots 10)	–	Ruiz-Peinado et al. (2011)
		Foliage	5.3–49.2	7.1–23.8	NW Spain	125	34–44	Diéguez-Aranda et al. (2009)

Table 6
Properties of the sample material used for volume and biomass functions for *Fagus sylvatica* by country and region: for details on the table and the content please see explanations provided for Table 5.

Forest region	Country	Compartments	DBH [cm]	Height [m]	Origin	No. Samples	Age [a]	References
North Europe	Finland	–	–	–	–	–	–	–
	Norway	–	–	–	–	–	–	–
Central-West Europe	Austria	Stem (volume)	–	–	Austria	933	–	Pollanschütz (1974)
		Branches	2.0–67.1	3.6–39.0	Austria	4213	35–125	Ledermann and Neumann (2006)
		Foliage	0.8–57.0	2.6–39.6	Switzerland	91	14–128	Burger (1953)
		Roots	4.0–53.0	7.0–28.0	Germany	27	44–127	Bolte et al. (2004)
	Belgium	Stem (volume)	–	–	Belgium	–	–	Dagnelie et al. (1985)
		Branches	5.7–62.1	9.2–33.9	Czech Republic	20	40–114	Cienciala et al. (2005)
		Foliage	2.0–33.0	3.5–22.5	Netherlands	38	8–59	Bartelink (1997)
		Roots	3.0–38.0	7.0–29.0	Central Europe	48	21–160	Wutzler et al. (2008)
	France	Aboveground	1.6–81.2	–	France	1293	–	Vallet et al. (2006)
	Germany	Wood volume	–	–	Germany	–	–	Kublin (2002)
		Foliage	2.0–33.0	3.5–22.5	Netherlands	38	8–59	Bartelink (1997)
	Netherlands	Aboveground	2.0–33.0	3.5–22.5	Netherlands	38	8–59	Bartelink (1997)
Central-East Europe	Czech Republic	Wood volume	–74.0	–38.0	Czechoslovakia	1886	–	Petráš and Pajtík (1991)
		Foliage, twigs	8.0–84.0	8.0–36.0	Czechoslovakia	285	–	Petráš et al. (1985)
		Roots	3.0–20.0	9.9 (mean)	NE France	16	24–35	Le Goff and Ottorini (2001)
	Poland	All	2.0–64.0	3.5–29.0	Europe	68	–	Muukkonen (2007)
	Romania	Aboveground	–	–	Romania	7070	–	Giurgiu et al. (1972)
South Europe	Italy	All	5.0–60.7	7.2–31.6	Italy	91	–	Tabacchi et al. (2011)
	Spain	All (excl. foliage)	9.5–74.8	9.0–30.9	Spain	72 (roots 14)	–	Ruiz-Peinado et al. (2011)
		Foliage	9.9–21.0	12.6–26.2	NW Spain	16	–	Diéguez-Aranda et al. (2009)

the same reference (Wirth et al., 2004), but Austria use in addition to DBH also the tree age for root biomass prediction. The additional variable has rather little effect for small diameters, while the results for Austria and Belgium strongly deviate after DBH of 40 cm (Fig. 6) and the root biomass of the oldest stand is for Belgium 33.7 t/ha (+27%) higher than for Austria. The choice of biomass or carbon estimation method is restricted to the availability of the input data. If a forest inventory does not provide certain

variables (e.g. age or crown height) then more general estimation methods must be used.

Carbon is derived by multiplying biomass with the carbon fraction (Eq. (1)). Research indicated that the carbon fraction in biomass differs by ecoregion (Thomas and Martin, 2012), tree species (Lamlom and Savidge, 2003) or by tree compartment (Lamlom and Savidge, 2006). Besides France, Belgium and Spain, most countries in this study use a carbon fraction of 0.5 as suggested by IPCC (2006) (Appendix A). Considering the literature this is a simplification of the complexity of nature, but necessary since no comprehensive studies exist.

Carbon reporting systems such as the FAO Statistics, the Kyoto protocol or the UNFCCC (United Nations Framework – Convention on Climate Change) are not only concerned with carbon stocks but mainly with changes in carbon stocks (fixation vs. emissions). The effect of the calculation methods presented in this study might be substantially smaller for estimating changes in carbon. Still since the tree results in Figs. 2–5 show different inclination across the DBH range, one can expect that the different methods procure different carbon increment rates for the same change in tree properties like an increase in DBH of 1 cm.

6. Conclusions

We present and compare the official biomass estimation methods from 12 different countries across Europe as they are used for the carbon reporting duties within the Kyoto Protocol under UNFCCC. True tree or stand biomass estimates are impossible to obtain so we compare and assess the country-specific estimation methods to provide a conceptual understanding of the different estimation procedures and how these differences may affect carbon predictions at the European scale. After addressing regional differences by clustering into European forest regions, deviations of single tree carbon and biomass as well as stand-level results decrease but remain throughout Europe (Figs. 2–5, Tables 3 and 4). These discrepancies can be explained with (i) differences in the sample material (Tables 5 and 6), (ii) the variables used in the biomass functions and (iii) the definition of the compartments (Appendices B–M). No additional patterns according to the biomass calculation methods (allometric biomass functions or biomass expansion factors) are evident.

The quality of tree carbon calculations in Europe needs to be improved and systematic quality checks for providing consistent carbon estimation methods are required. These checks must include (i) the definition of the tree compartments, (ii) additional variables to capture differences in site conditions, management impacts, and age effects, (iii) the performance of biomass functions when applied beyond the range of the data set available for parametrization, (iv) representativeness of the functions and the used sample material in terms of covering the tree allometry and specific variability of trees in the region of interest and (v) plausibility checks with local sample material, especially when estimation systems from other regions are applied.

We strengthen the findings of the FPS COST ACTION E43 on "Harmonisation of National Inventories in Europe: Techniques for Common Reporting" (McRoberts et al., 2009; Ståhl et al., 2012) by quantifying the deviation caused by different carbon calculation methods in Europe, which can lead to differences in tree carbon up to 140 t/ha for *P. abies* and 90 t/ha for *F. sylvatica*. We also highlight new issues discovered like the high discrepancies in young stands or the effect of additional tree variables such as crown length or tree age. Choosing and modifying the carbon calculation methodology is the responsibility of each country and NFI organization. However, this is a critical task that should be coordinated across countries because it has such significant ramifications such as its influence on climate change mitigation policy.

Conflict of interests

The authors declare that they have no conflict of interest.

Acknowledgements

This work is part of the project FORMIT ('Enhancing the FORest MITigation potential of European Forests') – financed by DG Research and Innovation within the Seventh Framework Program. The research leading to these results has received funding from the European Union Seventh Framework Programme under grant agreement n° 311970. We further want to acknowledge support from Estonian Ministry of Education and Research (grant n° IUT21-4). The Polish research was supported by funds for science in the years 2013–2016 allocated to an international co-financed project. We thank Loretta Moreno for proofreading the manuscript. We are also thankful to several persons who supported us in preparing the calculation methodology and the manuscript, Isabel Cañellas (Spain), Katarina Merganičová (Czech Republic), Klemens Schadauer, Md. Humain Kabir and Georg Kindermann (Austria). We further want to thank the editor and the anonymous reviewers for their helpful comments that substantially improved the quality of this work.

Appendix A. General details on carbon estimation

Tree carbon gets calculated according to the following general equation.

Table A.1
Carbon fraction (CC) for converting biomass into carbon.

Carbon fraction [/]					
Country	*Picea abies*	*Pinus sylvestris*	*Fagus sylvatica*	*Quercus robur*	*Betula pendula*
Austria	0.5	0.5	0.5	0.5	0.5
Belgium	0.5	0.5	0.49	0.5	0.5
Czech Republic	0.5	0.5	0.5	0.5	0.5
Finland	0.5	0.5	0.5	0.5	0.5
France	0.475	0.475	0.475	0.475	0.475
Germany	0.5	0.5	0.5	0.5	0.5
Italy	0.5	0.5	0.5	0.5	0.5
Netherlands	0.5	0.5	0.5	0.5	0.5
Norway	0.5	0.5	0.5	0.5	0.5
Poland	0.5	0.5	0.5	0.5	0.5
Romania	0.5	0.5	0.5	0.5	0.5
Spain	0.506	0.509	0.486	0.484	0.485

Table A.2
Dry wood density (wd) for converting volume into biomass.

Dry wood density [t dry biomass/m^3]					
Country	*Picea abies*	*Pinus sylvestris*	*Fagus sylvatica*	*Quercus robur*	*Betula pendula*
Austria	0.362	0.450	0.561	0.579	0.551
Belgium	0.380	0.480	0.560	0.600	0.550
Czech Republic	0.380	0.430	0.570	0.550	0.520
France	0.438	0.438	0.546	0.546	0.546
Germany – branch	0.490	0.490	0.540	0.570	0.540
Germany – stem	0.360	0.360	0.490	0.540	0.490
Romania	0.370	0.420	0.585	0.560	0.525

Table A.3
Root-to-shoot ratio (RS) for deriving root biomass with aboveground biomass (BM).

Root-to-shoot ratio [/]					
Country	*Picea abies*	*Pinus sylvestris*	*Fagus sylvatica*	*Quercus robur*	*Betula pendula*
France	0.30	0.30	0.28	0.28	0.28
Germany – BM < 50 t/ha (*Picea, Pinus*), BM < 75 t/ha (*Fagus, Betula*)	0.46	0.46	0.43	0.35	0.43
Germany – BM 50–150 t/ha (*Picea, Pinus*), BM 75–150 t/ha (*Fagus, Betula*)	0.32	0.32	0.26	0.35	0.26
Germany – BM > 150 t/ha	0.23	0.23	0.24	0.35	0.24
Italy	0.29	0.36	0.20	0.20	0.24
Poland	0.23	0.23	0.24	0.24	0.24

$$C_{tree} = CC * (dsm + dbm + dfm + drm) \quad (A.1)$$

where C_{tree} is the total carbon content of a tree [kg], *CC* is the carbon fraction [/] given for each country in Table A.1, *dsm* is the dry stem biomass [kg], *dbm* the dry branch biomass [kg], *dfm* the dry foliage biomass [kg] and *drm* the dry root biomass [kg].

If applicable in the country-specific methodology, dry wood density *wd* to derive biomass using volume estimates are provided in Table A.2 and root-to-shoot ratio *RS* for deriving root biomass in Table A.3.

Some of the biomass calculation methods consider different compartments than the above mentioned. To get comparable results, the results of these sub-compartments are aggregated to the compartments stem, branch and roots according to the following equations:

$$dsm = dswm + dsbm \quad (A.2)$$

$$dbm = dabm + ddbm \quad (A.3)$$

$$drm = dstm + dcrm + dfrm \quad (A.4)$$

with *dsm* dry stem biomass, *dswm* dry stem wood biomass, *dsbm* dry stem bark biomass, *dbm* dry branch biomass, *dabm* dry alive branch biomass, *ddbm* dry dead branch biomass, *drm* dry root biomass, *dstm* dry stump biomass, *dcrm* dry coarse root biomass, *dfrm* dry fine root biomass, all quantities in [kg].

The biomass functions of the Czech Republic and Spain separate branches into different diameter classes (e.g. Spain Ruiz-Peinado et al., 2011, 2012; Diéguez-Aranda et al., 2009 and Balboa-Murias et al., 2006a,b; for the Czech Republic Petráš et al., 1985). As foliage biomass is included in the branch biomass, for calculating branch biomass solely foliage biomass get substracted, see Eq. (A.5).

$$dbm = dbm1 + dbm2 + dbm3 + dbm4 + dbm5 - dfm \quad (A.5)$$

With *dbm*1 thick branches with diameter >7 cm, *dbm*2 medium branches with diameter 2–7 cm, *dbm*3 thin branches and twigs with diameter <2 cm, *dbm*4 thin branches with diameter 0.5–2 cm, *dbm*5 twigs with diameter <0.5 cm, *dfm* foliage biomass.

In the following chapters the biomass calculations are described for each country in detail. Often used variables are *DBH* diameter at breast height, at 1.3 m above ground, *H* tree height from ground to tree top, *HC* crown height from ground to living crown (first living branch), *CR* crown ratio calculated $CR = (H - HC)/H$, *wd* dry wood density.

Carbon fraction (*CC*), dry wood density (*wd*) and Root-to-shoot ratios (*RS*) are coefficients most calculation methods use and are therefore presented accumulated for all calculation methods here.

Appendix B. Biomass calculation in Finland

Allometric biomass functions dependent on DBH, tree height and crown length are used for calculating biomass for tree compartments (stem wood, stem bark, living branches, dead branches, foliage (leaves/needles), stump, coarse roots (diameter >1 cm)) (Repola, 2008, 2009) and fine roots (diameter <1 cm) (Härkönen et al., 2011) (see Table B.1).

The chosen methodology is largely identical then the method from the Finnish NIR report. It differs merely in the choice of coefficients used for estimating fine root biomass (Härkönen et al., 2011; Statistics Finland, 2013). It uses allometric biomass functions developed in Finland.

Model type 1:

$$dswm, dsbm, \ldots = cf * exp(c0 + c1 * dk/(dk + c2) + c3 * ln(H) + c4 * H + cf2) \quad (B.1)$$

Model type 2:

$$dswm, dsbm, \ldots = cf * exp(c0 + c1 * dk/(dk + c2) + c3 * H/(H + c4) + c5 * ln(CL) + cf2) \quad (B.2)$$

$$dk = 2 + 1.25 * DBH \quad (B.3)$$

$$dfrm = f_{fr} * dfm \quad (B.4)$$

with *dk* stump diameter [cm], *DBH* [cm], *H* [m], *CL* crown length [m], *CR* crown ratio [/], coefficients *ci, cf, cf*2 and f_{fr} are given below. f_{fr} are valid for semi-fertile sites (Härkönen et al., 2011).

For broadleaf trees and *dfm CR* is used instead ln(*CL*). For broadleaf trees and *dabm CL* instead ln(*CL*).

F. sylvatica is not native in Finland. Therefore Finland is excluded from analysis for this tree species.

Table B.1
Coefficients for calculating biomass for Finland (Repola, 2008, 2009).

Coefficients for biomass by compartments for Finland									
Compartment	*c*0	*c*1	*c*2	*c*3	*c*4	*c*5	*cf*	*cf*2	Model type
Picea abies									
dswm	−3.555	8.042	14	0.869	0.015	0	1	0.009	1
dsbm	−4.437	10.071	18	0.261	0	0	1	0.029	1
dabm	−3.023	12.017	14	−5.722	5	1.033	1	0.0425	2
dfm	−0.085	15.222	4	−14.446	1	1.273	1	0.0575	2
ddbm	−5.317	6.384	18	0.982	0	0	1.208	0	1
dstm	−3.964	11.73	26	0	0	0	1	0.0615	1
dcrm	−2.294	10.646	24	0	0	0	1	0.1095	1
Pinus sylvestris									
dswm	−3.721	8.103	14	5.066	12	0	1	0.0055	2
dsbm	−4.695	8.727	12	0.228	0	0	1	0.0355	1
dabm	−5.166	13.085	12	−5.189	8	1.11	1	0.0415	2
dfm	−1.748	14.824	4	−12.684	1	1.209	1	0.0625	2
ddbm	−5.318	10.771	16	0	0	0	0.913	0	1
dstm	−6.753	12.681	12	0	0	0	1	0.027	1
dcrm	−5.55	13.408	15	0	0	0	1	0.0395	1
Betula pendula, *Quercus robur*									
dswm	−4.879	9.651	12	1.012	0	0	1	0.004035	1
dsbm	−5.433	10.121	12	2.647	20	0	1	0.02739	2
dabm	−5.067	14.614	12	−5.074	12	0.092	1	0.035855	2
dfm	−20.856	22.32	2	0	0	2.819	1	0.027185	2
ddbm	−7.996	11.824	16	0	0	0	2.1491	0	1
dstm	−3.574	11.304	26	0	0	0	1	0.03348	1
dcrm	−3.223	6.497	22	1.033	0	0	1	0.07477	1

Table C.1
Coefficients for calculating biomass for Norway (Marklund, 1988; Petersson and Ståhl, 2006).

Coefficients for biomass by compartment for Norway					
	*a*0	*a*1	*a*2	*a*3	*a*4
Picea abies					
dswm	−2.3032	7.2309	14	0.0355	0.7030
dsbm	−3.4020	8.3089	15	0.0147	0.2295
dabm	−1.2063	10.9708	13	−0.0124	−0.4923
ddbm	−4.6351	3.6518	18	0.0493	1.0129
dfm	−1.8551	9.7809	12	0	−0.4873
drm	4.58761	10.4404	138	0	0
Pinus sylvestris					
dswm	−2.6864	7.6066	14	0.02	0.8658
dsbm	−3.2765	7.2482	16	0	0.4487
dabm	−2.5413	13.3955	10	0	−1.1955
ddbm	−5.8926	7.1270	10	−0.0465	1.106
dfm	−3.4781	12.1095	7	0.0413	−1.565
drm	3.4428	11.0654	113	0	0
Quercus robur, *Betula pendula*					
dswm	−3.3045	8.1184	11	0	0.9783
dsbm	−4.0778	8.3019	14	0	0.7433
dabm	−3.3633	10.2806	10	0	0
ddbm	−6.6237	11.2872	30	−0.3081	2.6821
drm	6.1708	10.0111	225	0	0

Appendix C. Biomass calculation in Norway

The methodology is taken from the Norwegian NIR report (Climate and Pollution Agency, 2013; oral communication Rasmus Astrup, 2013). It uses allometric biomass functions developed in Sweden. For aboveground biomass the functions from Marklund (1988) and for belowground biomass (minimum root diameter 2 mm) from Petersson and Ståhl (2006) are used. The functions for alive branches for *P. abies* and *P. sylvestris* also contain the biomass of needles (Marklund, 1988). To compare with other results the foliage biomass is calculated with separate functions.

$$dswm, dsbm, \ldots = exp(a0 + a1 * DBH/(DBH + a2) + a3 * H + c4 * ln(H)) \quad (C.1)$$

For the broad leaf species foliage biomass is assumed to be a constant proportion of stem biomass (de Wit et al., 2006):

$$dfm = dswm * 0.021 \quad (C.2)$$

DBH [cm] (for *drm DBH* [mm]), *H* [m], *drm* [g dry weight], coefficients *a*0–*a*4 are given in Table C.1 (Marklund, 1988; Petersson and Ståhl, 2006).

Appendix D. Biomass calculation in Austria

The presented method corresponds widely with the method for forest carbon calculation used in the Austrian National Inventory report for the Kyoto reporting (Umweltbundesamt, 2013) (see Tables D.1–D.3).

Dry stem biomass (dsm) get calculated using stem volume and species-specific wood density (Gschwantner et al., 2010).

$$dsm = V * wd \quad (D.1)$$

$$V = (DBH/200)^2 * \pi * H * FF \quad (D.2)$$

with *DBH* [cm] and *H* [m]

$$FF = c1 + c2 * ln^2(DBH) + c3/H + c4/DBH + c5/DBH^2 + c6/DBH/H + c7/DBH^2/H \quad (D.3)$$

with *DBH* and *H* [dm] where *V* stem volume [m^3], *FF* form factor, *wd* dry wood density given in Appendix A [kg dry BM/m^3], which is calculated using wood density and shrinkage factor by tree species from Wagenführ and Scheiber (1985), *ci* coefficients for form factor calculations (Pollanschütz, 1974; Schieler, 1988; Gabler and Schadauer, 2008) are given below.

Dry branch mass (*dbm*) is calculated for *P. abies* (including foliage biomass), *F. sylvatica, B. pendula* (same function as for *F. sylvatica)* and *Q. robur* using allometric functions from Ledermann and Neumann (2006):

$$dbm = cf * exp(a + b * ln(DBH) + c * H/DBH + d * ln(CR)) \quad (D.4)$$

with *DBH* [cm], *H* [m], the species-specific parameters *a–d* and *cf* given below in the following table.

For *P. abies dfm* is substracted from *dbm* to get comparable results.

Foliage biomass (*dfm*) is calculated for *P. abies*, *F. sylvatica, B. pendula* and *Q. robur* using allometric functions of Burger (1947, 1949, 1953) modified after Lexer and Hoenninger (2001).

$$dfm = a * DBH^b \quad (D.5)$$

dbm and *dfm* for *P. sylvestris* after Hochbichler et al. (2006):

$$dbm, dfm = cf * exp(a + b * ln(DBH) + c * ln(H)) \quad (D.6)$$

with *DBH* [cm], *H* [m], the species-specific parameters *b*0, *b*1, *cf* and *a–d* are given below.

Root mass (*drm*) get calculated for *P. abies*, *F. sylvatica, B. pendula* and *Q. robur* using the biomass functions of Wirth et al. (2004), Bolte et al. (2004) and Offenthaler and Hochbichler (2006). Only Bolte et al. (2004) provide the minimum diameter of the samples (2 mm).

$$drm = cf * exp(a + b * ln(DBH) + c * ln^2(DBH) + d * ln(A)) \quad (D.7)$$

And for *P. sylvestris* (Offenthaler and Hochbichler, 2006):

$$drm = 0.038872 * DBH^{2.066783} \quad (D.8)$$

with *DBH* [cm], *A* is tree age [a], the species-specific parameters *a–d* and *cf* are given below.

Appendix E. Biomass calculation in Belgium

The below presented methodology is the result of a literature review. The volume calculation method is identical in the Belgium NIR report (Flemish Environment Agency, 2013). It is a combination of volume functions, expansion factors and allometric biomass functions from Belgium, Austria, the Czech Republic, Germany, France and Netherlands (see Tables E.1 and E.2).

$$V = b0 + b1 * c_{130} + b2 * c_{130}^2 + b3 * c_{130}^3 + b4 * H + b5 * c_{130}^2 * H \quad (E.1)$$

$$dsm = V * wd \quad (E.2)$$

with *V* merchantable timber volume [m^3] with a minimal diameter of 7 cm (circumference 22 cm), c_{130} (circumference at 1.3 m height) = $DBH \cdots \pi$, *H* [m], *b*0–*b*5 coefficients according to Dagnelie et al. (1985) given below in the following table, *wd* dry wood density are taken from Vande Walle et al. (2005) are given in Appendix A.

If there are no appropriate biomass functions for Belgium available, the allometric functions from other countries are used. The functions are selected to give realistic results across the DBH and height range of the analysed trees.

For *dbm*, *dfm* and *drm* of *P. sylvestris* (Xiao et al., 2003 cited in Zianis et al., 2005), for *dbm* of *F. sylvatica, B. pendula* and *Q. robur* (Cienciala et al., 2005 cited in Zianis et al., 2005), for *dfm* Bartelink (1997) and for *drm* Wutzler et al. (2008):

$$dbm = b0 * DBH^{b1} \quad (E.3)$$

$$dfm = f0 + f1 * DBH^{b2} \quad (E.4)$$

$$drm = r0 * DBH^{r1} \quad (E.5)$$

The coefficients are given in the following table.

For *P. abies* and *dbm* (including needles) Ledermann and Neumann (2006), for *dfm* (not added to total biomass to avoid double counting) Bartelink (1996), for *drm* Wirth et al. (2004):

$$dbm = b0 * exp(b1 + b2 * ln(DBH) + b3 * H/DBH) \quad (E.6)$$

$$dfm = exp(f0 + f1 * ln(DBH) + f2 * ln(H)) \quad (E.7)$$

$$drm = r0 * exp(r1 + r2 * ln(DBH)) \quad (E.8)$$

with *DBH* [cm], *H* [m], coefficients given below.

Minimum diameter for root biomass is only provided by Xiao et al. (2003) and is 5 mm.

Appendix F. Biomass calculation in France

The below presented methodology is selected based on available literature on biomass in forests for France (INRA, 2004). It is largely identical then the method from the French NIR report (CITEPA, 2013). It combines volume functions with expansion factors developed in France (see Table F.1).

$$FF = (a + b * CBH + c * CBH^{0.5}/H) * (1 + d/CBH^2) \quad (F.1)$$

$$V = FF * (\pi/40000) * CBH^2 * H \quad (F.2)$$

$$dsm + dbm = V * wd \quad (F.3)$$

$$dfm = V * wd * 0.02 \quad (F.4)$$

$$drm = RS * (dsm + dbm + dfm) \quad (F.5)$$

Table D.1
Coefficients for calculating form factor for Austria (Pollanschütz, 1974; Schieler, 1988; Gabler and Schadauer, 2008).

Coefficients for form factor for Austria							
	*c*1	*c*2	*c*3	*c*4	*c*5	*c*6	*c*7
Picea abies	0.46818	−0.013919	−28.213	0.37474	−0.28875	28.279	0
Pinus sylvestris	0.435949	−0.014908	5.21091	0	0.028702	0	0
Fagus sylvatica	0.686253	−0.037151	−31.0674	−0.386321	0.219462	49.6163	−22.3719
Quercus robur	0.115631	0	65.9961	1.20321	−0.930406	−215.758	168.477
Betula pendula	0.42831	−0.06643	0	0	0	8.4307	0

Table D.2
Coefficients for calculating branch and foliage biomass for Austria (Ledermann and Neumann, 2006 and Burger, 1947, 1949, 1953 modified after Lexer and Hoenninger, 2001)

Coefficients for branch biomass for Austria						For foliage biomass			
	a	*b*	*c*	*d*	*cf*	*a*	*b*	*c*	*cf*
Picea abies	−1.9576	2.0252	0.1451	0.9154	1.051	0.0956	1.56	–	–
Pinus sylvestris	−3.2856	2.1684	0.1473	–	1.041	−3.8876	1.5904	0.2348	1.0417
Fagus sylvatica, Betula pendula	−3.3205	2.5568	−0.1092	0.6002	1.212	0.0217	1.7	–	–
Quercus robur	−1.2943	1.9445	0	1.2137	1.280	0.0270	1.7	–	–

Table D.3
Coefficients for calculating root biomass for Austria (Wirth et al., 2004; Bolte et al., 2004; Offenthaler and Hochbichler, 2006).

Coefficients for root biomass for Austria					
	a	*b*	*c*	*d*	*cf*
Picea abies	−8.35049	4.56828	−0.33006	0.28074	1.0406
Fagus sylvatica, Betula pendula	−4	2.32	0	0	1.08
Quercus robur	−3.97478	2.52317	0	0	1.0505

Table E.1
Coefficients for calculating stem volume for Belgium (Dagnelie et al., 1985).

Coefficients for stem volume for Belgium						
	*b*0	*b*1	*b*2	*b*3	*b*4	*b*5
Picea abies	−0.01093	0.001395	−9.6E−06	−2.5E−07	−0.00279	4.9E−06
Pinus sylvestris	−0.03984	0.001551	−6.2E−06	4.8E−08	7.4E−05	2.96E−06
Fagus sylvatica	−0.01557	0.000923	−7.1E−06	−7.7E−08	−0.00135	4.04E−06
Quercus robur	−0.00227	0.000124	1.26E−05	−5.9E−08	−0.00167	3.75E−06
Betula pendula	−0.01139	−0.0001	2.83E−05	−1.9E−07	−0.0006	3.08E−06

Table E.2
Coefficients for calculating branch, foliage and root biomass for Belgium (Ledermann and Neumann, 2006; Wirth et al., 2004; Bartelink, 1997; Wutzler et al., 2008; Cienciala et al., 2005; Xiao et al., 2003).

Coefficients for branch biomass					For foliage biomass			For root biomass		
	*b*0	*b*1	*b*2	*b*3	*f*0	*f*1	*f*2	*r*0	*r*1	*r*2
Picea abies	1.102	−1.1635	1.7459	−0.9499	−1.346	3.351	−2.201	1.0554	−5.3789	2.9211
Pinus sylvestris	0.0022	2.9122	0	0	0	0.00445	2.2371	0.3399	1.4728	0
Fagus sylvatica, Quercus robur, Betula pendula	0.021	2.471	0	0	0.375	0.0024	2.517	0.0282	2.39	0

Table F.1
Coefficients for calculating tree volume for France (Vallet et al., 2006).

Coefficients for tree volume for France				
	a	*b*	*c*	*d*
Picea abies	0.631	−0.000946	0	0
Pinus sylvestris	0.297	0.000318	0.384	204
Quercus robur, Betula pendula	0.471	−0.000345	0.377	0
Fagus sylvatica	0.395	0.000266	0.421	45.4

with *FF* Form factor for tree volume estimation, $CBH = DBH \cdot \pi$ (circumference at 1.3 m height), *H* [m], *V* [m^3] aboveground tree volume, *a–d* coefficients according to Vallet et al. (2006) given in the following table, *wd* wood density and *RS* root-to-shoot ratio given in Appendix A. Minimum root diameter is not defined.

Foliage biomass *dfm* is considered to be 2% of the total aboveground biomass.

Appendix G. Biomass calculation in Germany

The methodology presented below is identical to the method used in the German NIR report (Federal Environmental Agency, 2012) using the same volume functions as the German Forest Inventory (Bundeswaldinventur) (see Table G.1).

Wood volume, wood density and expansion factors are used to calculate biomass. Raw wood volume (minimum diameter 7 cm) (Kublin, 2002) is calculated with the functions implemented in the program BDAT 2.0 (Kublin, 2002) depending on species, DBH, tree height and *d*7 (diameter at height of 7 m). The estimation of the variable *d*7 is done by the program BDAT 2.0 for trees, as these values are not included in the dataset. Tree wood volume is calculated with raw wood volume and expansion factors (see Table G.1) derived from Grundner and Schwappach (1952) cited in Federal Environmental Agency (2012).

Foliage biomass is included in the estimates for coniferous species. Its share can be estimated with respective biomass functions for foliage, for *P. abies* from Schwarzmeier (2000), for *P. sylvestris* from Xiao et al. (2003), for *B. pendula* from Hytönen et al. (1995), for *F. sylvatica* from Bartelink (1997) and for *Q. robur* from Curiel Yuste et al. (2005). The volume functions are from Germany, the functions for the remaining compartments from other European countries.

$$dsm = V_{RW} * wd\_stem \quad (G.1)$$

$$V_{TW} = a + V_{RW} * b \quad (G.2)$$

$$dbm = (V_{TW} - V_{RW}) * wd\_branch \quad (G.3)$$

$$drm = RS * (dsm + dbm + dfm) \quad (G.4)$$

$$dfm = a + b * DBH^c * H^d \quad (G.5)$$

Table G.1
Coefficients for converting raw wood volume to tree wood volume (Federal Environmental Agency, 2012) and for calculating foliage biomass for Germany (Schwarzmeier, 2000; Xiao et al., 2003; Hytönen et al., 1995; Bartelink, 1997; Curiel Yuste et al., 2005).

Coefficients for tree wood volume for Germany			Coefficients for foliage biomass			
	a	*b*	*a*	*b*	*c*	*d*
Picea abies, age <60 years	0.036697	1.148143	0	0.0026146	2.6763	0
Picea abies, age >60 years	0	1.177947	0	0.0026146	2.6763	0
Pinus sylvestris, age <60 years	0.009946	1.156659	0	0.112269	2.2371	0
Pinus sylvestris, age >60 years	0.036883	1.076103	0	0.112269	2.2371	0
Betula pendula	0.017493	1.121933	0	0.0003	2	0.9583
Fagus sylvatica, age <60 years	0.011942	1.207371	0.375	0.0024	2.517	0
Fagus sylvatica, age 61–100 years	0.008184	1.196184	0.375	0.0024	2.517	0
Fagus sylvatica, age >100 years	0.030255	1.128104	0.375	0.0024	2.517	0
Quercus robur	0.101879	1.051529	0	0.0024	2.6081	0

with V_{RW} rawwood volume [m^3], V_{TW} total wood volume [m^3], *DBH* [cm], *H* [m], *wd_stem* is wood density stem, *wd_branch* wood density branch (Kollmann, 1982 cited in Federal Environmental Agency, 2012) and *RS* root-to-shoot ratio are given in Appendix A, *a*, *b* coefficients for calculating V_{TW} (Federal Environmental Agency, 2012) and for *dfm* are given in Table G.1. Minimum root diameter is not defined.

Appendix H. Biomass calculation in the Netherlands

The chosen method is a combination of the allometric biomass functions published in Nabuurs et al. (2005) also used in the NIR report of the Netherlands (National Institute for Public Health and the Environment, 2013) and biomass fractions calculated using results from the EFISCEN project (Schelhaas et al., 1999; Vilén et al., 2005). The allometric biomass functions published in Nabuurs et al. (2005) use publications providing species-dependent allometric biomass functions and conversion factors from Europe and the European part of Russia. For *Q. robur* the allometric function of Hochbichler (2002) is used, for *F. sylvatica* of Bartelink (1997), for *B. pendula* of Johansson (1999), for *P. sylvestris* and *P. abies* of Hamburg et al. (1997) (see Tables H.1 and H.2).

$$BM_{ABG} = a0 * DBH^{a1} * H^{a2} \quad \text{(H.1)}$$

$$BM_{total} = BM_{ABG} * (1 + RS) \quad \text{(H.2)}$$

with *DBH* [cm] (for *B. pendula DBH* [mm], *H* [m], BM_{ABG} total aboveground biomass [kg dry weight], BM_{total} total tree biomass [kg dry weight], *RS* age-dependent root-to-shoot ratio calculated using biomass fractions from Vilén et al. (2005) given in the next table. Minimum root diameter is not defined. The species-specific publications given above provide the coefficients for the aboveground biomass (*a*0–*a*2) and are cited in Nabuurs et al. (2005).

Total above ground biomass get divided into tree compartments by multiplying with estimates for biomass fractions.

$$dsm, dbm, \ldots = f\_i * BM_{total} \quad \text{(H.3)}$$

f_i are given below.

Biomass fractions were calculated within the EFISCEN project (Schelhaas et al., 1999; Vilén et al., 2005) and are based on the biomass allocation functions. For *P. abies* based on the functions of Wirth et al. (2004) for aboveground biomass and for coarse roots on Lehtonen et al. (2004) for fine roots. For *P. sylvestris* on the

Table H.1
Coefficients for calculating aboveground biomass for the Netherlands (Hochbichler, 2002; Bartelink, 1997; Johansson, 1999 and Hamburg et al., 1997 cited in Nabuurs et al., 2005).

Coefficients for aboveground biomass for the Netherlands			
	*a*0	*a*1	*a*2
Quercus robur	0.41354	2.14	0
Fagus sylvatica	0.0798	2.601	0
Betula pendula	0.00029	2.50038	0
Pinus sylvestris	0.0217	1.9634	0.9817
Picea abies	0.0533	1.791	0.8955

Table H.2
Age-dependent fraction values for calculating biomass in tree compartments for the Netherlands.

Biomass fractions dependent on tree age [years] for the Netherlands											
Picea abies	20	30	40	50	60	70	80	90	100	110	1000
f_stem	0.385	0.474	0.562	0.617	0.642	0.650	0.644	0.639	0.634	0.628	0.619
f_branch	0.349	0.256	0.173	0.130	0.111	0.104	0.106	0.108	0.111	0.115	0.121
f_roots	0.100	0.132	0.166	0.178	0.182	0.188	0.195	0.201	0.205	0.209	0.213
f_foliage	0.167	0.138	0.099	0.077	0.065	0.058	0.055	0.052	0.050	0.048	0.047
RS	0.111	0.152	0.199	0.216	0.223	0.231	0.243	0.251	0.258	0.264	0.271
Pinus sylvestris	30	40	50	60	80	100	120	1000			
f_stem	0.357	0.504	0.583	0.624	0.661	0.679	0.688	0.691			
f_branch	0.368	0.258	0.195	0.163	0.135	0.125	0.123	0.127			
f_roots	0.109	0.138	0.154	0.163	0.169	0.171	0.168	0.165			
f_foliage	0.167	0.101	0.068	0.050	0.035	0.026	0.021	0.018			
RS	0.122	0.160	0.182	0.195	0.204	0.206	0.203	0.197			
Fagus sylvatica, *Quercus robur*, *Betula pendula*	40	60	80	100	120	140	1000				
f_stem	0.600	0.674	0.692	0.693	0.712	0.721	0.721				
f_branch	0.100	0.108	0.118	0.129	0.108	0.095	0.089				
f_roots	0.261	0.191	0.174	0.165	0.167	0.171	0.176				
f_foliage	0.044	0.022	0.016	0.014	0.013	0.013	0.014				
RS	0.350	0.237	0.211	0.198	0.200	0.206	0.214				

functions of Cienciala et al. (2006) for aboveground biomass and on Marklund (1988) for root biomass. For *F. sylvatica, B. pendula* and *Q. robur* on Bartelink (1997) and Cienciala et al. (2005) for aboveground biomass and Le Goff and Ottorini (2001) for root biomass.

In the EFISCEN database there are no specific biomass fractions for the Netherlands available. Therefore the conversion factors developed for Germany/Austria were selected as these are probably most comparable with the conditions of forests in the Netherlands.

Appendix I. Biomass calculation in the Czech Republic

The presented method of calculating carbon is developed using volumetric functions applied in volume tables for Czechoslovakia (Petráš and Pajtík, 1991), density of wood and bark of tree species (Klement et al., 2010) and published allometric biomass functions (Drexhage and Colin, 2001; Petráš et al., 1985). It combines volume functions, biomass expansion factors and allometric biomass functions from the Czech Republic (see Tables I.1–I.3).

$$dswm, dsbm, \ldots = V_i * wd * I_i \quad \text{(I.1)}$$

$$dfm, drm, dbm5 = b1 * (DBH + b2)^{b3} * H^{b4} * b5 \quad \text{(I.2)}$$

where V_i is the volume of a certain compartment [m^3], *wd* is wood density [kg/m^3] given in Appendix A and I_i correction index (if applicable) derived from Požgaj et al. (1993), Chmelař (1992) and Miles and Smith (2009).

Minimum root diameter is 5 mm (Drexhage and Collin, 2001). The correction indices for individual tree species and *b*1–*b*5 coefficients for biomass calculation are given below.

$$dsm = BM_{wood>7cmUB} + dsbm \quad \text{(I.3)}$$

$$dbm = BM_{wood<7cmUB} + dbm5 \quad \text{(I.4)}$$

where $BM_{wood>7cmUB}$ is the biomass of wood under bark with diameter equal to or above 7 cm [kg dry BM], *dsbm* is biomass of bark [kg dry BM], $BM_{wood<7cmUB}$ is biomass of wood under bark with diameter below 7 cm [kg dry BM], *dbm*5 is biomass of green twigs [kg dry BM] as previously described. The individual biomass parts are calculated as follows:

$$BM_{wood>7cmUB} = V_{wood>7cmUB} * wd \quad \text{(I.5)}$$

$$BM_{wood<7cmUB} = V_{wood<7cmUB} * wd * I_{wood<7cm} \quad \text{(I.6)}$$

$$dsbm = V_{bark} * wd * I_{bark} \quad \text{(I.7)}$$

The volume of individual parts of the tree were calculated using two-parameter regressions applied in volume tables for Czechoslovakia and compiled or modified by Petráš and Pajtík (1991). The volume of the different parts of tree (tree, stem, wood with diameter equal to or above 7 cm under bark, wood with diameter below 7 cm under bark) is calculated using volumetric equations.

The compartment is indicated by the lower index. *OB* indicate volume over bark and *UB* under bark. If this is not stated, the used formula is valid for both *OB* and *UB*.

General equation for all different volumes of *P. abies* is:

$$V_i = a0 * (DBH + a1)^{a2} * H^{a3} - a4 * (DBH + a5)^{a6} * H^{a7} \quad \text{(I.8)}$$

For *F. sylvatica*:

$$V_i = FF_i * \pi * DBH^2 * H/40000 \quad \text{(I.9)}$$

$$FF_{stem} = a0 + a1 * DBH + a2 * DBH^2 + a3 * DBH^3 + a4 * H + a5 * H * DBH + a6 * DBH^2 * H + a7 * DBH^3 * H \quad \text{(I.10)}$$

$$FF_{wood>7cm} = a0 + a1/DBH + a2/DBH^2 + a3/DBH^3 + a4 * H + a5 * H * DBH + a6 * DBH^2 * H + a7 * DBH^3 * H \quad \text{(I.11)}$$

$$FF_{treeOB} = a0 + a1/H + a2/H^2 + a3/DBH + a4 * H/DBH + a5 * H^2/DBH + a6/DBH^2 + a7/DBH^2/H + a8/DBH^2/H^2 + a9/DBH^3 + a10/DBH^3 * H + a11/DBH^3 * H^2 \quad \text{(I.12)}$$

For *Q. robur*:

$$FF_{stem} = a0 + a1/DBH + a2/DBH^2 + a3/DBH^3 + a4 * H + a5 * H * DBH + a6 * DBH^2 * H + a7 * DBH^3 * H \quad \text{(I.13)}$$

$$FF_{wood>7cm}, FF_{treeOB} = a0 + a1/H + a2/H^2 + a3/DBH + a4 * H/DBH + a5 * H^2/DBH + a6/DBH^2 + a7/DBH^2/H + a8/DBH^2/H^2 + a9/DBH^3 + a10/DBH^3 * H + a11/DBH^3 * H^2 \quad \text{(I.14)}$$

Table I.1
Correction indices of wood density for the Czech Republic (Požgaj et al., 1993; Chmelař, 1992; Miles and Smith, 2009).

Correction indices of wood density for the Czech republic					
	Picea abies	*Pinus sylvestris*	*Fagus sylvatica*	*Quercus robur*	*Betula pendula*
I bark	1.25	0.95	1.2	1	1.13
I wood <7 cm	1.2	1.1	1.1	1.1	1.1

Table I.2
Coefficients for calculating biomass for the Czech Republic (Drexhage and Colin, 2001; Petráš et al., 1985).

Coefficients for biomass calculations for the Czech republic							
		*b*1	*b*2	*b*3	*b*4	*b*5	Reference
Picea abies	Twigs	0.016	1	1.788	0.679	0.468	Petráš et al. (1985)
Picea abies	Foliage	0.015	1	1.831	0.564	0.426	Petráš et al. (1985)
Picea abies	Roots	0.020	0	2.360	0	1	Drexhage and Colin (2001)
Pinus sylvestris	Twigs	0.236	1	1.842	−0.434	0.457	Petráš et al. (1985)
Pinus sylvestris	Foliage	0.119	1	1.857	−0.360	0.425	Petráš et al. (1985)
Pinus sylvestris	Roots	0.013	0	2.740	0	1	Drexhage and Colin (2001)
Fagus sylvatica, Quercus robur, Betula pendula	Twigs	0.076	1	2.245	−0.559	0.401	Petráš et al. (1985)
Fagus sylvatica, Quercus robur, Betula pendula	Foliage	0.029	1	2.432	−0.600	0.365	Petráš et al. (1985)
Fagus sylvatica, Betula pendula	Roots	0.022	0	2.540	0	1	Drexhage and Colin (2001)
Quercus robur	Roots	0.028	0	2.440	0	1	Drexhage and Colin (2001)

Table I.3
Coefficients for volume calculation for the Czech Republic (Petráš and Pajtík, 1991).

Regression coefficients for volumetric equations for the Czech Republic														
	Compartment	*a*0	*a*1	*a*2	*a*3	*a*4	*a*5	*a*6	*a*7	*a*8	*a*9	*a*10	*a*11	*a*12
Fagus sylvatica	stemOB	6.77E−01	−1.43E−02	2.92E−04	−2.11E−06	−3.13E−03	2.67E−04	−5.91E−06	4.19E−08					
Fagus sylvatica	stemUB	5.84E−01	−1.14E−02	2.49E−04	−1.88E−06	−2.77E−03	2.40E−04	−5.40E−06	3.87E−08					
Fagus sylvatica	wood ⩾7cm OB	5.65E−01	−2.33E+00	3.93E+01	−2.34E+02	−1.42E−03	−1.83E−06	6.21E−07	−4.77E−09					
Fagus sylvatica	wood ⩾7cmUB	5.42E−01	−3.12E+00	4.43E+01	−2.36E+02	−1.07E−03	−1.86E−05	8.81E−07	−6.00E−09					
Fagus sylvatica	treeOB	5.99E−01	−2.02E−01	4.49E+00	5.99E+00	−4.41E−01	6.10E−03	−2.97E+00	−1.09E+02	8.99E+01	6.66E+01	−1.09E+01	6.35E−01	
Pinus sylvestris	stemOB	3.03E−05	2.08E+00	−1.25E−02	9.61E−01									
Pinus sylvestris	stemUB	2.26E−05	2.12E+00	−1.27E−02	9.80E−01									
Pinus sylvestris	wood ⩾7cmOB					7.20E−02	−2.12E+00	1.37E+00						
Pinus sylvestris	wood ⩾7cmUB					6.43E−02	−2.12E+00	1.37E+00						
Pinus sylvestris	treeOB					3.60E+01	8.11E−01	1.38E+00	3.03E−05	2.08E+00	−1.25E−02	9.61E−01	1.00E+02	
Betula pendula	stemOB	0.00E+00	1.32E+00	−2.30E−04	6.43E+01	−2.04E+01	8.00E+00	−2.32E−01						
Betula pendula	stemUB								1.00E+00	−1.00E−02	1.73E+01	5.05E−03	1.00E−01	−2.06E+00
Betula pendula	wood ⩾7cmOB	−4.50E+00	1.08E+00	−1.15E−03	3.12E+04	−2.32E+01	5.50E+00	−1.43E−01						
Betula pendula	wood ⩾7cmUB								1.00E+00	−1.00E−02	1.73E+01	5.05E−03	1.00E−01	−2.06E+00
Betula pendula	treeOB	0.00E+00	1.11E+00	−4.80E−04	8.30E+04	−2.60E+01	8.00E+00	−1.50E−01						
Quercus robur	stemOB	4.62E−01	4.31E−01	7.46E−01	−9.06E−01	9.96E−04	−6.73E−06	−9.82E−07	7.75E−09					
Quercus robur	stemUB	3.59E−01	−5.25E−01	3.09E+00	−3.14E+00	3.21E−03	−5.84E−05	2.66E−07	−1.96E−09					
Quercus robur	wood ⩾7cmOB	4.47E−01	5.98E+00	−2.09E+00	−1.49E+01	8.70E−02	1.06E−03	−2.69E+01	1.68E+01	−2.21E−01	2.23E+02	−5.39E+01	−1.01E+00	
Quercus robur	wood ⩾7cmUB	4.53E−01	2.16E+00	9.10E+00	−1.21E+01	1.81E−01	−4.01E−03	−6.83E+00	9.44E+00	−2.44E−02	3.37E+01	−9.10E+00	−2.16E+00	
Quercus robur	treeOB	5.24E−01	4.24E+00	−6.60E+00	−7.81E+00	2.67E−01	−7.01E−03	3.74E+01	−2.14E+00	1.15E−01	−2.95E+01	1.73E+00	−9.29E−02	
Picea abies	stemOB	4.01E−05	1.00E+00	1.82E+00	1.13E+00	0.00E+00	0.00E+00	0.00E+00	0.00E+00					
Picea abies	stemUB	3.20E−05	1.00E+00	1.85E+00	1.15E+00	0.00E+00	0.00E+00	0.00E+00	0.00E+00					
Picea abies	wood ⩾7cmOB	4.01E−05	1.00E+00	1.82E+00	1.13E+00	9.29E−03	1.00E+00	−1.02E+00	8.96E−01					
Picea abies	wood ⩾7cmUB	3.20E−05	1.00E+00	1.85E+00	1.15E+00	8.29E−03	1.00E+00	−1.02E+00	8.96E−01					
Picea abies	treeOB	4.45E−05	1.00E+00	1.81E+00	1.13E+00	0.00E+00	0.00E+00	0.00E+00	0.00E+00					

For *B. pendula*:

$$V_{OB} = (H + a0)^{a1} * (a2 + a3 * exp(a4 * (DBH + a5)^{a6})) \quad (I.15)$$

$$V_{UB} = V_{OB} * (a7 + a8 * (a9 * exp(a10 * (V_{OB} + a11)^{a12}))) \quad (I.16)$$

For *P. sylvestris*:

$$V_{stem} = a0 * (DBH + 1)^{a1 + a2 * log(DBH+1)} * H^{a3} \quad (I.17)$$

$$V_{wood>7cm} = V_{stem} - a4 * (DBH + 1)^{a5} * H^{a6} \quad (I.18)$$

$$V_{treeOB} = V_{stemOB} + a4 * (DBH + 1)^{a5} / H^{a6} * a7 * (DBH + 1)^{a8 + a9 * log(DBH+1)} * H^{a10} / a11 \quad (I.19)$$

In case no regression equation was available, the required volume was calculated from the available volumes following the principles below:

$$percent\_bark = max\{V_{wood>7cmOB} - V_{wood>7cmUB})/V_{wood>7cmOB}; V_{stemOB} - V_{stemUB})/V_{stemOB}\} \quad (I.20)$$

$$V_{wood<7cmOB} = V_{treeOB} - V_{wood>7cmOB} \quad (I.21)$$

$$V_{wood<7cmUB} = (1 - percent\_bark) * V_{wood<7cmOB} \quad (I.22)$$

$$V_{bark} = V_{treeOB} - V_{wood>7cmUB} - V_{wood<7cmUB} \quad (I.23)$$

In the listed equations, FF_i the form factor for volume estimates [/], V_i volume of tree compartments [m^3], *percent_bark* is proportional content of bark [/], *DBH* is tree diameter at breast height in [cm], and *H* is tree height in [m] and parameters *a*0 to *a*12 are regression coefficients derived for the respective species and listed in the following table.

Appendix J. Biomass calculation in Poland

Allometric biomass functions using tree height and/or diameter are used for estimating aboveground biomass in Poland. For *P. sylvestris* models developed with sample material from 18 Scots pines stands in Bory Lubuskie (western Poland) are used (Zasada et al., 2008). Due to lack of appropriate published biomass functions for *P. abies, F. sylvatica* and *Q. robur* in Poland generalized biomass functions for Europe are applied (Muukkonen, 2007). For *B. pendula* height- and diameter-dependent functions developed in Finland are used (Repola, 2008) (see Table J.1).

For *P. sylvestris*:

$$dswm, dsbm, \ldots = a0 * DBH^{a1} * H^{a2} \quad (J.1)$$

With *DBH* [mm], *H* [m]

For *P. abies*, *F. sylvatica* and *Q. robur*:

$$dsm, dsbm, \ldots = exp(a0 + a1 * DBH/(DBH + a2)) \quad (J.2)$$

With *DBH* [cm]

For *B. pendula*:

Model type 1:

$$dswm, dsbm, \ldots = cf * exp(a0 + a1 * dk/(dk + a2) + a3 * ln(H) + cf2) \quad (J.3)$$

Model type 2:

$$dswm, dsbm, \ldots = cf * exp(a0 + a1 * dk/(dk + a2) + a3 * H/(H + a4) + cf2) \quad (J.4)$$

$$dk = 2 + 1.25 * DBH \quad (J.5)$$

dk and *DBH* [cm], *H* [m], all parameters are given below.

Root-to-shoot ratios are the official values used in official Polish reportings on changes in carbon stocks of the living biomass under the Kyoto Protocol which are the weighted average of the default coefficients proposed by IPCC (2006).

$$drm = RS * (dswm + dsbm + dfm + dabm + ddbm) \quad (J.6)$$

RS is given in Appendix A. Minimum root diameter is not defined.

Appendix K. Biomass calculation in Romania

Tree biomass is calculated using the volume functions developed in Romania by Giurgiu et al. (1972) used in the Romanian NIR report combined with biomass expansion factors. The

Table J.1
Coefficients for calculating biomass for Poland (Zasada et al., 2008; Repola, 2008; Muukkonen, 2007).

Coefficients for biomass calculation for Poland								
	*a*0	*a*1	*a*2	*a*3	*a*4	*cf*	*cf*2	Model type
Pinus sylvestris								
dswm	0.00041	1.627725	1.390374	–	–	–	–	–
dsbm	0.000192	2.117192	–	–	–	–	–	–
dabm	0.0000038	3.653659	−1.6008	–	–	–	–	–
ddbm	0.0000072	2.433082	–	–	–	–	–	–
dfm	0.000212	2.30978	−0.58099	–	–	–	–	–
Picea abies								
dsm	−3.043	11.784	9.328	–	–	–	–	–
dbm	−0.537	10.093	40.426	–	–	–	–	–
dfm	−1.360	7.308	19.662	–	–	–	–	–
Fagus sylvatica, Quercus robur								
dsm	−0.657	10.730	17.394	–	–	–	–	–
dbm	−2.128	13.295	26.095	–	–	–	–	–
dfm	−2.480	9.511	26.771	–	–	–	–	–
Betula pendula								
dswm	−4.879	9.651	12	1.012	–	1	0.004035	1
dsbm	−5.401	10.061	12	2.657	20	1	0.02743	2
dabm	−4.152	15.874	16	−4.407	10	1	0.051975	2
ddbm	−8.335	12.402	16	–	–	2.0737	0	2
dfm	−29.566	33.372	2	–	–	1	0.0385	2

calculated volume includes above ground tree compartments excluding foliage. Wood density values from the Global wood density database (Zanne et al., 2009; Chave et al., 2009) and biomass fractions calculated using results from the EFISCEN project (Vilén et al., 2005) (see Tables K.1 and K.2).

$$log10(V_{abg}) = a0 + a1 * log10(DBH) + a2 * (log10(DBH))^2 + a3 * log10(H) + a4 * (log10(H))^2 \quad (K.1)$$

$$BM_{ABG} = V_{ABG} * wd \quad (K.2)$$

$$dsm, dbm, \ldots = f\_i * BM_{ABG} \quad (K.3)$$

where V_{ABG} aboveground tree volume [m^3], BM_{ABG} aboveground tree biomass [kg], *DBH* [cm], *H* [m], *wd* dry wood density [kg/m^3] from the Global wood density database (Zanne et al., 2009; Chave et al., 2009) in Appendix A, coefficients *a*0–*a*4 and *f_i* age-dependent biomass fractions are given below. Minimum root diameter is not defined.

Appendix L. Biomass calculation in Italy

The methodology is a combination of the allometric biomass functions developed with sample material from Italy from Tabacchi et al. (2011) and the conversion parameters from Federici et al. (2008). *dsm* includes stem and branches > 5 cm diameter and *dbm* includes foliage and branches < 5 cm diameter (Tabacchi et al., 2011). The Italian NIR report for the Italian Greenhouse Gas Inventory for the period 1990–2010 (ISPRA, 2013) use growing stock reported by the NFI (MAF-ISAFA, 1988) in combination with biomass expansion factors, wood density and root-shoot ratios citing Federici et al. (2008). Growing stock is calculated with allometric functions, which are developed with a subset of the sample material used for the models used in this work (Tabacchi et al., 2011). Since *Q. robur* and *B. pendula* are not covered in Tabacchi et al. (2011), we use the models from *Quercus pubescens* Willd. for the first and from "Altre latifoglie" (other broadleaves) for the second species from the same reference (see Table L.1).

$$dsm = s0 + s1 * DBH^2 * H + s2 * DBH \quad (L.1)$$

$$dbm = b0 + b1 * DBH^2 * H + b2 * DBH \quad (L.2)$$

$$drm = RS * (dsm + dbm) \quad (L.3)$$

with *DBH* [cm], *H* [m], *s*0–*s*2 and *b*0–*b*2 according to Tabacchi et al. (2011) given in table below, *RS* according to Federici et al. (2008) in Appendix A. Minimum root diameter is not defined.

Appendix M. Biomass calculation in Spain

Until now for international reporting, carbon stock in living biomass was calculated using the method of "Change in Carbon Stocks" described in the GPG-LULUCF (IPCC, 2006). Biomass expansion factors were based on large dataset collected in the Ecological Forest Inventory of Catalonia, Spain (Gracia et al., 2002; Mäkipää et al., 2005). Root biomass is estimated with an expansion factor according to IPCC methodology (IPCC, 2006) (see Table M.1).

In future for international reporting on forest biomass allometric functions are probably used. These functions are developed in Spain and are dependent on DBH and/or tree height (Ruiz-Peinado et al., 2011, 2012; Diéguez-Aranda et al., 2009).

For *P. abies* (functions from *Abies alba*), *P. sylvestris* and *F. sylvatica* the functions from Ruiz-Peinado et al. (2011) and Ruiz-Peinado et al. (2012) are used, for *B. pendula* (functions from *Betula alba*) from Diéguez-Aranda et al. (2009) and for *Q. robur* from Balboa-Murias et al. (2006a, 2006b). The minimum root diameter is not given; the authors state however that fine roots are not captured by their excavation method (Ruiz-Peinado et al., 2011, 2012).

As there are no explicit functions for foliage biomass given in Ruiz-Peinado et al. (2011, 2012), the foliage biomass functions from Diéguez-Aranda et al. (2009) are used. For *P. abies* and for *P. sylvestris* the function from *Pinus pinaster* are used, for *F. sylvatica* the function from *Betula alba* (Diéguez-Aranda et al., 2009).

The general equation for *P. abies* and *P. sylvestris* is:

$$dsm, dbm1, \ldots = a * DBH^b * H^c + d * H \quad (M.1)$$

For *P. sylvestris*, *dbm1* = 0 for *DBH* <= 37.5 cm, if DBH > 37.5 cm:

$$dbm1 = 0.54 * (DBH - 37.5)^2 - 0.0119 * (DBH - 37.5)^2 * H \quad (M.2)$$

The general equation for *F. sylvatica*, *Q. robur* and *B. pendula* is:

$$dsm, dbm1, \ldots = a * DBH^b * H^c + d * DBH^2 + e \quad (M.3)$$

Table K.1
Coefficients for aboveground volume calculation for Romania (Giurgiu et al., 1972).

Coefficients for aboveground volume for Romania					
	*a*0	*a*1	*a*2	*a*3	*a*4
Picea abies	−4.18161	2.08131	−0.11819	0.70119	0.14818
Pinus sylvestris	−3.84672	1.82103	−0.04107	0.35677	0.33491
Fagus sylvatica	−4.11122	1.30216	0.23636	1.26562	−0.07966
Quercus robur	−4.13329	1.88001	0.04880	0.95371	−0.06364
Betula pendula	−4.16999	2.27038	−0.21540	0.30765	0.36826

Table K.2
Age-dependent biomass fractions for calculating biomass in compartments for Romania.

Biomass fractions dependent on tree age [years] for Romania											
Picea abies	20	30	40	50	60	70	80	90	100	110	1000
Stem	0.525	0.649	0.765	0.826	0.853	0.862	0.859	0.855	0.851	0.845	0.836
Branches	0.475	0.351	0.235	0.174	0.147	0.138	0.141	0.145	0.149	0.155	0.164
Roots	0.136	0.180	0.226	0.238	0.242	0.249	0.260	0.269	0.275	0.281	0.288
Foliage	0.227	0.189	0.135	0.103	0.086	0.077	0.073	0.070	0.067	0.065	0.063
Pinus sylvestris	30	40	50	60	80	100	120	1000			
Stem	0.493	0.661	0.749	0.793	0.830	0.845	0.848	0.845			
Branches	0.507	0.339	0.251	0.207	0.170	0.155	0.152	0.155			
Roots	0.150	0.181	0.198	0.208	0.213	0.213	0.208	0.201			
Foliage	0.230	0.132	0.087	0.063	0.044	0.032	0.026	0.022			
Fagus sylvatica, Quercus robur, Betula pendula	40	60	80	100	120	140	1000				
Stem	0.857	0.862	0.855	0.843	0.869	0.883	0.890				
Branches	0.143	0.138	0.145	0.157	0.131	0.117	0.110				
Roots	0.373	0.244	0.215	0.201	0.204	0.209	0.218				
Foliage	0.063	0.028	0.020	0.017	0.016	0.016	0.017				

Table L.1
Coefficients for calculation biomass for Italy (Tabacchi et al., 2011).

Coefficients for biomass calculations for Italy						
	*s*0	*s*1	*s*2	*b*0	*b*1	*b*2
Picea abies	−5.9426	0.01321	0.78369	5.9459	0.0040669	−0.21054
Pinus sylvestris	0.65786	0.017176	0	2.1336	0.0045864	0
Fagus sylvatica	−0.83814	0.024865	0	2.504	0.0051283	0
Quercus robur	1.0832	0.029634	−0.49794	−8.2101	0.0030396	1.7561
Betula pendula	−9.1098	0.0073484	2.3666	−3.6118	0.004319	0.74127

Table M.1
Coefficients for calculating biomass for Spain (Ruiz-Peinado et al., 2011, 2012; Diéguez-Aranda et al., 2009; Balboa-Murias et al., 2006a, 2006b).

Coefficients for biomass calculation in Spain					
Picea abies	*a*	*b*	*c*	*d*	
dsm	0.0189	2	1	0	
dbm1 + dbm2	0.0584	2	0	0	
dbm3	0.0371	2	0	0.968	
dfm	0.1081	1.51	0	0	
drm	0.101	2	0	0	
Pinus sylvestris					
dsm	0.0154	2	1	0	
dbm2	0.0295	2.742	−0.899	0	
dbm3	0.53	2.199	−1.153	0	
dfm	0.1081	1.51	0	0	
drm	0.13	2	0	0	
Fagus sylvatica	*a*	*b*	*c*	*d*	*e*
dsm	0.0182	2	1	0.0676	0
dbm2	0.0792	2	0	0	0
dbm3	0.00226	2	1	0.093	0
dfm	0.0346	1.645	0	0	0
drm	0.106	2	0	0	0
Quercus robur					
dswm	0.01823	2	1	0	−5.714
dsbm	0.00111	2	1	0.03154	−1.5
dbm1	3.427E−09	4.959	2.31	0	0
dbm2	0.00341	2	1	0	4.268
dbm4	0.03851	1.784	0	0	0
dbm5	0.00012	2	1	0	1.379
dfm	0.0101985	1.667	0.7375	0	0
drm	0.0116	1.949	0.9625	0	0
Betula pendula					
dswm	0.1485	2.2223	0	0	0
dsbm	0.031	2.186	0	0	0
dbm2	0.1374	1.76	0	0	0
dbm4	0.05	1.618	0	0	0
dbm5	0.0372	1.581	0	0	0
dfm	0.0346	1.645	0	0	0
drm	1.042	1.254	0	0	0

For *F. sylvatica dbm1* = 0 for *DBH* <= 22.5 cm, if *DBH* > 22.5 cm:

$$dbm1 = 0.83 * (DBH - 22.5)^2 - 0.0248 * (DBH - 22.5)^2 * H \quad (M.4)$$

For *B. pendula*:

$$dbm1 = 1.515 * exp(0.0904 * DBH) \quad (M.5)$$

All functions with biomass in [kg], *DBH* [cm] and *H* [m], coefficients *a*–*e* are given below.

Appendix N. Supplementary material

Supplementary data associated with this article can be found, in the online version, at http://dx.doi.org/10.1016/j.foreco.2015.11.016.

References

Araújo, T.M., Higuchi, N., Andrade de Carvalho Junior, J., 1999. Comparison of formulae for biomass content determination in a tropical rain forest site in the state of Para, Brazil. For. Ecol. Manage. 117, 43–52.

Assmann, E., 1970. The Principles of Forest Yield Study. Pergamon press, New York, 506 p.

Balboa-Murias, M.A., Rodríguez-Soalleiro, R., Merino, A., Álvarez-González, J.G., 2006a. Temporal variations and distribution of carbon stocks in aboveground biomass of radiata pine and maritime pine pure stands under different silvicultural regimes. For. Ecol. Manage. 237, 29–38.

Balboa-Murias, M.A., Rojo, A., Álvarez, J.G., Merino, A., 2006b. Carbon and nutrient stocks in mature *Quercus robur* L. stands in NW Spain. Ann. Forest Sci. 63 (5), 557–565.

Bartelink, H.H., 1996. Allometric relationships on biomass and needle area of Douglas-fir. For. Ecol. Manage. 86 (1–3), 193–203.

Bartelink, H.H., 1997. Allometric relationships for biomass and leaf area of beech (*Fagus sylvatica* L). Ann. Forest Sci. 54, 39–50.

Bolte, A., Rahmann, T., Kuhr, M., Pogoda, P., Murach, D., Gadow, K.V., 2004. Relationships between tree dimension and coarse root biomass in mixed stands of European beech (Fagus sylvatica L.) and Norway spruce (Picea abies[L.] Karst.). Plant Soil 264, 1–11. http://dx.doi.org/10.1023/B:PLSO.0000047777.23344.a3.

Burger, H., 1947. Holz, Blattmenge und Zuwachs. VIII. Mitteilung. Die Eiche. Mitteilungen der schweizerischen Anstalt für forstliches Versuchswesen 25, 211–279 (in German).

Burger, H., 1949. Holz, Blattmenge und Zuwachs. X. Mitteilung. Die Buche. Mitteilungen der schweizerischen Anstalt für forstliches Versuchswesen 26, 419–468 (in German).

Burger, H., 1953. Holz, Blattmenge und Zuwachs. XIII. Mitteilung. Fichten im gleichaltrigen Hochwald. Mitteilungen der schweizerischen Anstalt für forstliches Versuchswesen 29, 38–130 (in German).

Canadell, J.G., Le Quere, C., Raupach, M.R., Field, C.B., Buitenhuis, E.T., Ciais, P., Canadell, J.G., Que, C. Le, Conway, T.J., Gillett, N.P., Houghton, R.A., Marland, G., 2007. Contributions to accelerating atmospheric CO2 growth from economic activity, carbon intensity, and efficiency of natural sinks. PNAS 104, 18866–18870.

Chave, J., Coomes, D., Jansen, S., Lewis, S.L., Swenson, N.G., Zanne, A.E., 2009. Towards a worldwide wood economics spectrum. Ecol. Lett. 12, 351–366.

Chmelař, T., 1992. Variability of the conventional wood density of spruce *Picea abies* (L.) Karst branches in dependence on the position of branches in crown. Lesnictvi (Prague) 38 (2), 127–135 (in Czech).

Cienciala, E., Černý, M., Apltauer, J., Exnerová, Z., 2005. Biomass functions applicable to European beech. J. Forest Sci. 51 (4), 147–154.

Cienciala, E., Černý, M., Tatarinov, F., Apltauer, J., Exnerová, Z., 2006. Biomass functions applicable to Scots pine. Trees 20 (4), 483–495.

CITEPA, 2013. Rapport National d'Inventaire pour la France au Titre de la Convention Cadre des Nations Unies sur les Changement Climatiques et du Protocole de Kyoto, partie 1., 713 p. (in French).

Climate and Pollution Agency, 2013. National Inventory Report, Greenhouse Gas Emissions 1990–2011.

Curiel Yuste, J., Konôpka, B., Janssens, I.A., Coenen, K., Xiao, C.W., Ceulemans, R., 2005. Contrasting net primary productivity and carbon distribution between neighboring stands of *Quercus robur* and *Pinus sylvestris*. Tree Physiol. 25 (6), 701–712.

Dagnelie, P., Palm, R., Rondeux, J., et al., 1985. Tables de cubage des arbres et des peuplements forestiers. Les Presses Agronomiques de Gembloux, Gembloux, Belgium (in French).

De Wit, H.A., Palosuo, T., Hylen, G., Liski, J., 2006. A carbon budget of forest biomass and soils in southeast Norway calculated using a widely applicable method. For. Ecol. Manage. 225, 15–26. http://dx.doi.org/10.1016/j.foreco.2005.12.023.

Diéguez-Aranda U, Rojo Alboreca A, Castedo-Dorado F, Álvarez González JG, Barrio-Anta M, Crecente-Campo F, González González JM, Pérez-Cruzado C, Rodríguez Soalleiro R, López-Sánchez CA, Balboa-Murias MA, Gorgoso Varela JJ, Sánchez Rodríguez F, 2009. Herramientas selvícolas para la gestión forestal sostenible en Galicia. Xunta de Galicia. ISBN: 978-84-692-7395-1 (in Spanish).

Drexhage, M., Gruber, F., 1999. Above- and below-stump relationships for *Picea Abies*: estimating root system biomass from breast-height diameters. Scand. J. For. Res. 14, 328–333.

Drexhage, M., Colin, F., 2001. Estimating root system biomass from breast-height diameters. Forestry 74 (5), 491–497.

Eastaugh, C.S., Kangur, A., Korjus, H., Kiviste, A., Zlatanov, T., Velickkov, I., Srdjevic, B., Srdjevic, Z., Hasenauer, H., 2013. Scaling issues and constraints in modelling of forest ecosystems: a review with special focus on user needs. Baltic Forest. 19, 316–330.

Eastaugh, C.S., 2014. Relationships between the mean trees by basal area and by volume: reconciling form factors in the classic Bavarian yield and volume tables for Norway spruce. Eur. J. For. Res. 133, 871–877.

EUROSTAT, 2012. Europe in Figures, Eurostat Yearbook 2012, European Union, 698 p.

FAO, 2013. FAO STATISTICAL YEARBOOK, World Food and Agriculture, Food and Agriculture Organization of the United Nations, Rome, 307 p.

FOREST EUROPE, UNECE, FAO, 2011. State of Europe's Forests 2011. Status and Trends in Sustainable Forest Management in Europe, 344 p.

Federal Environmental Agency, 2012. Submission under the United Nations Framework Convention on Climate Change and the Kyoto Protocol. National Inventory Report for the German Greenhouse Gas Inventory 1990–2011, 885 p.

Federici, S., Vitullo, M., Tulipano, S., De Lauretis, R., Seufert, G., 2008. An approach to estimate carbon stocks change in forest carbon pools under the UNFCCC: the Italian case. iForest – Biogeosciences For. 1, 86–95.

Flemish Environment Agency, 2013. Belgium's Greenhouse Gas Inventory (1990–2011) National Inventory Report submitted under the United Nations Framework Convention on Climate Change and the Kyoto Protocol.

Gabler, K., Schadauer, K., 2008. Methods of the Austrian Forest Inventory 2000/02 Origins, Approaches, Design, Sampling, Data Models, Evaluation and Calculation of Standard Error, vol. 135. BFW-Berichte; Schriftenreihe des Bundesforschungs- und Ausbildungszentrums für Wald, Naturgefahren und Landschaft, Wien, 132 p.

Giurgiu, V., Decei, I., Armasescu, S., 1972. Biometria arborilor si arboretelor din Romania- Tabele endrometrice. Ed. Ceres, Bucuresti, Romania (in Romanian).

Gracia, C., Sabatè, S., Vayreda, J., Ibáñez, J.J., 2002. Aboveground Biomass Expansion Factors and Biomass Equations of Forests in Catalonia. Presentation at the COST E21 Meeting, Besalu (Spain) July 2002.

Gruber, F., 1987. Das Verzweigungssystem und der Nadelfall der Fichte (*Picea abies* (L.) Karst.) als Grundlage zur Beurteilung von Waldschäden. Ber. Forschungszentrum Waldökosysteme/Waldsterben, Reihe A, 26 (in German).

Grundner, F., Schwappach, A., 1952. Massentafeln zur Bestimmung des Holzgehaltes stehender Waldbäume und Waldbestände. 10. Aufl. Verlag Paul Parey, Berlin, Hamburg, 216 p. (in German).

Gschwantner, T., Gabler, K., Schadauer, K., Weiss, P., 2010. National forest inventory reports, chapter 1: Austria. In: Tomppo, E., Gschwantner, T.H., Lawrence, M., McRoberts, R.E. (Eds.), National Forest Inventories: Pathways for Common Reporting. Springer, Heidelberg, Dordrecht, London, New York, pp. 57–71.

Guo, Z., Fang, J., Pan, Y., Birdsey, R., 2010. Inventory-based estimates of forest biomass carbon stocks in China: a comparison of three methods. For. Ecol. Manage. 259 (7), 1225–1231.

Hamburg, S.P., Zamolodchikov, D.G., Korovin, G.N., Nefedjev, V.V., Utkin, A.I., Gulbe, J.I., Gulbe, T.A., 1997. Eestimating the carbon content of Russian forests; a comparison of Phytomass/Volume and Allometric Projections. Mitig. Adapt. Strat. Glob. Change 2, 247–265.

Härkönen, S., Lehtonen, A., Eerikäinen, K., et al., 2011. Estimating forest carbon fluxes for large regions based on process-based modelling, NFI data and Landsat satellite images. For. Ecol. Manage. 262, 2364–2377.

Hasenauer, H., 1994. Ein Einzelbaumwachstumssimulator für ungleichaltrige Fichten-Kiefern- und Buchen-Fichtenmischbestände. Forstl. Schriftenreihe, Univ. f. Bodenkultur, Wien. Österr. Ges. f. Waldökosystemforschung und experimentelle Baumforschung. 152 p. (in German).

He, L., Chen, J.M., Pan, Y., et al., 2012. Relationships between net primary productivity and forest stand age in U.S. forests. Global Biogeochem. Cycles 26, 1–19.

Hochbichler, E., 2002. Vorläufige Ergebnisse von Biomasseninventuren in Buchen- und Mittelwaldbeständen. In: Dietrich, H.P., Raspe, S., Preuhsler, T. (Eds.), Inventur von Biomasse- und Nährstoffvorräten in Waldbeständen, Forstliche Forschungsberichte, vol. 186. LWF, München, Germany, pp. 37–46 (in German).

Hochbichler, E., Bellos, P., Lick, E., 2006. Biomass functions for estimating needle and branch biomass of spruce (*Picea abies*) and Scots pine (*Pinus sylvestris*) and branch biomass of beech (*Fagus sylvatica*) and oak (*Quercus robur* and *petrea*). Aust. J. Forest Sci. 123, 35–46.

Hytönen, J., Saarsalmi, A., Rossi, P., 1995. Biomass production and nutrient uptake of short-rotation plantations. Silva Fennica 29 (2), 117–139.

INRA, 2004. Rapport final du projet CARBOFOR, Sequestration de Carbone dans les grands ecosystemes forestiers en France. Quantification, spatialisation, vulnerabilite et impacts de differents scenarios climatiques et sylvicoles. Programme GICC 2001 "Gestion des impacts du changement climatique" Convention Gip ECOFOR n 3/2001, 138 p. (in French).

IPCC, 2006. CHAPTER 4 FOREST. In: Eggleston, H.S., Buendia, L., Miwa, K., Ngara, T., Tanabe, K. (Eds.), 2006 IPCC Guidelines for National Greenhouse Gas Inventories, Prepared by the National Greenhouse Gas Inventories Programme. IGES, Japan, 83 p.

ISPRA, 2013. Italian greenhouse gas inventory 1990–2011, National Inventory Report 2013. Italy, Rome, p. 516.

Jalkanen, A., Mäkipää, R., Ståhl, G., Lehtonen, A., Petersson, H., 2005. Estimation of the biomass stock of trees in Sweden: comparison of biomass equations and age-dependent biomass expansion factors. Ann. Forest Sci. 62, 845–851.

Jenkins, J.C., Chojnacky, D.C., Heath, L.S., Birdsey, R.A., 2003. National-scale biomass estimators for United States tree species. Forest Sci. 49 (1), 12–35.

Johansson, T., 1999. Biomass equations for determining fractions of pendula and pubescent birches growing on abandoned farmland and some practical implications. Biomass Bioenergy 16 (3), 223–238.

Ketterings, Q.M., Coe, R., Van Noordwijk, V., Ambagau, Y., Palm, C.A., 2001. Reducing uncertainty in the use of allometric biomass equations for predicting above-ground tree biomass in mixed secondary forests. For. Ecol. Manage. 146, 199–209.

Kittenberger, A., 2003. Generierung von Baumverteilungsmustern. diploma thesis. Universität für Bodenkultur, Wien, 79 p. (in German).

Klement, I., Réh, R., Detvaj, J., 2010. Základné charakteristiky lesných drevín – spracovanie drevnej suroviny v odvetví spracovania dreva. Národné lesnícke centrum, ISBN 978-80-8093-112-4 (in Czech).

Klopf, M., Thurnher, C., Hasenauer, H., 2011. Benutzerhandbuch MosesFramework. Universität für Bodenkultur, Wien, 124 p. (in German).

Kollmann, F., 1982. Technologie des Holzes und der Holzwerkstoffe. Springer-Verlag, Berlin, Heidelberg, New York (in German).

Kublin, E., 2002. Verfahrens- und Programmbeschreibung zum erweiterten BWI-Unterprogramm BDAT 2.0. Forstliche Versuchs- und Forschungsanstalt Baden-Württemberg, 30 p. (in German).

Lamlom, S.H., Savidge, R.A., 2003. A reassessment of carbon content in wood: variation within and between 41 North American species. Biomass Bioenergy 25, 381–388.

Lamlom, S.H., Savidge, R.A., 2006. Carbon content variation in boles of mature sugar maple and giant sequoia. Tree Physiol. 26, 459–468.

Lang, M., Nilson, T., Kuusk, A., Kiviste, A., Hordo, M., 2007. The performance of foliage mass and crown radius models in forming the input of a forest reflectance model: a test on forest growth sample plots and Landsat 7 ETM+ images. Remote Sens. Environ. 110 (4), 445–457.

Lawrence, D.M., Oleson, K.W., Flanner, M.G., et al., 2011. Parameterization improvements and functional and structural advances in Version 4 of the Community Land Model. J. Adv. Model Earth Syst. 3, M03001.

Le Goff, N., Ottorini, J.M., 2001. Root biomass and biomass increment in a beech (*Fagus sylvatica* L.) stand in North-East France. Ann. Forest Sci. 58, 1–13.

Ledermann, T., Neumann, M., 2006. Biomass equations from data of old long-term experimental plots. Aust. J. Forest Sci. 123 (1/2), 47–64.

Lehtonen, A., Mäkipää, R., Heikkinen, J., Sievänen, R., Liski, J., 2004. Biomass expansion factors (BEFs) for Scots pine, Norway spruce and birch according to stand age for boreal forests. For. Ecol. Manage. 188, 211–224.

Lexer, M.J., Hoenninger, K., 2001. A modified 3D-patch model for spatially explicit simulation of vegetation composition in heterogeneous landscapes. For. Ecol. Manage. 144, 43–65.

Lorey, T., 1878. Die mittlere Bestandeshöhe. Allgemeine Forst- und Jagdzeitung 54, 149–155.

MacLean, R.G., Ducey, M.J., Hoover, C.M., 2014. A comparison of carbon stock estimates and projections for the Northeastern United States. Forest Sci. 60 (2), 206–213.

MacPeak, M.D., Burkart, L.F., Weldon, D., 1990. Comparison of grade, yield, and mechanical properties of lumber produced from young fast-grown and old slow- grown planted slash pine. Forest Products J. 40 (1), 11–14.

MAF-ISAFA, 1988. Inventario Forestale Nazionale. Sintesi metodologica e risultati. Ministero dell'Agricoltura e delle foreste. Istituto Sperimentale per l'assestamento forestale e per l'Alpicoltura, Trento (in Italian).

Marklund, L.G., 1988. Biomassafunktioner för tall, gran och björk i Sverige. Rapporter Skog; 45: 1–73. Sveriges Landbruksuniversitet (in Swedish).

Marschall, J., 1992. Hilfstafeln für die Forsteinrichtung, fifth ed. Österreichischer Agrarverlag, Wien (in German).

Mátyás, C., Ackzell, L., Samuel, C.J.A., 2004. EUFORGEN Technical Guidelines for genetic conservation and use for Scots pine *(Pinus sylvestris)*. International Plant Genetic Resources Institute, Rome, Italy, 6 p.

Mäkipää, R., Cienciala, E., Green, C., Gracia, C., Lehtonen, A., Muukkonen, P., Sabate, S., Somogyi, Z., Weiss, P., 2005. Multi-source inventory methods for quantifying carbon stocks and stock changes in European forests. Action COST CarboInvent. Final report for Deliverable 2.2. Document No.: WP2-D2.2-Metla. Date: October 28.

McGroddy, M., Daufresne, T., Hedin, L., 2004. Scaling of C:N:P stoichiometry in forests worldwide: implications of terrestrial Redfield-type ratios. Ecology 85 (9), 2390–2401.

McRoberts, R.E., Tomppo, E., Schadauer, K., Vidal, C., Chirici, G., Lanz, A., Cienciala, E., Winter, S., Smith, W.B., 2009. Harmonizing national forest inventories. J. Forest., 179–187

Miles, P.D., Smith, W.B., 2009. Specific Gravity and Other Properties of Wood and Bark for 156 Tree Species Found in North America. Research Note NRS-38.

Mitchell, S.R., Harmon, M.E., O'Connell, K.E.B., 2012. Carbon debt and carbon sequestration parity in forest bioenergy production. GCB Bioenergy 4, 818–827.

Mohren, G.M.J., Hasenauer, H., Köhl, M., Nabuurs, G.J., 2012. Forest inventories for carbon change assessments. Curr. Opinion Environ. Sustain. 4 (6), 686–695.

Montero, G., Ruiz-Peinado, R., Muñoz, M., 2005. Producción de biomasa y fijación de CO2 por los bosques españoles. Monografías INIA: Serie forestal 13. Instituto Nacional de Investigación y Tecnología Agraria y Alimentaria, Ministerio de Investigación y Ciencia. Madrid. ISBN 84-7498-512-9 (in Spanish).

Muukkonen, P., 2007. Generalized allometric volume and biomass equations for some tree species in Europe. Eur. J. Forest Res. 126 (2), 157–166.

Müller-Starck, G., Baradat, P., Bergmann, F., 1992. Genetic variation within European tree species. New Forest. 6 (1–4), 23–47.

Nabuurs, G., Schelhaas, M., Pussinen, A., 2000. Validation of the European Forest Information Scenario Model (EFISCEN) and a Projection of Finnish Forests. Silva Fennica 34 (2), 167–179.
Nagel, J., 1999. Konzeptuelle Überlegungen zum schrittweisen Aufbau eines waldwachstum-kundlichen Simulationssystems für Nordwestdeutschland (A concept for the development of a forest growth model for Northwest Germany). Schriften aus der Forstlichen Fakultät der Universität Göttingen und der Niedersächsischen Forstlichen Versuchsanstalt, J.D. Sauerländer's Verlag, Frankfurt am Main, 128 p.
Nabuurs, G., van den Wyngaert, I., Daamen, W., Helmink, A., de Groot, W., Knol, W., Kramer, H., Kuikman, P., 2005. National system of greenhouse gas reporting for forest and nature areas under UNFCCC in The Netherlands. Alterra-Report 1035 (1), 57 p.
National Institute for Public Health and the Environment, 2013. Greenhouse gas emission in The Netherlands 1990–2011, National Inventory Report 2013, 258 p.
Offenthaler, I., Hochbichler, E., 2006. Estimation of root biomass of Austrian forest tree species. Aust. J. Forest Sci. 123 (1/2), 65–86.
Pan, Y., Birdsey, R., Fang, J., Houghton, R., Kauppi, P., Kurz, W., Hayes, D., 2011. A large and persistent carbon sink in the World's forests. Science 333, 988–992.
Petráš, R., Košút, M., Oszlányi, J., 1985. Leaf biomass of trees in spruce, pine and beech. Lesnícky časopis 31 (2), 121–136 (in Slovak).
Petráš, R., Pajtík, J., 1991. Sústava česko-slovenských objemových tabuliek drevín. Lesnícky časopis 37 (1), 49–56 (in Slovak).
Petersson, H., Ståhl, G., 2006. Functions for below-ground biomass of *Pinus sylvestris, Picea abies, Betula pendula* and *Betula pubescens* in Sweden. Scand. J. For. Res. 21 (S7), 84–93.
Pietsch, S.A., Hasenauer, H., 2002. Using mechanistic modeling within forest ecosystem restoration. For. Ecol. Manage. 159, 111–131.
Pietsch, S.A., Hasenauer, H., Thornton, P.E., 2005. BGC-model parameters for tree species growing in central European forests. For. Ecol. Manage. 211 (3), 264–295.
Pollanschütz, J., 1974. Formzahlfunktionen der Hauptbaumarten Österreichs. Informationsdienst Forstliche Bundesversuchsanstalt Wien 153, 341–343 (in German).
Požgaj, A., Chovanec, D., Kurjatko, S., Babiak, M., 1993. Štruktúra a vlastnosti dreva. Príroda, Bratislava, 486 p. ISBN 80-07-00600-1 (in Slovak).
Pretzsch, H., Biber, P., Dursky, J., 2002. The single tree-based stand simulator SILVA: construction, application and evaluation. For. Ecol. Manage. 162, 3–21.
Repola, J., 2006. Models for vertical wood density of scots Pine, Norway spruce and birch stems, and their application to determine average wood density. Silva Fennica 40 (4), 673–685.
Repola, J., 2008. Biomass equations for birch in Finland. Silva Fennica 42 (4), 605–624.
Repola, J., 2009. Biomass equations for Scots Pine and Norway Spruce in Finland. Silva Fennica 43 (4), 625–647.
Ruiz-Peinado, R., Del Rio, M., Montero, G., 2011. New models for estimating the carbon sink capacity of Spanish softwood species. Forest Syst. 20 (1), 176–188.
Ruiz-Peinado, R., Montero, G., Del Rio, M., 2012. Biomass models to estimate carbon stocks for hardwood tree species. Forest Syst. 21 (1), 42–52.
Running, S., Nemani, R., Heinsch, F., Zhao, M., Reeves, M., Hashimoto, H., 2004. A continuous satellite-derived measure of global terrestrial primary production. Bioscience 54, 547–560.
Schelhaas, M.J., Varis, S., Schuck, A., Nabuurs, G.J., 1999. EFISCEN's European Forest Resource Database. European Forest Institute, Joensuu, Finland.
Schieler, K., 1988. Methodische Fragen in Zusammenhang mit der österreichischen Forstinventur. Diploma Thesis, Universität für Bodenkultur, Vienna, Austria. 99 p. (in German).
Schmidt-Vogt, H., 1977. Die Fichte. Band 1. Paul Parey, Hamburg (in German).
Schwarzmeier, M., 2000. Erhebung der oberirdischen Biomassevorräte von Fichtenbestanden (*Picea abies* (L.) Karst.) im Bereich der Waldklimastationen Ebersberg und Flossenbürg. Diploma Thesis, Fachhochschule Weihenstephan, Fachbereich Forstwirtschaft, Germany, 155 p. (in German).
Seidl, R., Lexer, M.J., Jäger, D., Hönninger, K., 2005. Evaluating the accuracy and generality of a hybrid patch model. Tree Physiol. 25 (7), 939–951.
Shinozaki, K., Yoda, K., Hozumi, K., Tira, T., 1964a. A quantitative analysis of plant form- the pipe model theory I. Basic analysis. Japanese J. Ecol. 14, 97–105.
Shinozaki, K., Yoda, K., Hozumi, K., Tira, T., 1964b. A quantitative analysis of plant form- the pipe model theory II. Further evidence of the theory and its application in forest ecology. Japanese J. Ecol. 14, 133–139.
Skrøppa, T., 2003. EUFORGEN Technical Guidelines for genetic conservation and use for Norway pruce (*Picea abies*). International Plant Genetic Resources Institute, Rome, Italy, 6 p.
Ståhl, G., Cienciala, E., Chirici, G., Lanz, A., Vidal, C., Winter, S., McRoberts, R.E., Rondeux, J., Schadauer, K., Tomppo, E., 2012. Bridging national and reference definitions for harmonizing forest statistics. Forest Sci. 58 (3), 214–223.
Statistics Finland, 2013. Greenhouse Gas emissions in Finland 1990–2011, National Inventory Report under the UNFCCC and the Kyoto Protocol.
Sterba, H., 1976. Ertragstafeln der ÖBF, Inst. f. forstl. Ertragslehre, Univ. f. Bodenkultur, Wien (in German).
Sterba, H., Monserud, R.A., 1997. Applicability of the forest stand growth simulator PROGNAUS for the Austrian part of the Bohemian Massif. Ecol. Model. 98, 23–34.
Tabacchi, G.,, Di Cosmo, L., Gasparini, P., Morelli, S., 2011. Stima del volume e della fitomassa delle principali specie forestali italiene, Equazioni di previsione, tavole del volume e tavole della fitomassa arborea epigea, 415 p. Trento: Consiglio per la Ricerca e la sperimentazione in Agricoltura, Unita di Ricerca per il Monitoraggio e la Pianificazione Forestale (in Italian).
Thomas, S.C., Martin, A.R., 2012. Carbon content of tree tissues: a synthesis. Forests 3, 332–352.
Thornton, P.E., 1998. Description of a Numerical Simulation Model for Predicting the Dynamics of Energy, Water, Carbon and Nitrogen in a Terrestrial Ecosystem. University of Montana, Missoula.
Thornton, P.E., Law, B.E., Gholz, H.L., Clark, K.L., Falge, E., Ellsworth, D.S., et al., 2002. Modeling and measuring the effects of disturbance history and climate on carbon and water budgets in evergreen needleleaf forests. Agric. For. Meteorol. 113 (1–4), 185–222.
Thurnher, C., Gerritzen, T., Maroschek, M., Lexer, M.J., Hasenauer, H., 2013. Analysing different carbon estimation methods for Austrian forests. Aust. J. Forest Sci. 130 (3), 141–166.
Tomppo, E., Gschwantner, T., Lawrence, M., McRoberts, R.E., 2010. National Forest Inventories: Pathways for common reporting. Springer, Berlin, 610 p.
Umweltbundesamt, 2013. Austria's National Inventory Report 2013, Submission under the United Nations Framework on Climate Change and the Kyoto Protocol. Umweltbundesamt GmbH (Federal Environment Agency Ltd) Vienna, Austria, Vienna.
Uri, V., Aosaar, J., Varik, M., Kund, M., 2010. The growth and production of some fast growing deciduous tree species stands on abandoned agricultural land. Forest. Stud. 52, 18–29.
Vallet, P., Dhôte, J.-F., Moguédec, G. Le, Ravart, M., Pignard, G., 2006. Development of total aboveground volume equations for seven important forest tree species in France. For. Ecol. Manage. 229, 98–110. http://dx.doi.org/10.1016/j.foreco.2006.03.013.
Vande Walle, I., Van Camp, N., Perrin, D., Lemeur, R., Verheyen, K., van Wesemael, B., Laitat, E., 2005. Growing stock-based assessment of the carbon stock in the Belgian forest biomass. Ann. For. Sci. 62, 853–864. http://dx.doi.org/10.1051/forest:2005076.
VEMAP Members, 1995. Vegetation/Ecosystem Modeling and Analysis Project (VEMAP): comparing biogeography and biogeochemistry models in a continental-scale study of terrestrial ecosystem responses to climate change and CO2 doubling. Global Biogeochem. Cycles 9 (4), 407–437.
Veroustraete, F., Sabbe, H., Eerens, H., 2002. Estimation of carbon mass fluxes over Europe using the C-Fix model and Euroflux data. Remote Sens. Environ. 83, 376–399.
Vilén, T., Meyer, J., Thürig, E., Lindner, M., Green, T., 2005. Multi-source inventory methods for quantifying carbon stocks and stock changes in European forests – CarboInvent. EFI, 31.
Wagenführ, R., Scheiber, C., 1985. Holzatlas, second ed. VEB Fachbuchverlag, Leibzig (in German).
Waring, R., Schroeder, P., Oren, R., 1982. Application of the pipe model theory to predict canopy leaf area. Can. J. For. Res. 12, 556–560.
Westfall, J.A., 2012. A comparison of above-ground dry-biomass estimators for trees in the Northeastern United States. Northern J. Appl. Forest. 29 (1), 26–34.
Wirth, C., Schumacher, J., Schulze, E.D., 2004. Generic biomass functions for Norway spruce in Central Europe–a meta-analysis approach toward prediction and uncertainty estimation. Tree Physiol. 24 (2), 121–139.
Wutzler, T., Wirth, C., Schumacher, J., 2008. Generic biomass functions for Common beech (*Fagus sylvatica*) in Central Europe: predictions and components of uncertainty. Can. J. For. Res. 38 (6), 1661–1675.
Xiao, C.W., Curiel Yuste, J., Janssens, I.A., Roskams, P., Nachtergale, L., Carrara, A., Sanchez, B.Y., Ceulemans, R., 2003. Above- and belowground biomass and net primary production in a 73-year-old Scots pine forest. Tree Physiol. 23 (8), 505–516.
Zanne, A.E., Lopez-Gonzalez, G., Coomes, D.A., Ilic, J., Jansen, S., Lewis, S.L., Chave, J., et al., 2009. Data from: Towards a worldwide wood economics spectrum. Dryad Digital Repository.
Zasada, M., Bronisz, K., Bijak, S., Wojtan, R., Tomusiak, R., Dudek, A., Michalak, K., 2008. Empirical formulae for determination of the dry biomass of aboveground parts of the tree. Sylwan 3, 27–39 (in Polish).
Zhao, M., Running, S.W., 2010. Drought-induced reduction in global terrestrial net primary production from 2000 through 2009. Science 329, 940–943.
Zianis, D., Muukkonen, P., Mäkipää, R., Mencuccini, M., 2005. Biomass and stem volume equations for tree species in Europe. Silva Fennica, Monographs, 63 p.

9.3. Paper 3

Neumann, M., **Moreno, A.,** Thurnher, C., Mues, V., Härkönen, S., Mura, M., Bouriaud, O., Lang, M., Cardellini, G., Thivolle-Cazat, A., Bronisz, K., Merganič, J., Alberdi, I., Astrup, R., Mohren, F., Zhao, M., Hasenauer, H., 2016b. Creating a Regional MODIS Satellite-Driven Net Primary Production Dataset for European Forests. Remote Sens. 8, 1–18.

remote sensing

MDPI

Article

Creating a Regional MODIS Satellite-Driven Net Primary Production Dataset for European Forests

Mathias Neumann [1,*], Adam Moreno [1], Christopher Thurnher [1], Volker Mues [2], Sanna Härkönen [3,4], Matteo Mura [5,6], Olivier Bouriaud [7], Mait Lang [8], Giuseppe Cardellini [9], Alain Thivolle-Cazat [10], Karol Bronisz [11], Jan Merganic [12], Iciar Alberdi [13], Rasmus Astrup [14], Frits Mohren [15], Maosheng Zhao [16] and Hubert Hasenauer [1]

1 Institute of Silviculture, Department of Forest and Soil Sciences, University of Natural Resources and Life Sciences, Vienna 1190, Austria; adam.moreno@boku.ac.at (A.M.); Cthurnhe@groupwise.boku.ac.at (C.T.); hubert.hasenauer@boku.ac.at (H.H.)
2 Centre for Wood Science, World Forestry, University of Hamburg, Hamburg 21031, Germany; volker.mues@uni-hamburg.de
3 Department of Forest Sciences, University of Helsinki, Helsinki 00014, Finland; sanna.harkonen@helsinki.fi
4 Finnish Forest Research Institute, Joensuu 80101, Finland
5 Department of Bioscience and Territory, University of Molise, 86090 Pesche (IS), Italy; matteo.mura@unifi.it
6 geoLAB—Laboratory of Forest Geomatics, Department of Agricultural, Food and Forestry Systems, Università degli Studi di Firenze, Firenze 50145, Italy
7 Facuty of Forestry, Universitatea Stefan del Mare, Suceava 720229, Romania; obouriaud@gmail.com
8 Tartu Observatory, Tõravere 61602, Estonia; Mait.Lang@emu.ee
9 Division Forest, Nature and Landscape, Department of Earth and Environmental Sciences, KU Leuven—University of Leuven, Leuven 3001, Belgium; giuseppe.cardellini@kuleuven.be
10 Technological Institute, Furniture, Environment, Economy, Primary Processing and Supply, Champs sur Marne 77420, France; Alain.THIVOLLECAZAT@fcba.fr
11 Laboratory of Dendrometry and Forest Productivity, Faculty of Forestry, Warsaw University of Life Sciences, Warsaw 02-776, Poland; karol.bronisz@wl.sggw.pl
12 Faculty of Forestry and Wood Sciences, Czech University of Life Sciences, Prague 16521, Czech Republic; j.merganic@forim.sk
13 Departamento de Selvicultura y Gestión de los Sistemas Forestales, INIA-CIFOR, Madrid 28040, Spain; alberdi.iciar@inia.es
14 Norwegian Institute for Bioeconomy Research, Ås 1431, Norway; rasmus.astrup@nibio.no
15 Forest Ecology and Forest Management Group, Wageningen University, Wageningen 6700, The Netherlands; frits.mohren@wur.nl
16 Department of Geographical Sciences, University of Maryland, Collage Park, MD 20742, USA; zhaoms@umd.edu
* Correspondence: mathias.neumann@boku.ac.at; Tel.: +43-1-47654-4059

Academic Editors: Lars T. Waser and Prasad S. Thenkabail
Received: 5 April 2016; Accepted: 25 June 2016; Published: 29 June 2016

Abstract: Net primary production (NPP) is an important ecological metric for studying forest ecosystems and their carbon sequestration, for assessing the potential supply of food or timber and quantifying the impacts of climate change on ecosystems. The global MODIS NPP dataset using the MOD17 algorithm provides valuable information for monitoring NPP at 1-km resolution. Since coarse-resolution global climate data are used, the global dataset may contain uncertainties for Europe. We used a 1-km daily gridded European climate data set with the MOD17 algorithm to create the regional NPP dataset MODIS EURO. For evaluation of this new dataset, we compare MODIS EURO with terrestrial driven NPP from analyzing and harmonizing forest inventory data (NFI) from 196,434 plots in 12 European countries as well as the global MODIS NPP dataset for the years 2000 to 2012. Comparing these three NPP datasets, we found that the global MODIS NPP dataset differs from NFI NPP by 26%, while MODIS EURO only differs by 7%. MODIS EURO also agrees with NFI NPP across scales (from continental, regional to country) and gradients (elevation, location, tree age, dominant species, etc.). The agreement is particularly good for elevation, dominant

species or tree height. This suggests that using improved climate data allows the MOD17 algorithm to provide realistic NPP estimates for Europe. Local discrepancies between MODIS EURO and NFI NPP can be related to differences in stand density due to forest management and the national carbon estimation methods. With this study, we provide a consistent, temporally continuous and spatially explicit productivity dataset for the years 2000 to 2012 on a 1-km resolution, which can be used to assess climate change impacts on ecosystems or the potential biomass supply of the European forests for an increasing bio-based economy. MODIS EURO data are made freely available at ftp://palantir.boku.ac.at/Public/MODIS_EURO.

Keywords: NPP; bioeconomy; forest inventory; NFI; climate; carbon; biomass; downscaling; increment; MOD17

1. Introduction

Net primary production (NPP), the difference between Gross Primary Production (GPP) and plant autotrophic respiration, is the net carbon or biomass fixed by vegetation through photosynthesis. NPP represents the allocation rate of photosynthetic products into plant biomass and can be used to measure the quantity of goods provided to society by ecosystems [1–3]. NPP of forest ecosystems is essential to estimate the potential supply of biomass for bioenergy, fiber and timber supply. NPP is also a key variable to assess environmental change impacts on ecosystems [4] since any variation in the growing conditions influences the carbon cycle due to changes in carbon uptake and/or respiration. As interest grows in utilizing forests for a "bio-based economy" [5,6], more accurate and realistic forest productivity estimates become increasingly important. In addition, competing forest ecosystem services, such as biodiversity or and nature conservation, need to be considered to ensure sustainable use of our forests and to avoid unsustainable over-exploitation of renewable resources.

Within the EU-28 160.9 million ha or 37.9% of the total land area are covered with forests [7]. These forests provide resources for the timber industry, the energy sector (24.3% of the energy in the EU-28 is generated from renewable sources of which 64.2% consists of forest biomass and waste [8]), but also for non-timber ecosystem services such as clean air, water, biodiversity or protection against natural hazards. Accurate and consistent forest information is a precondition for assessing the production and harvesting potential of forest resources in Europe.

There are conceptually different data sources and methods to assess forest productivity like:

(i) The MODIS algorithm MOD17 uses remotely sensed satellite-data and climate data to predict spatially and temporally continuous NPP and GPP (Gross Primary Production or carbon assimilation) based on an ecophysiological modelling approach [2]. In addition to satellite reflectance data and climate data, it requires the biophysical properties of land cover types, which are stored in the Biome Property Look-Up Tables (BPLUT) [9].

(ii) National forest inventory data can be used to assess the timber volume stocks as well as volume increment and removal, if repeated observations are available [10]. This terrestrial bottom-up approach collects forest information by measuring sample plots arranged on a systematic grid design across larger areas. In combination with biomass expansion factors or biomass functions, volume or tree information can be converted into biomass or carbon estimates to account for differences in wood densities, the carbon fraction and different allocation into compartments [11,12].

(iii) Flux towers record the gas-exchange in plant-atmosphere interactions [13], which can be used to derive GPP from Net Ecosystem exchange (NEE). NEE is estimated using eddy covariance data, climate measurements and other ancillary data [14].

Net Primary Production (NPP) from (i) top-down satellite-driven MOD17 algorithm and (ii) bottom-up NPP estimates using terrestrial forest inventory data were compared in a pilot study for Austria on national scale [15]. Top-down and bottom-up refer to the level of scaling of the primary recorded information (for MOD17 1-km remote sensing products and for Terrestrial NPP single tree observations). Our definition for top-down differs from traditional carbon cycle modelling [16]. This study wants to extend and test this concept for Europe on a continental scale.

For this purpose, we obtain two wall-to-wall spatially-explicit and consistent MODIS NPP datasets by acquiring the global dataset using global climate driver and by creating a regional dataset MODIS EURO using 1-km European climate data. We evaluate these two datasets by comparing with the NPP derived from forest inventory data from 12 European countries. We assess the reliability and potential discrepancies of the MODIS satellite-driven top-down versus the terrestrial bottom-up NPP estimates from continental to national scale and across different gradients like location, elevation or stand density. This will provide a better understanding of the reliability of remote sensing based NPP estimates, which could be used also for regions, where no terrestrial measurements are available.

2. Materials and Methods

We used two conceptually different methods to estimate NPP, (i) the MODIS NPP algorithm MOD17 and (ii) terrestrial forest inventory data and tree carbon estimation methods. Both have their respective strengths and weaknesses. MODIS NPP has the advantage of providing spatially continuous estimates with a consistent methodology, which is important for any large-scale studies. It incorporates biogeochemical principles in mechanistic modelling environment and the vegetation feedback to climate conditions through changes in Leaf Area Index and absorbed radiation [17]. It does not distinguish between different vegetation apart from general Land Cover types, has a coarse spatial resolution and might not be able to represent specific local conditions due to its calibration to global conditions. In contrast, terrestrial forest inventory NPP assesses the actual carbon allocation by trees and captures local small-scale effects (e.g., site conditions, tree age or forest management) as well as regional differences in estimating tree carbon [12,18]. It covers only the increment of trees assessed by the inventory system and might not capture local specifics of litter fall and fine root turnover very well, since broad model assumptions have to be used.

2.1. MODIS NPP

Since the year 2000, the MOD17 product provides spatially and temporally continuous NPP estimates across the globe [17]. The algorithm behind uses the reflectance data from the sensor MODIS (MODerate resolution Imaging Spectroradiometer) of the TERRA and AQUA satellites operated by National Aeronautics and Space Administration of the United States (NASA). MOD17 provides GPP and NPP estimates at a 1-km resolution [2,17] and incorporates basic biogeochemical principles adopted from Biome-BGC [19]. It integrates a light use efficiency logic using remotely sensed vegetation information to estimate GPP (Equation (1)) with a maintenance and growth respiration module to derive NPP (Equation (2)).

$$GPP = LUE_{max} \times f_{Tmin} \times f_{vpd} \times 0.45 \times SW_{rad} \times FPAR \quad (1)$$

$$NPP = GPP - R_M - R_G \quad (2)$$

LUEmax is the maximum light use efficiency, which get adjusted by f_{Tmin} and f_{vpd} to address water stress due to low temperature (Tmin) and vapor pressure deficit (VPD). SWrad is short wave solar radiation load, of which 45% is photosynthetically active. FPAR is the fraction of absorbed photosynthetic active radiation. R_M is the maintenance respiration and is estimated using LAI (Leaf Area Index), climate data and biome-specific parameters. R_G is the growth respiration and is estimated to be approx. 25% of NPP. The complete algorithm is documented in [18] and more details are found in the cited literature therein.

The MOD17 algorithm requires climate data, FPAR and LAI (leaf area index) data as well as land cover data, which is derived from MODIS reflectance data [20]. We obtained the global MODIS NPP product (MOD17A3 Version 055) provided by the Numerical Terradynamic Simulation Group (NTSG) at University of Montana available at ftp://ftp.ntsg.umt.edu/pub/MODIS/NTSG_Products/. This data set (hereafter called MODIS GLOB) covers the period of 2000 to 2012, which is the time period covered by our terrestrial data (see next chapter), and provides the annual NPP in $gC \cdot m^{-2} \cdot year^{-1}$.

The source of FPAR and LAI input is MODIS15 LAI/FPAR Collection 5, which was temporally gap filled to close data gaps due to unfavorable atmospheric conditions such as cloudiness or heavy aerosol presence [9]. For Land cover, we used the land cover product MOD12Q1 Version 4 Type 2 [21] representing the conditions in year 2001.

Climate data are important input into the MODIS NPP algorithm and climate data have a strong impact on the MODIS NPP results [15,22]. MODIS GLOB uses the global climate data set NCEP2 [23] described in the following Section 2.2. In Europe, we have high quality daily climate data, the E-OBS data set [24], which was recently downscaled to a 1-km resolution [25].

We next ran the MOD17 algorithm with the downscaled European climate data [25] and obtained an additional MODIS NPP estimate for the period 2000–2012 (hereafter called MODIS EURO), which differ from MODIS GLOB provided by NTSG only in the used daily climate input data. We used the same FPAR, LAI and Land cover input, as used for the global NPP product, MODIS GLOB. MODIS EURO covers our study region, the EU-28 including Norway, Switzerland and the Balkan states (see Figure 1) and is made available under ftp://palantir.boku.ac.at/Public/MODIS_EURO.

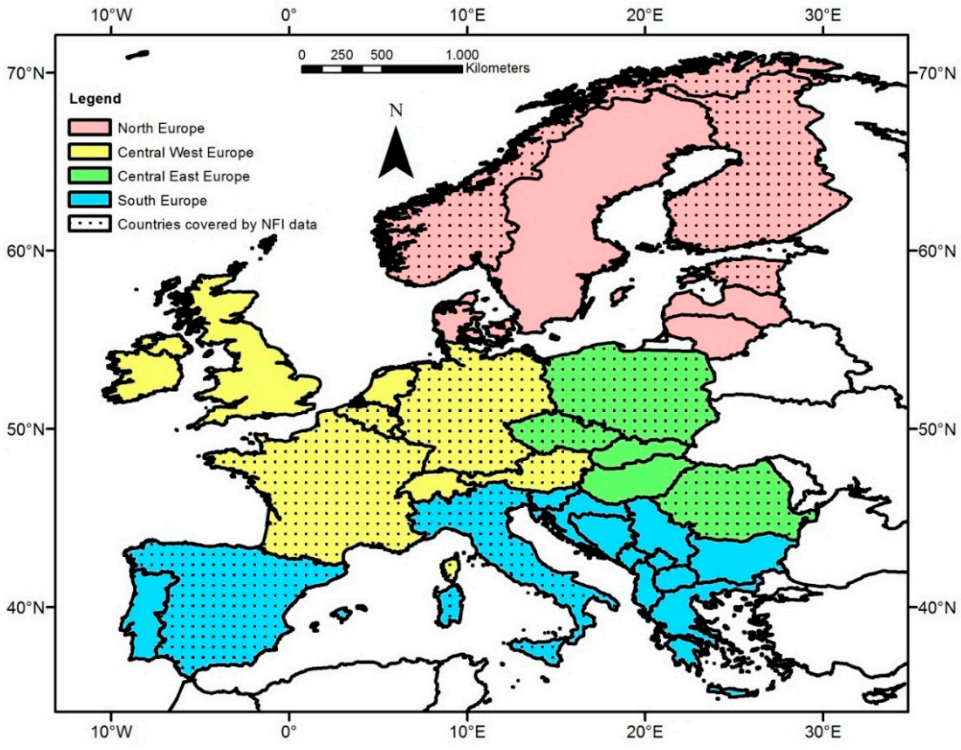

Figure 1. Our study region separated into four regions, countries with forest inventory data for estimating terrestrial National Forest Inventory (NFI) Net Primary Production (NPP) are marked with dots.

2.2. Climate Data

As outlined, the two MODIS NPP estimates, MODIS GLOB and MODIS EURO, differ only in the daily climate data input: MODIS GLOB employs the global NCEP2 climate data set [23] and MODIS

EURO uses European downscaled climate data [25]. We provide here a brief overview of the two climate data sets.

The NCEP2 data set (NCEP-DOE Reanalysis 2) is a reanalyzed global daily climate data set with a spatial resolution of 1.875° × 1.875°. This corresponds to approx. 220 km at the equator at latitude 0° (approx. 136 × 220 km at latitude 50°). To compensate the coarse spatial resolution, for MODIS GLOB the climate data for the 1 km MODIS pixels was deduced with an bilateral interpolation method based on the neighboring NCEP2 pixels [9].

The downscaled climate data used for MODIS EURO provide daily climate data on a 0.0083° × 0.0083° resolution (approx. 1 × 1 km at the equator and approx. 0.6 × 1 km at 50° latitude) [25]. This data set was developed out of the E-OBS gridded climate data set (0.25° resolution, using data from 7852 climate stations) [24] in conjunction with the WorldClim data set [26].

2.3. Terrestrial NFI NPP

Terrestrial forest data such as national forest inventory (NFI) data assess accumulated carbon on a systematic grid using a permanent plot design. From repeated observations of diameter at breast height (DBH) and/or tree height (H) in combination with biomass functions or biomass expansion factors the carbon accumulation of trees is estimated. Since this method is based on single tree measurements and local biomass studies, NPP derived from forest inventory data incorporates local effects such as weather patterns, climate anomalies, stand age, differences in biomass allocation, site and soil effects and different forest densities due to forest management [15,27].

We obtained 196,434 forest inventory plots covering 12 European countries. In Europe, each country has its own National Forest Inventory (NFI) system, which all have different measurement periods, sampling designs and methodologies [10] (Table S1 in the Supplementary Material). Thus, we first had to develop a harmonized and consistent terrestrial dataset for estimating Terrestrial NPP. We calculated NPP using the forest inventory data according to Equation (3).

$$\mathrm{NPP} = \mathrm{CARB_{INC}} + \mathrm{FR_{TO}} + \mathrm{C_{LF}} \quad (3)$$

$\mathrm{CARB_{INC}}$ is the carbon increment of trees ($\mathrm{gC \cdot m^{-2} \cdot year^{-1}}$). $\mathrm{FR_{TO}}$ is the carbon used for fine root turnover [28,29]. Fine root turnover $\mathrm{FR_{TO}}$ is assumed to be equal to the carbon flow into litter $\mathrm{C_{LF}}$ [27,30]. Both processes are controlled by the same factors and the assumption of similarity between the above- and belowground turnover of short-living plant organs is supported by recently collected European data on fine root turnover [29] and litter fall [31]. $\mathrm{C_{LF}}$ is the flow of carbon into litter ($\mathrm{gC \cdot m^{-2} \cdot year^{-1}}$) estimated using a climate-sensitive and species-dependent model [31] and is calculated as:

$$\text{Broadleaf-dominated}: \mathrm{C_{LF}} = \mathrm{CF} \exp(2.643 + 0.726\,\mathrm{Ln(T + 10)} + 0.181\,\mathrm{Ln(P)}) \quad (4)$$

$$\text{Coniferous-dominated}: \mathrm{C_{LF}} = \mathrm{CF} \exp(2.708 + 0.505\,\mathrm{Ln(T + 10)} + 0.240\,\mathrm{Ln(P)}) \quad (5)$$

CF is the carbon fraction of dry biomass which is set equal to 0.5 [11]. T is the mean annual temperature from the year 2000 to 2012 (°C). P is the mean annual precipitation 2000 to 2012 [mm]. For temperature and precipitation we use the European climate data [25] to capture important small-scale regional effects such as elevation or topography in a more realistic way. Equation (4) is applied for all plots where broadleaf species contribute most to total basal area and Equation (5) is used for coniferous-dominated plots (see Table S2 of the Supplementary Material).

We used data from nine National Forest Inventories (Austria, Czech Republic, Germany, France, Finland, Norway, Poland, Romania, Spain), and three Regional Forest Inventories (Belgium, Estonia, Italy). We grouped our 12 countries in four geographic regions, North Europe, Central-West Europe, Central-East Europe and South Europe [7], to address the large environmental, elevational and climatic

gradients in Europe. Countries within a region should have similar climatic and edaphic conditions as well as similar tree allometries and allocation patterns [32]. The original locations of the inventory plots were falsified to the nearest pixel of the MODIS grid to guarantee the locations of the plots remain unknown. Temporal consistency with the MODIS data (available since year 2000) was ensured by using only inventory data, which provide $CARB_{INC}$ (Equation (3)) for the time period 2000 to 2012. Figure 1 shows our study region with the four geographic regions completely covered by MODIS EURO, and the 12 countries, where we have NFI NPP.

Although all our terrestrial forest inventory data assess properties of trees, there are different sampling methods and increment calculation by country in place, which may strongly affect the resulting estimates [33,34]. Four different methods to estimate tree carbon increment $CARB_{INC}$ are used in our data: (1) repeated observations of fixed area plots (used in Norway, Poland, Belgium); (2) repeated angle count sampling (for Austria, Germany, Finland); (3) increment cores (France, Romania, Italy); as well as increment predictions from (4) tree growth models (Czech Republic, Estonia, Italy). Tree growth model predictions were used if no increment observations, either from repeated observations or from increment cores, were available.

In the Supplementary Material, we provide all details for our 12 inventory data sets, the local sampling system, the available data and the used increment method (Table S1 in the Supplementary Material).

The tree carbon results for determining carbon increment $CARB_{INC}$ (Equation (3)) were estimated using the carbon calculation method applied by the local forest inventory organization and compiled in [32]. Local biomass functions and biomass expansion factors were used to derive tree biomass and carbon fractions to convert biomass into carbon. In the Supplementary Material, we provide a detailed description on processing the NFI data, the tree carbon estimates and stand variables to describe the represented forests (e.g., mean age, basal area or stand density index).

Using this methodology, we processed the forest inventory data from the 12 countries (Table S1) and derived harmonized carbon stocks for all inventory plots. The forest inventory data set consists of 196.434 plots, harmonized across 12 European countries. We applied the carbon increment method for each country and calculated NPP by inventory plot (hereafter called NFI NPP) using Equations (3)–(5).

2.4. Analysis of NPP Results

We thus have three NPP sources: two using the MOD17 algorithm with different daily climate data: (i) MODIS GLOB produced by the Numerical Terradynamic Simulation Group (NTSG) at University of Montana and (ii) MODIS EURO by running the original MOD17 algorithm and the latest BPLUTs parametrized by [9] with downscaled daily climate data from Europe [25] as well as (iii) Terrestrial NFI NPP using forest inventory data from the 12 countries (Table S1) and local carbon estimation methods [32].

We compared the three NPP datasets across Europe, by our 4 regions (Figure 1) and the 12 countries to analyze our results across different spatial scaling. We extracted for each forest inventory plot at the corresponding MODIS cell the average NPP from MODIS GLOB and MODIS EURO for 2000 to 2012. We next computed for all plots the difference between the two MODIS NPP estimates and the Terrestrial NFI NPP (ΔNPP_{GLOB} = MODIS GLOB minus NFI NPP and ΔNPP_{EURO} = MODIS EURO minus NFI NPP).

We used each NFI plot separately and did not compute average values for MODIS pixels. This avoided smoothing effects due to different spacing between inventory grid points and the plot clusters used in some countries (Table S1).

To analyze the effect of gradients on the NPP results, we collected potentially meaningful meta-information such as plot location (Longitude and Latitude in WGS1984), Elevation (EU-DEM 30 m resolution), MODIS Land Cover type or forest characteristics (dominant tree species, mean age, stand density, tree height, etc.) and analyzed patterns of ΔNPP_{GLOB} and ΔNPP_{EURO} across these gradients.

Terrestrial and remote sensing NPP estimates exhibited discrepancies in previous research [15,18] and as explanation the authors suggested changes in stand density, which are commonly caused by forest management and disturbances [15,18]. Since major parts of the forests in Europe are managed [7] and affected by natural disturbances such as wind damage or forest fire [35], they should have experienced changes in stand density as compared to unmanaged forests. Stand density directly affects terrestrial NPP estimates by its impact on the development of DBH and H of the remaining trees after forest management operations until canopy closure is reached. On the other hand MODIS NPP is based on the "big leaf" concept and assumes a full coverage of forest area. We thus use Stand density index (SDI) [36] in the analysis of our NPP estimates.

3. Results

NPP estimated using the MOD17 algorithm has the advantage of providing spatial- and temporal-continuous NPP estimates across Europe on a 1-km resolution and Figure 2 illustrates this by showing MODIS EURO for the years 2000 to 2012. Note that MODIS EURO also covers not-forest land cover types such as crops, shrub- or grassland.

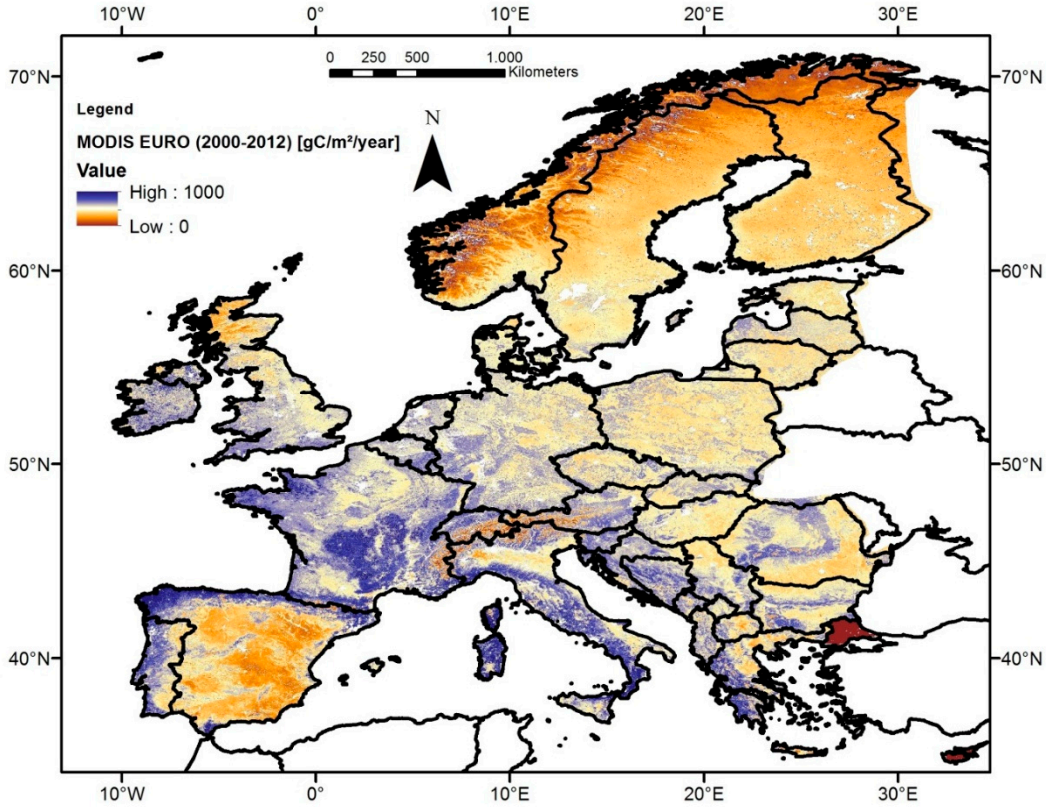

Figure 2. MODIS EURO NPP on 1-km resolution representing average NPP for the period 2000–2012 using European daily climate data (available under ftp://palantir.boku.ac.at/Public/MODIS_EURO).

Terrestrial NFI NPP is driven by forest information collected by field crews. Thus it provides NPP and the carbon accumulation by forest stands during a certain time period. Table 1 gives a summary of the forest inventory results by country, by region and the whole dataset, with the terrestrial NFI NPP at the right side.

Table 1. Summary of the forest inventory results: Number of plots with data, Time period covered by NFI NPP, Mean elevation (range Minimum–Maximum) in meter above sea level (EU-DEM 30 m resolution). For the following plot statistics we provide mean and standard deviation: Mean quadratic DBH (cm), Mean Tree height (m), Basal area at 1.3 m height ($m^2 \cdot ha^{-1}$), Stem number (ha^{-1}), Tree carbon per hectare ($gC \cdot m^{-2}$), Median age class, SDI Stand Density Index [36] (for details on this variables see Supplementary Material), NPP is the NFI Net primary production ($gC \cdot m^{-2} \cdot year^{-1}$) according to Equation (3), For Czech Republic we only have country means. Empty cells (-) indicate that this variable is not available from the NFI data set. At the end of each section, statistics of the region are given and at the bottom of the table summary statistics for whole Europe.

Region	Country	Number of Plots	Time Period	Mean Elevation (min–max) (m)	Mean DBH (cm)	Mean Tree Height (m)	Basal Area ($m^2 \cdot ha^{-1}$)	Stem Number (ha^{-1})	Tree Carbon ($gC \cdot m^{-2}$)	Median Age (Years)	SDI	NPP ($gC \cdot m^{-2} \cdot year^{-1}$)
North Europe	Estonia	19930	2000–2010	66 (2–275)	17 ± 8	17 ± 7	19 ± 8	1540 ± 2554	5240 ± 2929	40–60	449 ± 192	509 ± 163
	Finland	6442	2000–2008	141 (1–400)	18 ± 7	14 ± 5	18 ± 8	3522 ± 13251	4859 ± 3020	40–60	400 ± 236	446 ± 173
	Norway	9562	2000–2009	391 (0–1253)	15 ± 6	9 ± 3	15 ± 12	930 ± 682	4003 ± 3691	60–80	368 ± 265	442 ± 143
	all	35379	2000–2010	161 (0–1253)	16 ± 7	14 ± 7	18 ± 9	1736 ± 5983	4856 ± 3199	40–60	419 ± 224	482 ± 162
Central-West Europe	Austria	9562	2000–2009	912 (113–2299)	32 ± 14	21 ± 7	32 ± 19	987 ± 1070	10364 ± 6973	60–80	688 ± 396	681 ± 251
	Belgium	512	2009–2013	39 (2–278)	29 ± 12	18 ± 6	30 ± 13	660 ± 446	11507 ± 6475	40–60	648 ± 279	671 ± 195
	France	33152	2001–2011	444 (0–2707)	23 ± 11	15 ± 7	23 ± 15	778 ± 602	8083 ± 6457	60–80	512 ± 298	649 ± 254
	Germany	5894	2000–2008	344 (−5–1879)	28 ± 12	22 ± 7	31 ± 14	833 ± 814	11811 ± 6371	60–80	628 ± 302	754 ± 185
	all	49120	2000–2013	514 (−5–2707)	25 ± 12	17 ± 8	25 ± 17	824 ± 749	9034 ± 6698	60–80	564 ± 328	667 ± 253
Central-East Europe	Czech Rep.	13929	2001–2004	541 (138–1503)	25	20	33	812	17340 ± 10858	60–80	809 ± 441	643 ± 266
	Poland	17281	2005–2013	193 (−4–1459)	23 ± 9	18 ± 5	29 ± 14	883 ± 614	10656 ± 6623	40–60	612 ± 263	720 ± 288
	Romania	5509	2003–2011	542 (−1–1968)	24 ± 11	-	28 ± 15	878 ± 723	10355 ± 7256	40–60	582 ± 289	571 ± 164
	all	36719	2001–2013	443 (−4–1968)	23 ± 10	18 ± 5	28 ± 15	881 ± 673	12376 ± 8793	40–60	652 ± 345	649 ± 248
South Europe	Italy	15183	2002–2009	860 (7–2891)	20 ± 8	12 ± 4	22 ± 13	839 ± 636	6315 ± 4897	20–40	497 ± 293	635 ± 179
	Spain	60033	2000–2008	842 (1–2549)	23 ± 13	10 ± 4	13 ± 11	491 ± 516	4003 ± 3918	40–60	288 ± 246	606 ± 293
	all	75216	2000–2009	831 (1–2891)	22 ± 12	10 ± 4	15 ± 12	561 ± 560	4469 ± 4237	40–60	330 ± 269	578 ± 275
All countries	-	196434	–	548 (−5–2891)	22 ± 11	13 ± 7	20 ± 15	900 ± 2646	7298 ± 6916	40–60	469 ± 325	597 ± 252

Our NFI dataset covers the full elevational and latitudinal range of forest conditions in Europe including different site conditions, tree species, development stages or management practices. For most countries we have more than 5000 inventory plots (exception: Belgium with 512 plots) and in most cases a plot spacing of at least 4 by 4 km (Table S1). This dataset also provides information on forest properties such as tree age, carbon stocks or stand density and Table 2 indicates that these characteristics vary across Europe.

Table 2. NPP and ΔNPP (always using median) for the whole dataset ("All Countries"), for each country separately and for each region (MODIS NPP using global climate data—MODIS GLOB; MODIS NPP using local European climate data—MODIS EURO and NPP using forest inventory data—NFI NPP); ΔNPP and Rel. ΔNPP both for MODIS GLOB and MODIS EURO. Positive differences indicate that MODIS NPP overestimates NFI NPP and vice versa.

NPP and ΔNPP ($gC \cdot m^{-2} \cdot year^{-1}$)		MODIS	MODIS		ΔNPP		Rel. ΔNPP [%]	
		GLOB	EURO	NFI NPP	GLOB	EURO	GLOB	EURO
	All Countries	**680**	**577**	**539**	**141**	**38**	**26%**	**7%**
North Europe	Finland	471	399	414	57	−15	14%	−4%
	Norway	484	406	409	75	−3	18%	−1%
	Estonia	534	504	492	42	12	9%	3%
	all	519	479	461	58	18	13%	4%
Central-West Europe	Austria	739	612	634	105	−22	17%	−4%
	Belgium	732	599	644	88	−45	14%	−7%
	France	787	666	604	183	62	30%	10%
	Germany	692	602	716	−24	−114	−3%	−16%
	all	759	645	615	144	30	23%	5%
Central-East Europe	Czech Republic	696	618	553	143	65	26%	12%
	Poland	641	571	659	−19	−88	−3%	−13%
	Romania	713	562	565	148	−3	26%	−1%
	all	677	592	595	82	−3	14%	−1%
South Europe	Italy	862	657	635	227	22	36%	4%
	Spain	632	555	503	129	52	26%	10%
	all	691	584	519	172	65	33%	13%

3.1. NPP Estimates across Different Scales

Comparing all our three NPP estimates on a European scale allowed us to explore the general behaviour and evaluate the agreement of the two remote sensing driven NPP products, MODIS GLOB and MODIS EURO, with the terrestrial driven NFI NPP estimates (Figure 3).

Re-running the MOD17 algorithm with local climate data reduced the remotely sensed MODIS NPP in terms of median, mean and variation as compared to the global climate driver (Figure 3). NFI NPP is close to MODIS EURO regarding median and mean, but show larger variation. In addition, Figure 3 confirms that our data is clearly right-skewed (NFI NPP in particular).

Zooming in and examining the different NPP estimates by ecoregion and country allowed us to analyze our results on a higher spatial resolution and to assess local effects such as different regional growing conditions, the impact of local biomass allometries or tree species composition [32] as well as the potential effect of different forest management practices in Europe [7].

We provide in Table 2 the median NPP for the three NPP sources (MODIS GLOB, MODIS EURO and NFI NPP) and the differences between MODIS and NFI NPP (ΔNPP_{GLOB} and ΔNPP_{EURO}), both in absolute values in $gC \cdot m^{-2} \cdot year^{-1}$ and normalized in relation to NFI NPP (Rel. ΔNPPi in %). Results are given in Table 2 for Europe, by country and for the four eco-regions [7].

At the European level, the MODIS GLOB gives an NPP of 680 $gC \cdot m^{-2} \cdot year^{-1}$, the MODIS EURO resulted in 577 $gC \cdot m^{-2} \cdot year^{-1}$, and the NPP from the NFI data exhibit a value of 539 $gC \cdot m^{-2} \cdot year^{-1}$. The differences in NPP (ΔNPP_{GLOB}) using the global dataset MODIS GLOB are larger than ΔNPP_{EURO} using the regional dataset MODIS EURO (+26% vs. +7%). The same pattern is evident across all four

regions and most countries. Only for Poland and Germany ΔNPP_{GLOB} is smaller than ΔNPP_{EURO}. ΔNPP_{GLOB} is positive for most countries (negative in only 2 countries), while the discrepancy of MODIS EURO is more randomly distributed in Europe and the 4 regions (ΔNPP_{EURO} positive in 5 countries and negative for 7 countries). In addition, Table 2 shows that Rel. ΔNPP_{EURO} is smaller than 10% for all countries except five (France, Germany, Czech Republic, Poland and Spain).

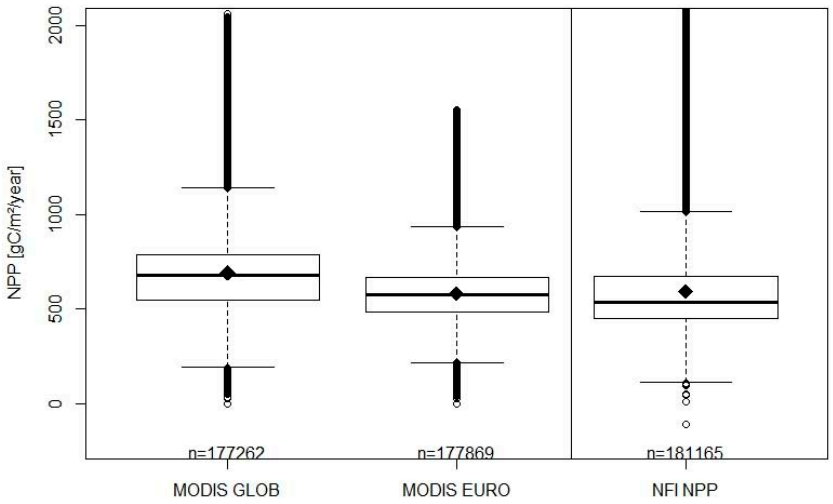

Figure 3. Comparison of MODIS GLOB and MODIS EURO with NFI NPP: The box represent the Median and the 25th and 75th percentile, the diamond give the arithmetic mean, the whiskers extend to 1.5 of the interquartile range, values outside this range are indicated by circles, on the bottom the number of values represented by the boxplots are given. The number of observations is different since climate data is missing for certain pixels to compute MODIS NPP. To enhance the interpretability of the image, NFI NPP results larger 2100 $gC \cdot m^{-2} \cdot year^{-1}$ (445 observations) are not shown, but are included in the boxplot.

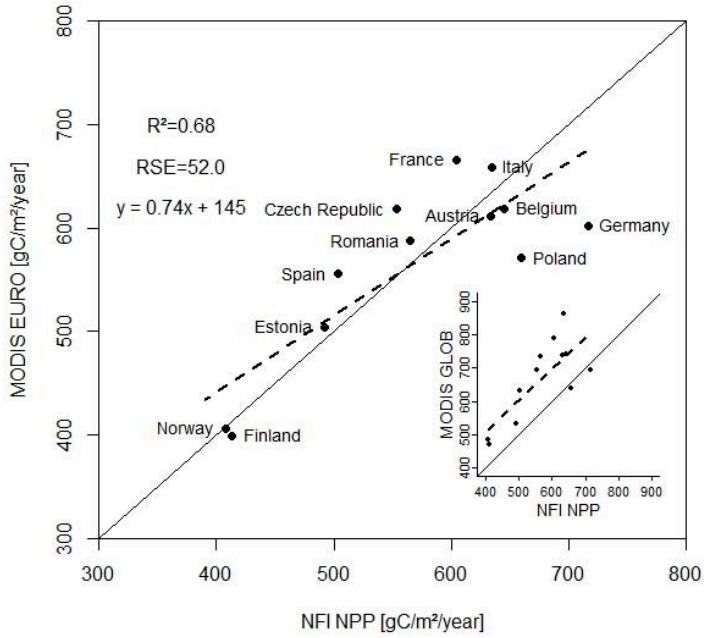

Figure 4. Comparison of MODIS EURO using European climate data and NFI NPP (MODIS GLOB vs. NFI NPP in the subplot in the bottom-right corner), we present median by country, solid line is 1:1 line, dashed line represents the linear trend of the 12 countries, Coefficient of determination R^2, Residual standard error (RSE) and the trend function are given.

This suggests that the discrepancy between MODIS EURO and NFI NPP is smaller than for MODIS GLOB and NFI NPP and we wanted to confirm this along the NPP gradient by showing the country medians in Figure 4.

Figure 4 provides the results by country of the NPP estimates resulting from the NFI data versus MODIS EURO with an R^2 0.68, a residual standard error (RSE) of 52.0 $gC \cdot m^{-2} \cdot year^{-1}$ or 9.7% of median of the NFI NPP. Aside from Germany and Poland MODIS EURO and NFI NPP are similar across the NPP gradient for the analyzed countries. The results for MODIS GLOB in the right corner exhibit consistent overestimation of NFI NPP, smaller agreement (R^2 = 0.59) and larger error (RSE 80.6 $gC \cdot m^{-2} \cdot year^{-1}$ equal 15.0% of median NFI NPP).

We used in Figure 4 the aggregated NPP of all inventory plots of one country, since the spatial coverage and thus the error structure of the two NPP sources are very different (one MODIS pixel covering 1 km^2 or 100 ha and the size of an NFI plot ranging from approx. 0.01 to 0.2 ha; Table S1). A direct plot-to-pixel comparison is provided in Figure S1 in the Supplementary Material.

3.2. NPP across Elevational, Latitudinal and Longitudinal Gradients

From Figures 3 and 4 as well as Table 2, we can see that the top-down MODIS EURO NPP estimates are consistent with the bottom-up terrestrial driven forest inventory NPP estimates at the European, regional and country level. Next, we investigated whether any patterns across gradients between MODIS EURO and NFI NPP may exist. For this purpose, we showed here ΔNPP_{EURO} for selected gradients, Elevation, Latitude and Longitude. We chose these gradients, since they have a strong effect on environmental and climatic conditions such as growing season length or weather patterns, but also on tree allometries and species composition, and are irrespective of country borders.

We aggregated our results into classes to increase the readability and show Figure 5 the results for whole Europe (results on the different regions are available in Figures S2–S5 in the Supplementary Material). Images for additional gradients like tree age, tree height, MODIS land cover and dominant tree species are provided in Figures S6–S9 in the Supplementary Material.

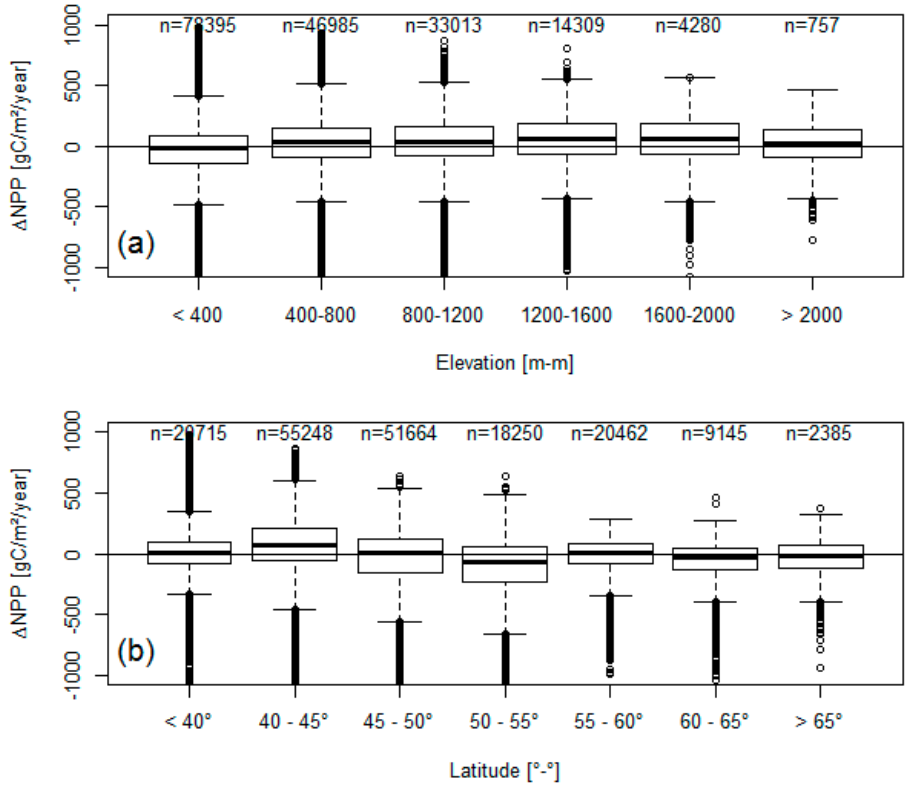

Figure 5. *Cont.*

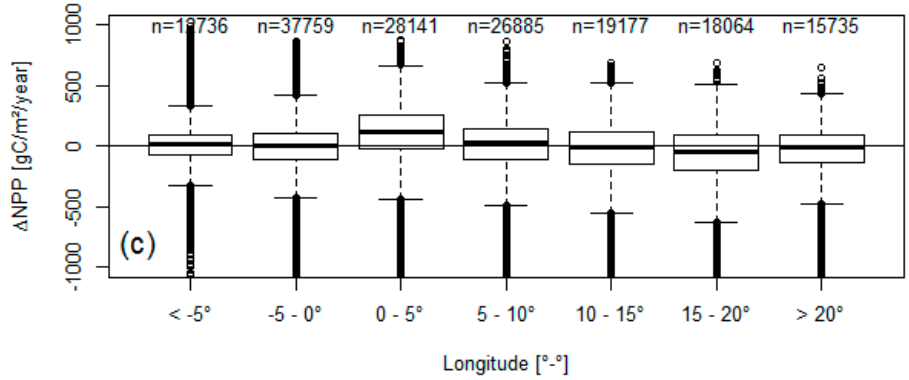

Figure 5. NPP Difference (ΔNPP) MODIS EURO minus NFI NPP by Elevation classes (**a**), by Latitude (**b**) and by Longitude (**c**), properties of illustration analogous to Figure 3, on the top the number of values represented by the boxplots are given.

Grouping by elevation in Figure 5a does not indicate striking differences and shows, that the agreement between MODIS EURO and NFI NPP is consistent across the elevational gradients. At certain latitude and longitude classes however local discrepancies exist, which may correspond to the findings in Table 2 and Figure 4.

3.3. Stand Density Effects

We analyzed ΔNPP_{EURO} (differences in NPP between MODIS EURO versus NFI NPP) by SDI (Stand Density Index [36] calculated with Equation (S10) in the Supplementary Material) for all of Europe (Figure 6).

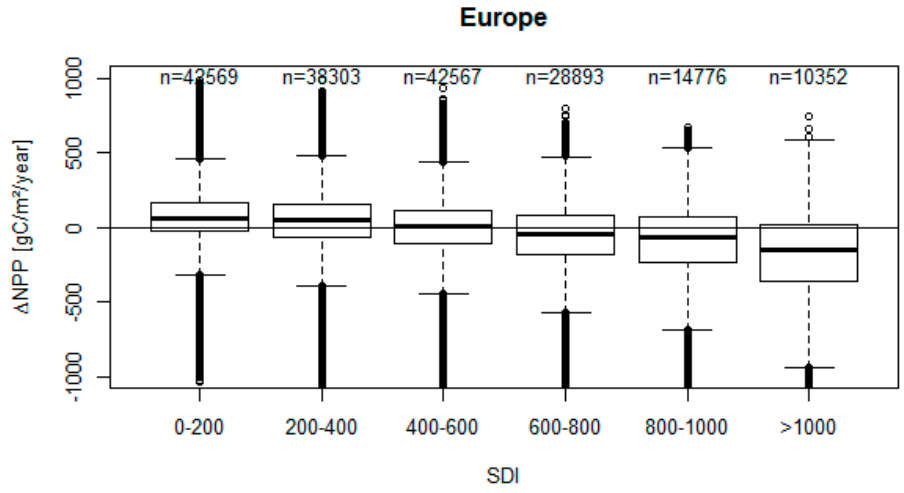

Figure 6. NPP Difference (ΔNPP) MODIS EURO minus NFI NPP by Stand Density Index classes (SDI), for details see Figure 5.

ΔNPP shows in Figure 6 a significant trend by stand density index SDI (using linear regression; R 0.31; $\Delta NPP = 103.1 - 0.247 \times SDI$; $p < 0.001$), which confirms that differences in stand density have an effect in our data from the 12 European countries. MODIS EURO NPP estimates are higher than NFI NPP at low SDI classes, while at intermediate SDI classes no discrepancies are evident (Figure 6). At high SDI classes MODIS EURO are lower than NFI NPP.

We analyzed the effect of SDI for each country, since SDI could be an explanation for the discrepancies visible in Table 2, Figures 4 and 5. Local effects of forest management intensity, disturbances or differences in the local inventory data design and methodology (Table S1) could

lead to differences in SDI. We performed similar graphical analysis as shown in Figure 6 for each country and present here as examples two "extreme" countries: (i) France—positive ΔNPP +10%, with MODIS EURO overestimating NFI NPP; and (ii) Germany—negative ΔNPP −16%, where MODIS EURO underestimates NFI NPP.

For France, MODIS EURO and NFI NPP results agree at high stand density and show discrepancies at low stand density (Figure 7a). Apparently, MODIS EURO does well in capturing the NPP of stands with high densities, but does not agree with NFI NPP from very open stands. The same patterns are also visible for other countries, where MODIS EURO overestimates NFI NPP such as Spain or Czech Republic (not shown).

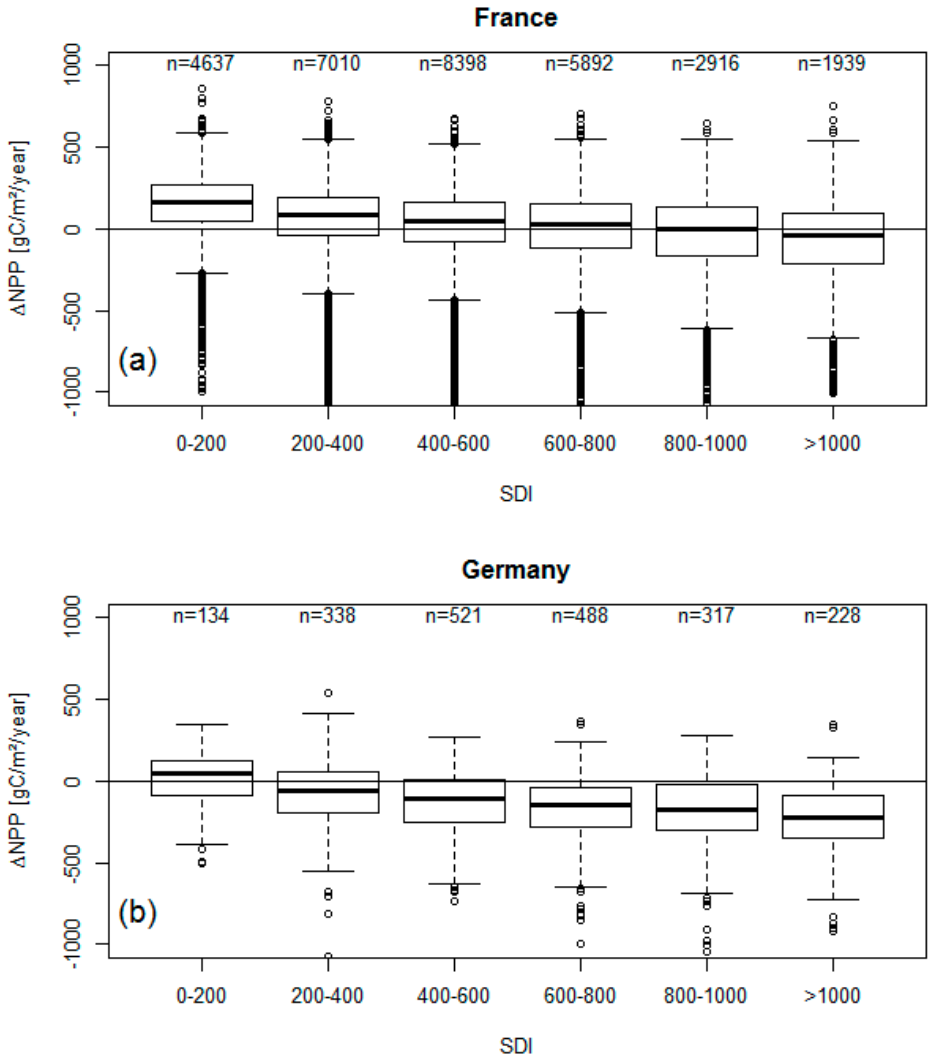

Figure 7. NPP Difference (ΔNPP) MODIS EURO minus NFI NPP by Stand Density Index classes (SDI) for selected countries: France (**a**)—MODIS EURO overestimates NFI NPP (on average positive ΔNPP) and Germany (**b**)—MODIS EURO underestimates NFI NPP (on average negative ΔNPP), for details see Figure 5.

For Germany on the other hand, MODIS EURO and NFI NPP are similar at low stand density classes, but show increasing deviations with increasing stand densities (Figure 7b). We see the same result for other countries as well, where MODIS EURO underestimates NFI NPP such as Poland (not shown). This may be seen as an indication that besides stand density an additional driver might cause discrepancies between MODIS EURO versus terrestrial NFI NPP.

4. Discussion

Top-down satellite driven MODIS NPP (Net Primary Production) estimates using local European daily climate data (MODIS EURO) exhibit smaller differences from the bottom-up terrestrial forest inventory NFI NPP estimates (Table 1) than the original MODIS GLOB estimates using global climate data (Figure 3; Table 2). This confirms that the output from the climate sensitive MOD17 algorithm can be substantially improved by using enhanced daily climate data [22] and supports the findings of the pilot study in Austria [15] by extending the focus to a continental scope. The local European daily climate data [25] used for MODIS EURO reduced across scales from continental (Figure 3) to national scale (Figure 4) substantially the differences between NPP using the MOD17 algorithm and terrestrial forest inventory data (Table 2). Both NPP estimates are also consistent across various gradients (elevation, latitude and longitude in Figure 5 and tree age, tree height, MODIS Land cover type and dominant species in Figures S6–S9).

In this study we evaluated MODIS EURO in comparison to the global MODIS NPP dataset [17] using our terrestrial NFI NPP. The specific methodologies and differences of our forest inventory data sets (Table S1) and missing information on fine roots and litter fall do not permit a proper validation of NPP. Since the forest inventory data was collected with a different purpose [10], it contains a different error structure due to the small sample plot size and large grid spacing (one or very few plots within a MODIS pixel) as compared to the continuous 1-km MODIS grid.

The large variations and local discrepancies apparent in this study (Figure 3; Table 2) are also reflected in a study on evaluating NPP and GPP (Gross Primary Production) from the MOD17 algorithm for North and South America [37]. While the authors reported no general bias in the MODIS NPP product, they found over- as well underestimation especially for certain locations and forest biomes of more than 30%. This study shows that in Europe discrepancies between MODIS EURO and terrestrial NFI NPP exceeds 10% in three out of twelve countries (Table 2).

This study improves the knowledge on explaining discrepancies between remote sensing and terrestrial NPP estimates by highlighting the effect of stand density index (SDI). Forests with stand density of 200 or lower are expected to have gaps, canopy cover below 100% and low competition between trees. Under such conditions the NFI NPP is substantial lower than MODIS NPP (Figures 6 and 7). This can be explained that at low stand density a substantial share of NPP is undetected by the forest inventory system (gaps filled with young trees or shrubs below diameter threshold), while MODIS NPP is able to capture these gaps via leaf area index provided by the satellite [15]. Figure S10 in Supplementary Material confirms that the stand density related trend of ΔNPP in Figures 6 and 7 is mainly caused by NFI NPP, which shows a stronger increase with SDI than MODIS NPP.

Since we tested this effect with MODIS GLOB as well, we can conclude that any MODIS productivity estimates irrespective from the used climate input cannot detect such important effects adequately. The relatively large pixel size of 1-km apparently does not allow MODIS NPP to capture small scale patterns such as clear-cuts, thinning operations or disturbance events, while a forest inventory can detect them better. This confirms the findings of the pilot study in Austria [15] and indicates that differences in stand density needs consideration also on the much larger European scale.

MODIS EURO agrees very well with NFI NPP at average stand densities (Figure 6). This could be explained with the calibration of the BPLUT tables used in the MOD17 algorithm [9] using large-scale global terrestrial NPP data [27]. The calibration data most likely represents average forest conditions and may not capture very open or very dense forests adequately. The NFI NPP on the one hand represents the conditions of the (small) area covered by an inventory plot, while MODIS NPP provides a smoothed average NPP of a 1-km pixel. A consistent stand density map at 1-km resolution would be needed to test this hypothesis.

But NFI NPP estimates capture not only differences in stand density and forest management, they are also strongly influenced by local tree allometries and local carbon estimation methods [38]. For Germany, stand density cannot explain the observed discrepancies satisfactory in Figure 7b.

In fact the results are quite different compared to whole Europe (Figure 6), France (Figure 7a) or our pilot study [15]. Germany is planning to modify the currently used tree biomass estimation methodology [39] which is used in this study, for future carbon assessments. Following reanalysis of existing data [40] and collection and analysis of new sample data [41], improved biomass functions were developed for Germany [42]. This new updated methodology results in approx. 5% lower aboveground biomass estimates. Thus future German NFI NPP estimates will be lower as well, which will most likely reduce the gap between MODIS and NFI NPP observed for this country in this study. This suggests that, interpretation of discrepancies between NPP estimates needs consideration of the tree carbon estimation methods, since they directly affect increment estimates.

However, there might be other potential drivers leading to inconsistencies both in MODIS EURO and NFI NPP, that could be analyzed in future studies.

Concerning NFI NPP, few countries do not consider adequately the contribution of small trees to the NPP of a forest, either by not considering the ingrowth of small trees [33] or a particular large diameter threshold in some countries (Table S1). This could explain, why in Spain and France MODIS EURO is higher than NFI NPP, as we were not able to include ingrowth here and thus the French and the Spanish NFI NPP estimates might not represent the NPP of their forests sufficiently.

The accuracy of the litter fall and fine root estimates for NFI NPP (Equations (3)–(5) need further research as well. The litter fall models used in this study were derived in a meta-analysis using Eurasian litter fall data [31]. They have substantial variation in the used input data and might contain potential inaccuracy, when applied in certain regions. In addition, the estimates for litter fall and fine roots are driven by the same climate data than MODIS EURO. Although the specific climate input differs (periodic average climate used in Equations (4) and (5) for NFI NPP versus daily maximum, minimum temperature and precipitation used in MOD17), it cannot be ruled out yet that the climate source explains the better match of MODIS EURO and NFI NPP. Thus, the performance of the currently used approach and alternative options for instance by using Foliage mass and Leaf longevity [43] needs to be tested using European litter fall data.

Potential errors in the MODIS EURO product could involve wrong classification of forest biomes by MODIS Land cover [44], limitations of the global parameters of the MOD17 algorithm capturing European forest conditions (see discrepancies in NPP for evergreen broadleaf forests in Figure S3), mismatches in LAI and FPAR by region or forest fragmentation [45].

5. Conclusions

In this study we created a regional Net Primary Production (NPP) dataset by running the MOD17 algorithm with local European climate data on 1-km resolution for the years 2000 to 2012 (MODIS EURO). We additionally obtained the global MODIS NPP product (MODIS GLOB) and evaluated the two MODIS NPP datasets with bottom-up forest inventory driven NPP (NFI NPP). We thus compared two conceptually different methods for assessing forest productivity across Europe, and test whether local climate data enhances the ability of the MOD17 algorithm to capture European forest conditions.

Running the MOD17 algorithm with local daily climate data substantially improves the quality of MODIS satellite-driven NPP across Europe as compared to the global NPP product (MODIS GLOB). Top-down satellite-driven MODIS EURO and bottom-up NFI NPP agree by regions and by countries, across gradients by longitude, latitude and elevation, if potential discrepancies by stand density due to forest management or the used carbon estimation methods are addressed.

This newly created MODIS EURO dataset is a consistent, continuous, spatial and temporal explicit forest productivity measure of the European forest area providing realistic estimates, which compare well with forest inventory information. This is important since reliable wall-to-wall forest productivity estimates are increasingly important for the growing bio-economy or for increasing our knowledge on other forest ecosystem services such as carbon sequestration.

As long as the MODIS program (based on Satellite "Terra" launched in 1999 and "Aqua" in 2002) is operational and local climate data is available, we can obtain reliable large-scale forest productivity

measures for European forests. Since the lifetime of the satellites carrying the MODIS sensor is unknown, we strongly suggest the implementation and testing of this concept in the upcoming European satellite technologies such as the Copernicus Programme to ensure consistent and realistic productivity estimates also in the future.

MODIS EURO data are made freely available for 2000 until 2012 under ftp://palantir.boku.ac.at/Public/MODIS_EURO.

Supplementary Materials: The following are available online at www.mdpi.com/2072-4292/8/7/554/s1, Table S1: Summary of the properties of the different forest inventory datasets, Table S2: Tree species groups used in this study, description and selected tree species, Figure S1: Direct pixel-to-plot comparison of MODIS EURO and NFI NPP, Figure S2: For North Europe ΔNPP grouped by Elevation, Latitude and Longitude, Figure S3: For Central-West Europe ΔNPP grouped by Elevation, Latitude and Longitude, Figure S4: For Central-East Europe ΔNPP grouped by Elevation, Latitude and Longitude, Figure S5: For South Europe ΔNPP grouped by Elevation, Latitude and Longitude, Figure S6: Difference ΔNPP grouped by age classes, Figure S7: Difference ΔNPP grouped by tree height classes, Figure S8: Difference ΔNPP grouped by MODIS Land cover types, Figure S9: Difference ΔNPP grouped by dominant species, Figure S10: MODIS EURO and NFI NPP by Stand density Index (SDI) classes.

Acknowledgments: This work was conducted as part of the collaborative project "FORest management strategies to enhance the MITigation potential of European forests" (FORMIT). The research leading to these results has received funding from the European Union Seventh Framework Programme under grant agreement n° 311970. Special thanks to all the field crews collecting the sample data for the inventory plots. We are also grateful to the responsible people from the various forest inventory organizations for providing us with the data of their forest inventory systems and thereby making this work possible in the first place. We also want to acknowledge the open data policy of NASA and the work of the MODIS land product science team providing us with the FPAR and LAI products. We further want to thank Loretta Moreno for proof reading the manuscript. We want to thank in particular the editor and the anonymous reviewer on their helpful comments on an earlier draft of the manuscript.

Author Contributions: M.N. conceived and designed the study, coordinated compiling the NFI NPP dataset, calculated the forest inventory results for Austria and wrote the first draft of the manuscript, A.M. and C.T. developed the code for computing MODIS EURO and maintain the ftp-server, V.M. calculated the forest inventory results for Germany, S.H. for Finland, M.M. for Italy, O.B. for Romania, M.L. for Estonia, G.C. for Belgium, A.T. for France, K.B. for Poland, J.M. for Czech Republic, I.A. for Spain, R.A. for Norway, M.Z. provided the original MOD17 code and helped in preparation of the input data, F.M. and H.H. coordinated and supervised the analysis and the manuscript writing, all authors contributed equally in writing and revising the manuscript.

Conflicts of Interest: The authors declare no conflict of interest.

References

1. Gower, S.T.; Kucharik, C.J.; Norman, J.M. Direct and Indirect Estimation of Leaf Area Index, f APAR, and Net Primary Production of Terrestrial Ecosystems. *Remote Sens. Environ.* **1999**, *70*, 29–51. [CrossRef]
2. Running, S.W.; Nemani, R.R.; Heinsch, F.A.; Zhao, M.; Reeves, M.; Hashimoto, H. A Continuous Satellite-Derived Measure of Global Terrestrial Primary Production. *Bioscience* **2004**, *54*, 547–560. [CrossRef]
3. Imhoff, M.L.; Bounoua, L.; DeFries, R.; Lawrence, W.T.; Stutzer, D.; Tucker, C.J.; Ricketts, T. The consequences of urban land transformation on net primary productivity in the United States. *Remote Sens. Environ.* **2004**, *89*, 434–443. [CrossRef]
4. Friedlingstein, P. A steep road to climate stabilization. *Nature* **2008**, *451*, 297–298. [CrossRef] [PubMed]
5. Enriquez, J. GENOMICS: Genomics and the World's Economy. *Science* **1998**, *281*, 925–926. [CrossRef] [PubMed]
6. McCormick, K.; Kautto, N. The Bioeconomy in Europe: An Overview. *Sustainability* **2013**, *5*, 2589–2608. [CrossRef]
7. FOREST EUROPE State of Europe's Forests 2015. Available online: http://www.foresteurope.org/docs/fullsoef2015.pdf (accessed on 27 June 2016).
8. EUROSTAT Europe in Figures—Eurostat Yearbook. Available online: http://ec.europa.eu/eurostat/ (accessed on 26 February 2016).
9. Zhao, M.; Heinsch, F.A.; Nemani, R.R.; Running, S.W. Improvements of the MODIS terrestrial gross and net primary production global data set. *Remote Sens. Environ.* **2005**, *95*, 164–176. [CrossRef]
10. Tomppo, E.; Gschwantner, T.; Lawrence, M.; McRoberts, R. *National Forest Inventories: Pathways for Common Reporting*; Springer: Berlin, Germany, 2010; p. 610.

11. IPCC Good Practice Guidance for Land Use, Land-Use Change and Forestry, CHAPTER 4 FOREST. In *2006 IPCC Guidelines for National Greenhouse Gas Inventories, Prepared by the National Greenhouse Gas Inventories Programme*; Eggleston, H.S., Buendia, L., Miwa, K., Ngara, T., Tanabe, K., Eds.; IGES: Kanagawa, Japan, 2006; p. 83.
12. Zianis, D.; Muukkonen, P.; Mäkipää, R.; Mencuccini, M. Biomass and stem volume equations for tree species in Europe. *Silva Fenn. Monogr.* **2005**, *4*, 63.
13. Baldocchi, D. "Breathing" of the terrestrial biosphere: Lessons learned from a global network of carbon dioxide flux measurement systems. *Aust. J. Bot.* **2008**, *56*, 1–26. [CrossRef]
14. Jung, M.; Reichstein, M.; Margolis, H.A.; Cescatti, A.; Richardson, A.D.; Arain, M.A.; Arneth, A.; Bernhofer, C.; Bonal, D.; Chen, J.; et al. Global patterns of land-atmosphere fluxes of carbon dioxide, latent heat, and sensible heat derived from eddy covariance, satellite, and meteorological observations. *J. Geophys. Res.* **2011**, *116*, G00J07. [CrossRef]
15. Neumann, M.; Zhao, M.; Kindermann, G.; Hasenauer, H. Comparing MODIS Net Primary Production Estimates with Terrestrial National Forest Inventory Data in Austria. *Remote Sens.* **2015**, *7*, 3878–3906. [CrossRef]
16. Jiang, F.; Chen, J.M.; Zhou, L.; Ju, W.; Zhang, H.; Machida, T.; Ciais, P.; Peters, W.; Wang, H.; Chen, B.; et al. A comprehensive estimate of recent carbon sinks in China using both top-down and bottom-up approaches. *Sci. Rep.* **2016**, *6*. [CrossRef] [PubMed]
17. Zhao, M.; Running, S.W. Drought-induced reduction in global terrestrial net primary production from 2000 through 2009. *Science* **2010**, *329*, 940–943. [CrossRef] [PubMed]
18. Hasenauer, H.; Petritsch, R.; Zhao, M.; Boisvenue, C.; Running, S.W. Reconciling satellite with ground data to estimate forest productivity at national scales. *For. Ecol. Manag.* **2012**, *276*, 196–208. [CrossRef]
19. Thornton, P.E. *Description of a Numerical Simulation Model for Predicting the Dynamics of Energy, Water, Carbon and Nitrogen in a Terrestrial Ecosystem*; University of Montana: Missoula, MT, USA, 1998; p. 280.
20. Yang, W.; Huang, D.; Tan, B.; Stroeve, J.C.; Shabanov, N.V.; Knyazikhin, Y.; Nemani, R.R.; Myneni, R.B. Analysis of Leaf Area Index and Fraction of PAR absorbed by Vegetation Products from the Terra MODIS sensor: 2000–2005. *IEEE Trans. Geosci. Remote Sens.* **2006**, *44*, 1829–1842. [CrossRef]
21. Friedl, M.; Sulla-Menashe, D.; Tan, B.; Schneider, A.; Ramankutty, N.; Sibley, A.; Huang, X. MODIS Collection 5 global land cover: Algorithm refinements and characterization of new datasets. *Remote Sens. Environ.* **2010**, *114*, 168–182. [CrossRef]
22. Zhao, M.; Running, S.W.; Nemani, R.R. Sensitivity of Moderate Resolution Imaging Spectroradiometer (MODIS) terrestrial primary production to the accuracy of meteorological reanalyses. *J. Geophys. Res.* **2006**, *111*, G01002. [CrossRef]
23. Kanamitsu, M.; Ebisuzaki, W.; Woollen, J.; Yang, S.-K.; Hnilo, J.J.; Fiorino, M.; Potter, G.L. NCEP–DOE AMIP-II Reanalysis (R-2). *Bull. Am. Meteorol. Soc.* **2002**, *83*, 1631–1643. [CrossRef]
24. Haylock, M.R.; Hofstra, N.; Klein Tank, A.M.G.; Klok, E.J.; Jones, P.D.; New, M. A European daily high-resolution gridded data set of surface temperature and precipitation for 1950–2006. *J. Geophys. Res.* **2008**, *113*, D20119. [CrossRef]
25. Moreno, A.; Hasenauer, H. Spatial downscaling of European climate data. *Int. J. Climatol.* **2015**. [CrossRef]
26. Hijmans, R.J.; Cameron, S.E.; Parra, J.L.; Jones, P.G.; Jarvis, A. Very high resolution interpolated climate surfaces for global land areas. *Int. J. Climatol.* **2005**, *25*, 1965–1978. [CrossRef]
27. Olson, R.J.; Johnson, K.R.; Zheng, D.L.; Scurlock, J.M.O. *Global and Regional Ecosystem Modeling: Databases of Model Drivers and Validation Measurements*; Oakridge Laboratory: Oak Ridge, TN, USA, 2001; p. 95.
28. Jackson, R.; Mooney, H.; Schulze, E. A global budget for fine root biomass, surface area, and nutrient contents. *Proc. Natl. Acad. Sci. USA* **1997**, *94*, 7362–7366. [CrossRef] [PubMed]
29. Finér, L.; Ohashi, M.; Noguchi, K.; Hirano, Y. Fine root production and turnover in forest ecosystems in relation to stand and environmental characteristics. *For. Ecol. Manag.* **2011**, *262*, 2008–2023. [CrossRef]
30. Raich, J.; Nadelhoffer, K. Belowground carbon allocation in forest ecosystems: Global trends. *Ecology* **1989**, *70*, 1346–1354. [CrossRef]
31. Liu, C.; Westman, C.J.; Berg, B.; Kutsch, W.; Wang, G.Z.; Man, R.; Ilvesniemi, H. Variation in litterfall-climate relationships between coniferous and broadleaf forests in Eurasia. *Glob. Ecol. Biogeogr.* **2004**, *13*, 105–114. [CrossRef]

32. Neumann, M.; Moreno, A.; Mues, V.; Härkönen, S.; Mura, M.; Bouriaud, O.; Lang, M.; Achten, W.M.J.; Thivolle-Cazat, A.; Bronisz, K.; et al. Comparison of carbon estimation methods for European forests. *For. Ecol. Manag.* **2016**, *361*, 397–420. [CrossRef]
33. Hasenauer, H.; Eastaugh, C.S. Assessing Forest Production Using Terrestrial Monitoring Data. *Int. J. For. Res.* **2012**. [CrossRef]
34. Huber, M.O.; Eastaugh, C.S.; Gschwantner, T.; Hasenauer, H.; Kindermann, G.; Ledermann, T.; Lexer, M.J.; Rammer, W.; Schörghuber, S.; Sterba, H. Comparing simulations of three conceptually different forest models with National Forest Inventory data. *Environ. Model. Softw.* **2013**, *40*, 88–97. [CrossRef]
35. Seidl, R.; Schelhaas, M.-J.; Rammer, W.; Verkerk, P.J. Increasing forest disturbances in Europe and their impact on carbon storage. *Nat. Clim. Chang.* **2014**, *4*, 806–810. [CrossRef] [PubMed]
36. Reineke, L. Perfecting a stand-density index for even-aged forests. *J. Agric. Res.* **1933**, *46*, 627–638.
37. Turner, D.P.; Ritts, W.D.; Cohen, W.B.; Gower, S.T.; Running, S.W.; Zhao, M.; Costa, M.H.; Kirschbaum, A.A.; Ham, J.M.; Saleska, S.R.; et al. Evaluation of MODIS NPP and GPP products across multiple biomes. *Remote Sens. Environ.* **2006**, *102*, 282–292. [CrossRef]
38. MacLean, R.G.; Ducey, M.J.; Hoover, C.M. A Comparison of Carbon Stock Estimates and Projections for the Northeastern United States. *For. Sci.* **2014**, *60*, 206–213. [CrossRef]
39. *Austrias National Inventory Report 2012: Umweltbundesamt Submission under the United Nations Framework Convention on Climate Change and the Kyoto Protocol 2012 National Inventory Report for the German Greenhouse Gas Inventory 1990–2010*; Umweltbundesam: Dessau, Germany, 2012; p. 827.
40. Kändler, G.; Bösch, B. Methodenentwicklung für die 3. Bundeswaldinventur: Modul 3 Überprüfung und Neukonzeption einer Biomassefunktion—Abschlussbericht. *Tech. Rep. FVA-BW* **2013**, 1–72. (In German)
41. Neubauer, M.; Demant, B.; Bolte, A. Tree-based estimator for below-ground biomass of *Pinus sylvestris* L. *Forstarchiv* **2015**, *86*, 42–47.
42. Umweltbundesamt Berichterstattung unter der Klimarahmenkonvention der Vereinten Nationen und dem Kyoto- Protokoll 2014 Nationaler Inventarbericht zum Deutschen Treibhausgasinventar 1990–2012. *Clim. Chang.* **2014**, *24*, 965. (In German)
43. He, L.; Chen, J.M.; Pan, Y.; Birdsey, R.; Kattge, J. Relationships between net primary productivity and forest stand age in U.S. forests. *Glob. Biogeochem. Cycles* **2012**, *26*, 1–19.
44. Moreno, A.; Neumann, M.; Hasenauer, H. Optimal Resolution for Linking Remotely Sensed and Forest Inventory Data in Europe. *Remote Sens. Environ.* **2016**, *183*, 109–119. [CrossRef]
45. Härkönen, S.; Lehtonen, A.; Manninen, T.; Tuominen, S.; Peltoniemi, M. Estimating forest leaf area index using satellite images: Comparison of *k*-NN based Landsat-NFI LAI with MODIS- RSR based LAI product for Finland. *Boreal Environ. Res.* **2015**, *6095*, 181–195.

9.4. Paper 4

Moreno, A., Neumann, M., Hasenauer, H., 2016. Optimal resolution for linking remotely sensed and forest inventory data in Europe. Remote Sens. Environ. 183.

Remote Sensing of Environment 183 (2016) 109–119

Contents lists available at ScienceDirect

Remote Sensing of Environment

journal homepage: www.elsevier.com/locate/rse

Optimal resolution for linking remotely sensed and forest inventory data in Europe

Adam Moreno *, Mathias Neumann, Hubert Hasenauer

Institute of Silviculture, Department of Forest and Soil Sciences, University of Natural Resources and Life Sciences, Vienna, Peter-Jordan-Str. 82, A-1190 Wien, Austria

ARTICLE INFO

Article history:
Received 27 February 2016
Received in revised form 17 May 2016
Accepted 26 May 2016
Available online xxxx

Keywords:
NFI
Europe
Resolution
Aggregation
Optimization
Forest inventory
Remote sensing

ABSTRACT

Forests provide critical ecosystem services that ensure the sustainability of the environment and society. To manage forests on large scales, spatially explicit gridded data that describes the characteristics of these forests over the entire study area are required. There have been multiple efforts to create such data on regional and global scales. This type of gridded spatially explicit data on forest characteristics are typically done by integrating terrestrial forest inventory (NFI) and satellite-based remotely sensed data. Many studies that incorporate remotely sensed data and forest inventory data often directly compare pixels to inventory plots. The standard resolution of 0.0083° is typically used to integrate these two types of data sets. There is an assumption that, when producing gridded data sets incorporating forest inventory data, the finer the resolution the better the information. This assumption may seem intuitive, however at this resolution, in Europe, each 0.0083° cell has on average 1 NFI plot, which results in a sample with 0 degrees of freedom that represents 0.02% of the cell area. In this study, we challenge this assumption and we quantify the optimal resolution with which to compare and combine remotely sensed and NFI data from the largest collated and harmonized NFI data set in Europe including 196,434 plots. We determined that aggregating data with an original resolution of 0.0083° to between 0.0664° and 0.266° (or ×8 to ×32) produces the best agreement between these two forest inventory and remotely sensed data sets, and the lowest standard error in NFI data, and maintains the majority of the local-level spatial heterogeneity.

1. Introduction

Forests provide critical ecosystem services that ensure the sustainability of the environment and society (Costanza, Fisher, Mulder, Liu, & Christopher, 2007; Richmond, Kaufmann, & Myneni, 2007). Forests are under threat of large scale disturbances and mortality due to a changing climate (McDowell & Allen, 2015; Schröter et al., 2005; van Mantgem et al., 2009). There are, however, ways that we can manage forests that can mitigate and adapt to this change (Spittlehouse, 2005). Forest management on large scales, i.e., regional or continental, requires spatially-explicit gridded data that describe the characteristics of these forests. Multiple efforts have been made to create such data on regional and global scales (Beaudoin et al., 2014; Crowther et al., 2015; Moreno, Neumann, & Hasenauer, 2016; Simard, Pinto, Fisher, & Baccini, 2011). Such data sets require integrating terrestrial and remotely sensed data which must be derived using one resolution to make the data set consistent. The resolution chosen has an impact on the quality of the output (Blackard et al., 2008; Jenkins, Birdsey, & Pan, 2001; Wilson, Lister, & Riemann, 2012). Therefore, an optimal resolution on which to link these two independent data sets should be quantified.

Gridded, spatially-explicit data on forest characteristics are derived by integrating terrestrial national forest inventory (NFI) and satellite-based remotely sensed data. Typically, these studies use forest properties measured by satellites to extrapolate NFI data across an entire study area, with the assumption that an NFI plot represents a remotely sensed data cell covering the same location. Then, a number of different techniques, such as k-nearest neighbors, are used to match similar remotely sensed cells that do not have any underlying NFI data with those that do (Beaudoin et al., 2014; Crowther et al., 2015; Simard et al., 2011).

Additionally, remotely sensed data are used to study many aspects of the global biosphere (Justice et al., 2002). Such data can be used to measure productivity, cover type, and deforestation (Hansen et al., 2013; Justice et al., 2002; Running et al., 2004). To calibrate and validate these data sets, researchers again use terrestrial empirical observations such as those obtained from NFIs (Hasenauer, Neumann, Moreno, & Zhao, 2014; Hasenauer, Petritsch, Zhao, Boisvenue, & Running, 2012; Turner et al., 2006).

There is an assumption that when producing gridded data sets that incorporate, or are compared to, NFI data the finer the resolution the better the resulting information. This assumption may seem intuitive, however, to incorporate these two types of data together, they must be comparable spatially, thematically and temporally (Tomppo et al.,

* Corresponding author.
E-mail address: adam.moreno@boku.ac.at (A. Moreno).

http://dx.doi.org/10.1016/j.rse.2016.05.021
0034-4257/

2008). Many studies that incorporate remotely sensed data and forest inventory data often directly compare pixels to inventory plots (Crowther et al., 2015; Gallaun et al., 2010; Simard et al., 2011). A common resolution on which these studies are done is 1 km^2 (0.0083°). Fixed area NFI plots typically have areas of 200 m^2 (Tomppo et al., 2010). Therefore, 1 plot is 0.02% of a 1 km^2 cell. One sample, that represents less than 1% of the total population, results in no confidence in the sample's (forest inventory plot) ability to describe the population (remotely sensed cell). If then new datasets are generated based on this relationship, then the output may be spurious. Studies often use this one-to-one relationship to then create national, regional or even global datasets of forest characteristics (Beaudoin et al., 2014; Crowther et al., 2015; Tomppo et al., 2008). Aggregated data that incorporate more samples within a cell may lead to more accurate and realistic results.

Beyond the difference in plot size versus cell size, there are other hurdles involved in combining these two datasets across countries that are often overlooked. Methods to obtain NFI data differ across countries (Tomppo et al., 2010). Some countries use fixed area plots, which give a specific size to every sample plot. While other countries use angle count sampling, which determines which trees are counted in a sample using the tree diameter and the distance to the plot center (Bitterlich, 1952). Each sampling technique will produce a different description of a forest (Motz, Sterba, & Pommerening, 2010). Also, the country-level sampling design through space and time varies by country, from a regularly spaced grid that is the same every year, to randomized points that change every year (Tomppo et al., 2010). All of these factors affect the confidence in the NFI data at different scales. The variance in confidence through scales has an effect on the reliability of data that is produced by incorporating remotely sensed and NFI data (Seidl et al., 2013).

There are also political hurdles that hinder the use NFI data spatially. In Europe, there is no coherent NFI database from which to obtain all inventory data for the entire continent (Neumann et al., 2016). Researchers must, therefore, obtain data from each country, individually. When obtaining this data, most countries will not provide the exact location of the inventory plots out of concern for compromising the samples. These countries then provide data with a falsified location within a certain radius or within a certain grid cell (Moreno et al., 2016). The perfect link between remotely sensed data and NFI data would be to use fine resolution remotely sensed data that covers the NFI plot and only the NFI plot. However, because NFI data are given with falsified locations, this is not possible. The lack of an overarching and open NFI system or database for Europe has hindered the ability of researchers to understand how NFI data behave throughout the continent on different scales.

Additionally, inventory sample plots are meant to be used as aggregations to derive average results for a region, and not as single data points (Tomppo et al., 2010). The minimum aggregation on which NFI data is released by national organizations typically depends on the variation of the variable of interest, the sample design grid and the desired confidence interval and a single plot provides an undefined confidence interval. Therefore, to improve the confidence in NFI data and the comparability with remotely sensed data, both datasets must be aggregated until an acceptable error/confidence is reached. The optimal resolution at which to compare these two types of data and the benefits and draw-backs of aggregation are currently not quantified on the continental scale for Europe. An optimal resolution with which to combine remotely sensed and NFI data will justify a resolution that is not arbitrarily chosen based on data limitations or assumptions, but on which resolution produces the most accurate results. This will, in turn improve our confidence in the European and global scale data on forests that can be used to inform forest managers and policy makers on how best to improve forest stewardship that will benefit the environment and society, today and into the future.

In this paper, we quantify the optimal aggregation step at which to compare NFI and remotely sensed data in Europe. We accomplish this by assessing NFI data from 11 countries in Europe along with different gridded data sets. The objectives of this paper are:

1. Assess the agreement of remotely sensed data at their original resolution with NFI data
2. Quantify the loss of information with aggregation
3. Assess how aggregation affects agreement between remotely sensed and NFI data sets
4. Quantify the standard error of NFI variables at various aggregation steps
5. Determine the optimal resolution on which to combine remotely sensed and NFI data

2. Data

We use NFI data in conjunction with 4 remotely sensed land cover products.

2.1. Forest inventory data

We use national forest inventory (NFI) data from 11 European countries, Austria (Gabler and Schadauer 2008), Belgium (region Flanders) (Wouters et al. 2008), Czech Republic, Finland (Tomppo and Tuomainen in Tomppo et al., 2010), France (Nikolas et al. in Tomppo et al., 2010), Germany (Kandler, 2009), Norway (Tomppo et al., 2010), Poland, Romania (Marin et al. in Tomppo et al., 2010), Spain (Alberdi et al. in Tomppo et al., 2010), and Regional or Provincial Forest inventory (RFI, PFI) from 5 provinces in Italy (Trento, Sicily, Umbria, Piemonte and Liguria) (Neumann et al., 2016). This is currently the largest harmonized plot level forest inventory data set of Europe and includes 196,434 plots (Neumann et al., 2016). We use only data taken between 2000–2010 so as to match the same time period as the remotely sensed data products we use with no resamples in our dataset. We chose these countries because of accessibility and because they cover a latitudinal gradient throughout the continent. Datasets have been collated and harmonized by Neumann et al. (2016). The plot locations were falsified by the respective national organization responsible for the forest inventory to avoid revealing the location of the sample plots. The plot location was either altered into a random direction not to exceed more than 100 m or the plot locations were re-projected onto the center of the MODIS land cover grid (0.0083°) (Fig. 1).

Each NFI system has a different sampling density, arrangement of the sample plots and sampling method (Table 1). The sampling method has an effect on the uncertainty in results (Bergseng, Ørka, Næsset, & Gobakken, 2014; Hasenauer & Eastaugh, 2012; Hasenauer et al., 2012). Some countries in our dataset use angle count sampling (ACS) while the majority use fixed area plots (FAP) (Table 1) (Bitterlich, 1952).

Basal area factor for ACS determines the trees sampled based on their size and distance to the center of a plot. Both the basal area factor for ACS and the plot area for FAP vary in our NFI data. The size of the subplots range from 250 m^2 in Norway to almost 2000 m^2 in Spain. Six countries have their plots aligned in clusters, 5 countries as single plots on each grid point. When arranged in clusters, the number of plots varies between 2 to 18 plots in each cluster. All NFI systems use a systematic sample plot grid with constant distance between grid points. The grid distance varies by country and ranges from 0.5 km (provinces Sicily and Piemonte in Italy) to more than 10 km in Northern Finland. In Finland and Romania the grid distance also changes within the country which leads to a varying number of samples within these countries spatially (Table 1, Fig. 1).

2.2. MODIS land cover

Moderate Resolution Imaging Spectroradiometer (MODIS) land cover-type product (MCD12Q1; Hansen et al., 2002) is a global land

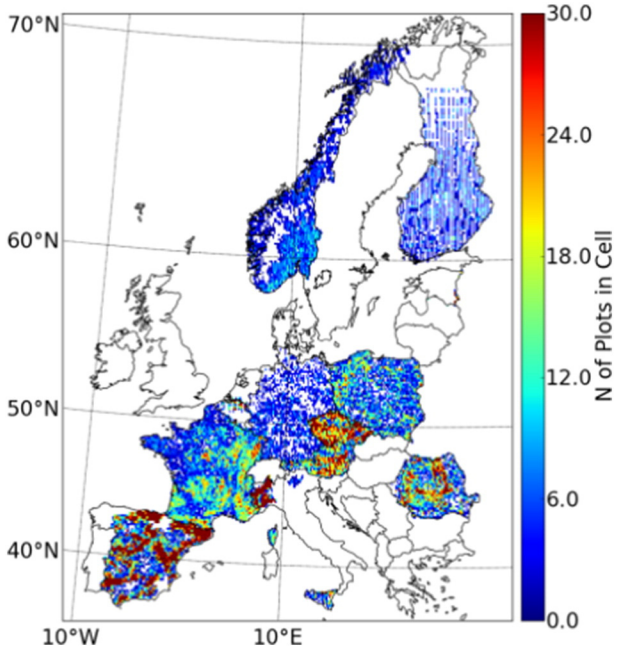

Fig. 1. Coverage of terrestrial forest inventory data and number of plots per cell (0.133° resolution).

cover data set derived with a decision tree system using spectral information and NDVI (normalized difference vegetation index) derived from the MODIS sensor along with temperature data. The decision tree algorithm executing the land cover type classification uses training data derived from the International Geosphere Biosphere Programme's (IGBP) University of Maryland land cover legend. We use the aggregated MODIS Land Cover product with a 1 × 1 km (0.0083°) using the classification system from the University of Maryland (UMD) (Friedl et al. 2010). We use the year 2000 and 7 MODIS classes in this study: evergreen broadleaf, evergreen needle leaf, deciduous broadleaf, deciduous needle leaf, mixed forest, woody savanna, and non-forest. Forest type is determined using the following rules: A cell is given a forest classification if it has 60% forest cover or higher. If the cell is designated as forest, then it is assigned the dominate forest type if that forest type has over 60% of the share of forest. If no forest type has over 60% of the share of forest cover then it is given a "mixed forest" designation. If the cell has 30%–60% forest cover, then it is given the classification "woody savanna".

2.3. Global Land Cover 2000

The Global Land Cover 2000 (GLC2000) (Mayaux et al., 2006) made by the Joint Research Center in Europe is based on the VEGA 2000 dataset, which is acquired by the VEGETATION sensor on board SPOT-4 and SPOT-5. The data were then synthesized to create a consistent global land cover data set with a 0.0083° resolution for the year 2000. The GLC2000 utilizes the U.N. Food and Agriculture Organization's Land Cover Classification System (LCCS) and has 22 classes (Di Gregorio, 2005). Using this classification system as a basis, regional groups were mandated to utilize a bottom up approach to classify the remotely sensed data for their specific area. We used 6 classes in GLC2000: evergreen broadleaf, evergreen needle leaf, deciduous broadleaf, deciduous needle leaf, mixed forest, and non-forest. The GLC2000 uses the same classification rules as MODIS, except it has a forest cover threshold of 15% as opposed to MODIS' 60% and there is no "woody savanna" designation.

2.4. CORINE Land Cover (CLC)

The CORINE Land Cover data set is a product of the Coordination of Information on the Environment program initiated by the European Commission operated by the European Environmental Agency (Bossard, Feranec, & Otahel, 2000). The version used in this study is CLC 2006 (Bossard et al., 2000). For CLC 2006 satellite data from SPOT-4 and/or IRS LISS II, two dates were used in combination with a supervised classification scheme. The CLC 2006 is generated automatically with expert opinion influencing the final classification (Bossard et al., 2000). The CLC map covers Europe, Turkey and Iceland, excluding Great Britain, Greece and Switzerland on a 0.00158° resolution. It distinguishes 48 different land cover types, 12 in the class "Forest and semi natural areas". We reduced CLC classes to 6 including: agroforestry, broad-leaved forest, coniferous forest, mixed forest, transitional woodland, and non-forest. The CLC forest types are classified in the same manner as MODIS except CLC refers to the "woody savanna" designation as "transitional woodland". CLC uses a 30% forest cover threshold before a cell is classified as forest after which a forest type must have 75% share of the forest to acquire a specific forest type; otherwise it is classified as mixed forest or transitional woodland.

2.5. Tree species map for European forests (EFI)

The European Forest Institute's map of forest species is based on a statistical interpolation of the International Co-operative Programme on assessment and monitoring of air (ICP) forest inventories and various remotely sensed climate and orographic variables using both kriging and logistic regression models. It distinguishes 20 different tree species groups on a 0.0083° resolution, provides proportional share of each tree species in a cell and covers all of Europe (Brus et al., 2011). For building the regression models and validation, terrestrial data from the ICP Forest Level 1 plots and NFI data from 18 European countries were used. The dominant tree species is derived for every cell, irrespective of the percent forest cover within a cell. This data set does not include a non-forest class.

Table 1
Characteristics of NFI systems used for this study. Sampling method can be either Angle count sampling (ACS) or Fixed area plots (FAP). Basal area factor is required for countries with ACS. Plot area is required for the countries with FAP. Arrangement of sample plots indicates whether the plots are arranged as single plots or within clusters. The distance between each cluster/single plot and the number of sample plots in our dataset are given.

Country	Sampling Method	Basal Area Factor [m^2/ha]	Plot Area [m^2]	Arrangement of sample plots	Distance between plots [km]	N of Plots
Austria	ACS + FAP	4	21.2	Clusters of 4 plots	3.889 × 3.889	9167
Belgium	FAP	–	15.9–1017.9	Single plots	1 × 0.5	2495
Czech Rep.	FAP	–	28.3–500	Clusters of 2 plots	2 × 2	13,929
Finland	ACS	2 (S) 1.5 (N)	–	Clusters of 14–18	6–8 (S) 6–11 (N)	6232
France	FAP	–	113–706	Single Plots	2 × 2	32,107
Germany	ACS	4	–	Clusters of 4 plots	4 × 4 or 8 × 8	6153
Italy	FAP	–	50–600	Single plots	0.5 × 0.5 or 1 × 1	19,852
Norway	FAP	–	250	Single plots	3 × 3	9200
Poland	FAP	–	200–500	Cluster of 5 plots	4 × 4	13,546
Romania	FAP	–	200–500	Cluster of 4 plots	4 × 4 or 2 × 2	16,605
Spain	FAP	–	78.5–1963.5	Single plots	1 × 1	69,853

Table 2
Aggregation steps and their corresponding resolution in degrees and the cell size range in Europe in km.

Aggregation step (N of orig. cells on a side)	Resolution (Decimal degrees)	Cell area range North–South (km^2)
1	0.008	0.3–0.7
2	0.016	1.1–2.8
4	0.033	4.4–11.3
8	0.066	17.6–45.2
16	0.133	70.7–180.9
32	0.266	283.2–723.1
64	0.533	1140.7–2887.6
128	1.066	4624.4–11,587.7

3. Methods

3.1. Assess the agreement of remotely sensed data on their original resolution with NFI data

We analyzed NFI data from 6 countries where we have complete coverage with a continuous grid and include the tree level data and species designations required to determine dominate forest type per plot. These countries included: Austria, Germany, Norway, Finland, Czech Republic, and Spain. We classified the NFI forest type according to the rules of the remote sensing data to which we are comparing (e.g., we use the classification scheme for MODIS and the rules set forth for each class on the NFI data when comparing these 2 datasets). All plots within a remote sensing cell are used together within the rules to determine the forest type.

We used confusion matrices to analyze the amount of agreement between the NFI and remotely sensed data for each remotely sensed dataset (Lewis & Brown, 2001). The confusion matrices include all of the cover type classifications used in the remote sensing dataset in question. All matrices, except those associated with the EFI dataset, include a "non-forest" classification. The EFI dataset does not include this classification. The percent agreement is the percentage of cells that have the same forest type and non-forest classification in both the remotely sensed and the NFI data.

3.2. Quantify the loss of information with aggregation

We aggregated each land cover map and the NFI data at various aggregation steps. MODIS, EFI and GLC2000 all have a similar original resolution of 0.0083°. These datasets were aggregated by 2, 4, 8, 16, 32, 64, and 128 times the original resolution (Table 2). For example, the first aggregation step is 2×2 original resolution cells and the second is 4×4 original resolution cells and so forth. The accompanying NFI dataset is aggregated by using the land cover definition rules, described in the data section, under each cell at the aggregated resolution. We use a constant resolution in decimal degrees which means that the surface area a cell represents varies by latitude, increasing from north to south (Table 2). The area of a cell is calculated as:

$$A = R^2 * \{(sinlat1 - sinlat2) * (lon2 - lon1)$$

A is the area of the cell. R is the radius of the Earth equal to 6371 km. *lat*1 and *lon*1 are the latitude and longitude of the upper left corner of the cell and *lat*2 and *lon*2 are for the bottom right corner of the cell. The latitudinal range is from 34.59° to 71.34° and our longitudinal range is from −10.83° to 34.25°.

CLC has an original resolution of 0.00158°. Countries within our NFI dataset have falsified plot locations within a 0.0083° cell. Therefore we could not match CLC on its original resolution with NFI data directly. We therefore aggregated both CLC and the NFI data from the original resolution of 0.00158° up to 0.0079°, or 5×5 CLC pixels, which is similar to the MODIS original resolution which was used for the falsification of the NFI plot coordinates. We then aggregated CLC and the underlying NFI data to 2, 4, 8, 16, 32, 64 and 128 times the 0.0079° resolution. We aggregated based on the same rules as the original CLC dataset.

We then quantified the loss of local level information as we aggregated. We did this by calculating the Shannon equitability index (Hill, 2015) of the original resolution cells associated with each aggregation step. The Shannon equitability index is calculated as:

$$E_H = \frac{H}{\ln(S)}$$

E_H is Shannon's equitability index, S is the number of classes of the original resolution cells within an aggregated cell and H is Shannon's diversity index calculated as:

$$H = -\sum_{i=1}^{S} p_i * \ln(p_i)$$

p_i is the proportion of class i in S — the total number of classes in the cell. The Shannon's equitability index (E_H) is a normalized Shannon's diversity index creating values from 0 to 1. The lower the E_H is the higher the diversity. We use this index to assess how diverse the cells are that are aggregated together. When we are on the original resolution the E_H is 1 because the output cell value perfectly reflects the input information, which is itself the original resolution cell values. As we aggregate, more cells from the original resolution will be used to determine the aggregated cell's value. An aggregated cell only has 1 value but represents multiple original resolution cells. Therefore, the lower the E_H – the higher the heterogeneity in original resolution cell value proportions within an aggregated cell – the more loss of information there will be. If all original resolution cell values that make up an aggregated cell are the same then the E_H will be 1 and there will be no loss of information due to aggregation. If there are multiple species but complete evenness in the proportions, which also produces E_H equal to 1, then any classification is as valid as any other amongst the classifications present. More than likely, a cell such as this would be classified as woody savannah or mixed forest which reflects the equal influence of all cells that make up the aggregated value. A lower E_H will occur when there are uneven proportions which would, if un-aggregated, result in heterogeneous individual classifications in diverse proportions that are missed when aggregated. Such a forest will most likely receive a specific classification (e.g. evergreen needle leaf forest or deciduous broad leaf forest) which dominates the landscape thereby negating any effect the minority forest cover types has on the final aggregated value.

3.3. Assess how aggregation affects agreement of remotely sensed data sets and NFI data

We assessed how aggregation affects the agreement between remotely sensed and NFI data by using the aggregated data sets we produced earlier along with confusion matrices to quantify the percent agreement at each aggregation step. Here we compared the aggregated NFI data with the corresponding aggregated data of each of the 4 gridded cover type data sets in our study. The percent agreement is the percent of remotely sensed cell's that have the same land cover type as the corresponding NFI data at each aggregation step.

Table 3
Land Cover classification percent agreement between remotely sensed and national forest inventory data.

Cover type data	Austria	Czech Republic	Germany	Norway	Finland	Spain	All
CLC	60%	40%	64%	56%	39%	31%	40%
EFI	60%	56%	69%	69%	59%	44%	50%
MODIS	45%	24%	60%	47%	37%	13%	27%
GLC2000	50%	48%	65%	50%	44%	32%	41%
Mean	47%	41%	52%	47%	40%	30%	39%

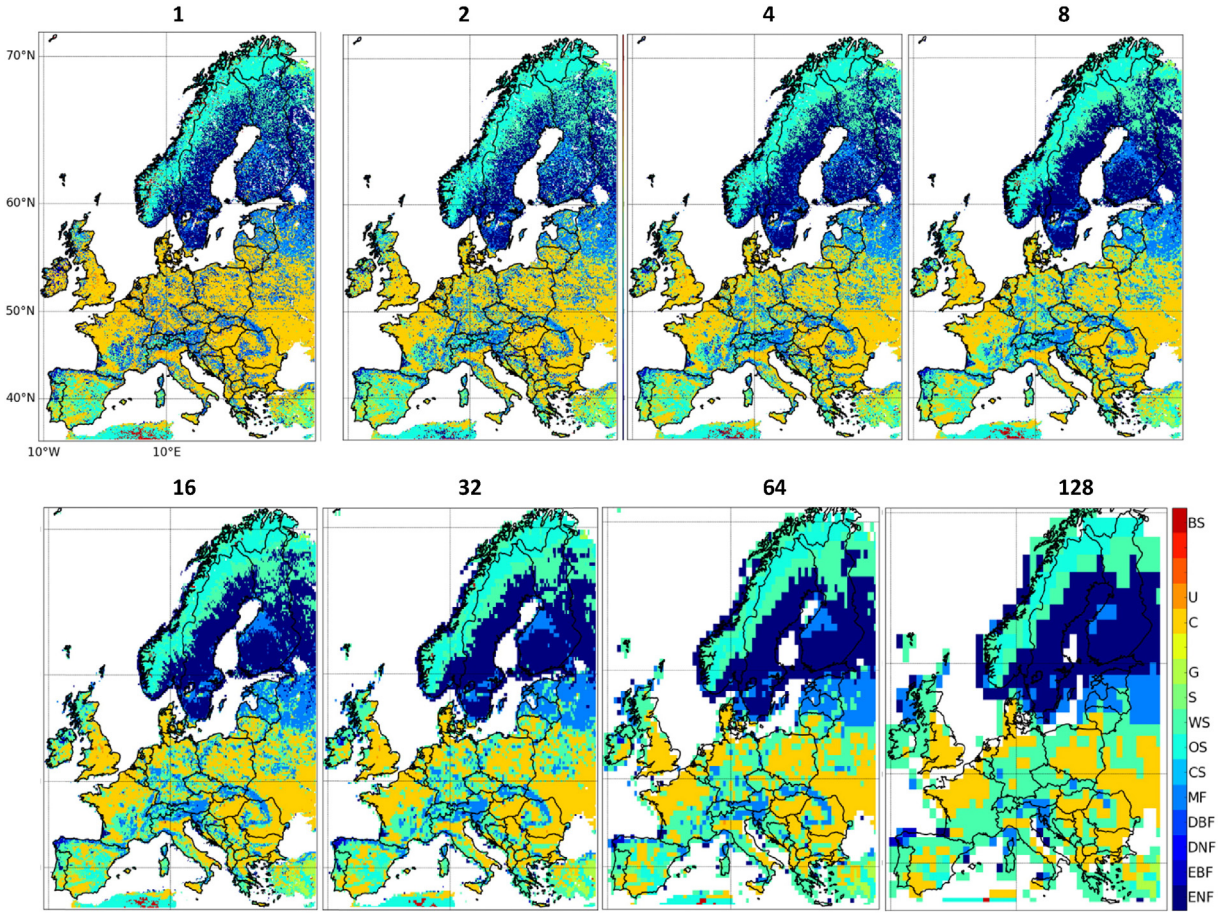

Fig. 2. MODIS Land-cover data, as an example, at each aggregation step (ENF = Evergreen Needle-leaf Forest; EBF = Evergreen Broadleaf Forest; DNF = Deciduous Needle-leaf Forest; DBF = Deciduous Broadleaf Forest; MF = Mixed Forest; CS = Closed Shrubland; OS = Open Shrubland; WS = Woody Savannah; S = Savannah; G = Grassland; C = Cropland; U = Urban; BS = Barren/Sparse).

3.4. Quantify the standard error of NFI variables at various aggregation steps

To assess the impact of the aggregation on the confidence in NFI variables and their ability to accurately describe forest characteristics, we analyze 3 NFI variables: basal area, mean age and mean height. Basal area, mean age and height are directly derived from the tree data assessed on the plots and incorporate no model assumptions. Deriving basal area, mean age and height does not require information on forest cover percentage or species information so we could include data from 5 other countries: Belgium, France, Italy, Poland and Romania. Basal area is calculated according to the following equation.

$$BA = \Sigma\left(\frac{Dbh^2 \cdot \pi \cdot Nrep}{40000}\right)$$

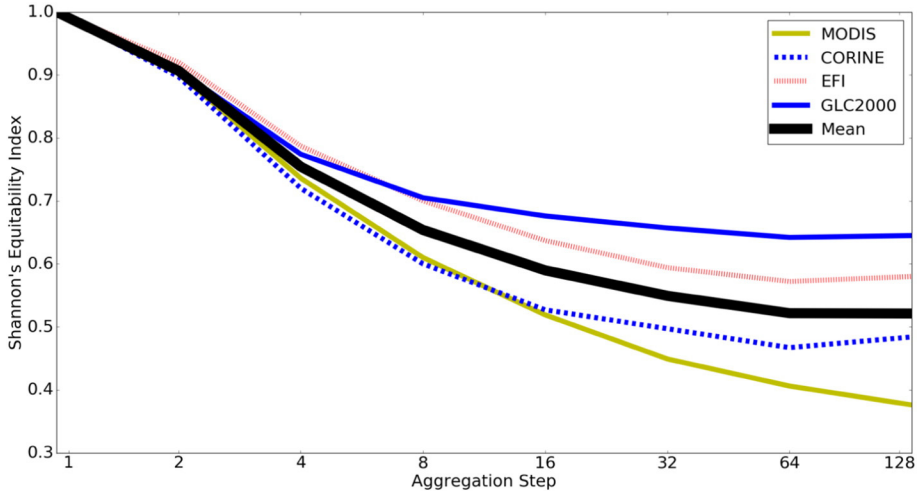

Fig. 3. Mean Shannon's Equitability Index of the original resolution data within each aggregated cell for 4 cover type data sets: MODIS, CORINE, an European Forestry Institute species map (EFI) and Global Land Cover 2000 (GLC2000).

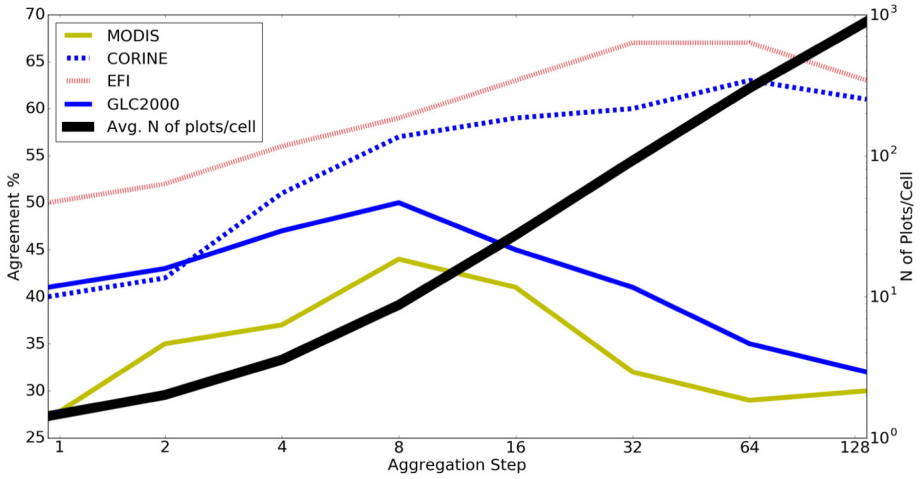

Fig. 4. Effect of aggregation on percent agreement between remotely sensed cover type data sets: MODIS, CORINE, an European Forestry Institute species map (EFI) and Global Land Cover 2000 (GLC2000) and national forest inventory forest cover type and the average number of NFI plots within each cell.

BA is the basal area [m^2/ha]. *Dbh* is diameter at breast height (1.3 m) [cm]. *Nrep* is the represented stem number [ha^{-1}]; for fixed area plots $Nrep = 10{,}000/A$ *and* $Nrep = (4 \cdot k)/(dbh^2 \cdot \pi)$ *for angle count sampling.* *A* is the plot area [m^2] and *k* is the basal area factor [m^2/ha] (Table 1).

We then aggregated these variables using the same aggregation steps we used in the previous analyses and calculated the standard error. The base resolution was 0.0083°; same as the original resolution on the gridded data sets we analyzed earlier. Standard error for each pixel is calculated as:

$$SE = \frac{\sigma}{\sqrt{N}}$$

SE is the standard error, σ is the standard deviation of the NFI data in a cell, and N is the number of plots within a cell. We calculated the SE for each variable for each country at each aggregation step. We also calculated the SE for all of Europe at each aggregation step and the slope of the resulting curve. The slope of the mean is calculated as:

$$Slope = SE_i - SE_{i-1}$$

SE_{i-1} is the SE of the aggregation step before the target aggregation step. SE_i is the standard error of the target aggregation step. For example, if we are calculating the slope for aggregation step 8 then the slope equals $SE_8 - SE_4$. We analyze 3 variables — basal area, age, and height so that we can assess the overall effect aggregation has on NFI SE instead of how it affects just one variable.

3.5. Determine the optimal resolution on which to combine remotely sensed and NFI data

To determine the optimal resolution on which to combine remotely sensed and NFI data we assessed the 3 effects of aggregation that we analyzed: Loss of information, agreement between remotely sensed and NFI data, and the standard error of the underlying NFI data. We normalized the curve of each of these effects by dividing each curve by their respective maximum values. This allows us to directly compare the proportional effects of aggregation on each curve. We used the mean curve for each effect we analyzed. For the SE curve we inversed the data so that a 1 refers to the lowest SE value, i.e., the least error. This creates 3 curves, one for each effect, with values from 0 to 1 at each aggregation step. A 1 value would be the most desired value for each effect, i.e., the least loss of information, the best agreement and the lowest standard error. These 3 curves were then added together and normalized once again. The resulting curve is the sum of three effects of aggregation. We also calculated the slope of this curve just as we did for SE.

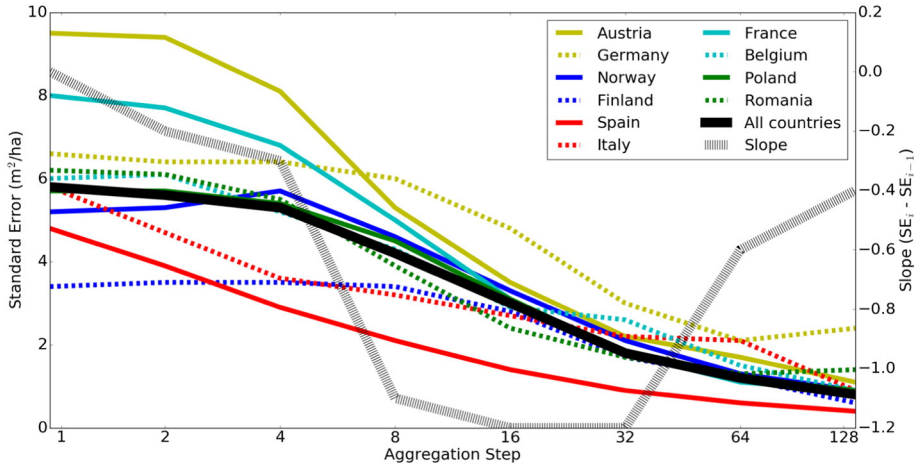

Fig. 5. Standard Error of basal area for 10 countries from national forest inventories, the mean of all countries and the slope of the mean.

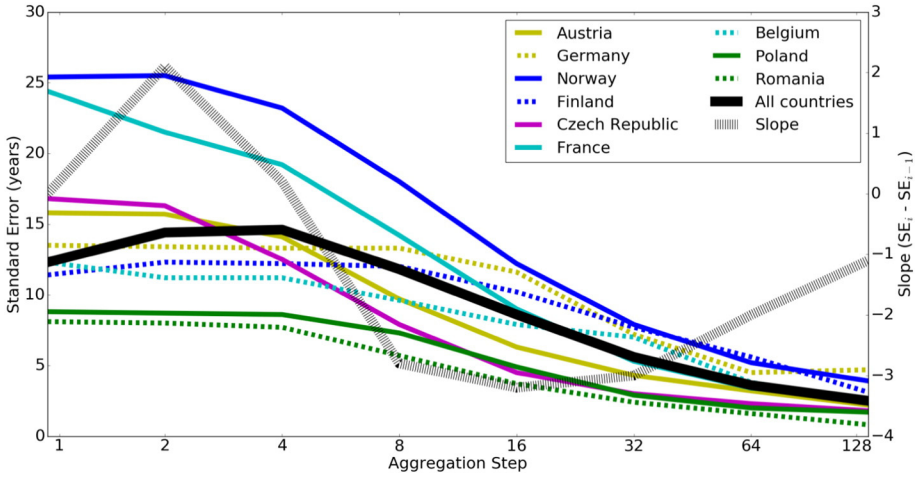

Fig. 6. Standard Error of mean forest age for 8 countries from national forest inventories, the mean of all countries and the slope of the mean.

4. Results

4.1. Assess the agreement of land cover remotely sensed data on their original resolution with NFI data

We compared land cover classification from NFI data for the original MODIS, EFI and GLC2000 datasets to assess how well currently used gridded data products agree with NFI data at a 0.0083° resolution – at or near native resolution. We also compared NFI data with the CLC dataset at a 0.0079° resolution (5 × 5 the original cell resolution). Results of the confusion matrices show a mean agreement percentage of 39% for all land cover datasets and for all 6 countries (Table 3). The mean accuracy of the datasets varies by country ranging from 30% in Spain to 52% in Germany.

The results for the individual land cover datasets show that EFI has the highest country-level percent agreement including 69% agreement in Germany and Norway. The land cover dataset with the lowest agreement is the MODIS data with 27% agreement. The lowest country-level accuracy is Spain in the MODIS dataset. CLC, which is the finest resolution European focused dataset in our study, has an agreement percentage of 40% which is 1% lower than GLC2000, a global dataset – though produced in Europe.

4.2. Quantify the loss of information with aggregation

We assessed how much information is lost due to aggregation, by aggregating land cover datasets at various aggregation steps using the rules set in the original dataset (Fig. 2). The gridded data visually shows that on the continental scale there is little effect for the first few aggregation steps. At aggregation step 32 there is then a clear difference from the original resolution (Fig. 2). Qualitatively it is clear from the images that there is loss of information as we aggregated, however, we also quantified this loss of information (Fig. 3). The Shannon's Equitability Index (E_H) curves show that, on the mean, as we suspected qualitatively, there is not much loss of information on the first few aggregation steps (Fig. 3). Each dataset loses information at different rates. MODIS loses the most information with aggregation whereas GLC loses the least information.

4.3. Assess how aggregation affects agreement of remotely sensed data sets and NFI data

We assessed how aggregation effects the agreement between remotely sensed and NFI data by aggregating at different aggregation steps and quantifying the agreement. Aggregating from the original resolution increases agreement between the remotely sensed and NFI data sets in every data set in our study (Fig. 4). The average number of plots within a cell increases almost linearly on a logarithmic scale with aggregation. The dataset that receives that greatest increase in agreement is the CLC data set with an increase of 23% from its original resolution at aggregation step 64. The EFI dataset has the highest agreement at every aggregation step. MODIS has the lowest agreement at every aggregation step and begins to merge with GLC2000 by the last aggregation step. MODIS' highest agreement is only 4% higher than CLC at its

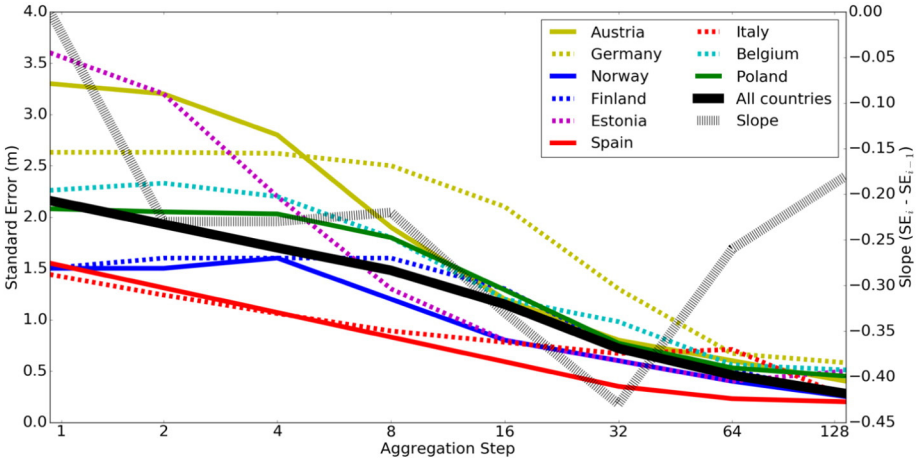

Fig. 7. Standard Error of forest height for 8 countries from national forest inventories, the mean of all countries and the slope of the mean.

original resolution. Neither MODIS nor GLC2000 ever reach the level of agreement seen in the EFI data at its lowest agreement percentage. The two global datasets have similar patterns in agreement through the aggregation steps, as do the two European datasets. The two global datasets, GLC2000 and MODIS, have an agreement peak at aggregation step 8 then decline ending with approximately the same agreement in the last aggregation step. The European datasets continue to increase in agreement, until just before our last aggregation step, ending with approximately the same percent agreement (Fig. 4).

4.4. Quantify the standard error of NFI variables at various aggregation steps

We assessed how well the underlying NFI data are able to describe the real world forest within a cell by quantifying the standard error at various aggregation steps. We chose 3 variables that do not require model assumptions, such as volume or carbon, so that there should not be variation in calculation methods from country to country. We calculated the standard error of the NFI data at every aggregation step for: basal area, mean height and mean age for each individual country. We also did this for all countries together to find the mean European pattern. The base resolution of 0.0083° for basal area has the largest variation in country-level standard error values (Fig. 5). As we aggregated data, the variation in the standard error decreased. The country with the lowest standard error in the base resolution is Belgium. By the 4th aggregation step, Spain has the lowest standard error. Austria has the highest standard error, until Germany surpasses it after aggregation step 4. Some countries have similar patterns in the standard error in basal error through the aggregation steps. For example, Spain and Italy as well as Poland and Romania have similar patterns. The basal area standard error is affected differently for different countries. Spain and Italy have an immediate decline in standard error on the first aggregation step. Most countries have a gradual decrease in the first few aggregation steps, followed by a steeper decline, then a leveling off in the final steps. The European standard error follows this same pattern with a basal area standard error in the base resolution of 5.8. The slope of the European standard error shows the aggregation steps that produce the greatest improvement are 16 and 32. After this inflection point, the effect of aggregation on the standard error begins to diminish (Fig. 5).

The aggregation effect on the standard error of age has the same properties as that of basal error (Fig. 6). The age standard error shows decreasing variation with aggregation and the same concave down decreasing curves. With respect to age, however, the European standard error increases with the first 2 aggregation steps and then decreases. Again, the inflection point is at aggregation step 16. For individual countries, Norway has the highest standard error, and Romania has the lowest.

The standard error with respect to tree height varies by more than 100% from the lowest country value to the highest in the base resolution (Fig. 7). Austria has the highest standard error with 3.3 m and Italy has the lowest with 1.44 m. Again, there are groupings of countries that behave in the same way. Austria and Germany both have high standard errors compared to the other countries and have similar curves. Belgium and Poland also have similar curves. Italy and Spain show different curves compared to all of the other countries. The European standard error has an almost linear downward trend, with the slope varying by 0.25 m from the aggregation step that shows the greatest improvement, to the step with the least. The inflection point is at aggregation step 32. The end of the curve indicates that the benefit of aggregation begins to flatten out towards the end.

4.5. Determine the optimal resolution on which to combine remotely sensed and NFI data

We quantified the optimal resolution on which to integrate remotely sensed and NFI data by combining the 3 previous aggregation effects analyzed in this study: information loss, agreement and standard error of NFI data. We took the mean curves of each effect of aggregation and normalized them (Fig. 8). This shows that the greatest effect that aggregation has is on the SE of the NFI dataset with an 80% improvement from its original resolution to the largest aggregation step. The information represented at each aggregation step, as calculated by the E_H, declines by nearly 50% from the original resolution data. The cover-type agreement has the best agreement at aggregation step 8 which is 25% greater than the agreement on the original resolution. We then summed up all of these effects and normalized the resultant curve to understand how they interact. This weights each effect equally. The slope of this curve shows that there is a negative benefit from aggregation until aggregation step 8. The results also show that the inflection point is between aggregation steps 8 and 32 (Fig. 8). The slope curve demonstrates the benefit from aggregation. Before the 8th aggregation step aggregation has slightly negative benefits. After aggregation step 32, aggregation has diminishing benefits.

5. Discussion

We analyzed the effect aggregation has on the information (heterogeneity) represented by the gridded data, the agreement between NFI and remotely sensed data derived products, and the accuracy of the underlying NFI data when linking these two types of data sets. At a resolution of 0.0083°, the original resolution for the gridded datasets we

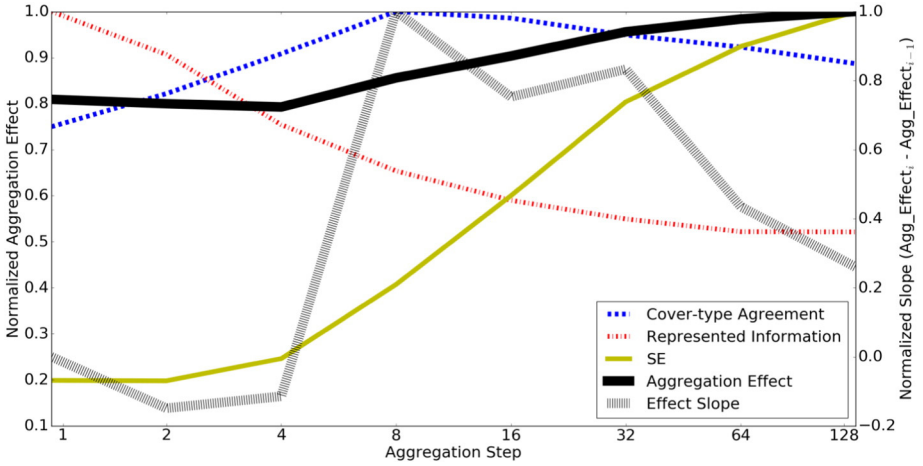

Fig. 8. Three normalized effects of aggregation: Represented Information, Cover-type agreement, and the Standard Error (SE) of the underlying NFI data. Aggregation Effect is the normalized sum of the 3 curves. Effect Slope is the Aggregation Effect value minus the preceding Aggregation Effect value.

analyzed, on average there is approximately 1 corresponding NFI plot within a grid cell (Fig. 4). The average area of 1 NFI plot represents 0.02% of the total area of a grid cell at this resolution, with zero degrees of freedom. This constitutes an undefinable confidence in the comparability of these two types of datasets essentially making the NFI point 1 single random sample that represents 1/5,000ths of the population. Therefore, at this resolution the two datasets are not directly comparable, and so the results in this study are not a validation of the remotely sensed datasets we used, and should not be taken as an error analysis but rather as an agreement/comparability analysis. This result alone demonstrates why linking remotely sensed and NFI data at a 0.0083° (1 km^2) resolution should be avoided.

The amount of information represented by each cell as we aggregated diminished (Fig. 2, Fig. 3). This is because at every aggregation step each cell can only represent 1 cover-type class. As we aggregated, each aggregated cell will encompass more cells from the original data. As we combine more cells from the original data the likelihood that these cells are heterogeneous increases. The more heterogeneous the cells are that are aggregated together the more information is lost because in the end all of these cells are represented by one value in the aggregated data set. At the larger aggregation steps the information curve flattens out because at this point spatial heterogeneity is already low and there is not much more information to lose.

We chose to analyze agreement of cover type because there are multiple independently produced gridded data sets that cover all of Europe. Other variables on forest characteristics have very limited data available for continental analysis. By analyzing multiple datasets we can isolate the effect of aggregation instead of assessing the accuracy of one gridded data product. On the original resolution (0.0083°), the EFI dataset has the highest agreement with NFI data (Table 3). This is primarily because the EFI dataset does not include a non-forest designation which removes a step in the classification method used by the other datasets. The other datasets first get a designation of forest or non-forest, where disagreement can occur, and then if it is designated as forest, it will be assigned a forest type, where further disagreement can follow. MODIS has the most disagreement between the two datasets. To exemplify why comparison at this resolution should be avoided let us examine the MODIS agreement at the original resolution in further detail.

The majority of the disagreements using MODIS occur in the evergreen needle-leaf forest (ENF) class in the NFI data, even though this category also has the most cells that also agree. NFI data indicates that ENF is the largest forest type, and 30% of the time, MODIS classifies the same cells as ENF. However, more often than not, ENF in the NFI data are classified as mixed forest or woody savannah in the MODIS data. Even though the NFI plot associated with a MODIS cell gives a forest classification, there are no other plots within the same cell to define the density of the forest cover and therefore cannot distinguish between an ENF and a woody savannah. Additionally, even if the majority of the trees within a NFI plot area are ENF, as explained earlier, this is not representative of the entire MODIS cell. Just outside of that plot the rest of the cell could contain agriculture or another tree species type. Therefore, MODIS would not be incorrect if it had a different classification than the NFI data. So in this case, we cannot say whether either dataset is correct at this resolution, we can only say that we cannot compare these two datasets at this resolution for processing or analysis. This confirms that, at this resolution, these two datasets should not be combined.

As we aggregated cells, both regional European datasets (EFI and CLC) as well as both Global datasets (MODIS and GLC2000) behave in two distinct patterns (Fig. 4). The European datasets tend to increase more gradually and see agreement improvement into the larger aggregation steps. The global datasets increase more rapidly in agreement, followed by a steep decline after aggregation step 8. This indicates that the overall distribution of forest classes in the remotely sensed data for Europe are more representative of the overall distribution of classes in the NFI data than the global datasets. This can be demonstrated if we examine an extreme case, by aggregating all European cells to 1 single cell. This would require assessing the distribution and proportions of all cells at the original resolution and all NFI plots together. If the proportions of cover types in the remotely sensed data aligned with the proportions in the NFI data, and the rules for classification are properly implemented, then the extreme single cell aggregation would have the same value in both datasets. That does not guarantee that at a finer resolution they would agree. It is possible that at the finer 0.0083° resolution, every cell disagrees with the underlying NFI data. However, if the total European distribution of classes is the same, then the data will improve with aggregation. The more agreement the remotely sensed data and the NFI data have spatially, the earlier we will see a benefit from aggregation. However, if the overall distribution of classes on larger scales is not aligned, then as aggregation continues towards this single cell, the datasets will diverge; as can be seen in the global datasets. The benefit we get from the first few aggregation steps is that we eliminate any location disagreement between the in-situ data and the remotely sensed data, as well as getting a more representative sample within each cell from the NFI data. At middle resolutions, the agreement is on the forest or watershed level (Fig. 2, Fig. 4). The global datasets agree with NFI data most at this forest/watershed level. The European datasets have higher agreement at that level, but the highest agreement is seen at aggregation step 64 (Fig. 2, Fig. 4). This indicates that the regional European datasets have more agreement in the distribution of classes at every scale than the global datasets but with the most distribution agreement at the landscape level.

The effect that aggregation has on the SE reflects the limitations of the NFI dataset for spatial use and exemplifies why NFIs were designed for use in aggregates and not as individual values. The number of underlying NFI plots in each cell increases exponentially in accordance with the exponential increase in cell size as we aggregated (Fig. 4). More NFI plots within a cell will yield a lower standard error (SE), given that the standard deviation does not increase exponentially as well. Lower SE gives higher confidence in the data's ability to represent a population, in this case a grid cell. The SE in all three forest characteristics studied – basal area, age and height – have high inter-country variation, which declines with aggregation (Fig. 5, Fig. 7). This indicates that the standard deviation does not increase at the same rate as the increase in NFI sample plots per cell. The standard error varies by country because of the different sampling techniques at the plot and country-level (such as sampling grid size), heterogeneity of the landscape, and forest management practices. These factors influence the number of samples that will be combined at each aggregation step and the standard deviation from plot to plot within a cell. For example, Austria has a high standard error in basal area and height because Austria has high variation in elevation and many small scale forest owners which affect the height and basal area of a forest, increasing the standard deviation of these variables. Countries that have similar SE patterns with aggregation reflect that they have similar country-wide sampling grids and landscapes. Basal area and age behave similarly with inflection points at aggregation step 32 (Fig. 5, Fig. 6). At this point the benefits of aggregation diminish and we quickly loose spatial variability (Fig. 2). It should also be noted that because most countries have permanent sample grids and the area a remotely sensed cell represents varies with a constant degree resolution by latitude that aggregation will improve agreement and SE in the south earlier with aggregation than in the north. Projections with a constant area, as opposed to constant degrees, would show similar results but with cells in the north being affected at the same rate as in the south.

Considering the loss of spatial information, agreement between remotely sensed and NFI data, and the standard error of NFI with aggregation, we conclude that the best resolution to compare these two datasets is between aggregation step 8 and 32 or 0.0664° and 0.266° respectively which provides 9 to 92 plots per cell respectively (Table 2, Fig. 4, Fig. 8). We must consider that with every aggregation step we are losing information on local scales that are valuable to forest managers and researchers (Fig. 2, Fig. 3). However, the agreement between

remote sensing and NFI data are the lowest and the standard error is the highest at the finest resolution (Fig. 8). Therefore we recommend using an aggregated dataset (greater than 0.0083°) when combining remotely sensed and NFI data. The inflection points in the standard error curves indicate that aggregation step 16 or 32 has the most benefit while maintaining the most local level information (Fig. 5, Fig. 7). Whether a researcher prefers to combine these datasets on the finer or coarser end of our recommendation depends on the trade-offs they are willing to make. At finer resolutions within our recommendation the remotely sensed data will depict more heterogeneity with higher agreement between the remotely sensed and NFI data. However, the SE of the NFI data will be lower than at larger aggregation steps giving less confidence in the underlying NFI data's ability to accurately depict the real world situation. At the coarser end of the recommendation the SE will be low giving high confidence in the underlying NFI data with approximately the same level of agreement between the remotely sensed and NFI data. However, the heterogeneity in the data will decrease. The trade-offs that are acceptable should depend on which scale the research is focused. At smaller scales, a finer resolution may be more appropriate because heterogeneity in data might be important. However, at the continental scale local level heterogeneity may not be the most important factor and so a coarse scale could be the better option. On any scale, we recommend using a resolution no lower than 0.0664°.

Our recommendation agrees with studies from the U.S. that have shown that based on their forest sampling method, the minimum aggregation for combining forest inventory data with gridded data is between approximately 0.133° (approx. aggregation step 16) to 0.5° (approx. aggregation step 64) (Blackard et al., 2008; Jenkins et al., 2001). Further, other research in the U.S. has shown that using forest inventory plots do not accurately describe a 0.0083° resolution cell and that to perform a nearest neighbor method – used in many studies that combine this type of data – the data must be aggregated to at least 0.075° resolution – coarser than our aggregation step 8 (Wilson et al., 2012). These studies, however, did not quantify the benefits and drawbacks of aggregation to find an optimal resolution as we did in this study.

6. Conclusion

Harmonizing NFI data across countries into a gridded dataset to be used in conjunction with remotely sensed data requires the use of one consistent resolution. The resolution chosen has a large effect on the quality of, and the confidence in the output data. Studies that link in-situ and remotely sensed data often do so on a 0.0083° resolution primarily because it is commonly used and because this is the finest resolution of many remote sensing products. It is assumed that the finer the resolution is, the better the information produced will be. This study challenges that assumption by quantifying various effects aggregation has on the confidence and accuracy of the combination of remotely sensed and NFI data in Europe. It might seem intuitive that the finest resolution should lead to more accurate results; however our study shows that, based on our current data availability and remote sensing abilities in Europe, aggregating to larger resolutions produces more agreement between these two datasets and less error in the underlying NFI data at a higher rate than the loss of local level spatial heterogeneity. Though we focused on Europe, this study is applicable to other continents and to global studies that link inventory and remote sensing data.

Larger resolutions will change the conceptual meaning of the resulting data. This difference requires a landscape level outlook as opposed to a stand or forest level outlook that finer resolutions provide. If forest managers and policy makers are not able to make decisions using a resolution that produces the most accurate and realistic results, then policies for data accessibility must change. NFI data that provide the exact location of plots would allow researchers to use the most high resolution satellite data, such as Landsat (30 m^2 resolution), Sentinel (10 m^2 resolution), Spot data (1.5 m^2 resolution) or LiDAR (<1 m resolution), to create gridded data on forest ecosystems on the order of meters instead of kilometers. This would permit researchers to match the exact plot area with remotely sensed data allowing direct comparisons which we showed, given our current state of data accessibility, cannot be done. Such data would give us a better understanding of the state of forests and forest resources throughout Europe across political boundaries. As an example, this better understanding of European forests would allow researchers to quantify the affect that different forest management practices have on the landscape compared with one another or target vulnerable or underperforming forests in regards to ecosystem services. Harmonization and linking of NFI and remotely sensed data could be done by a committee of scientists or by national centers then collated before public release, thus preserving the secrecy of exact plot locations to the general public.

Acknowledgments

We thank Loretta Moreno for revising our manuscript. We would also like to thank all the researchers that make their data freely and publicly available allowing this kind of research. The research leading to these results has received funding from the European Union Seventh Framework Programme under grant agreement no. 311970 (FORMIT).

References

Beaudoin, A., Bernier, P. Y., Guindon, L., Villemaire, P., Guo, X. J., Stinson, G., ... Hall, R. J. (2014). *Mapping attributes of Canada's forests at moderate resolution through k NN and MODIS imagery. 532.* (pp. 521–532), 521–532 (January).

Bergseng, E., Ørka, H. O., Næsset, E., & Gobakken, T. (2014). Assessing forest inventory information obtained from different inventory approaches and remote sensing data sources. *Annals of Forest Science*, *1432*, 1–13 (http://doi.org/10.1007/s13595-014-0389-x).

Bitterlich, W. (1952). Die Winkelzählprobe: Ein optisches Meßverfahren zur raschen Aufnahme besonders gearteter Probeflächen für die Bestimmung der Kreisflächen pro Hektar an stehenden Waldbeständen. *Forstwissenschaftliches Centralblatt*, *71*(7), 215–225.

Blackard, J. a., Finco, M. V., Helmer, E. H., Holden, G. R., Hoppus, M. L., Jacobs, D. M., Lister, A. J., Moisen, G. G., Nelson, M. D., Riemann, R., et al. (2008). Mapping U.S. forest biomass using nationwide forest inventory data and moderate resolution information. *Remote Sensing of Environment*, *112*(4), 1658–1677 (http://doi.org/10.1016/j.rse.2007.08.021).

Bossard, M., Feranec, J., & Otahel, J. (2000). *CORINE land cover technical guide: Addendum 200040, .*

Brus, D. J., Hengeveld, G. M., Walvoort, D. J., Goedhart, P. W., Heidema, A. H., Nabuurs, G. J., & Gunia, K. (2012). Statistical mapping of tree species over Europe. *European Journal of Forest Research*, *131*(1), 145–157.

Costanza, R., Fisher, B., Mulder, K., Liu, S., & Christopher, T. (2007). Biodiversity and ecosystem services: A multi-scale empirical study of the relationship between species richness and net primary production. *Ecological Economics*, *61*(2–3), 478–491 (http://doi.org/10.1016/j.ecolecon.2006.03.021).

Crowther, T. W., Glick, H. B., Covey, K. R., Bettigole, C., Maynard, D. S., Thomas, S. M., Smith, J. R., Hintler, G., Duguid, M. C., Amatulli, G., et al. (2015). *Mapping tree density at a global scale.* (Nature). (http://doi.org/10.1038/nature14967).

Di Gregorio, A. (2005). *Land cover classification system.* Classification Concepts and User Manual: LCCS. Food and Argicultural Organization (No. 8).

Friedl, M. A., Sulla-Menashe, D., Tan, B., Schneider, A., Ramankutty, N., Sibley, A., & Huang, X. (2010). MODIS Collection 5 global land cover: Algorithm refinements and characterization of new datasets. *Remote Sensing of Environment*, *114*(1), 168–182.

Gallaun, H., Zanchi, G., Nabuurs, G. J., Hengeveld, G., Schardt, M., & Verkerk, P. J. (2010). EU-wide maps of growing stock and above-ground biomass in forests based on remote sensing and field measurements. *Forest Ecology and Management*, *260*(3), 252–261 (http://doi.org/10.1016/j.foreco.2009.10.011).

Gabler, K., & Schadauer, K. (2008). *Methods of the Austrian forest inventory 2000/02: origins, approaches, design, sampling, data models, evaluation and calculation of standard error.* Naturgefahren und Landschaft: Bundesforschungs-und Ausbildungszentrum für Wald.

Hansen, M., DeFries, R., Townshend, J. R., Sohlberg, R., Dimiceli, C., & Carroll, M. (2002). Towards an operational MODIS continuous field of percent tree cover algorithm: Examples using AVHRR and MODIS data. *Remote Sensing of Environment*, *83*(1–2), 303–319 (http://doi.org/10.1016/S0034-4257(02)00079-2).

Hansen, M. C., Potapov, P. V., Moore, R., Hancher, M., Turubanova, S. A., Tyukavina, A., Thau, D., Stehman, S. V., Goetz, S. J., Loveland, T. R., et al. (2013). High-resolution global maps of 21st-century forest cover change. *Science*, *342*(6160), 850–853 (New York, N.Y.). (http://doi.org/10.1126/science.1244693).

Hasenauer, H., & Eastaugh, C. S. (2012). Assessing Forest production using terrestrial monitoring data. *International Journal of Forestry Research*, *2012*, 1–8 (http://doi.org/10.1155/2012/961576).

Hasenauer, H., Petritsch, R., Zhao, M., Boisvenue, C., & Running, S. W. (2012). Reconciling satellite with ground data to estimate forest productivity at national scales. *Forest*

Ecology and Management, *276*, 196–208 (http://doi.org/10.1016/j.foreco.2012.03.022).

Hasenauer, H., Neumann, M., Moreno, A., & Zhao, M. (2014). *Large scale estimation of biomass increment by combing terrestrial and satellite driven data.*

Hill, M. O. (2015). Diversity and evenness : A unifying notation and its consequences. *Ecology*, *54*(2), 427–432 (http://doi.org/10.2307/1934352).

Jenkins, J., Birdsey, R., & Pan, Y. (2001). Biomass and NPP estimation for the mid-Atlantic region (USA) using plot-level forest inventory data. *Ecological Applications*, *11*(4), 1174–1193.

Justice, C., Townshend, J. R., Vermote, E., Masuoka, E., Wolfe, R., Saleous, N., ... Morisette, J. (2002). An overview of MODIS land data processing and product status. *Remote Sensing of Environment*, *83*(1–2), 3–15 (http://doi.org/10.1016/S0034-4257(02)00084-6).

Kandler, G. (2009). *The design of the second German national forest inventory.* Proceedings of the Eighth Annual Forest Inventory and Analysis Symposium.

Lewis, H., & Brown, M. (2001). A generalized confusion matrix for assessing area estimate from remotely sensed data. *International Journal of Remote Sensing*, *22*(16), 3223–3235 (http://doi.org/10.1080/01431160152558332).

Mayaux, P., Eva, H., Gallego, J., Strahler, A. H., Herold, M., Member, S., Agrawal, S., Naumov, S., De Miranda, E. E., Di Bella, C. M., et al. (2006). Validation of the Global Land Cover 2000 Map*44*(7), 1728–1739.

McDowell, N. G., & Allen, C. D. (2015). Darcy's law predicts widespread forest mortality under climate warming. *Nature Climate Change*, *5*(May), 669–672 (http://doi.org/10.1038/nclimate2641).

Moreno, A., Neumann, M., & Hasenauer, H. (2016). *The state of forest resources across Europe. Remote sensing, submitted.*

Motz, K., Sterba, H., & Pommerening, A. (2010). Sampling measures of tree diversity. *Forest Ecology and Management*, *260*(11), 1985–1996. http://dx.doi.org/10.1016/j.foreco.2010.08.046.

Neumann, M., Moreno, A., Mues, V., Härkönen, S., Mura, M., Bouriaud, O., Lang, M., Achten, W. M. J., Thivolle-Cazat, A., Bronisz, K., et al. (2016). Comparison of carbon estimation methods for European forests. *Forest Ecology and Management*, *361*, 397–420. http://dx.doi.org/10.1016/j.foreco.2015.11.016.

Richmond, A., Kaufmann, R. K., & Myneni, R. B. (2007). Valuing ecosystem services: A shadow price for net primary production. *Ecological Economics*, *64*(2), 454–462. http://dx.doi.org/10.1016/j.ecolecon.2007.03.009.

Running, S. W., Nemani, R. R., Heinsch, F. A., Zhao, M., Reeves, M., & Hashimoto, H. (2004). A continuous satellite-derived measure of global terrestrial primary production. *Bioscience*, *54*(6), 547 (http://doi.org/10.1641/0006-3568(2004)054[0547:ACSMOG]2.0.CO;2).

Schröter, D., Cramer, W., Leemans, R., Prentice, I. C., Araújo, M. B., Arnell, N. W., Bondeau, A., Bugmann, H., Carter, T. R., Gracia, C. A., et al. (2005). Ecosystem service supply and vulnerability to global change in Europe. *Science*, *310*(5752), 1333–1337 (New York, N.Y.). (http://doi.org/10.1126/science.1115233).

Seidl, R., Eastaugh, C. S., Kramer, K., Maroschek, M., Reyer, C., Socha, J., ... Hasenauer, H. (2013). Scaling issues in forest ecosystem management and how to address them with models. *European Journal of Forest Research*, *132*(5–6), 653–666 (http://doi.org/10.1007/s10342-013-0725-y).

Simard, M., Pinto, N., Fisher, J., & Baccini, A. (2011). Mapping forest canopy height globally with spaceborne lidar. *Geophysical Research*, *116*(G04021).

Spittlehouse, D. L. (2005). Integrating climate change adaptation into forest management. *Forestry Chronicle*, *81*(5), 691–695 (http://doi.org/10.5558/tfc81691-5).

Tomppo, E., Olsson, H., Ståhl, G., Nilsson, M., Hagner, O., & Katila, M. (2008). Combining national forest inventory field plots and remote sensing data for forest databases. *Remote Sensing of Environment*, *112*(5), 1982–1999 (http://doi.org/10.1016/j.rse.2007.03.032).

Tomppo, E., Gschwantner, T., Lawrence, M., McRoberts, R. E., Gabler, K., Schadauer, K., ... Cienciala, E. (2010). *National forest inventories: Pathways for common reporting.*

Turner, D. P., Ritts, W. D., Cohen, W. B., Gower, S. T., Running, S. W., Zhao, M., ... Ahl, D. E. (2006). Evaluation of MODIS NPP and GPP products across multiple biomes. *Remote Sensing of Environment*, *102*(3–4), 282–292 (http://doi.org/10.1016/j.rse.2006.02.017).

van Mantgem, P. J., Stephenson, N. L., Byrne, J. C., Daniels, L. D., Franklin, J. F., Fule, P. Z., ... Veblen, T. T. (2009). Widespread increase of tree mortality rates in the Western United States. *Science*, *323*(5913), 521–524 (http://doi.org/10.1126/science.1165000).

Wilson, B. T., Lister, A. J., & Riemann, R. I. (2012). A nearest-neighbor imputation approach to mapping tree species over large areas using forest inventory plots and moderate resolution raster data. *Forest Ecology and Management*, *271*, 182–198 (http://doi.org/10.1016/j.foreco.2012.02.002).

Wouters, J., Quataert, P., Onkelinx, T., & Bauwens, D. (2008). *Ontwerp en handleiding voor de tweede regionale bosinventarisatie van het Vlaamse Gewest.* Report INBO.

9.5. Paper 5

Moreno, A., Neumann, M, Hasenauer, H. In revision for submission. “The state of forest resources across Europe“

The State of Forest Resources across Europe

Adam Moreno[1*], Mathias Neumann[1], Hubert Hasenauer[1]

[1]Institute of Silviculture

University of Natural Resources and Life Sciences, Vienna

Peter Jordan Straße 82

A – 1190 Vienna, Austria

Tel.:+43 – 1 – 476 54 – 4078

e-mail: adam.moreno@boku.ac.at

[*]Corresponding author

6.4. 2016

The State of Forest Resources across Europe

Abstract

A consistent pan-European gridded data set on the state of forest resources would allow researchers, policy makers and conservationists to study and understand European forests independent of political boundaries and along different gradients such as elevation, latitude, and climate. Although National Forest Inventory (NFI) data provide information on the characteristics of forests including carbon content, volume, height, and age such data does not exist across Europe. The creation of pan-European gridded data sets on forest resources have been hindered by varying NFI systems, spatial and temporal discrepancies in data collection, data accessibility and countries without NFIs. The purpose of this study is to use existing European data to develop a consistent pan-European data set for total live tree carbon, volume, mean tree height and mean tree age by integrating remotely sensed along with harmonized NFI data from 12 different European countries. We produce a pan-European map for each of the four key variables on a 0.133° grid representing the time period 2000-2010. We used this data to assess the state of forest resources across Europe showing that mountainous regions have the highest levels of carbon and volume, central Europe has the tallest mean tree heights and Austria and Northern Scandinavia have the oldest mean tree ages. Cross-validation of the data indicates that the error varies by forest characteristic but shows negligible biases for all. We compared our carbon and volume data with that of the UN Food and Agriculture Organization's Forest Resources Report which indicate similar results. We also compared our height and age data with global height and European age datasets and found that these forest characteristics are more difficult to compare because of differences in the definitions used for age and height and the underlying datasets. Our gridded datasets provide consistent information on the state of forest resources across Europe and can be obtained at ftp://palantir.boku.ac.at/Public/ForestResources.

Key words: Carbon, volume, forest resources, gridded data, Europe, age, height

1. Introduction

European forests contain approximately a third of the world's temperate forest biomass (Pan et al., 2011). The state of forest resources in Europe are measured using forest inventories. There are 28 member countries in the European Union and even more forest inventories (Daamen et al., 2010; Tomppo et al., 2008). Each forest inventory is conducted independently from one another with some countries (e.g. Italy) applying different inventory systems for each province. European NFI data is not collected and distributed from one freely accessible database. Users must obtain each forest inventory dataset individually from the responsible organization. Some NFI's require legally binding written contracts, while some data portals are only provided in the native language of individual countries. Thus, collecting and analyzing NFI data across different European countries is challenging. Additionally, individual country reporting without centralized oversight has been shown to hinder the effectiveness of multi-country climate mitigation and monitoring schemes which is currently done because of no centralized dataset on forest resources (Kollmuss et al., 2015).

Approximately every 5 years, the United Nations Food and Agricultural Organization (FAO) publish the Global Forest Resource Assessment (FRA) report to collate National Forest Inventory data (NFI). This report gives country-level information on forest characteristics such as volume and live tree carbon (FAO 2010). Several sampling and calculation methods are permitted for reporting to the FAO that are outlined within the guidelines set forth in the Intergovernmental Panel on Climate Change's National Green House Gas Inventory reporting (IPCC et al., 2006). This makes comparing data across countries using FAO FRA data ambiguous because different carbon calculation methods used by various European countries may produce different carbon estimates (Neumann et al., 2016b).

Researchers have attempted to create a harmonized NFI dataset for Europe (Schelhaas et al., 2006). The European Forest Information Scenario Model (EFIScen) project gathered data from several different European countries and created a freely available database. EFIScen is a matrix model and predicts the probability of key forest characteristics (e.g. Volume/ha, stem number, etc.) over time within a given jurisdiction. Thus the EFIScen data, which originate from NFI data, is grouped into jurisdictions, or site types, giving limited flexibility in spatial analysis (i.e., by

elevation, latitude, climate, or proximity to human development). A precondition for each grouped jurisdiction is a minimum number of inventory plots so that the accumulated data provided are statistically sound. Within the EFIScen project, this data was then used to create various gridded datasets (Brus et al., 2011; Gallaun et al., 2010; Vilén et al., 2012). These gridded datasets, however, have limited accessibility due to restrictions upon data sharing or not being provided on a public data portal.

On the global scale, Simard et al. (2011) created a map of canopy height and Crowther *et al.* (2015) mapped tree density. The local applicability of global datasets is diminished by a lack of enough data to accurately represent small areas. The European forests in the global tree density map are represented by research plots operated by members of The International Co-operative Programme's forest inventories on Assessment and Monitoring of Air Pollution Effects on Forest (ICP Forests) (http://icp-forests.net/) along with various remotely sensed products to create a gap-filled dataset at a 1x1 km resolution (Crowther et al., 2015). The ICP Forests plot data is scattered throughout Europe with only 6,000 plots with each plot covering only a very small part of a 1x1 km pixel. Crowther et al. (2015) admit that there is high confidence in tree density on the global scale and low confidence at smaller scales. Instead of NFI data, Simard et al. (2011) use previously produced space based LiDAR data and topographic maps (Lefsky et al., 2005) to create a 1x1km map of canopy height. Global datasets are designed to be used on global scales. At finer scales the accuracy of these datasets diminishes.

There have also been attempts to create country or regional level maps of forest data (Maselli et al., 2014; Ruiz-Labourdette et al., 2012). Datasets that are focused on local scales tend to be more accurate at that scale. However, this data may not be directly comparable to similar/related datasets from nearby areas as methodology may differ. Herein lays the tradeoff between scale and accuracy. Today, no pan-European gridded data set exists based off of consistently applied datasets and one methodology for various forest characteristics that is also accurate at local scales.

The purpose of this study is to create a pan-European gridded dataset of total live tree carbon, volume, mean tree height, and mean tree age to allow a consistent assessment of forest resources in Europe. Such data, hitherto unavailable, will support sustainable forest

management decisions across countries by assessing the role of forests for a growing bio-economy sector, quantifying the mitigation potential of European forests, and for analyzing the ecosystem services provided by European forests. We collate NFI data from 196,434 inventory plots from 12 different European countries and several remote sensing and other gridded data products representing the time period 2000 to 2010.

The objectives of our study are:

1. Develop an algorithm to combine NFI and remotely sensed gridded data to produce a gridded wall to wall cross European data set for total tree live carbon, volume, height and mean tree age.
2. Cross-validate the pan-European gridded data sets.
3. Compare and evaluate the newly created pan European gridded datasets with other previously produced data.

2. Data

For our study we obtained terrestrial bottom up observations (NFI data, Biogeographic Regions Forested area, FAO FRA, EFIscen) and remotely sensed top down data (MODIS Land Cover, MODIS NPP, MODIS NPP Trend, Tree Canopy Height, and Site Quality). We use these data sets for three distinct purposes: algorithm development, cross-validation, and comparison. The data consists of point data, gridded data and regional statistics (Table 1).

Table 1: Description of datasets used in this study. *Data* refers to the different data sets as outlined in the data section, *Point* refers to single inventory points, *Gridded* indicates raster data, *Country Stats* is the country level statistics, *Jurisdiction Stats* are data given for different jurisdictions on the sub-country level; x indicates that this data set is used to create, validate or compare against this output variable. *Alg* – this data set was used within the algorithm to create the output variables, *Val* – this data set was used to cross validate the output data, and *Com* – this data set was used to compare versus output variable(s).

Data	Type	Carbon	Volume	Height	Age	Use
NFI	Point	x	X	x	x	Alg/Val
MODIS Land Cover	Gridded	x	X	x	x	Alg
Biogeographical Regions	Gridded	x	X	x	x	Alg
MODIS NPP	Gridded	x	X	x	x	Alg
MODIS NPP Trend	Gridded	x	X	x	x	Alg
Tree Canopy Height	Gridded	x	X	x	x	Alg/Com
Site Quality	Gridded	x	X	x	x	Alg
Forested Area	Gridded	x	X			Alg
FAO FRA	Country Stats	x	X			Com
EFIScen	Jurisdiction Stats				x	Com

2.1 NFI

The NFI (National Forest Inventory) data used for this study come from 12 countries in Europe: Austria, Belgium, the Czech Republic, Estonia, France, Finland, Germany, Italy, Norway, Poland, Romania, and Spain. Each of these countries have a different sampling grid design and have implemented either a fixed area or angle count sampling plot system (Table 2). The data

originates from forest inventory data collected during the time period 2000-2010 by Neumann et al. (2015). Each country has different measurement times so as to create a harmonized data set our data represents the mean forest conditions during this 10 year time period. The data consists of 196,434 plots with locations falsification on a .0083° grid.

Table 2: Summary of the NFI characteristics by country. The sampling method can be either Angle Count Sampling (ACS) or a Fixed Area Plots (FAP). A basal area factor is required for countries with ACS. Plot area is required for the countries with FAP. The arrangement of sample plots indicates whether the plots are arranged as single plots or within clusters. Some countries have varying distances between plots/clusters depending on location.

Country	Sampling Method	Basal Area Factor [m^2/ha]	Plot Area [m^2]	Arrangement of Sample Plots	Distance between plots [km]	N of Plots
Austria	ACS+FAP	4	21.2	Clusters of 4 plots	3.889 x 3.889	9167
Belgium	FAP	-	15.9 - 1017.9	Single plots	1x0.5	2495
Czech Rep.	FAP	-	28.3 - 500	Clusters of 2 plots	2x2	13929
Estonia	Taxation	-	Undefined	Random	-	19930
Finland	ACS	2 (S) 1.5 (N)	-	Clusters of 14 – 18	6-8 (S) 6-11 (N)	6232
France	FAP	-	113 - 706	Single Plots	2x2	32107
Germany	ACS	4	-	Clusters of 4 plots	4x4 or 8x8	6153
Italy	FAP	-	50-600	Single Plots	0.5x0.5 or 1x1	19852
Norway	FAP	-	250	Single Plots	3x3	9200
Poland	FAP	-	200 - 500	Cluster of 5 Plots	4x4	13546
Romania	FAP	-	200 - 500	Cluster of 4 Plots	4x4 or 2x2	16605
Spain	FAP	-	78.5 - 1963.5	Single Plots	1x1	69853

We aggregated the plot level forest variables (live tree carbon, volume, mean tree height, and mean tree age) to a 0.133° resolution (area range: 75 – 175km^2) by averaging the plot variables to make gridded terrestrial data to reach an acceptable level of confidence in the gridded terrestrial data (Figure 1, methods section) (Moreno et al., 2016). The size of the grid cells varies according to latitude due to the curvature of the earth and map projection. Carbon data is given as tons of live tree carbon per hectare including carbon in the stem, branches, foliage, coarse roots, foliage and fine roots but does not include soil or dead-wood carbon.

Volume is given as m^3 per hectare and has different definitions from country to country. Some countries define volume as the merchantable timber or growing stock while others define it as

the total tree volume including branches (Neumann et al 2016). These differences in the definitions make a complete harmonization of volume difficult as we cannot parse apart the various components that make the volume estimates. We used the individual countries' definitions of volume within our data set.

Age is given as age classes. Each country has different age classes. Fortunately, it was possible to harmonize the age classes into 1 standard set. These age classes are: 0-20, 21-40, 41-60, 61-80, 81-100, 101-120, and >120 in years. Height is given as the mean height of all trees within a plot.

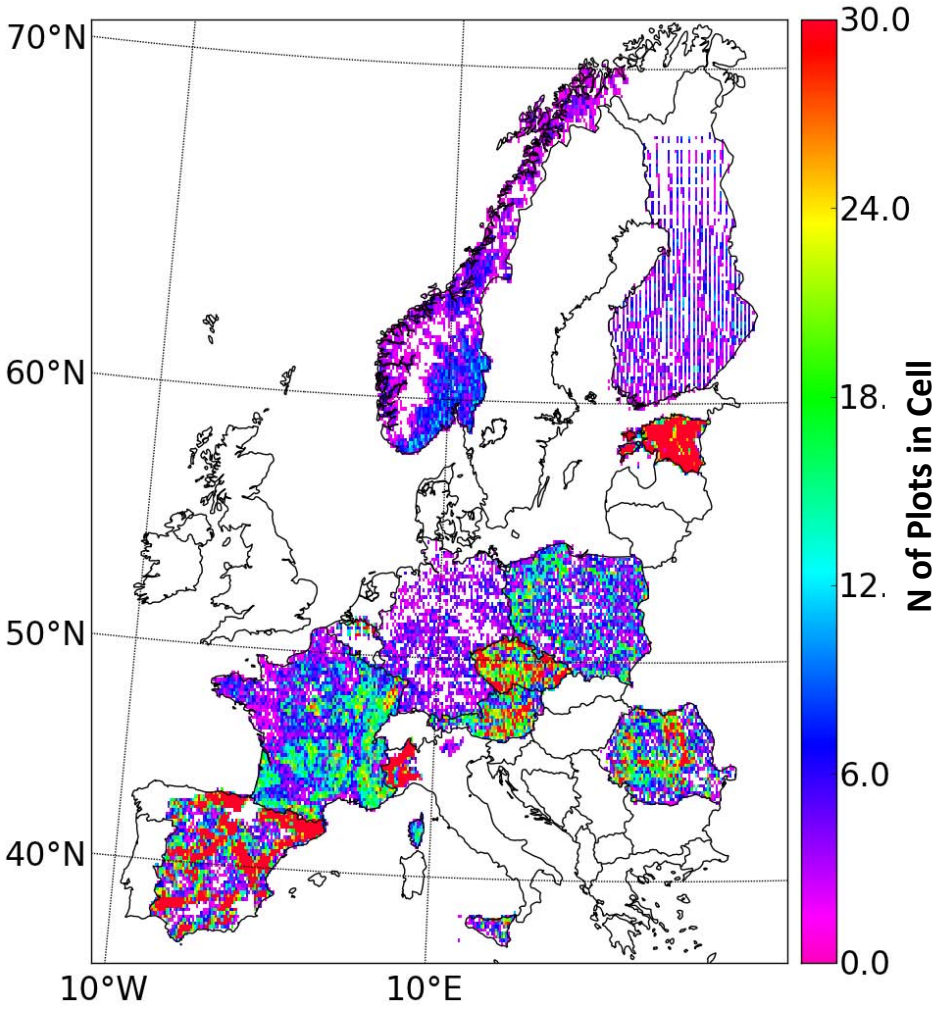

Figure 1: Gridded terrestrial data based off of NFI data. The color indicates the number of NFI plots within a given gridded terrestrial cell (0.133° resolution, 75–175km^2). Note: Estonia is the only country in our data where the NFI is based on a non-systematic inventory grid design. Thus the number of plots per grid cell is disproportionally high.

2.2 MODIS Land cover

The Moderate resolution Imaging Spectroradiometer (MODIS) is a sensor on the Terra and Aqua satellites. MOD12 land cover is given at a 0.0083° resolution (in Europe cell area range: 0.27 – 0.71 km^2, approximately 1km^2 at the equator) globally and includes 11 vegetative cover types: evergreen broad leaf, deciduous broad leaf, evergreen needle leaf, deciduous needle leaf, woody savanna, savanna, crops, open shrub lands, closed shrub lands, grassland, and

mixed forest (Friedl et al., 2002). The land cover data is produced by implementing the MODIS 12 Q1 collection 4 land cover classification algorithm. This algorithm is a supervised classification that gap fills the International Geosphere-Biosphere Program Data and Information System (IGBP) using annual data from the MODIS sensor for classification.

2.3 Biogeographical Regions

Biogeographical regions were collated from individual EU member countries' reports and are given on a 1x1 km resolution. Biogeographical regions include: Alpine, Arctic, Black Sea, Continental, Mediterranean, Pannonian, Steppic, Atlantic, and Boreal (European Environment Agency, 2012). We aggregated bioregions to produce 3 different bioregion maps, thereby creating clustering options for our parameterization process described in the methods section. One map has 6 regions: Alpine, Continental, Mediterranean, Pannonian, Boreal (includes: Norwegian Alpine, and Arctic regions), and Atlantic. Another map includes 3 regions: Northern Europe (includes: Arctic, Norwegian Alpine, and Boreal regions), Central Europe (includes: Atlantic, Continental, Pannonian, and Steppic regions) and Southern Europe (includes: Mediterranean region). The third map has no bioregion designations and is only a mask of Europe. See the methods section for further explanation into why we created 3 different bioregion options.

2.4 MODIS NPP and MODIS NPP Trend

Net Primary Production (NPP) is derived using the MOD17 algorithm. This algorithm, using MODIS fraction of Photosynthetically Active Radiation (FPAR), Leaf Area Index (LAI), land cover, climate data and a biome-property lookup table, calculates global NPP data every 8 days (Running *et al.*, 2004). The MODIS NPP dataset we use in this study is an improved NPP dataset focusing on and producing values of NPP for European Forests (Neumann et al., 2016a). This NPP data is derived using the original MOD17 algorithm and a European regional climate dataset (Moreno and Hasenauer, 2015) covering daily weather data for minimum and maximum temperatures as well as daily precipitation data across Europe. This NPP data set is freely available at ftp://palantir.boku.ac.at/Public/EuroNPP

The NPP trend data result from a linear regression fit line for annual values by cell for the original 0.00833° resolution from 2000–2010. The trend is then given as the slope of the linear regression line. We then aggregate to the 0.133° resolution by finding the average trend within the larger cell area.

2.5 Tree Canopy Height

Tree canopy height data is produced by gap-filling Geoscience Laser Altimeter System (GLAS) data from the Ice, Cloud, and Land Elevation Satellite (ICESat) that covers the globe with 65m footprint vertical profiles on north-south transects (Simard et al. 2011). This data has large areas without empirical observations. Simard et al. (2011) gap-filled GLAS data using annual mean precipitation, precipitation seasonality, annual mean temperature, temperature seasonality, elevation, tree cover percentage, and protection status as co-variates. They define canopy height as the height of the tallest tree or the average height of the three tallest trees which may be seen as similar to dominate height definitions commonly used for forest inventories. In practicality the canopy height in this data set is the distance in elevation between the lowest ground and highest canopy points within a cell. The result is a global gridded data set at 0.0083° resolution. This data was both calibrated and validated using 98 plot points in Uganda, Africa and 120 flux tower sites scattered globally.

2.6 Site Quality

We define site quality as the product of 3 normalized gridded datasets: average growing season length, average annual short wave solar radiation (SWRad), and average annual vapor pressure deficit (VPD). Average growing season length is defined as the average time between the onset of increasing MODIS Leaf Area Index (LAI) in the spring and the end of decreasing autumn LAI beginning the winter steady state LAI (Myneni et al., 2002). LAI was chosen because it has clear seasonality for all tree species that can be encountered throughout Europe (Tian, 2004). The result is the relative growing season length in a cell compared to other locations in Europe.

SWRad and VPD are both calculated using the MtClim algorithm with newly downscaled gridded climate data and the GTOPO30 DEM (data available from the U.S. Geological Survey) as

inputs (Moreno & Hasenauer, 2015; Thornton & Running, 1999). This algorithm uses the DEM to derive east and west horizons, aspect and slope and uses these variables along with precipitation and day length to calculate the SWRad. VPD is a function of the difference between minimum and maximum temperatures which is also calculated in MtClim. These maps are then normalized by dividing all values by the maximum value in the dataset to get normalized values between 0 and 1. Site quality is then the product of these normalized maps. This data can be obtained at ftp://palantir.boku.ac.at/Public/ForestCharacteristics

2.7 Forested Area

Brus et al. (2011) developed a tree species composition map of Europe. This data is based on both the ICP level II plot data (www.icp-forests.org) and the European Forest Information Scenario Model database (EFIScen). They then used two types of methods to create gridded data. For those countries in which they had NFI data they performed ordinary kriging. In countries without NFI data the researchers gap-filled using a linear regression between species composition in known areas and various co-variates such as climate, topography and soil data. We obtained this map and masked them to create a map of forested versus non-forested areas. Using this forest/non-forest data on a 0.0083° resolution we can produce a percent forest cover map at our 0.133° resolution.

Forested area per cell is derived by multiplying the total surface area of a cell with the fraction of forest cover within that cell. The area of a cell varies by latitude and is calculated as:

$$Area = R^2 * (\sin(NLat) - \sin(SLat)) * (ELon - WLon) \qquad (1)$$

Where R = 6371 (the radius of the Earth in km), NLat and SLat are the northern and southern latitudes of the cell in degrees, respectively. Elon and WLon are the east and west longitudes in degrees of the cell, respectively. Different forest area data sets give different forest areas by country throughout Europe which can have a large impact on country level totals of forest characteristics (Table A1).

2.8 FAO FRA

The United Nations Food and Agriculture Organization (FAO) publish the Global Forest Resources Assessment (FRA) aggregating NFI data from most countries in the world and reporting variables such as live tree carbon and volume. We used the FRA 2010 report. Methods used for reporting to the FAO are outlined in the Good Practice Guidance for Land Use, Land-Use Change and Forestry (GPG-LULUCF) and the 2006 IPCC Guidelines for National Greenhouse Gas Inventories reports (IPCC, 2003; IPCC et al., 2006). These guidelines give several options as to the methodologies, in both calculation and sample design, which may be used to derive values that are then reported to the FAO for use in the FRA. For example, some countries use biomass expansion factors while others use biomass equations. Some reports are produced using a complete NFI data set measured by the country itself while other reports are produced using historical data or modeled data. In some instances FAO derives the data that they report themselves based off of historic data and that of similar countries without the use of direct current forest inventory data(FAO, 2010a).

2.9 EFIScen

The European Forest Information Scenario (EFIScen) Model database is a publically available collection of aggregated NFI data from 32 European countries (Schelhaas, et al. 2006). The data are derived from NFI data grouped into jurisdictions or site types. This database was created to work within the framework of a matrix model that predicts the probability of changes in forest characteristics (e.g., volume) over time given a specific jurisdiction. The data are categorized into age class, cover types, regions, and/or ownership by each individual country. These groupings where given to the researchers by individual countries preventing access to the original tree or plot level data. Each combination of species and other distinguishing characteristics, such as owner, forest type or site quality, has their own distribution of area per age class. The age classes as well as the other distinguishing characteristics are different for each country. For example, France provides the area covered by 20 different age classes categorized by State/Other public/Private grouped by 9 different tree species. Hungary, however, has 12 age classes categorized by Good/Medium/Poor site qualities for 6 tree species.

In these two examples France groups forests by ownership while Hungary groups by site quality.

EFIScen data has been mapped but is not spatially explicit beyond these grouping boundaries nor are the spatially explicit data sets publically available (Vilén et al., 2012). We converted age classes into the classes that fit our harmonized gridded terrestrial data. The age classes to which we converted EFIScen data are 0-20, 21-40, 41-60, 61-80, 81-100, 101-120, and >120.

3. Methods

Several methodological challenges existed in combining previously produced data to create a pan-European, wall-to-wall data set on forest resources. The previously existing data sets were developed for different purposes and the type of data (point versus gridded information) as well as the data collection method (terrestrial versus remotely sensed data) differs (Table 1). For example, the NFI data provide values for forest characteristics; however, publically available data are not spatially explicit below the country level and are not consistently available all over Europe. Further, countries who maintain NFI data have differing grid design and data collection system methods (Angle count sampling, Fixed area plot, surveying) (Table 2). Conversely, Simrad et al. (2011) tree canopy height data gives a spatially explicit data set on forest height but is not focused on Europe which decreases the reliability in European forests. Further, their method derives height estimates by calculating the difference between the lowest ground point and highest point in the canopy within a 0.00833° cell which can decrease accuracy on slopes. Other data such as the MODIS data provide consistent information for the NPP of European forests but are challenging to compare with NFI derived values (Moreno et al., 2016; Neumann et al., 2016a).

This disparate group of data derived for various purposes needs an algorithm to integrate them to derive consistent forest characteristics for live tree carbon, volume, mean tree height, and mean tree age across Europe akin to those values that come from NFI data, even for areas where NFI data are unavailable. For this study, we developed a gap-filling algorithm based on a two-step process: cluster analyses and kNN nearest neighbor (Figure 2).

Clustering is the process in which cells are grouped together based on similarity defined by the user. Clustering is often done using a k-means machine learning principle in which n number of centroids of each cluster is determined by minimizing the within cluster sum of squares from points in an n-dimensional space, based on co-variates, to the centroids (J.A. Hartigan and Wong, 1979). Cells are then clustered by the nearest centroid.

The k nearest neighbors algorithm (kNN) is a nearest neighbor machine learning algorithm method that finds the n closest points amongst a data set for every point within said data set within an n-dimensional space, based on co-variates (Manning and Schutze, 1999).

Our approach using clustering and nearest neighbors assumes that forest cells that share similar values, in our co-variates space, will have similar forest structure. The similarity of the forest cells is assessed by the following set of co variates: NPP, NPP trend, canopy height, and site quality. In our algorithm we use forest cells where we have gridded terrestrial data to gap fill similar forest cells where we do not have gridded terrestrial data (Figure 2).

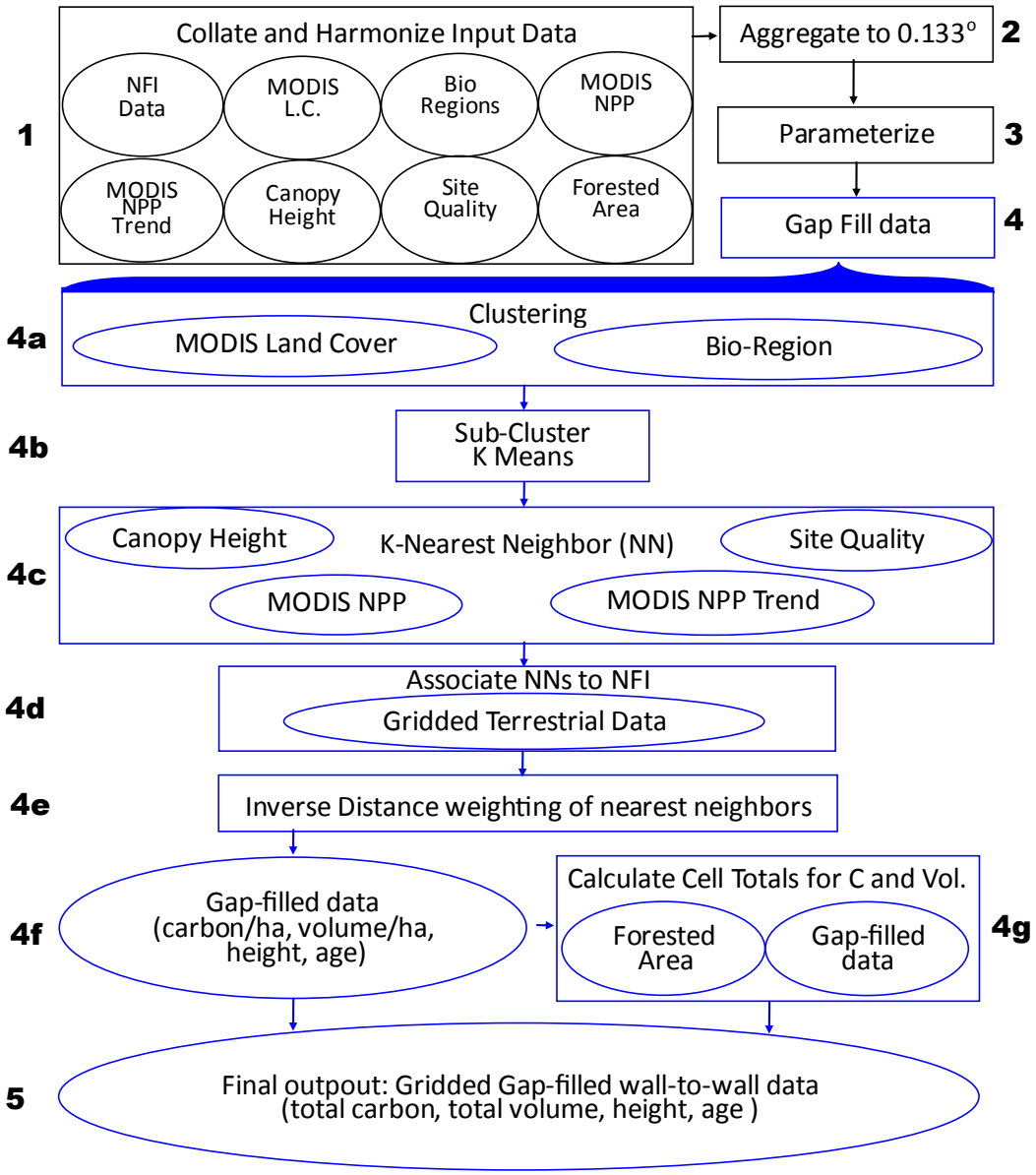

Figure 2: Methodology Flow-Chart. There are 6 steps in our methodology: 1) Collate and Harmonize Input Data, 2) Data aggregation, 3) Parameterization, 4) Gap-filling, 5) Final outputs. The gap filling algorithm is shown in more detail with steps 4a to 4g. Ovals represent data sets and rectangles represent processes. Ovals inside rectangles indicate that this data set was used within this process.

3.1 Collate and Harmonize Input Data and Data aggregation (Figure 2: step 1 and 2)

Our input gridded and remotely sensed data products were clipped and snapped to the extent and grid of the 0.0083° resolution European MODIS data, which was the limiting factor in

spatial extent (Figure 2: step 1). The NFI data was also processed to produce a corresponding gridded terrestrial data set with plots being averaged under mutual grid cells (Figure 2: step 1, Figure 1).

All datasets were then aggregated to a 0.133° resolution (approximately 75 – 175km^2) (Figure 2: step 2, table 2). Aggregation is necessary because a minimum number of NFI plots within a gridded terrestrial cell are needed to have sufficient statistical confidence in the derived cell value (Moreno et al., 2016). The required amount of NFI points per cell were dictated by the need of a confidence interval within 25% of the mean value on the European scale. At 0.0083° resolution (in Europe cell area range: 0.27 – 0.71 km^2) there is typically only 1 plot within a cell in Europe which gives an undefined confidence interval. At 0.133° resolution (in Europe cell area range: 75 – 175km^2) the confidence interval decreases to approximately 10% on average for the forest characteristics on which we focus (carbon, volume, height, age), with an average number of NFI plots per grid cell of 27 throughout Europe (Figure 1) (Moreno et al., 2016).

For non-categorical results derived from NFI data (carbon, volume, height) the aggregated cell value is an arithmetic mean of the plots within the cell. Carbon is the total live tree carbon including stem, branches, foliage and roots. We aimed to harmonize every variable as much as possible, however for volume, because of varying measurement techniques and volume definitions countries provided either stem volume over bark, total wood volume or total merchantable timber.

Height refers to the mean height of all trees within a cell. Categorical data such as mean age was assigned using the most frequent plot age class within a cell. Fraction of age class is given as the number of each age class divided by the number of plots within a cell. Harmonized volume and carbon estimations as well as age classes were obtained from Neumann et al., (2016).

3.2 Parameterization (Figure 2: step 3)

Parameterization was performed using an iterative algorithm that allowed assessment of hundreds of combinations of parameters to find the best combination for each forest characteristic in question defined by various statistical measures: Mean Bias Error (MBE), Mean

Absolute Error (MAE), Root Mean Squared Error (RMSE), Shift, Kurtosis, and Variance (Willmott and Matsuura, 2006). This was done by using a "leave one out" cross validation approach to test the gap-filling algorithm estimate versus the gridded terrestrial data (which is based off of NFI data) for each combination of parameter values (Kohavi, 1995). We evaluated the cell level error, indicated by the MBE, MAE and RMSE. We also evaluated the overall distribution error, given by its 3 moments: variance, skew and kurtosis. Analyzing both the overall distribution and cell level error informs us on the bias – variance trade off inherent to a kNN algorithm. We can either match the overall distribution or we can minimize the cell level error, but not both as they are mutually exclusive (Hero et al., 1996). The result of the parameterization is different for each forest characteristic (i.e., carbon, volume, height, age) based on which scale accuracy is maximized (i.e., whether we preferred larger scale distribution accuracy or finer scale cell level accuracy).

Our gap-filling algorithm has 5 parameters that must be optimized to achieve the desired output: number of bioregions, covertypes, k-means clusters, nearest neighbors and the strength of the inverse distance weighting. The number of bioregions refers to the number of regions we used for clustering cells. Our parameterization process determined whether 6, 3 or no bioregions produced the most accurate results. Covertypes could consist of 11 cover types or no covertypes, again the parameterization process determined the values that produced the most accurate results. We also determined how many k-means clusters to use within each bioregion/covertype group via parameterization, i.e. e.g., we may have a group of cells within the boreal bioregion that are evergreen needle leaf forests, and then via k-means we can further cluster this group of cells by as many clusters as the parameterization process determines produces the most accurate results. We also determined the number of nearest neighbors we used which defines the number of gridded terrestrial cells that will be used to calculate the gap-filling estimation. Finally, the strength of the inverse distance weighting determines how the "distance" in co-variate space affects the weighting of each nearest neighbor on the gap-filling estimate.

3.3 Gap-filling (Figure 2: step 4)

We create a pan-European gridded data set of total tree carbon, total volume, mean tree age and mean tree height on a 0.133° resolution by gap filling areas for which we have no gridded terrestrial data. The method for our gap-filling algorithm first clustered similar forests and then performed a nearest neighbor algorithm (kNN) on cells without gridded terrestrial data with cells that have gridded terrestrial data. The cells are first clustered by cover type, bioregion and k-means clustering (Figure 2: step 4a and 4b).

K-means clustering groups sub-clusters of cells so that the within-cluster sum of squares is minimized (John A Hartigan and Wong, 1979). This clustering is done to group forests with the same biophysical and site properties. The kNN was then performed on each cluster (Figure 2: step 4c). The kNN is based on a 4 dimensional "site characteristic" or covariate space with NPP, NPP trend, canopy height and site quality as the co-variates (Table 2). kNN finds the nearest cells within our co-variate space to our target cell. For every 0.133° cell without gridded terrestrial data within a cluster we performed a kNN algorithm.

The number of nearest neighbors used varies depending on the forest characteristic in question (carbon, volume, height, age). There is no "distance" limitation for the nearest neighbors in our co-variate space. The nearest neighbors are the closest cells that have gridded terrestrial data based on the Euclidian distance (Figure 2: step 4d). The values for the variable in question are then combined using an inverse distance weighting formula (Figure 2: step 4e). The strength of the weighting varies by variable. A value of 0 is no weighting, 1 means weighting by the distance, 2 means weighting by the distance squared, and so on. The strength of the weighting has no limit and is determined through our parameterization procedure.

We produce gridded gap filled data sets that have the same units as the original gridded terrestrial data, i.e., tons carbon/ha, m^3/ha, meters , and age-class (Figure 2: step 4f). Carbon and volume values in the gridded terrestrial are given as tons C/ha and m^3/ha. After a pan-European gridded data set was produced, carbon/ha and volume/ha were multiplied by the number of hectares of forest within in 0.133° cell using our forest/non-forest data set (Figure 2: step 4g). This results in total carbon per cell, and total volume per cell which reflects the total forest area per cell as the forested area is different for every cell. Height and age are unaffected

by the forest area as the size of a forest has no bearing on empirical measurements of these two forest characteristics.

4. Analysis and Results

4.1 Algorithm and Gridded Data

4.1.1 Algorithm Development and Parameterization

The resolution on which our output data were created (0.133° or approximately 16x16km) was chosen to maximize the confidence we have in the input gridded terrestrial data's ability to accurately portray the real world and agreement between the remotely sensed co-variates and the training gridded terrestrial data, while minimizing the spatial information lost through aggregation (Moreno et al., 2016). At a 0.0083° resolution ($1km^2$) there is, on average 1 plot per cell, with an average plot size of $200m^2$ representing 0.02% of a cell's area. One sample (NFI plot) that represents 0.02% of a population (a remotely sensed cell) with 0 degrees of freedom is not statistically meaningful. Therefore any data produced based on this relationship will be spurious. To avoid this problem we increased the number of samples within a cell through aggregation leading to 27 NFI plots per gridded terrestrial data cell on average (Figure 1).

The resolution is not limited by the remote sensing data but by the NFI data as NFI data was provided to us with falsified locations within 1km, and the need to have sufficient plots within a cell to reach our desired confidence levels. Our output data on a 0.133° resolution is designed to understand landscape level information and the spatial variability of forest characteristics. They are not designed to represent local level heterogeneity.

After already clustering by bioregion and covertype we then use the co-variates for k-means clustering and k-NN. The co-variates were chosen to represent different aspects of a given forest area. Input co-variates must delineate forest structure logically and correlate as little as possible otherwise inaccurate and biased outputs may result.

Site quality determines the temporal productivity curve and maximum possible rates of production and growing stock of a forest. We therefore use site quality to match forests with similar productivity curves. The NPP data is then a point on the productivity curve. The NPP

data in conjunction with the height data gives us an indication as to how much living biomass we can expect in this forest relative to other forests and where along the productivity curve a forest may lie in relation to other similar forests in its group. An absolute NPP value is not sufficient to determine placement on the productivity curve because NPP has a maxima followed by a decrease and eventual plateau. This results in multiple forest development stages having the same absolute NPP value. Height in this instance acts as a proxy for forest development.

NPP trend gives us 2 relevant pieces of information. First, it tells us if the forest is reaching a plateau or if it is increasing or decreasing in productivity rate and it also giving us an indication of management. Forests with similar ages and NPPs can have different forest structures based on previous management practices. In the absence of management one stand may be reaching a plateau or steady state NPP whereas another stand that has been managed and has a similar absolute NPP value may continue to have increasing productivity. Therefore the NPP trend map is an attempt to delineate forest structures that occur under the forest canopy and thus not captured by remote sensing data directly. Elevation alone was not used as a co-variate because it is yet another variable to predict site quality and we did not want to over represent this aspect of forest properties in our co-variate ensemble.

The algorithm requires parameterization for each forest characteristic. Each forest characteristic was parameterized individually as each characteristic behaves different spatially. The parameters used within our algorithm for each forest characteristic (carbon, volume, height, age) are a result of an automated parameterization algorithm to maximize accuracy at the scale we specified: cell, country or continental scale (Table 3).

Table 3: **Parameters of the gap-filling algorithm: N of Bioregions = number of bio-regions used, N of Cover types = number of cover types used, N of clusters = number of k-means clusters used, N of NN = Number nearest neighbors, I.D.W. = strength of inverse distance weighting (0 indicates normal averaging).**

Variable	N of Bioregions	N of Covertypes	N of clusters	N of NN's	I.D.W.
Volume	6	1	4	1	NA
Carbon	6	9	3	1	NA
Height	6	9	0	4	0
Age	6	9	0	4	0

Volume and carbon were parameterized to maximize accuracy at the regional to continental scale because we were interested in country-level and European statistics. Height and age, which can help estimate site quality and in biomass calculations, were maximized for more country to local scale accuracy.

Volume and carbon both used only 1 nearest neighbor (Table 3). These variables where clustered by bio regions and carbon was further clustered by cover type. Both variables were also further clustered by k-means indicating that there were groupings that were not covered by bioregion or cover type. Height and age parameters included 4 nearest neighbors. For clustering, both variables used 6 bio-regions and 9 covertypes with no k-means clusters indicating that bio-region and cover type sufficiently delineate groups according for forest age and height. No inverse distance weighting was used but instead values are simply averaged (Table 3).

4.1.2 Gridded Data

Next we were interested in understanding the spatial distribution of forest resources across Europe by producing gridded datasets of total live tree carbon, total volume, mean tree height and mean tree age. The gridded data, which show the state of forest resources across Europe, were derived using our parameterized algorithm (Figure 2,Table 3), with 4 co-variates - NPP, NPP trend, canopy height, site quality - along with input data from the available data sources (Table 1). The resulting output data are on a 0.133° resolution and represent the time period

2000-2010. The data sets give the landscape level spatial pattern of forest resources throughout Europe giving comparable cross-border values allowing not only country level assessments (Table A2) but also by latitude, elevation or any other spatial divisions. Using our available data we can analyze the spatial differences in forest resources across countries throughout Europe.

Carbon and volume values are provided as totals as opposed to per unit area values. This was done to allow comparison of country totals with other data sets and for determine high and low values of absolute carbon and volume values across Europe.

We created a mean tree height data set as opposed to the traditional dominant tree or tallest tree height because at a 0.133° resolution there will always be at least 3 tall trees. Consequently dominant tree height, which is meaningful at the plot level, gives little insight into the forest on such a large resolution. The mean tree height, however, informs us as to how tall the forest is on average within this cell and about the average site quality, forest management, and stand structure.

The mean tree age data gives a landscape level age profile of a forest. It provides information as to how old a forest is on the landscape level which is different than how age is traditionally thought of on the plot level. This allows us to understand forest age structure over large areas without focusing on plot level variance. This information can be useful for regional level planning and understanding how larger scale policies and management have affected the forest age structure across counties, states and countries.

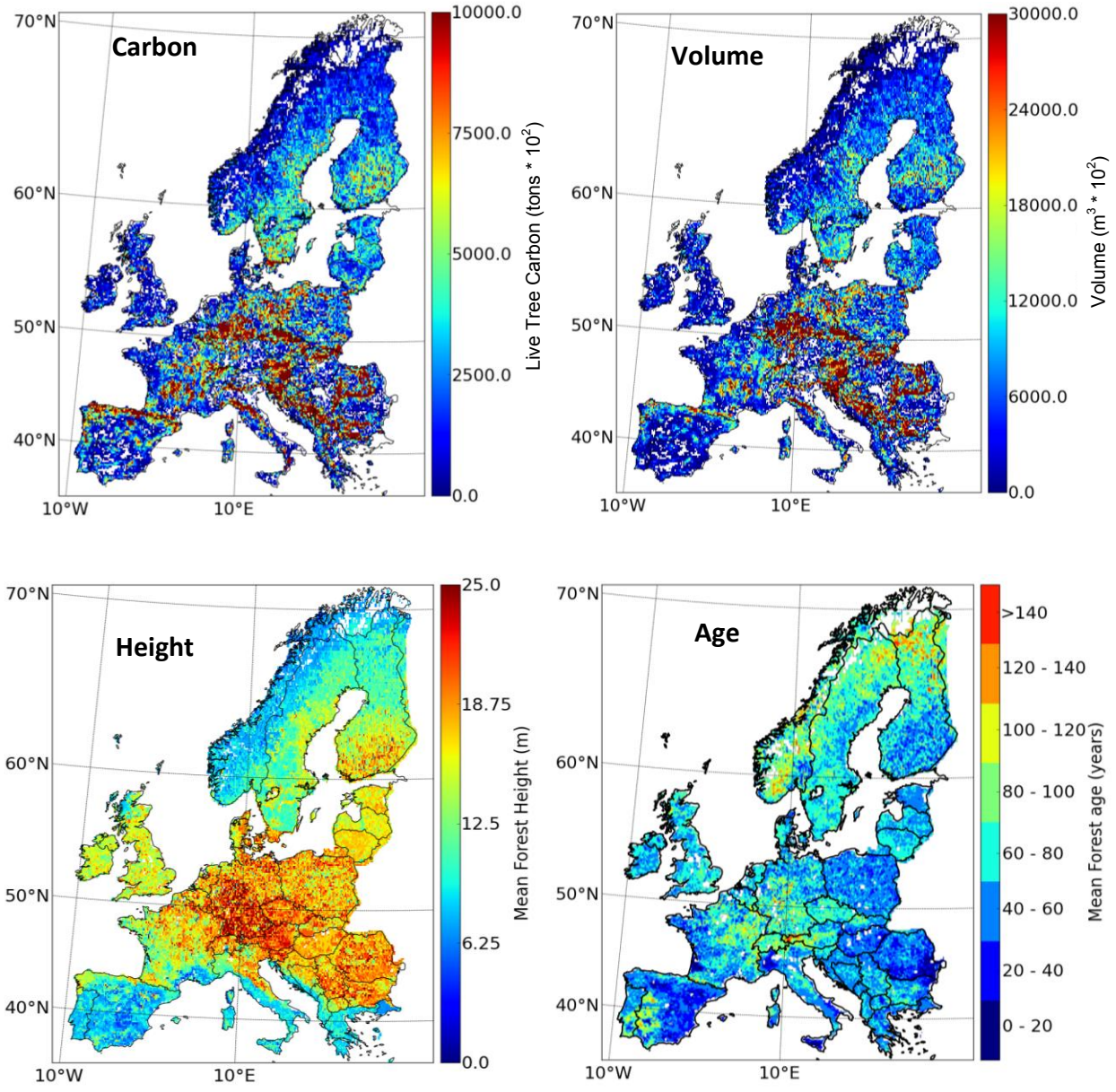

Figure 3: Total Live Tree Carbon (tons*10^2), Total Volume (m^3*10^2), Height (m), Mean tree age (age classes in years). 0.133° resolution. The total live tree carbon and total volume result from multiplying the c/ha and the m^3/ha by the total number of hectares of forest within each cell respectively. Height and mean tree age are unaffected by forest area.

4.3 Cross-validation

One crucial piece of information needed for any gridded forest data set (Figure 3) is the reliability and/or spatial accuracy and error of the information. Thus we next performed a "leave one out" cross validation for carbon, volume, height, age.

We first compared estimated grid cell values versus the corresponding gridded terrestrial cell data derived from the NFI values regardless to which country the cells belong. The accumulated results then give a European-wide validation estimate for the "leave one out" cross-validation.

This type of cross validation gives a more accurate and unbiased assessment of accuracy given large and non-random data as compared to sectional cross-validation, i.e. cross-validation by country or region (Kohavi, 1995). The statistics for validation are defined by Willmott and Matsuura (2006).

To place our error in the context of random error associated with our input gridded terrestrial data we evaluated the confidence interval of the NFI data within each gridded terrestrial data cell. Confidence interval is defined as:

$$CI = 1.96 * \frac{\sigma}{\sqrt{N}}$$

Where σ is the standard deviation of a cell and N is the number of plots within a cell. Given an α of 0.05 or we use a critical value of 1.96 as our constant. We can use the confidence interval at the European scale because each country samples at different distances, some including clusters or actual random samples, fulfilling the assumption of randomness.

The cross validation demonstrates the tradeoff decisions made in the parameterization process by showing the error at differing scales (Table 4). We provide the mean values for the original gridded terrestrial data and the cross-validated data as well as the corresponding standard deviations. We measure the bias via a mean bias error (MBE) and the accuracy with the mean absolute error (MAE) and the root mean squared error (RMSE). The difference between the MBE and the RMSE also provided information on the variation in the error. An equal MAE and RMSE mean that every cell has the same error. We also calculated the mean confidence interval

of the underlying NFI data. This puts our results and error in context with our confidence in the ability of the original NFI data to depict real world values.

Table 4: Results of leave one out cross-validation. GTD is the result of all gridded terrestrial data based on NFI data. CV is the cross-validation results. Standard deviation (SD), Mean bias error (MBE), Mean Absolute Error (MAE), Root Mean Squared Error (RMSE). CI is the average confidence interval of the NFI data that makes each gridded terrestrial data cell. N is the number of 0.133° cells evaluated.

Variable (units)	Mean GTD	Mean CV	SD GTD	SD CV	MBE	MAE	RMSE	CI-NFI	N
Carbon (tons/ha)	78	77.8	47	47.6	0.24	30.2	43.5	7.08	16430
Volume (m^3/ha)	221.2	221.1	188.2	191.1	0.03	110.5	188.1	22.7	16430
Height (m)	14.6	14.6	5.6	4.8	0.02	2.7	3.7	3.28	14601
Mean Age Class (class)	3.6	3.7	1.4	0.93	-0.1	1	1.4	NA	13854

We also analyzed the "leave-one-out" error spatially to further quantify the error behavior in our algorithm. We parsed the data spatially by country, latitude, and elevation. This allows us to understand how well we can capture forest structure spatially and the effects of moving up scales from individual cells to countries and to the continental scale. Some countries did not provide age or height which is reflected in the number of cell used in our analysis. Figures 4 to 7 provide the mean differences between estimated versus gridded data for carbon, volume, height and age by latitude (A), country (B) and elevation(C).

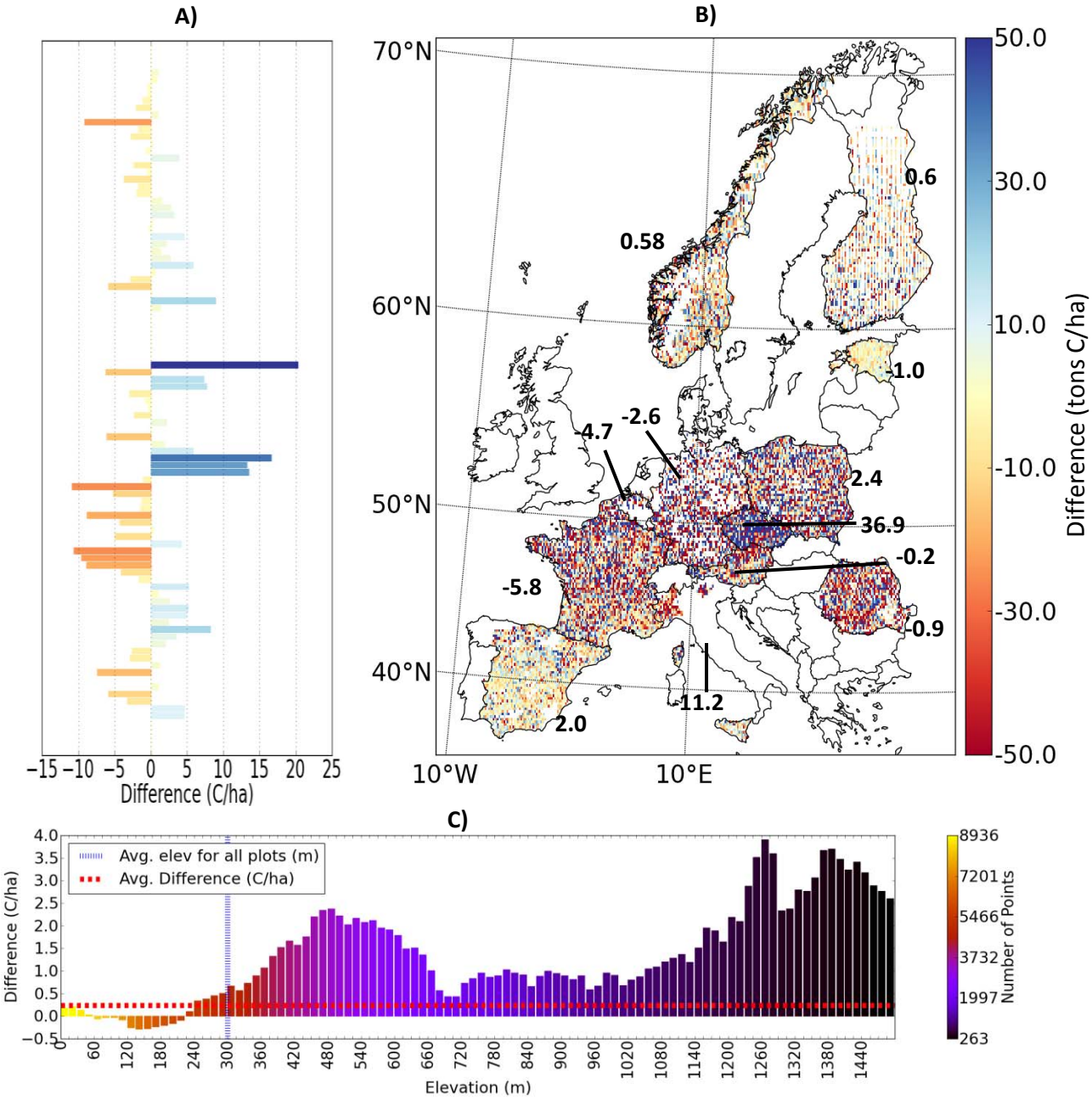

Figure 4: Tons C/ha Difference (gridded terrestrial data - Estimated): Values annotated on map are country averages. A) By Latitude; B) Spatial Distribution, annotated numbers indicate country average differences; C) By Elevation (colors indicate number of cells in partition).

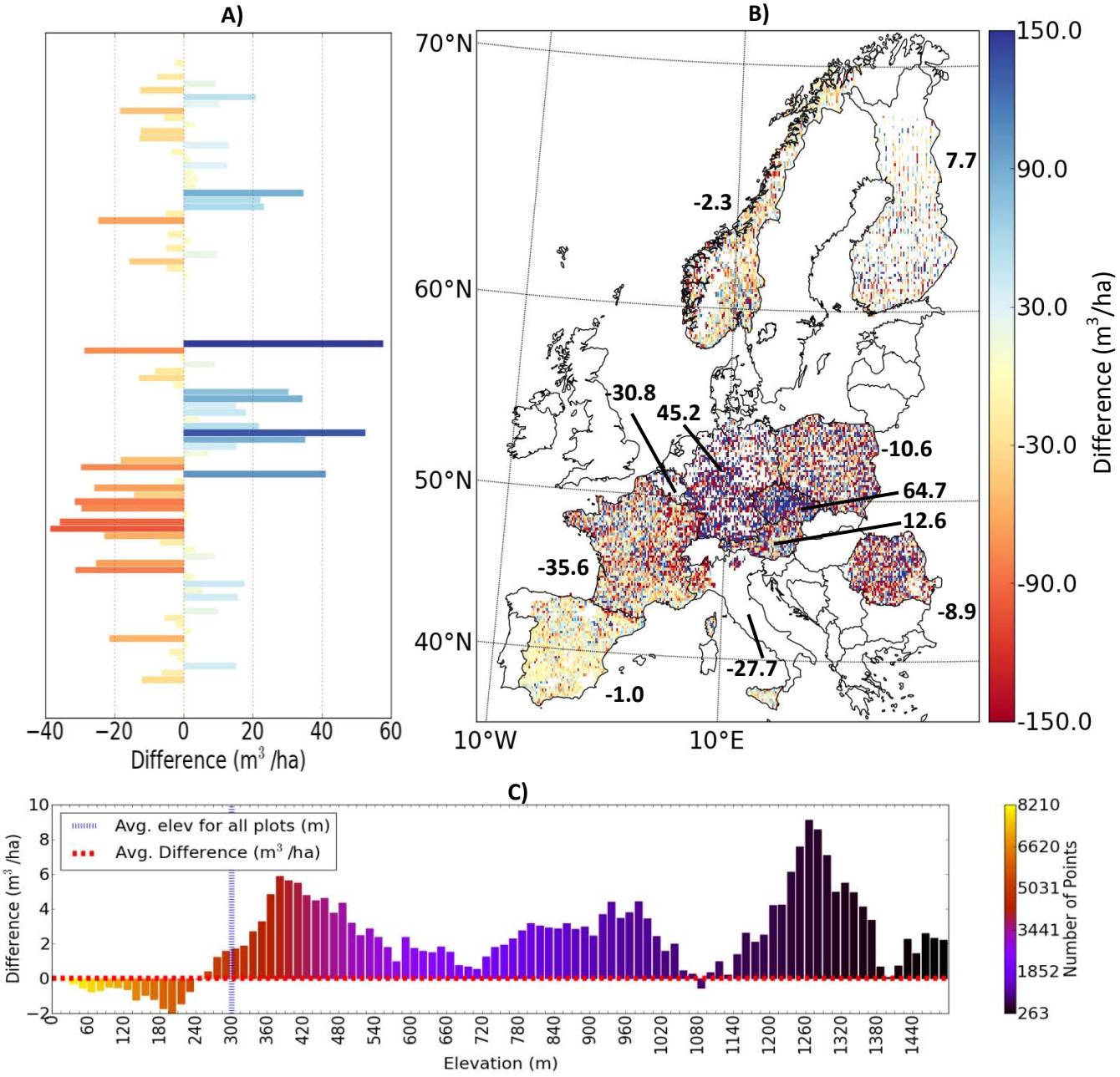

Figure 5: Volume/ha Difference (gridded terrestrial data - Estimated): Values annotated on map are country averages. A) By Latitude; B) Spatial Distribution, annotated numbers indicate country average differences; C) By Elevation (colors indicate number of cells in partition).

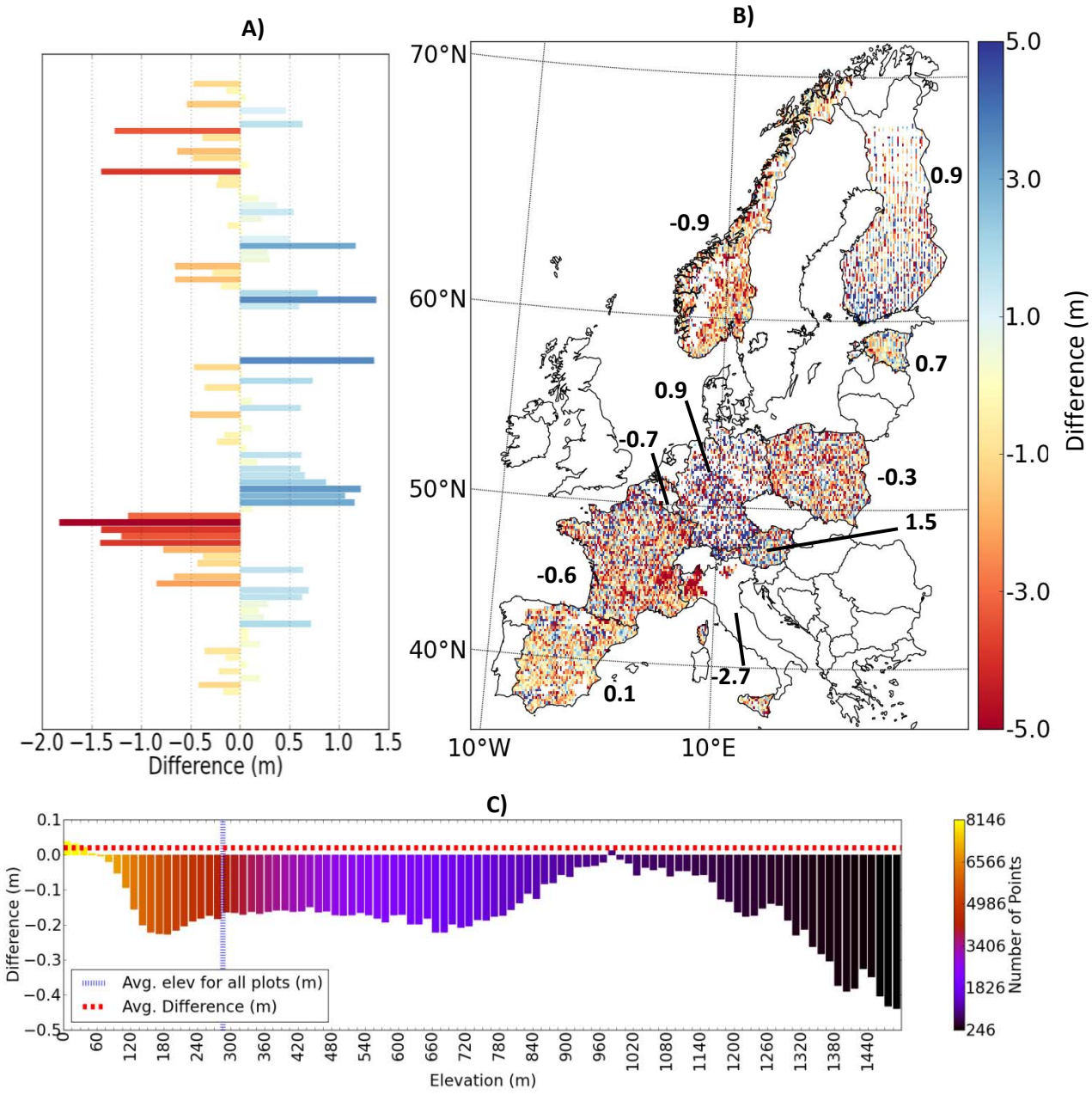

Figure 6: Mean tree height Difference (gridded terrestrial data - Estimated): Values annotated on map are country averages. A) By Latitude; B) Spatial Distribution, annotated numbers indicate country average differences; C) By Elevation (colors indicate number of cells in partition).

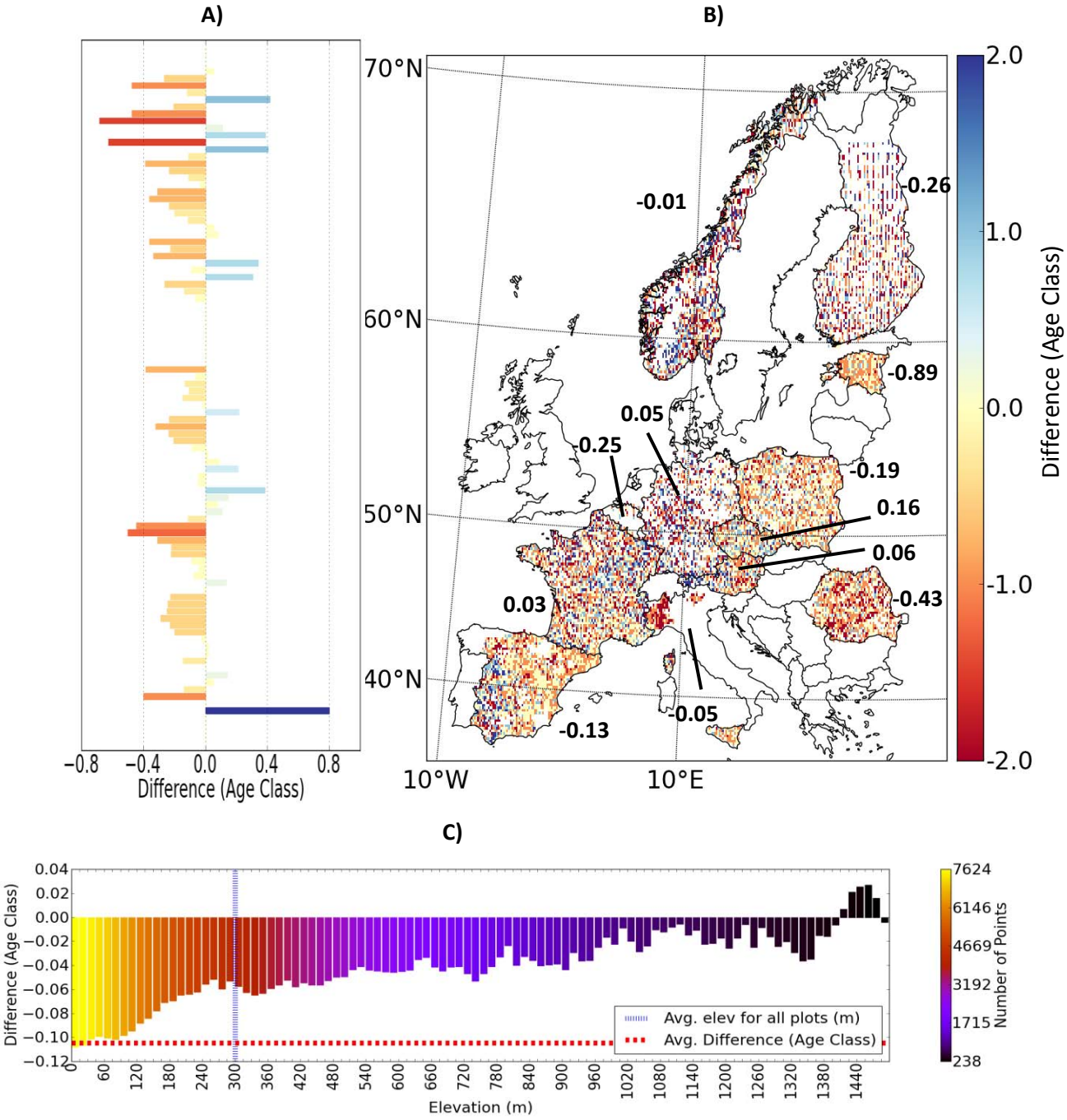

Figure 7: Mean tree age Class Difference (gridded terrestrial data - Estimated): Values annotated on map are country averages. A) By Latitude; B) Spatial Distribution, annotated numbers indicate country average differences; C) By Elevation (colors indicate number of cells in partition).

Next we tested the robustness of the input data, by performing a "country-wise" cross-validation where we estimated every cell with gridded terrestrial data using nearest neighbors that are not within the target cell's country. In other words, each grid cell is estimated using only other countries' data making each country an independent validation data set. This is again done for every gridded terrestrial data cell. This analysis shows how affected the results become once a section of data is removed (Table 5). If the input data is robust then there would be little difference between the leave one out cross validation and the country wise cross validation (Table 4 and 5). Large differences do occur between these two types of cross validations indicating that removing an entire country from our input data would greatly affect our ability to perform this analysis and that there is large variation between countries NFI values for the same forest characteristic (Table 4 and 5).

Table 5: Results of country wise cross-validation. GTDindicates the result of all gridded terrestrial data based on NFI data. CV indicates cross-validation results. Standard deviation (SD), Mean bias error (MBE), Mean Absolute Error (MAE), Root Mean Squared Error (RMSE). CI is the average confidence interval of the NFI data that makes up each cell. N is the number of 0.133° cells evaluated.

Variable (units)	Mean GTD	Mean CV	SD GTD	SD CV	MBE	MAE	RMSE	CI-NFI	N
Volume (m^3/ha)	203.1	185.2	179.3	186.1	-17.9	130.3	203.4	22.7	14799
Carbon (tons of carbon/ha)	77.1	66.2	48.6	58.6	-11.0	42.8	56.6	7.08	15518
Height (m)	14.3	10.0	5.7	8.1	-4.5	6.6	8.3	3.28	13689
Mean Age Class (class)	3.5	2.6	1.4	1.7	-1.4	1.7	2.3	N.A.	13080

4.4 Comparison with other datasets

To put our results into context we compared our data versus similar data sets that exist throughout Europe.

4.4.1 Carbon and Volume

Carbon sequestration of European forests helps to mitigate climate change effects and accurate forest carbon estimates give researchers and politicians the ability to assess the role of European forest within the global carbon cycle. Volume is an important forest characteristic for the economic sector. Volume, along with increment and age, is an important measure for maintaining sustainable harvests. No current spatially explicit gridded data set of forest carbon and volume specifically for Europe is publicly and

freely available for comparison with our work. For this reason, we obtained the FAO FRA data which is widely used to assess the carbon and volume storage by country across Europe and globally to compare with our data (Figure 8). FAO FRA data is given as country totals so to make data comparable we analyzed their data with country totals of our data.

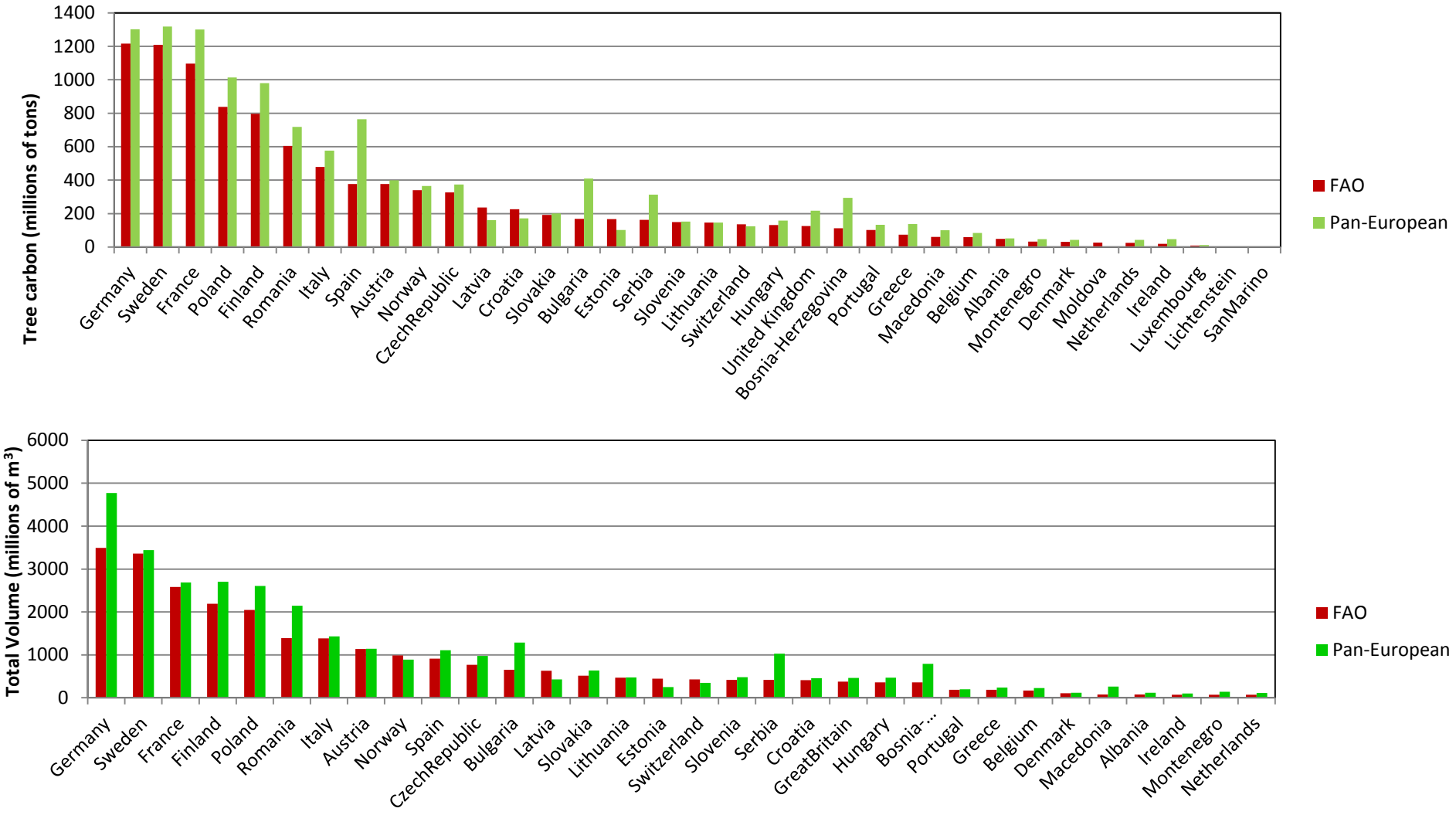

Figure 8: Total carbon and volume by country for the United Nation's Food and Agriculture Organization (FAO) and this study (Pan-European)

4.4.2. Height

Height is needed for calculating volume and biomass, is considered as a biodiversity indicator and in conjunction with age, is a measure of site quality (Chirici et al., 2012; McDill and Amateis, 1992). The latest wall-to-wall dataset similar to forest height for Europe is the tree canopy height data set developed by Simard et al. (2011) which is a global data set calculated from space based LiDAR data.

We compare European distributions of Simard (2011) tree canopy height predictions versus our mean tree height cross-validation and the original gridded terrestrial data (Figure 9). The original gridded terrestrial data acts as an empirical independent estimation. This allows us to assess our algorithm's estimated results versus the Simard method and the ground truth data. This comparison aims to show how different definitions of height make a difference and to put the error of our algorithm into context on the continental scale.

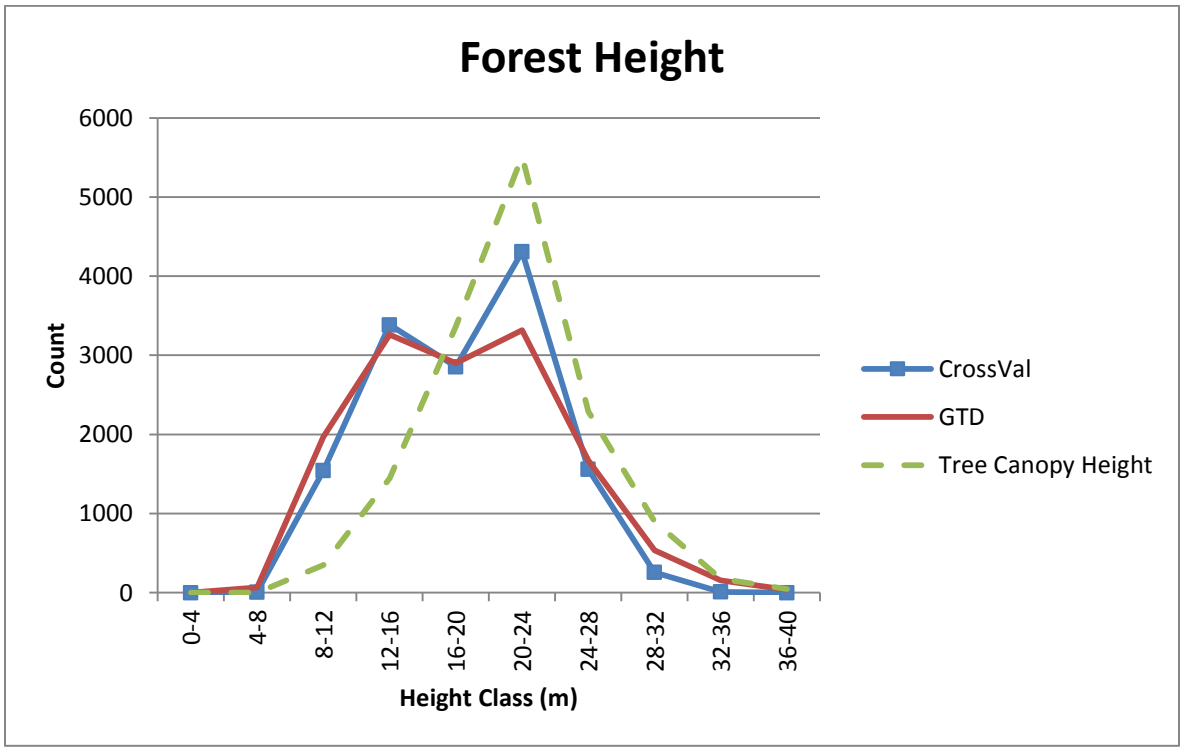

Figure 9: Distribution of cell forest height for our pan-European cross validated data in this study (CrossVal), the gridded terrestrial data (GTD) and the Tree Canopy Height data from Simard (2011) aggregated to 0.13°.

4.4.3. Age

Age is one of the most important and most difficult forest characteristics to measure and quantify. Forest age is used in productivity, mortality, biodiversity and biomass estimation methods. EFIScen is another European project that has attempted to quantify forest age throughout Europe. Original EFIScen data however, is not spatially explicit or harmonized across countries. We aggregated EFIScen data to create country-wide harmonized age class distributions that are comparable across countries (Data section). We compare this aggregated and harmonized EFIScen data to our age data for five countries (Figure 10). Three of these countries are completely gap-filled; one each from Northern, Central and Southern Europe: Sweden, Lithuania, and Croatia, respectively. The Austrian estimate is derived completely from gridded terrestrial data (based off of the original NFI data). The remaining country, Switzerland, is also completely gap-filled. To further investigate the comparison of age we also included the Swiss NFI data from their online data portal (Swiss Federal Institute for Forest Snow and Landscape Research, 2015). These particular countries are highlighted because they all show different aspects of the difficulty in quantifying forest age using different datasets (Figure 10).

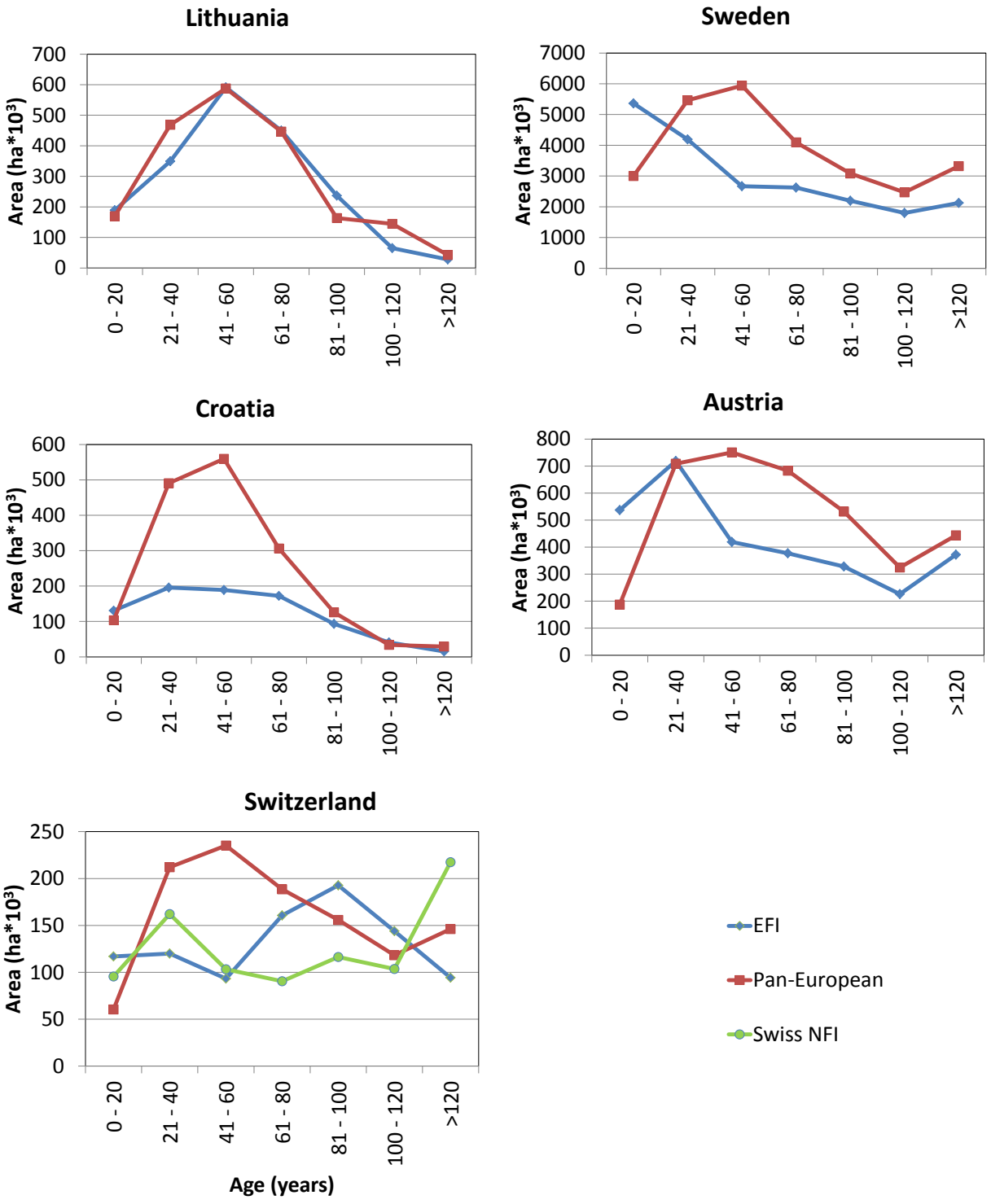

Figure 10: Area (ha) of age class by country for EFIScen and this study's data (Pan-European). Pan-European data for Lithuania, Sweden, Croatia, and Switzerland were completely derived through gap-filling. Pan-European Austrian data was completely given by the official NFI data. Swiss NFI data is from their publicly available data portal and includes uneven-aged forests which is not included in this graph and equals 308,200 ha.

5. Discussion

Using our newly created gridded pan-European data sets - total live tree carbon, volume, mean tree height and mean tree age - we assess the state of forest resources across Europe. The accumulated amount of carbon, and volume stored within European forest are $12238.0*10^6$tons and $32541.5*10^6$ m^3 respectively (Table A2 and Figure 3). The average height and age are 14.22m and age class 3.71 respectively (Table A2 and Figure 3). Our numbers are based on a combination of 8 different data sets including bottom up terrestrial information from national forest inventories and forest area as well top down remote sensing information across Europe (Table 1). The algorithm we developed combines our available data sources allowing us to estimate the state of forest resources in areas with no or missing terrestrial information (Figure 2). This procedure provides continuous harmonized data that depicts forest resources beyond national level statistics (Table A2). For our study we had access to 12 national forest inventory data sets including over 196,000 plot level information data points (currently the largest plot level forest inventory data set in Europe) however the algorithm allows for the easy integration of additional countries that would increase the accuracy of final output data (Figure 2) .

Areas with the highest amount of carbon and volume tend to be located in mountainous areas (Figure 3). Countries with high volume per hectare are Germany, Austria and the Czech Republic which are major timber producers. Large plantations in low elevations also have high totals of carbon and volume such as the *Forêt des Landes* in south-western France, plantations throughout Portugal and the managed forests of Germany (Figure 3). The lowest carbon and volume are found in areas that are dominated by agriculture, such as Spain and France or dominated by rangelands such as in Norway. In Scandinavia there are higher carbon to volume ratios caused by high wood densities and root to shoot ratios found in this region (Neumann, et al., 2016).

Central Europe has the largest proportion of tall tree values due to the high site quality in this region (Figure 3). Norway has a particularly high proportion of short trees as compared to the rest of Europe, corresponding to the fact that Norway has predominately open shrub land savanna landscapes. A distinct difference in tree height exists between central Europe and southern Europe as one crosses the Alps and enters the Mediterranean bioregion. The gridded data of forest height does not follow the pattern of any other forest characteristic (Figure 3). With low stand densities, a forest may be very tall but have low carbon and volume. Researchers use forest height as a proxy for age when necessary; however height is highly dependent on site quality and forest management (Wang and Klinka, 1995). In high elevation alpine forests, old trees do not have the ability to grow tall whereas in plantations young trees may be very tall.

The area in central Europe with the oldest mean tree age is in the state of Vorarlberg in Austria. This area is very steep and wet with many scattered human settlements hindering the harvesting of forests while providing a hospitable environment for tree growth. Other areas with continuous cover of older mean tree ages are northern Finland and Norway. These areas consist of sparse, slow growing forests that do not encourage forest harvesting which has led to older forests. Agricultural areas do not drive down the age of forest because these trees are typically not under rotation (Figure 3).

The "leave-one-out" biases for volume and carbon are less than 0.01% of the mean values (Table 4). These two variables - volume and carbon - show a similar standard deviation in the cross validation and the original gridded terrestrial data as of our parameterization choice in maximizing country to continental scale accuracy. The MAE and the RMSE are within a standard deviation demonstrating that the error is within the variability of the dataset.

Our algorithm is more accurate at lower elevations (Figures 4-7). This is caused by a higher number of points at lower elevations which lead to more accurate gap filling estimations. Spatially, for carbon, most countries show scattered areas that are both over and under estimated, with the exception of the Czech Republic (Figure 5). We underestimate the Czech Republic by an average of 36.9 tons C/ha. This is because the Czech Republic's gridded terrestrial data shows an exceptionally high carbon/ha and volume/ha which then leads to an underestimation when using other country values for estimates in the kNN. Variation in the error is higher when parsed by latitude than elevation because latitude creates more diverse strata than does elevation. The "country-wise" biases for volume and carbon show an underestimation of 18% and 21%, respectively (Table 4). The differences in bias and error between the "leave-one-out" and "country-wise" validations indicate the robustness of the input data. Some countries represent large portions of a bioregion, therefore not many points remain to choose from for gap-filling when a country is removed resulting in higher error. For example, Spain is in the Mediterranean bioregion and when removed in the "country-wise" validation the only data we can use to fill Spain with is from coastal Mediterranean France and portions of Italy.

All countries besides Italy and Austria have average height errors of less than 1 meter (Figure 6). The latitude with the largest overestimation is in the mid 40°s. Here we can see that the majority of this overestimation is due to northwestern Italy and southeastern France. This area contains high elevation mountains and our estimates tend to have higher error in higher elevations.

The standard deviation for age of the "leave-one-out" cross validation data decreased from the original NFI standard deviation because we used an average of 4 neighbors (Table 4). The MAE lies within the bounds of the normal variation of the dataset as it is smaller than the standard deviation. Spatially, over

and underestimations in mean age are scattered throughout Europe (Figure 7). We overestimate by under a half an age class at most latitudes with scattered latitudes having underestimations. We estimated age better with increasing elevation because the variation of observation decreases with elevation.

Volume and carbon estimations in this study are 21% higher than the FAO FRA estimates (Figure 8). We do not have spatially explicit datasets used for FAO reporting nor the access needed to compare calculation steps. Thus we cannot know for certain the cause behind this discrepancy. However, literature, understanding of the data and knowledge as to how carbon and volume are calculated in countries throughout Europe dictates that this discrepancy is driven by 4 factors: differences in calculation methods, the wall-to-wall nature of our gridded data, forest area designation and quality/variation of NFI data.

Our dataset and the FOA FRA are in agreement with respect to the top 8 countries with the most forest carbon stock (Figure 8). The top 3 countries with the smallest relative difference to FAO values - Lithuania, Slovenia, and Slovakia - are entirely gap-filled with a discrepancy from FAO FRA of 0.0%, 2.8%, and 4.8% respectively. Considering only countries for which we have gridded terrestrial data, there is an average estimation of 20% over the FAO estimate. However, Austria, which is entirely covered with gridded terrestrial data, has almost identical values in both our estimate and the FAO estimates.

Two countries that are completely gap-filled and have large discrepancies in volume between our data and FAO data are Serbia, and Bosnia-Herzegovina. We attribute these discrepancies to the quality of the FAO FRA data. FAO data for Serbia is based on incomplete NFI data (FAO, 2010b). and FAO data for Bosnia and Herzegovina is produced by the FAO themselves using historical datasets and no NFI data from Bosnia and Herzegovina (FAO, 2010a). The uncertainty information on the FAO data are unavailable in the FAO FRA reports not allowing further investigation into the cause of these discrepancies.

The largest difference in volume is in Germany (Figure 8). We have original NFI data for Germany and we use the same methodology used to produce volume estimates as those reported to the FAO. We attribute this discrepancy in volume estimates to the wall-to-wall nature of our data, forest area designation and high Czech NFI volume/ha values (Figure 3, 5). The German NFI data does not cover large portions of the country whereas our data covers all of Germany leading to the inclusion of sparsely forested areas not included in the NFI dataset, such as agricultural lands, which can add up to a noticeable amount of volume and carbon. These areas were gap-filled using our algorithm. When Czech

values were used to gap fill these areas, this led to higher than average volume estimates. Volume in countries that are similar to the Czech Republic according to our co-variates tended to be overestimated. Further, forest area again contributes to this discrepancy as data giving spatially explicit or country statistics on forest area differs greatly (Kempeneers et al., 2013; Seebach et al., 2011) (Table A1). The FAO FRA does not provide forest area maps which would allow us to further analyze the affect forest area designation has on the discrepancies in these estimates.

Carbon estimations are primarily driven by volume estimations, as calculating carbon first requires a volume estimate. Spain has the biggest carbon difference of any country between our data and FAO at nearly 50%. We have the original NFI data from Spain. Carbon (which includes above and below ground biomass) is derived from volume (which only includes above ground biomass) using root to shoot ratios. The Spanish root-to-shoot ratio is approximately 0.56 on average(Neumann et al., 2016b). Our data and FAO data show similar Spanish volume values. Therefore, FAO FRA for Spain must only represent above ground biomass further supporting our assumption that calculation method contributes to the discrepancies between our and the FAO FRA data. Without spatially explicit information on the uncertainty of FAO data it is not possible for us to analyze if our data or FAO data is more accurate to real world values; we can only analyze the discrepancies between the two data sets.

The height results show that that Simard's tree canopy height data is skewed toward taller heights. In the gridded terrestrial data and our cross-validated data there are two peaks in the distribution, at 12-16m and at 20-24m. The cross-validated data, however, is higher in the latter peak. Our data represents the average height of all trees within a cell. This data then gives an indication of the height profile of a forest on the landscape level. Simard's height data is the height from the lowest point on the ground to the highest point in the canopy. To exemplify how this definition difference affects results, let us consider a forest with 99% of forest cover as small trees with only 1% being tall trees. Our cell value will reflect a short height, whereas Simard will indicate a tall height. This difference in definition is exemplified in the skewness in Simard's tree canopy height data towards taller trees (Simard et al., 2011; Figure 3).

The age of a forest has many definitions (Cohen et al., 1995). Our study defines age as the average age of all trees within a cell. The EFIScen database is a collection of forest inventories that were compiled by separate countries to produce age class distributions, making its definition of age country-dependent. EFIScen age classes were not harmonized across countries and are given as area per age class per forest type. Further, the EFIScen data, aggregated to total forest area per country, includes values of forest

area that are up to 2 orders of magnitude different compared to our and FAO estimates (Table A1). This indicates that either the EFIScen data has different definitions of what constitutes a forest or the publicly available data set is incomplete.

In central Europe, Lithuania, which is completely gap-filled, shows a close agreement in the age class distribution between the EFIScen and data from this study (Figure 10). Sweden, however, has different distributions between the datasets with EFIScen having a continuously decreasing distribution and our data having a peak in the middle age classes. Croatia has a similar distribution between the two datasets, but there is a different total forest area (Table A1). The Croatian forestry company website states that there is 2,688,687 ha of total forest area (Hrvatske šume, 2015) which is larger than both the estimates from the datasets we analyzed (Table A1). Our dataset for Austria is derived completely from NFI data with no gap-filling; however, there is a large discrepancy between the two datasets. The reason behind all of these discrepancies is the differing definitions of age. Additionally, we do not include an uneven aged designation. This can lead to the discrepancy such as that which we find in the middle age classes in countries such as Austria (Figure 10). To further exemplify the difference age definition makes, we included Swiss NFI data into our analysis (Figure 10). Here the uneven aged stands, which comprise 308,200 ha of the Swiss NFI data, were not included in the distribution making a distinct difference in the age class distribution curve. In the Swiss data we see that 3 independently derived distributions of age have resulted in 3 distinctly different outcomes, exemplifying the difficulty in comparing age across data sets.

Our definition for age allows us to use our values as an indication of rotation length as it measures the average age of all trees which is rotation length dependent. To further examine our age estimate we compared our distributions with country statistics on management. The age pattern in Lithuania in our data indicates a common rotation length of 41-60 years and only a small portion of conservation area, indicated by the graph as a peak at age class 41-60, followed by a decreasing distribution and the lack of an increase in age class 8 (Figure 10). This agrees with Lithuanian forest statistics, which state that less than 1.2% of total forest area is in reserves in Lithuania (Fahy, 1999) and match the official pine age class distribution and optimal rotation lengths (Brukas et al., 2001; Hjortsø et al., 2006). In Sweden, 25% of forests are under conservation and the most common rotation length is 65-110 years (Swedish Forest Industries Federation, 2012). This can be seen in our Swedish distribution with an increase in age distribution until the 41-60 year age class, followed by a steep decline. There is then a large increase in the oldest age class which supports the fact that 25% of the area is under conservation. The South-East

European Forestry group says that 46% of Croatian forest is 40 – 80 years old (Lovrić et al., 2010). Both the EFIScen and our datasets agree with this statement by both showing a peak at this age class. Our data, however, shows a slight increase in the oldest age class, which also indicates a small percentage of protected area. That agrees with the 6% estimate by the Croatia Federal Forests (Hrvatske šume, 2015).

6. Conclusions

We developed a snap shot of the state of European forests across Europe based on variables common in forest inventories. We can produce any NFI variable, however in this study we focused on 4 characteristics: total live tree carbon, volume, mean tree height, and mean tree age. This data provides pan-European spatially explicit harmonized datasets of various forest characteristics using one methodology. It can be used to further our understanding of landscape-level forest dynamics as well as allow us to study the difference in forests across political boundaries. Further, the methodology and data developed here can be used as a check for international reporting such as that for the FAO. Data can be quickly checked and analyzed to find discrepancies that would then require further investigation. This data can also be used to fill in areas that have no data or decline to participate in such programs.

The data sets that we produced in this analysis are derived by combining available "bottom up" terrestrial data sources with "top down" satellite data records (Table 1). We grouped forests by cover type and bioregion as well as used 4 co-variates (i) site quality, (ii) NPP, (iii) NPP trend, and (iv) height to perform k-means clustering and k-nearest neighbor analysis (Figure 2). The information is provided as wall-to-wall data for live tree carbon, volume, mean tree height, and mean tree age class across European forests at a 0.133° (approximately 75 – 175km^2) resolution (Figure 2). Note that the algorithm developed can be used for any other forest characteristics and/or forest region (Figure 2). The code is freely available from the authors.

Our data will allow people interested in knowing the state of forest resources across Europe on the landscape scale to easily access information. Beyond Europe, this methodology can also be used in areas that have no accessible NFI data, whether due to financial, practical or political limitations. As long as there are similar forests that have NFI data one can use this methodology to fill in other areas. If this methodology is used internationally then it can also act as a way to check reporting errors and quantify forest characteristics for the purposes of global carbon mitigation schemes and negotiations. Our methodology shown here could be used by countries that do not have the means to produce their own NFI datasets, to partner with nations with similar forests and accompanying NFI data, to generate

information on the state of their forest resources. This could provide those countries without empirical NFI estimates more information to better negotiate at international meetings including the United Nations Framework Convention on Climate Change. All output data and the source code used to create it are freely and publicly available at ftp://palantir.boku.ac.at/Public/ForestResources.

Acknowledgments

We would like to thank Mrs. Loretta Moreno and Dr. Christopher Thurnher for reviewing and revising our manuscript. We would also like to thank all of those researchers and organizations who make their datasets publicly available allowing this kind of research possible. The research leading to these results has received funding from the European Union Seventh Framework Programme under grant agreement n°311970.

7. References

Brukas, V., Jellesmark Thorsen, B., Helles, F., Tarp, P., 2001. Discount rate and harvest policy: Implications for Baltic forestry. For. Policy Econ. 2, 143–156.

Brus, D.J., Hengeveld, G.M., Walvoort, D.J.J., Goedhart, P.W., Heidema, a. H., Nabuurs, G.J., Gunia, K., 2011. Statistical mapping of tree species over Europe. Eur. J. For. Res. 131, 145–157.

Chirici, G., Mcroberts, R.E., Winter, S., Bertini, R., Bra, U., Asensio, I.A., Bastrup-birk, A., Rondeux, J., Barsoum, N., 2012. National Forest Inventory Contributions to Forest Biodiversity Monitoring 58, 257–268.

Cohen, W.B., Spies, T. a., Fiorella, M., 1995. Estimating the age and structure of forests in a multi-ownership landscape of western Oregon, U.S.A. Int. J. Remote Sens. 16, 721–746.

Crowther, T.W., Glick, H.B., Covey, K.R., Bettigole, C., Maynard, D.S., Thomas, S.M., Smith, J.R., Hintler, G., Duguid, M.C., Amatulli, G., Tuanmu, M.-N., Jetz, W., Salas, C., Stam, C., Piotto, D., Tavani, R., Green, S., Bruce, G., Williams, S.J., Wiser, S.K., Huber, M.O., Hengeveld, G.M., Nabuurs, G.-J., Tikhonova, E., Borchardt, P., Li, C.-F., Powrie, L.W., Fischer, M., Hemp, a., Homeier, J., Cho, P., Vibrans, a. C., Umunay, P.M., Piao, S.L., Rowe, C.W., Ashton, M.S., Crane, P.R., Bradford, M. a., 2015. Mapping tree density at a global scale. Nature.

Daamen, A., Daamen, W.P., Wim, P., 2010. National Forest Inventories.

European Environment Agency, 2012. European Biogeographical Regions.

Fahy, O.& C.J., 1999. COST Action E27 Protected Forest Areas in Europe – Analysis and Harmonisation Country Report - Ireland. Ctry. Rep. Irel. 173–186.

Fao, 2010. Global Forest Resources Assessment 2010. Progress Towards Sustainable Forest Management. FAO Forestry Paper 147, Forestry Paper.

FAO, 2010a. Global forest resources assessment 2010 - Country report Bosnia and Herzagovina. Food Argicultural Organ. UN 34.

FAO, 2010b. Global forest resources assessment 2010 - Country report Serbia. Food Argicultural Organ. UN 34.

Friedl, M. a, McIver, D.K., Hodges, J.C.F., Zhang, X., Muchoney, D., Strahler, A.H., Woodcock, C.E., Gopal, S., Schneider, A., Cooper, A., Baccini, A., Gao, F., Schaaf, C., 2002. Global land cover mapping from MODIS: algorithms and early results. Remote Sens. Environ. 83, 287–302.

Gallaun, H., Zanchi, G., Nabuurs, G.J., Hengeveld, G., Schardt, M., Verkerk, P.J., 2010. EU-wide maps of growing stock and above-ground biomass in forests based on remote sensing and field measurements. For. Ecol. Manage. 260, 252–261.

Hartigan, J.A., Wong, M.A., 1979. Alorithm AS 136: A K-Means Algorithm. J. R. Stat. Soc. Ser. C (Applied Stat. 28, 100–108.

Hartigan, J.A., Wong, M.A., 1979. Algorithm AS 136: A k-means clustering algorithm. Appl. Stat. 28, 100–108.

Hero, A.O., Fessler, J. a., Usman, M., 1996. Exploring estimator bias-variance tradeoffs using the uniform CR bound. IEEE Trans. Signal Process. 44, 2026–2041.

Hjortsø, C.N., Stræde, S., Helles, F., 2006. Applying multi-criteria decision-making to protected areas and buffer zone management: A case study in the Royal Chitwan National Park, Nepal. J. For. Econ. 12, 91–108.

Hrvatske šume, 2015. Forests in Croatia [WWW Document]. URL http://portal.hrsume.hr/index.php/en/forests/general/forests-in-croatia

IPCC, 2003. Intergovernmental Panel on Climate Change Good Practice Guidance for Land Use , Land-Use Change and Forestry.

IPCC, Eggleston, S., Buendia, L., Miwa, K., Ngara, T., Tanabe, K., 2006. 2006 IPCC Guidelines for National Greenhouse Gas Inventories, Intergovernmental Panel on Climate Change.

Kempeneers, P., McInerney, D., Sedano, F., Gallego, J., Strobl, P., Kay, S., Korhonen, K.T., San-Miguel-Ayanz, J., 2013. Accuracy assessment of a remote sensing-based, pan-european forest cover map using multi-country national forest inventory data. IEEE J. Sel. Top. Appl. Earth Obs. Remote Sens. 6, 54–65.

Kohavi, R., 1995. A Study of Cross-Validation and Bootstrap for Accuracy Estimation and Model Selection. Int. Jt. Conf. Atificial Intell.

Kollmuss, A., Schneider, L., Zhezherin, V., 2015. Has Joint Implementation reduced GHG emissions ? Lessons learned for the design of carbon market mechanisms. Stockholm, Sweden.

Lefsky, M. a., Harding, D.J., Keller, M., Cohen, W.B., Carabajal, C.C., Del Bom Espirito-Santo, F., Hunter, M.O., De Oliveira, R., 2005. Estimates of forest canopy height and aboveground biomass using ICESat. Geophys. Res. Lett. 32, 1–4.

Lovrić, M., Martinić, I., Lovrić, N., Landekić, M., Sporčić, M., 2010. Assessment of progress towards sustainable forest management in Croatia through usage of quantitative Improved Pan-European Criteria and Indicators. South-East Eur. For. 1, 51–59.

Manning, C.D., Schutze, H., 1999. Foundations of statistical natural language processing, Cambridge: MIT Press.

Maselli, F., Chiesi, M., Mura, M., Marchetti, M., Corona, P., Chirici, G., 2014. Combination of optical and LiDAR satellite imagery with forest inventory data to improve wall-to-wall assessment of growing stock in Italy. Int. J. Appl. Earth Obs. Geoinf. 26, 377–386.

McDill, M.E., Amateis, R.L., 1992. Measuring Forest Site Quality Using the Parameters of a Dimensionally Compatible Height Growth-Function. For. Sci. 38, 409–429.

Moreno, A., Hasenauer, H., 2015. Spatial downscaling of European climate data. Int. J. Climatol.

Moreno, A., Neumann, M., Hasenauer, H., 2016. Optimal Resolution for Linking Remotely Sensed and Forest Inventory Data in Europe. Submitted.

Myneni, R.B., Hoffman, S., Knyazikhin, Y., Privette, J.L., Glassy, J., Tian, Y., Wang, Y., Song, X., Zhang, Y., Smith, G.R., Lotsch, A., Friedl, M., Morisette, J.T., Votava, P., Nemani, R.R., Running, S.W., 2002. Global products of vegetation leaf area and fraction absorbed PAR from year one of MODIS data. Remote Sens. Environ. 83, 214–231.

Neumann, M., Hasenauer, H., Moreno, A., 2016a. Estimating NPP for European Forests Submitted.

Neumann, M., Moreno, A., Mues, V., Härkönen, S., Mura, M., Bouriaud, O., Lang, M., Achten, W.M.J., Thivolle-Cazat, A., Bronisz, K., Merganič, J., Decuyper, M., Alberdi, I., Astrup, R., Mohren, F., Hasenauer, H., 2016b. Comparison of carbon estimation methods for European forests. For. Ecol. Manage. 361, 397–420.

Pan, Y., Birdsey, R. a, Fang, J., Houghton, R., Kauppi, P.E., Kurz, W. a, Phillips, O.L., Shvidenko, A., Lewis, S.L., Canadell, J.G., Ciais, P., Jackson, R.B., Pacala, S.W., McGuire, a D., Piao, S., Rautiainen, A., Sitch, S., Hayes, D., 2011. A large and persistent carbon sink in the world's forests. Science 333, 988–93.

Ruiz-Labourdette, D., Nogués-Bravo, D., Ollero, H.S., Schmitz, M.F., Pineda, F.D., 2012. Forest composition in Mediterranean mountains is projected to shift along the entire elevational gradient under climate change. J. Biogeogr. 39, 162–176.

Running, S.W., Nemani, R.R., Heinsch, F.A., Zhao, M., Reeves, M., Hashimoto, H., 2004. A Continuous Satellite-Derived Measure of Global Terrestrial Primary Production. Bioscience 54, 547.

Schelhaas, M. J., Varis, S., Schuck, A., & Nabuurs, G.J., 2006. EFISCEN Inventory Database. Joensuu, Finland.

Seebach, L.M., Strobl, P., San Miguel-Ayanz, J., Gallego, J., Bastrup-Birk, a., 2011. Comparative analysis of harmonized forest area estimates for European countries. Forestry 84, 285–299.

Simard, M., Pinto, N., Fisher, J., Baccini, A., 2011. Mapping forest canopy height globally with spaceborne lidar. Geophys. Res. 116.

Swedish Forest Industries Federation, 2012. Swedish Forestry: Forest and forest land [WWW Document]. URL http://www.svenskttra.se/MediaBinaryLoader.axd?MediaArchive_FileID=eb34da70-248d-4e78-b7cf-9592aca6c0db&FileName=Forest.pdf

Swiss Federal Institute for Forest Snow and Landscape Research, 2015. Swiss National Forest Inventory data portal.

Thornton, P.E., Running, S.W., 1999. An improved algorithm for estimating incident daily solar radiation from measurements of temperature, humidity, and precipitation. Agric. For. Meteorol. 93, 211–

228.

Tian, Y., 2004. Comparison of seasonal and spatial variations of leaf area index and fraction of absorbed photosynthetically active radiation from Moderate Resolution Imaging Spectroradiometer (MODIS) and Common Land Model. J. Geophys. Res. 109, D01103.

Tomppo, E., Olsson, H., Ståhl, G., Nilsson, M., Hagner, O., Katila, M., 2008. Combining national forest inventory field plots and remote sensing data for forest databases. Remote Sens. Environ. 112, 1982–1999.

Vilén, T., Gunia, K., Verkerk, P.J., Seidl, R., Schelhaas, M.J., Lindner, M., Bellassen, V., 2012. Reconstructed forest age structure in Europe 1950-2010. For. Ecol. Manage. 286, 203–218.

Wang, G.G., Klinka, K., 1995. Site-specific height curves for white spruce (Picea glauca [Moench] Voss) stands based on stem analysis and site classification. Ann. For. Sci. 52, 607–618.

Willmott, C.J., Matsuura, K., 2006. On the use of dimensioned measures of error to evaluate the performance of spatial interpolators. Int. J. Geogr. Inf. Sci. 20, 89–102.

Appendix

Table A1: Total forested area from EFIScen, this study (Pan-European) and FAO

Country	Total Forested Area (ha)		
	EFIScen	Pan-European	FAO
Austria	2,978,000	3,628,773	3,897,000
Belgium	146,259	703,669.8	679,880
Bosnia	22,750	2,425,217	2,185,000
Croatia	836,201	1,648,052	1,926,800
Czech	753,544.2	2,270,572	2,661,000
Denmark	442,309	421,174.5	548,000
Estonia	2,047,912	1,951,751	2,196,000
Finland	19,752,610	21,249,613	22,157,000
France	1,237,034	15,934,988	16,050,000
Germany	9,985,069	11,223,452	11,076,000
Hungary	1,860,640	1,598,186	2,047,400
Ireland	328,902	621,680.1	756,600
Italy	3,832,048	8,480,119	9,305,000
Latvia	2,621,752	2,977,663	3,376,800
Lithuania	1,908,979	2,022,840	2,175,600
Netherlands	306,029	344,775.2	365,000
Norway	5,946,577	8,975,334	10,217,800
Poland	8,814,881	9,348,988	9,391,800
Portugal	1,109,229	3,196,523	3,463,600
Romania	5,642,700	6,504,288	6,645,800
Slovakia	1,909,089	1,866,770	1,933,400
Slovenia	1,151,999	1,281,579	1,257,000
Sweden	20,966,537	27,370,952	28,203,000
Switzerland	1,139,901	1,116,430	1,249,200
United Kingdom	2,142,939	2,339,870	2,895,400
European Total	97,883,890	139,503,260	146,660,080

Table A2: Country Totals for carbon and volume and country averages for age class and height. Age class definitions in years: 1 = 0-20, 2 = 21-40, 3 = 41-60, 4 = 61-80, 5 = 81-100, 6 = 101-120, and 7 >120.

Country	Total Carbon (millions of Tons)	Total Volume (millions of m^3)	Age Class	Height (m)
Albania	51.64	118.18	3.50	10.59
Austria	398.40	1143.85	4.18	20.47
Belgium	84.69	228.10	3.97	18.37
Bosnia-Herzegovina	293.49	792.96	3.40	15.09
Bulgaria	408.81	1287.75	3.46	18.01
Croatia	171.44	460.45	3.28	15.21
CzechRepublic	373.06	978.11	4.09	19.65
Denmark	42.58	120.26	3.69	17.42
Estonia	101.29	249.14	3.20	16.40
Finland	979.23	2702.38	4.01	13.38
France	1299.62	2688.68	3.76	14.64
Germany	1302.26	4771.09	3.98	20.39
Greece	137.21	237.13	3.28	8.96
Hungary	157.67	470.96	2.87	17.99
Ireland	46.87	100.61	3.51	14.81
Italy	576.17	1433.58	3.21	12.17
Latvia	160.23	428.87	3.54	15.82
Lithuania	145.97	474.11	3.73	16.73
Macedonia	99.60	262.12	3.60	14.82
Montenegro	46.81	139.37	3.34	11.51
Netherlands	42.68	109.86	3.71	17.96
Norway	365.37	891.32	4.54	8.51
Poland	1012.93	2604.55	3.19	17.85
Portugal	132.74	198.43	3.83	8.64
Romania	718.52	2143.65	2.71	18.67
Serbia	312.70	1026.69	3.57	18.81
Slovakia	200.68	637.16	3.38	17.75
Slovenia	152.60	480.31	3.68	18.93
Spain	763.99	1107.65	3.03	9.10
Sweden	1318.34	3441.41	4.17	11.84
Switzerland	123.95	348.52	4.46	17.68
United Kingdom	216.48	464.22	3.73	14.89
Europe (per cell)	12238.0	32541.5	3.71	14.22